# Stereocontrolled Ring-Opening Polymerization of Lactide Monomers by Lewis-Acidic Metal Complexes

**Von der Fakultät für Mathematik, Informatik und Naturwissenschaften der**

**RWTH Aachen University**

**zur Erlangung des akademischen Grades eines**

**Doktors der Naturwissenschaften genehmigte Dissertation**

vorgelegt von

Diplom-Chemiker

Andreas Kapelski

aus

Rheinberg

Berichter: Universitätsprofessor Dr. rer. nat. Jun Okuda

Universitätsprofessor Dr. rer. nat. Iris M. Oppel

Tag der mündlichen Prüfung: 01. Februar 2013

Berichte aus der Chemie

**Andreas Kapelski**

# Stereocontrolled Ring-Opening Polymerization of Lactide Monomers by Lewis-Acidic Metal Complexes

Shaker Verlag
Aachen 2013

**Bibliographic information published by the Deutsche Nationalbibliothek**
The Deutsche Nationalbibliothek lists this publication in the Deutsche Nationalbibliografie; detailed bibliographic data are available in the Internet at http://dnb.d-nb.de.

Zugl.: D 82 (Diss. RWTH Aachen University, 2013)



Printed in Germany.

ISBN 978-3-8440-1798-4
ISSN 0945-070X

Shaker Verlag GmbH • P.O. BOX 101818 • D-52018 Aachen
Phone: 0049/2407/9596-0 • Telefax: 0049/2407/9596-9
Internet: www.shaker.de • e-mail: info@shaker.de

The work delinated here was carried out between October 2009 and October 2012 in the Laboratories of Prof. Dr. Jun Okuda at the Institute of Inorganic Chemistry at RWTH Aachen University, Germany

**Abbreviations**

| | |
|---|---|
| AcOH | Acetic acid, $CH_3COOH$ |
| Ada | adamantyl group, Tricyclo[3.3.1.1$^{3,7}$]decanyl |
| Ar | aromatic group |
| br | broad |
| $^t$Bu | *tert*-butyl group, -$C(CH_3)_3$, -$CMe_3$ |
| cum | cumyl group, -$C(CH_3)_2(C_6H_5)$, -$CMe_2Ph$ |
| d | doublet |
| DABCO | 1,4-Diazabicyclo[2.2.2]octan |
| DBU | 1,8-Diazabicyclo[5.4.0]undec-7-en |
| Do | donor atom |
| DSC | differential scanning calorimetry |
| f.e. | for example |
| equiv. | equivalent |
| Et | ethyl group, -$CH_2CH_3$ |
| EtAc | Ethyl acetate, $CH_3COOCH_2CH_3$ |
| EtOH | Ethanol, $CH_3CH_2OH$ |
| GC | gas chromatography |
| GPC | gel permeation chromatography |
| LA | lactide |
| m | multiplet |
| M | Metal |
| $M_n$ | number average molecular weight |
| $M_w$ | weight average molecular weight |
| Me | methyl group, -$CH_3$ |
| MeOH | Methanol, $CH_3OH$ |
| Mt | million tons |
| NMR | nuclear magnetic resonance |

| | |
|---|---|
| OTs | tosyl proup, *para*-toluene sulfonyl group |
| PDI | polydispersity index (=$M_w$/ $M_n$) |
| Ph | phenyl group, -$C_6H_5$ |
| PLA | Poly(lactide); Poly(lactic acid) |
| ppm | parts per million |
| q | quartet |
| quint | quintet |
| ROP | Ring-Opening Polymerization |
| t | triplet |

# Contents

# Chapter I

# Poly(lactide):

# A Biodegradable Polymer

# I. Poly(lactide): A Biodegradable Polymer

## I.1. General Introduction

### I.1.1. Biodegradable Polymers

Society's dependance on petrochemical resources is a challenging problem. These resources will be consumed some day. By virtue of growing ecological consciousness in chemical industry and academical research, replacing petrochemically based materials by products based on natural resources is a path to overcome this dependance.

Today, chemical industry strongly relies on petrochemical resources. In 2008 more than 280 Mt of polymers were produced worldwide,[1] but only neglicibly small 360 000 tons (0.1%) came from natural resources.[2] According to present forecasts, annual growth rates of 37% are expected, reaching a production capacity of 3.45 Mt of biorenewable polymers in 2020.[3] Overall, 90% of petrochemically derived polymers produced today can potentially be replaced.[3] One of the most prominent representatives of these biodegradable polymers is polylactide, also referred to as poly lactic(acid) (PLA).

The physical and chemical properties render PLA an attractive alternative to petrochemically derived polymers like polyethylene (PE), polypropylene (PP) or polystyrene (PS). Presently, PLA is already used in biomedical implants; for example as sutures; as packaging material, films or fibres.[4-6]

### I.1.2. From Corn to Polylactide (PLA)

Reports dating from the sixteenth century already describe polycondensation of lactic acid, resulting in a solid material.[7] However, PLA was not recognized specifically until Carothers *et al.* first mentioned Ring-Opening Polymerization (ROP) of lactide to PLA in 1932.[8] Nearly 40 years passed until in the 1970s the advantages and possible applications for biodegradable polymers were recognized. Industrial production of PLA started in the early 90s. Since that day, produced amounts grew every year.[9] Today, more than 150 000 t PLA are produced annually in the USA, Europe and Japan by companies such as Natureworks LLC, which

specialized in the production of PLA. The physical, chemical and processing characteristics of PLA have been reported in a number of reviews showing pioneering efforts that have been made over the last decades.[4,7,9-24]

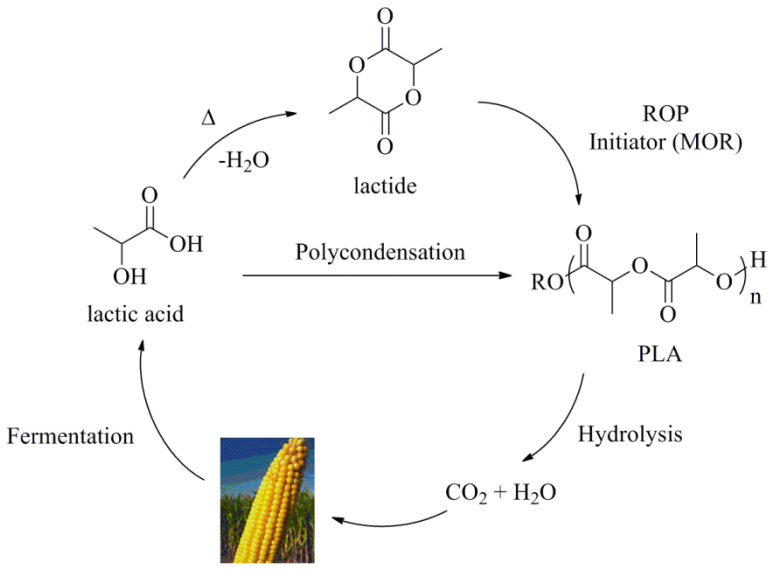


**Scheme 1.1.** Lifecycle of PLA

The lifecycle of PLA (Scheme 1.1.) starts from starch, corn or sugar feedstocks which are processed into glucose. By fermentation using bacteria of the genus lactobacillus, lactic acid is produced.[25] Lactic acid can directly be polycondensed into PLA. In terms of control over selectivity, molecular weight, molecular weight distribution (PDI) or melting point; lactic acid is reacted by condensation into its cyclic diester lactide (LA), that is polymerized by ring-opening polymerization (ROP) using an organometallic, organic or enzymatic initiator. Decomposition of PLA into $CO_2$ and $H_2O$ closes the lifecycle of PLA.

## I.1.3. Ring-Opening Polymerization (ROP) of Lactide Monomers

The nature of the initiator used for the ROP of lactide monomers determines the occuring mechanism. ROP can proceed cationic,[26-29] anionic,[30-33] via coordination-insertion mechanism or via activated monomer mechanism. The coordination-insertion mechanism (Scheme 1.2. **A**) is well understood and supported by detailed experimental and theoretical studies.[34-41]

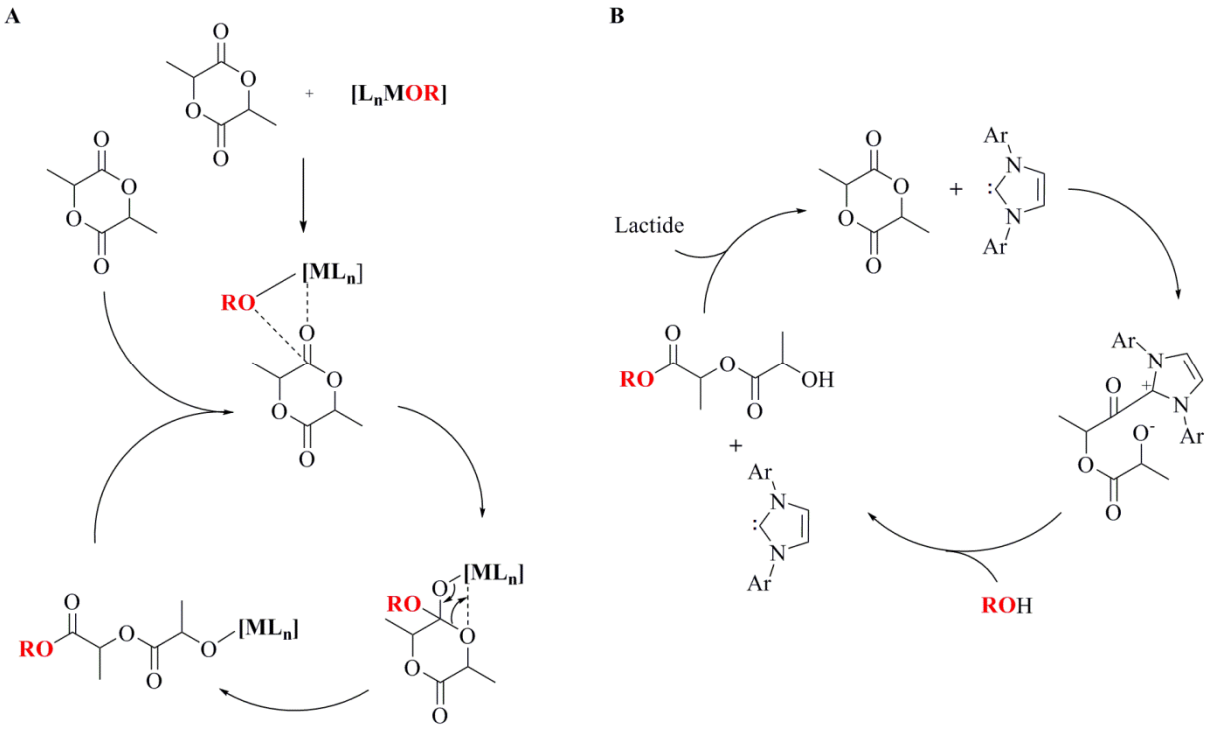


**Scheme 1.2.** Mechanisms of the ROP of lactide. **A**: coordination-insertion mechanism, **B**: activated monomer mechanism.

Commonly, organometallic initiators bearing Lewis-acidic metal centers are used. The metal is ligated by one or more mono- or multidentate ligands, determining electronical and sterical properties of the initiator. Amide, alkoxide or alkyl groups may be used as initiating groups. Lactide coordinates with one carbonyl oxygen to the Lewis acidic metal center, followed by nucleophilic attack of the initiator group at the carbonyl carbon. The lactide ring undergoes acyl-bond cleavage to create a new alkoxide species bonded to the metal center that subsequently attacks another lactide monomer as a nucleophile. Termination by hydrolysis yields hydroxy end capped polymers.

The activated monomer mechanism (Scheme 1.2. **B**) occurs, when organocatalysts or cationic initiators are used.[28,42] The nucleophilic initiator activates lactide by nucleophilic attack. Addition of a protic substrate, f.e. an alcohol, initiates polymerization by generating a ring-opened adduct which consists of an $\alpha$-chain bearing an ester from the initiating alcohol and an $\omega$-chain that is end capped with a secondary alcohol.

Theoretical calculations have identified loss of ring strain as driving force of the ROP. The standard enthalpy of the polymerization is -23 $kJ \cdot mol^{-1}$ and the standard entropy of polymerization is -0.04 $kJ.K^{-1}$ $mol^{-1}$ for the formation of PLA.[43]

Transesterification is the main side reaction during the ROP,[44] leading to scrambling in molecular weights. As a consequence, PDI values increase.[45] This can occur intra- or intermolecularly. In case of intramolecular transesterification, two neighboring polymer chains exchange their polymer ends forming short polymer chains and macrocyclic species. (Scheme 1.3.A) In intermolecular transesterification, chain redistribution takes place (Scheme 1.3.B).[35]

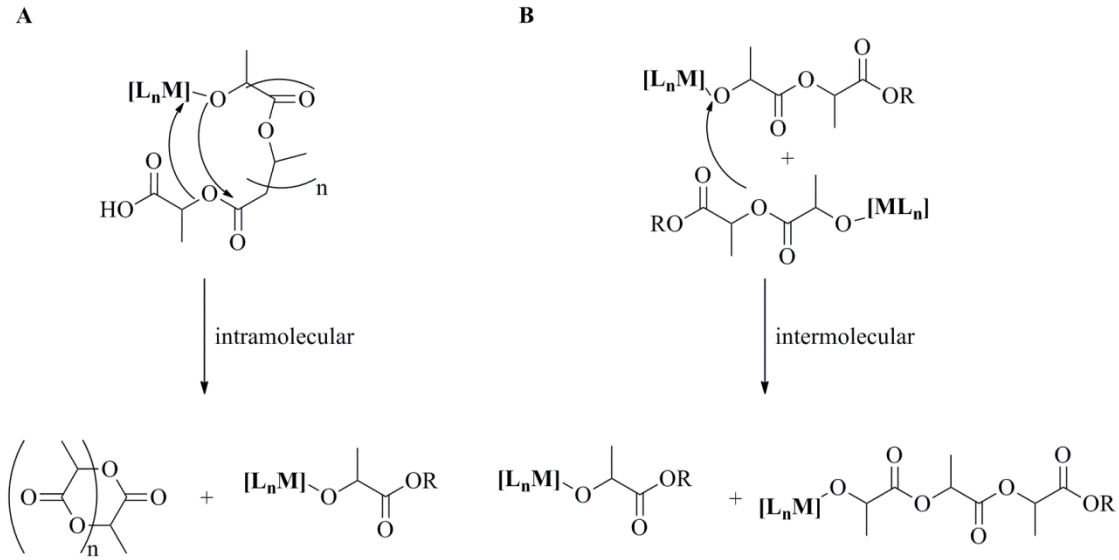


**Scheme 1.3. A**: Intramolecular and **B**: intermolecular transesterification

# I.2. Stereocontrolled ROP of Lactide

## I.2.1. Structure of Lactide Monomers and Poly(lactide)

Physical and mechanical properties of a polymeric material strongly depend on its molecular weight, PDI and stereochemistry. Lactide possesses two stereocenters resulting in three isomers: D-, L- and DL-lactide (*meso*-lactide) (Scheme 1.4.).

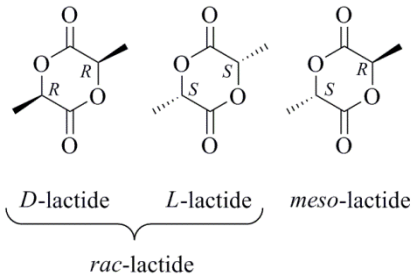


**Scheme 1.4.** Lactide isomers

The isomers are commercially available in pure form and as racemate, referred to as *rac*-lactide. Due to these stereocenters, stereocontrolled ROP of lactide monomers can result in a variety of PLA microstructures (Scheme 1.5.).

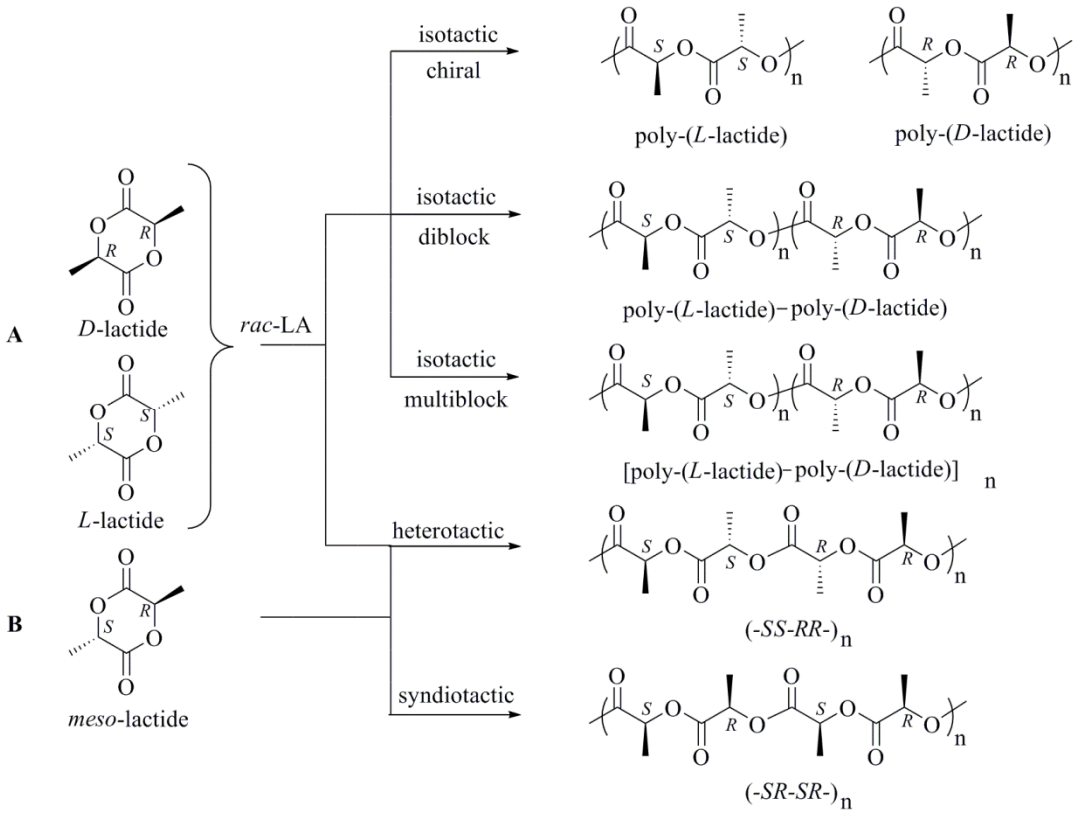


**Scheme 1.5.** PLA microstructures resulting from stereocontrolled ROP of **A**: *rac*-lactide and **B**: *meso*-lactide.

ROP of enantiopure D- and L-lactide gives isotactic PLA featuring all stereocenters along the polymer chain having the same configuration (*RRRRRR* or *SSSSSS*). ROP of *rac*-lactide can

result in isotactic diblock or multiblock PLA. Heterotactic PLA evolves from alternating insertion of D- and L- configured monomers out of *rac*-lactide; the stereocenters along the polymer chain doubly alternate (e.g. *SSRRSSRRSS*). ROP of *meso*-lactide can potentially result in formation of heterotactic or syndiotactic PLA. The stereocenters alternate along the polymer chain (e.g. *SRSRSRSRSR*). Atactic PLA is formed if no stereocontrol occurs. Side reactions like transesterification, chain termination or insertion errors influence the microstructure.

Polymer tacticity is identified by homonuclear decoupled $^{1}$H NMR and $^{13}$C NMR analysis of tetrad sequences.[46-47] In absence of side reactions like epimerization or transesterification, ROP of lactide monomers results in well-defined possible tetrad sequences. The chemical shifts of these tetrad sequences are shown in Scheme 1.6.

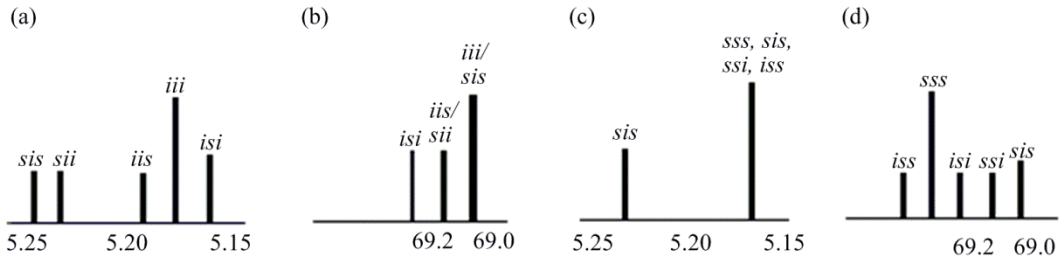


**Scheme 1.6.** Chemical shifts (in ppm) for diagnostic tetrad sequences. (a) $^{1}$H{$^{1}$H} NMR spectrum of poly(*rac*-lactide); (b) $^{13}$C{$^{1}$H} NMR spectrum of poly(*rac*-lactide); (c) $^{1}$H{$^{1}$H} NMR spectrum of poly(*meso*-lactide); (d) $^{13}$C{$^{1}$H} NMR spectrum of poly(*meso*-lactide).

The degree of stereoregularity is quantified as probability of *racemic* or *meso* enrichments along the polymer chain. The probability of forming a new *racemic* diad is referred to as $P_r$ and the probability of forming a new *meso* diad is refered to as $P_m$. These values are calculated from homonuclear decoupled $^{1}$H{$^{1}$H} NMR spectra of PLA.[14,48-49] A completely atactic polymer features $P_r = P_m = 0.50$. For ROP of *rac*-lactide, $P_r = 1.0$ ($P_m = 0$) describes perfectly heterotactic PLA and $P_m = 1.0$ ($P_r = 0$) describes isotactic PLA. For ROP of *meso*-lactide, $P_r = 1.0$ ($P_m = 0$) describes perfectly syndiotactic PLA while $P_m = 1.0$ ($P_r = 0$) describes heterotactic PLA. Analog, $P_i$ is used to describe isotacticity of PLA and $P_s$ describes syndiotacticity.

Tacticity of the polymer affects its melting ($T_m$) and glass transition temperature ($T_g$). Heterotactic PLA melts at $T_m$ = 130 °C, isotactic PLA shows $T_m$ = 180 °C. Annealing of an equimolar mixture of isotactic poly(L-lactide) and poly(D-lactide) results in stereocomplex PLA (Neo-PLA) with $T_m \approx 230$ °C (Scheme 1.7.).[14,50] Syndiotactic PLA is reported to melt at $T_m$ = 153 °C.[114]

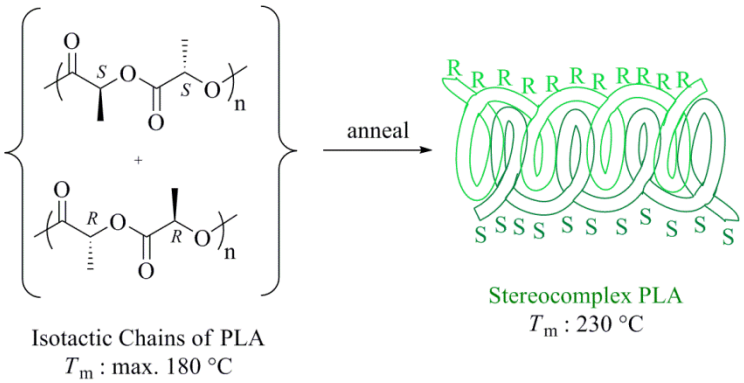


**Scheme 1.7.** Formation of stereocomplex PLA

## I.2.2. Metal-Based Initiators for the ROP of Lactide Monomers

Since the work of Kleine in 1959 who studied the preparation of PLA using metal-based initiators,[51] organometallic compounds have been investigated with regard to their applicability as initiators for the ROP of lactide monomers.

In industry, tin(II) bis(ethylhexanoate) $Sn(Oct)_2$ is the most widely established precatalyst for the production of PLA. Protic reagents or impurities such as alcohols, amines or lactic acid act as co-initiators (Scheme 1.8.).[52-54]

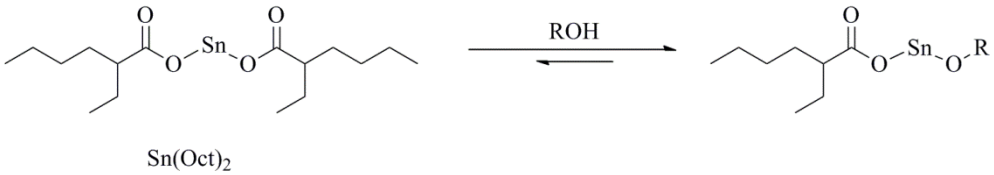


**Scheme 1.8.** Structure of $Sn(Oct)_2$ and its reaction with alcohols.

Mechanistic and kinetic aspects on the ROP initiated by $Sn(Oct)_2$ have been studied intensively by Penczek *et al.*[38] and Kowalski *et al.*[55] Application of Sn(II) initiators stays controversial because of their toxicity. Other metal alkoxides such as $[Al(O^iPr)_3]$[277-278] or

alkoxide clusters like $[Y_5(\mu\text{-}O)(O^iPr)_{13}]$[109] and $[Fe_5(\mu\text{-}O)(OEt)_{13}]$[171] were found to efficiently initiate ROP of lactides. The polymerization is less controlled due to more than one alkoxide groups that can potentially attack lactide. This results in relatively broad $M_w/M_n$ values. Consequently, well-defined single site initiators that efficiently control molecular weight, its distribution and stereoselectivity have experienced a tremendous development.

Today, numerous homogeneous catalysts have been reported to polymerize lactide monomers. They are highlighted in several comprehensive reviews.[4-5,7,9-18,20-21] Complexes based on alkaline earth metals magnesium[20,56-83,138,196] or calcium;[56,61,67,69,72,77,79,84-86] on scandium,[87-92] yttrium[9,20,87,89-91,93-105,107-120,] and the lanthanides,[20,87,89,96-97,103,106-110,116-117,121-127] on group 4 metals (titanium,[20,36,112,119,128-153,155-156] zirconium[36,131-133,135-143,147,153,155-165] and hafnium[131-133,139,141-142,155,156,159-161,163,165]), on iron,[20,32,166-171] nickel,[172] copper[172-173], or zinc[10-12,20,36,56-61,65,69,72-83,119,121,138,154,174-217] as well as in group 13 metals (aluminum,[20,27,35-37,48,104,114,154,183,188,203,206,211,218-269] gallium[270-271] and indium[272-280]) initiate ROP of lactide monomers.

Generally, these complexes consist of a Lewis acidic-metal center M, ancillary ligands $L_n$ and an initiating group R to form complexes of the type $[(L_n)MR]$. As initiating groups alkyls, amides, and halides are used.

## I.2.3. Isoselective ROP of *rac*-Lactide

Since *rac*-lactide is more easily accessible than *meso*-lactide, many efforts have been made to polymerize *rac*-lactide selectively.[5,14-15] Complexes of magnesium,[57] yttrium,[95,104] the lanthanides,[124] zinc,[57,189] aluminum[219-227,243,255,268] and gallium[270] show isoselective ROP of *rac*-lactide. Most outstanding results were achieved by using aluminum based complexes with Salan or Salen-type ligands. Effects of variations in the ligand backbone or the phenolate moiety were discussed by Gibson[252] and Dove.[14]

In 1996, Spassky *et al.* first reported formation of highly isotactic and crystalline poly(*rac*-lactide) by ROP of *rac*-lactide using enantiopure {(*R*)-SalBinap}Al(OR) (**I**, Scheme 1.9.).[268] At conversions less than 50%, predominantly poly(D-lactide) is formed while L-lactide remained in solution. This results from different polymerization rates with a rate constant for D-lactide 19 times higher than for L-lactide. A melting temperature $T_m$ = 187 °C was determined for the isolated polymer.

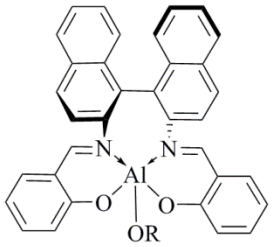


R = Me, O$^i$Pr

**I**

**Scheme 1.9.** {(*R*)-SalBinap}Al(OR) (**I**) by Spassky, 1996.[268]

In 2002, Feijen *et al.* reported that enantiopure *RR*-configured aluminum isopropoxide complex **II** with the Jacobsen ligand (Scheme 1.10) showed a preference of 20:1 for ROP of D-lactide ending up with $P_m$ = 0.93 at 85% conversion.[255] However, only a small initial monomer/initiator ratio of 62 was used in this reaction.

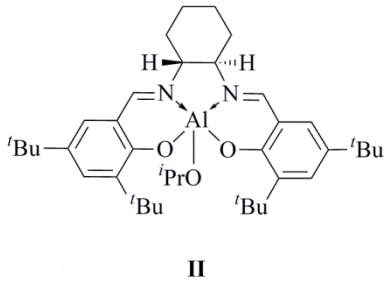


**II**

**Scheme 1.10.** Al-Salen complex **II** by Feijen, 2002.[255]

Highly isotacic stereoblock PLA with $P_m$ = 0.98 and $T_m$ = 207 °C was prepared by Nomura *et al.* in 2007 using achiral aluminum-Salen complex **III** with a rigid backbone and large $Si(CH_3)_2\{C(CH_3)_3\}$-groups in *ortho* and *para* position of the phenolate moiety (Scheme 1.11).[243]

Proceeding via chain-end mechanism, chirality of the polymer probably induces the chiral geometry of the flexible ligand, amplifying the efficiency of stereodifferentiation of L-lactide and D-lactide. Up to now, this is the highest isotactic stereoblock PLA reported for ROP of *rac*-lactide by an achiral catalyst/initiator system.

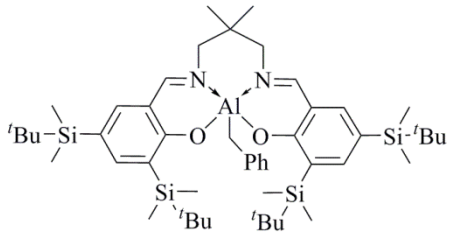

**III**

**Scheme 1.11.** Al-Salen complex **III** by Nomura, 2007.[243]

Very recently, Lin *et al.* prepared bulky substituted Aluminum Salen complexes **IV** that produce isotactic PLA from *rac*-lactide within 12 h at 70 °C in toluene solution. (Scheme 1.12.) The polymers showed melting points of $T_m$ = 203 °C and 205 °C.[219]

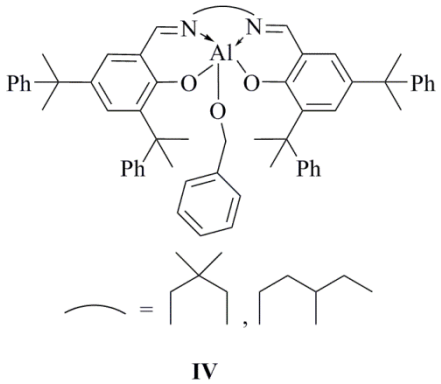

**IV**

**Scheme 1.12.** Al-Salen complexes **IV** by Lin, 2012.[219]

## I.2.4. Heteroselective ROP of *rac*-lactide

Different from ROP of *rac*-lactide to isotactic poly(*rac*-lactide) with selectivities of $P_m$ > 0.90 using aluminum Salen complexes, heterotactic poly(*rac*-lactide) is accessible with a greater variety of metals and ligands. Complexes of calcium,[61] magnesium,[57,59,65,68] scandium,[88-89] yttrium,[94,97,102-103] samarium,[126] zirconium,[141-142] zinc,[57,58-60,65,190,215] aluminum[96,234] and indium[274] have been studied intensely.

Coates *et al.* prepared dimeric zinc alkoxide complexes [(BDI)ZnO$^i$Pr]$_2$ supported by a *β*-diiminate ligand (**V**, Scheme 1.13.) that polymerized *rac*-lactide to highly heterotactic PLA ($P_r$ = 0.94) with 97% conversion in 2 h at 0 °C . A detailed study on the polymerization

kinetics and the effect of the substituents on the *β*-diiminate ligand on the catalytic activity were reported.[57]

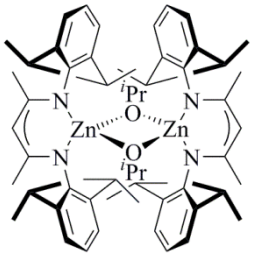


**V**

**Scheme 1.13.** [(BDI)ZnO$^{i}$Pr]$_2$ complex **V** by Coates, 2001.[57]

Remarkably high heteroselectivity in the ROP of *rac*-lactide was found for zirconium and hafnium amine tris(phenolate) alkoxides reported by Davidson *et al.* in 2008 (**VI**, Scheme 1.14.).[141] Performing ROP in toluene at 25 °C yields PLAs with $P_r$ = 0.98 (M = Zr) and $P_r$ = 0.97 (M = Hf). Polymerization is controlled due to the high steric bulk of the tris(phenolate) chelating system with one alkoxide group attached to the metal center. Notably, high heteroselectivity remains if the polymerization is performed solvent-free at 130 °C.[141]

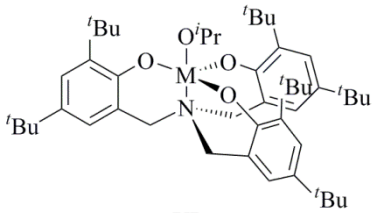


**VI**

**Scheme 1.14.** Tris(phenolate) alkoxide complexes **VI** by Davidson *et al.*, 2008.[141]

In 2004 Carpentier *et al.* first introduced highly heteroselective ROP of *rac*-lactide initiated by a group 3 metal complex (**VII**, Scheme 1.15.).[97] By further introducing sterically large cumyl groups instead of $^{t}$Bu groups on the phenolate moiety it was possible to increase heteroselectivity from $P_r$ = 0.80 up to $P_r$ = 0.90 (**VIII**, Scheme 1.15.).[110]

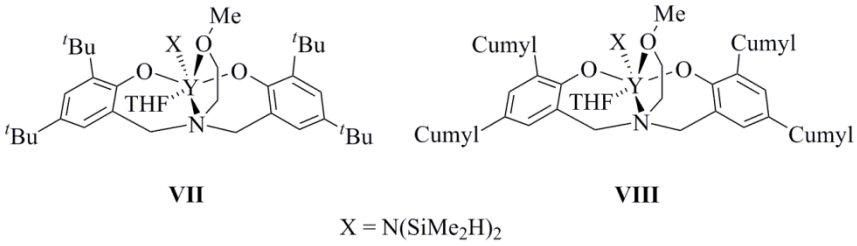


**VII** **VIII**

$X = N(SiMe_2H)_2$

**Scheme 1.15.** Yttrium complexes by Carpentier in 2004 (**VII**)[97] and 2006 (**VIII**).[110]

1,$\omega$-dithiaalkanediyl-bridged bis(phenolate) complexes of rare earth metals scandium, yttrium and lutetium by Okuda *et al.* rapidly polymerize *rac*-lactide to narrowly distributed PLA with heterotacticities of $P_r > 0.92$ (**IX**, Scheme 1.16.).[87-89] Heteroselectivity was reported to depend strongly on the bulk of the *ortho*-substituent $R_1$ of the phenolate moiety and the size of the ligand backbone.

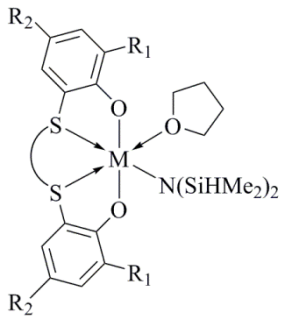


$M = Sc, Y, Lu$

$R_1, R_2 = H, {}^tBu, Me, Cumyl$

**IX**

**Scheme 1.16.** Rare earth metal bis(phenolate) complexes **IX** by Okuda *et al.*[87-89]

Highest heteroselectivity in ROP of *rac*-lactide was achieved by lanthanide mono(alkyl) complexes supported by ONNO-tetradentate diamine ligands reported by Cui *et al.*[96] (**X**, Scheme 1.17.). Polymers with heterotacticities up to $P_r = 0.99$ have been isolated, featuring high molecular weights and narrow $M_w/M_n$ values.

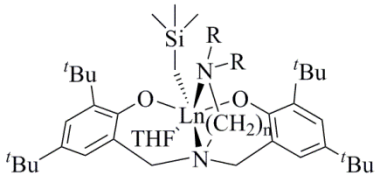


**X**

**Scheme 1.17.** Lanthanide complexes **X** by Cui *et al.*[96]

Trispyrazolyl-hydroborate complexes of non-toxic alkaline earth metal calcium reported by Chisholm *et al.* produced heterotactic poly(*rac*-lactides) (Scheme 1.18.) ($P_r$ = 0.90).[60]

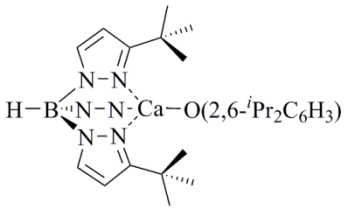


**X**

**Scheme 1.18.** Calcium tris(pyrazolyl)-hydroborate complex **X** by Chisholm *et al.*[60]

## I.2.5. Syndioselective ROP of *meso*-Lactide

Compared to the slow process of finding catalysts for stereocontrolled ROP of *rac*-lactide, pioneering results on stereocontrolled ROP of *meso*-lactide were already published in the late 90s.

In 1999, Coates used enantiopure (*R*)-configured aluminum SALEN complex **I** introduced by Spassky *et al.* in 1996 (Scheme 1.10) and achieved a syndiotacticity of $P_s$ = 0.96 being the highest syndiotacticity ever reported.[263] Analysis of crystalline polymer by DSC found a melting point of $T_m$ = 152 °C, following annealing at 95 °C for 1 h. ROP of *meso*-lactide with analogous racemic catalyst afforded atactic PLA.

Since great efforts have been made, finding exclusively catalysts to polymerize *meso*-lactide with even higher syndioselectivities, initiators of alkaline earth metals[67], rare earth metals[110], group 4 metals,[153,157] zinc,[57] aluminum[234,237,257] or indium[278] have been discovered for

syndioselective ROP of *meso*-lactide. However, syndiotacticities of PLAs do not exceed $P_s$ = 0.96.

## I.3. Outline

Objective of this thesis is investigation of stereocontrolled ROP of lactide monomers. Preliminary studies have already found 1,$\omega$-dithiaalkanediyl bridged bis(phenolate) complexes of rare earth elements and group 13 metals (aluminum, indium) as suitable initiators for stereocontrolled ROP of lactide monomers.

**Chapter II** describes syntheses and characterization of new racemic and achiral 1,$\omega$-dithiaalkanediyl bridged OSSO-type bis(phenols). Consequently, syntheses and characterization of new bis(phenolate) complexes of scandium and yttrium will be presented and discussed in **Chapter III**. **Chapter IV** deals with studies on activity and stereoselectivity of these complexes in ROP of *rac*- and *meso*-lactide. A detailed microstructure analysis of the polymers is additionally given.

In **Chapter V** ROP of *rac*- and *meso*-lactide initiated by indium (bis)phenolate complexes including detailed kinetic studies is presented. In the concluding **Chapter VI**, a new phenol-type proligand containing a macrocycle will be introduced. The syntheses of neutral and cationic alkaline earth metal complexes and their application in ROP of lactide monomers will be discussed.

## I.4. References


[1] Statistisches Bundesamt, Fachserie 4, Reihe 3.1, **2007**.

[2] L. Shen, J. Haufe, M. K. Patel, *Product Overview and Market Projection of Emerging Bio-based Plastics*, Copernicus Institute for Sustainable Development and Innovation, Utrecht University, Utrecht **2009**.

[3] European Bioplastics, PRO-BIP study **2007**.

[4] R. Auras, L.-T. Lim, S. E. M. Selke, H. Tsuji in *Poly(lactic acid) – Synthesis, Structures, Properties, and Applications*, John Wiley & Sons, Inc. Hoboken, New Jersey, **2010**.

[5] S. Inkinen, M. Hakkarainen, A.-C. Albertsson, A. Södergard, *Biomacromolecules* **2011**, *12*, 523-532.

[6] R. Auras, B. Harte, S. Selke, *Macromol. Biosci.* **2004**, *4*, 835-864.

[7] A. Södergård, M. Stolt, *Prog. Poly. Sci.* **2002**, *27*, 1123-1163.

[8] W. H. Carothers, G. L. Dorough, *J. Am. Chem. Soc.* **1932**, 761-772.

[9] R. H. Platel, L. M. Hodgson, C. K. Williams, *Polymer Reviews* **2008**, *48*, 11-63.

[10] I. dos Santos Vieira, S. Herres-Pawlis, *Eur. J. Inorg. Chem.* **2012**, *5*, 765-774.

[11] N. Ajellal, J.-F. Caprentier, C. Guillaume, S. M. Guillaume, M. Helou, V. Poirier, Y. Sarazin, A. Trifonov, *Dalton Trans.* **2010**, *39*, 8363-8376.

[12] J.-C. Buffet, J. Okuda, *Polym. Chem.* **2011**, *2*, 2758-2763.

[13] P. J. Dijkstra, H. Du, J. Feijen, *Polym. Chem.* **2011**, 2, 520-527.

[14] M. J. Sanford, A. P. Dove, *Chem. Soc Rev.* **2010**, *39*, 486-494.

[15] C. M. Thomas, *Chem. Soc. Rev*. **2010**, *39*, 165-173.

[16] C. K. Williams, M. A. Hillmyer, *Polym. Rev.* **2008**, *48*, 1-10.

[17] A. Amgoume, C. M. Thomas, J.-F. Carpentier, *Pure Appl. Chem*. **2007**, *79*, 2013-2030.

[18] O. Dechy-Cabaret, B. Martin-Vaca, D. Bourissou, *Chem. Rev*. **2004**, *104*, 6147-6176.

[19] A.-C. Albertsson, I. K. Varma, *Biomacromolecules* **2003**, *4*, 1466-1486.

[20] B. J. O'Keefe, M. A. Hillmyer, W. B. Tolman, *J. Chem. Soc., Dalton Trans*. **2001**, 2215-2224.

[21] R. E. Drumright, P. R. Gruber, D. E. Henton, *Adv. Mater*. **2000**, *12*, 1841-1846.

[22] Y. Ikada, H. Tsuji, *Macromol. Rapid Commun.* **2000**, *21*, 117-132.

[23] K. E. Uhrich, S. M. Cannizzaro, R. S. Langer, K. M. Shakesheff, *Chem. Rev.* **1999**, *99*, 3181-3198.

[24] E. Chiellini, R. Solaro, *Adv. Mater.* **1996**, *8*, 305-313.

[25] A. N. Vaidya, R. A. Pandey, S. Mudliar, M. S. Kumar, T. Chakrabarti, S. Devotta, *Crit. Rev. Environ. Sci. Technol.* **2005**, *35*, 429-467.

[26] I. G. Barskaya, Y. B. Lyudvig, R. R. Shifrina, A. L. Izyumnikov, *Vysokomolekulyarnye Soedineniya Seriya A* **1983**, *25*, 1283-1288.

[27] N. Emig, H. Nguyen, H. Krautscheid, R. Reau, J.-B. Cazaux, G. Bertrand, *Organometallics* **1998**, *17*, 3599-3608.

[28] D. Bourissou, B. Martin-Vaca, A. Dumitrescu, M. Graullier, F. Lacombe, *Macromolecules* **2005**, *38*, 9993-9998.

[29] M. Basko, P. Kubisa, *J. Polym. Sci., Polym Chem.* **2006**, *44*, 7071-7081.

[30] C. Stere, M. Iovu, A. Boborodea, D. S. Vasilescu, I. S. Fazakas-Anca, *Polym. Advan. Technol.* **1998**, *9*, 322-325.

[31] A. Bhaw-Luximon, D. Jhurry, N. Spassky, S. Pensec, J. Belleney, *Polymer* **2001**, *42*, 9651-9656.

[32] D. S. McGuinness, E. L. Marshall, V. C. Gibson, J. W. Steed, *J. Polym. Sci., Polym Chem.* **2003**, *41*, 3798-3803.

[33] S. Csihony, T. T. Beaudette, A. C. Sentman, G. W. Nyce, R. M. Waymouth, J. L. Hedrick, *Adv. Syn. Catal.* **2004**, *346*, 1081-1086.

[34] W. Dittrich, R. C. Schulz, *Angew. Makromol. Chem.* **1971**, *15*, 109.

[35] P. Dubois, C. Jacobs, R. Jérôme, P. Teyssié, *Macromolecules* **1991**, *24*, 2266-2270.

[36] H. R. Kricheldorf, M. Berl, N. Scharnagl, *Macromolecules* **1988**, *21*, 286-293.

[37] J. L. Eguiburu, M. J. Fernandez-Berridi, F. P. Cossío, J. San Román, *Macromolecules* **1999**, *32*, 8252-8258.

[38] A. Kowalski, A. Duda, S. Penczek, *Macromolecules* **2000**, *33*, 7359-7370.

[39] E. L. Marshall, V. C. Gibson, H. S. Rzepa, *J. Am. Chem. Soc.* **2005**, *127*, 6048-6051.

[40] M. Ryner, K. Stridsberg, A.-C. Albertsson, H. von Schenck, M. Svensson, *Macromolecules* **2001**, *34*, 3877-3881.

[41] R. Stephen, R. B. Sunoj, P. Ghosh, *Dalton Trans.* **2011**, *40*, 10156-10161.

[42] E. F. Connor, G. W. Nyce, M. Myers, A. Möck, J. L. Hedrick, *J. Am. Chem. Soc.* **2002**, *124*, 914-915.

[43] A. Duda, S. Penczek, *Macromolecules* **1990**, *23*, 1636-1639.

[44] H. R. Kricheldorf, I. Kreiser-Saunders, *Makromol. Chem.* **1990**, *191*, 1057-1066.

[45] S. Penczek, A. Duda, R. Szymanski, *Macromol. Symp.* **1998**, *132*, 441-449.

[46] K. A. M. Thakur, R. T. Kean, E. S. Hall, J. J. Kolstad T. A. Lindgren, M. A. Doscotch, J. I. Siepmann, E. J. Munson, *Macromolecules* **1997**, *30*, 2422-2428.

[47] M. T. Zell, B. E. Padden, A. J. Paterick, K. A. M. Thakur, R. T. Kean, M. A. Hillmyer and E. J. Munson, M*acromolecules* **2002**, *35*, 7700-7707.

[48] J. Belleney, M. Wisniewski, A. Le Borgne, *Eur. Polym. J.* **2004**, *40*, 523-530.

[49] J. Coudane, C. Ustariz-Peyret, G. Schwach, M. Vert, *J. Polym. Sci., Part A: Polym. Chem.* **1997**, *35*, 1651-1658.

[50] K. Fukushima, Y. Kimura, *Polym. Int.* **2006**, 626-642.

[51] J. Kleine, H. H. Kleine, *Makromol. Chem.* **1959**, *30*, 23-38.

[52] G. Rafler, J. Dahlmann, *Acta. Polym.* **1992**, *43*, 91-95.

[53] M. B. Bassi, A. B. Padias, H. K. Hall, *Polym. Bull.* **1990**, *24*, 227-232.

[54] A. J. Nijenhuis, D. W. Grijpma, A. J. Pennings, *Macromolecules* **1992**, *25*, 6419-6424.

[55] A. Kowalski, J. Libiszowski, T. Biela, M. Cypryk, A. Duda, S. Penczek, *Macromolecules* **2005**, *38*, 8170-8176.

[56] C. A. Wheaton, P. G. Hayes, B. J. Ireland, *Dalton Trans.* **2009**, *38*, 4832-4846.

[57] B. M. Chamberlain, M. Cheng, D. R. Moore, T. M. Ovitt, E. B. Lobkovsky, G. W. Coates, *J. Am. Chem. Soc.* **2001**, *123*, 3229-3238.

[58] M. H. Chisholm, N. W. Eilerts, J. C. Huffman, S. S. Iyer, M. Pacold, K. Phomphrai, *J. Am. Chem. Soc.* **2000**, *122*, 11845-11854.

[59] M. H. Chisholm, J. Gallucci, K. Phomphrai, *Inorg. Chem.* **2002**, *41*, 2785-2794.

[60] M. H. Chisholm, J. C. Gallucci, K. Phomphrai, *Inorg. Chem.* **2005**, *44*, 8004-8010.

[61] M. H. Chisholm, J. Gallucci, K. Phomphrai, *Chem. Commun.* **2003**, 48-49.

[62] B. Lian, C. M. Thomas, O. L. Casagrande, Jr., T. Roisnel, J.-F. Carpentier, *Polyhedron* **2007**, *26*, 3817-3824.

[63] J. Ejfler, M. Kobylka, L. B. Jerzykiewicz, P. Sobota, *Dalton Trans.* **2005**, 2047-2050.

[64] T. Chivers, C. Fedorchuk, M. Parvez, *Organometallics* **2005**, *24*, 580-586.

[65] M. H. Chisholm, J. C. Huffman, K. Phomphrai, *J. Chem. Soc., Dalton Trans.* **2001**, 222-224.

[66] I. L. Fedushkin, A. G. Morozov, V. A. Chudakova, G. K. Fukin, V. K. Cherkasov, *Eur. J. Inorg. Chem.* **2009**, *33*, 4995-5003.

[67] J.-C. Buffet, J. P. Davin, T. P. Spaniol, J. Okuda, *New. J. Chem.* **2011**, *35*, 2253-2257.

[68] L. F. Sánchez-Barba, A. Garcés, J. Fernández-Baeza, A. Otero, C. Alonso-Moreno, A. Lara-Sánchez, A. M. Rodríguez, *Organometallics* **2011**, *30*, 2775-2789.

[69] Y. Sarazin, V. Poirier, T. Roisnel, J.-F. Carpentier, *Eur. J. Inorg. Chem.* **2010**, *22*, 3423-3428.

[70] L. Wang, H. Ma, *Macromolecules* **2010**, *43*, 6535-6537.

[71] J. Ejfler, K. Krauzy-Dziedzic, S. Szafert, L. B. Jerzykiewicz, P. Sobota, *Eur. J. Inorg. Chem.* **2010**, *23*, 3602-3609.

[72] Y. Sarazin, B. Liu, T. Roisnel, L. Maron, J.-F. Carpentier, *J. Am. Chem. Soc.* **2011**, *133*, 9069-9087.

[73] Y. Wang, W. Zhao, D. Liu, S. Li, X. Liu, D. Cui, X. Chen, *Organometallics* **2012**, *31*, 4182-4190.

[74] C.-Y. Sung, C.-Y. Li, J.-K. Su, T.-Y. Chen, C.-H. Lin, B.-T. Ko, *Dalton Trans.* **2012**, *41*, 953-961.

[75] H.-J. Chuang, S.-F. Weng, C.-C. Chang, C.-C. Lin, H.-Y. Chen, *Dalton Trans.* **2011**, *40*, 9601-9607.

[76] V. Poirier, T. Roisnel, J.-F. Carpentier, Y. Sarazin, *Dalton Trans.* **2011**, *40*, 523-534.

[77] X. Xu, Y. Chen, G. Zou, Z. Ma, G. Li, *J. Organomet. Chem.* **2010**, *695*, 1155-1162.

[78] A. Garcés, L. F. Sánchez-Barba, C. Alonso-Moreno, M. Fajardo, J. Fernández-Baeza, A. Otero, A. Lara-Sánchez, I. López-Solera, A. María Rodríguez, *Inorg. Chem.* **2010**, *49*, 2859-2871.

[79] V. Poirier, T. Roisnel, J.-F. Carpentier, Y. Sarazin, *Dalton Trans.* **2009**, 9820-9827.

[80] P. L. Arnold, I. J. Casely, Z. R. Turner, R. Bellabarba, R. B. Tooze, *Dalton Trans.* **2009**, 7236-7247.

[81] Z. Zheng, G. Zhao, R. Fablet, M. Bouyahyi, C. M. Thomas, T. Roisnel, O. Casagrande Jr, J.-F. Carpentier, *New. J. Chem.* **2008**, *32*, 2279-2291.

[82] J.-C. Wu, B.-H. Huang, M.-L. Hsueh, S.-L. Lai, C.-C. Lin, *Polymer* **2005**, *46*, 9784-9792.

[83] A. P. Dove, V. C. Gibson, E. L. Marshall, A. J. P. White, D. J. Williams, *Dalton Trans.* **2004**, 570-578.

[84] M. H. Chisholm, J. C. Gallucci, K. Phomphrai, *Inorg. Chem.* **2004**, *43*, 6717-6725.

[85] H.-Y. Chen, H.-Y. Tang, C.-C. Lin, *Polymer* **2007**, *48*, 2257-2262.

[86] Z. Zhong, M. J. K. Ankoné, P. J. Dijkstra, C. Birg, M. Westerhausen, J. Feijen, *Polym. Bull.* **2001**, *46*, 51-57.

[87] H. Ma, T. P. Spaniol, J. Okuda, *Dalton Trans.* **2003**, 4770-4780.

[88] H. Ma, T. P. Spaniol, J. Okuda, *Angew. Chem.* **2006**, *118*, 7982-7985.

[89] H. Ma, T. P. Spaniol, J. Okuda, *Inorg. Chem.* **2008**, *47*, 3328-3339.

[90] J.-C. Buffet, A. Kapelski, J. Okuda, *Macromolecules* **2010**, *43*, 10201-10203.

[91] A. Kapelski, J.-C. Buffet, T. P. Spaniol, J. Okuda, *Chem. Asian. J.* **2012**, *7*, 1320-1330.

[92] J.-C- Buffet, J. Okuda, *Dalton Trans.* **2011**, *40*, 7748-7754.

[93] R. H. Platel, A. J. P. White, C. K. Williams, *Chem. Commun.* **2009**, 4115-4117.

[94] A. Amgoune, C. M. Thomas, J.-F. Carpentier, *Macromol. Rapid Commun.* **2007**, *28*, 693-697.

[95] W. Miao, S. Li, H. Zhang, D. Cui, Y. Wang, B. Huang, *J. Organomet. Chem.* **2007**, *692*, 4828-4834.

[96] X. Liu, X. Shang, T. Tang, N. Hu, F. Pei, D. Cui, X. Chen, X. Jing, *Organometallics* **2007**, *26*, 2747-2757.

[97] C.-X. Cai, A. Amgoune, C. W. Lehmann, J.-F. Carpentier, *Chem. Commun.* **2004**, 330-331.

[98] R. H. Platel, L. M. Hodgson, A. J. P. White, C. K. Williams, *Organometallics* **2007**, *26*, 4955-4963.

[99] R. H. Platel, A. J. P. White, C. K. Williams, *Inorg. Chem.* **2008**, *47*, 6840-6849.

[100] Y. Yang, S. Li, D. Cui, X. Chen, X. Jing, *Organometallics* **2007**, *26*, 671-678.

[101] L. M. Hodgson, A. J. P. White, C. K. Williams, *J. Polym. Sci., Part A: Polym. Chem.* **2006**, *44*, 6646-6651.

[102] L. M. Hodgson, R. H. Platel, A. J. P. White, C. K. Williams, *Macromolecules* **2008**, *41*, 8603-8607.

[103] A. Alaaeddine, A. Amgoune, C. M. Thomas, S. Dagorne, S. Bellemin-Laponnaz, J.-F. Carpentier, *Eur. J. Inorg. Chem.* **2006**, 3652-3658.

[104] A. Alaaeddine, C. M. Thomas, T. Roisnel, J.-F. Carpentier, *Organometallics* **2009**, *28*, 1469-1475.

[105] I. Westmoreland, J. Arnold, *Dalton Trans.* **2006**, 4155-4163.

[106] G. G. Skvortsov, M. V. Yakovenko, P. M. Castro, G. K. Fukin, A. V. Cherkasov, J.-F. Carpentier, A. A. Trifonov, *Eur. J. Inorg. Chem.* **2007**, 3260-3267.

[107] P. L. Arnold, J.-C. Buffet, R. Blaudeck, S. Sujecki, C. Wilson, *Chem. Eur. J.* **2009**, *15*, 8241-8250.

[108] P. L. Arnold, J.-C. Buffet, R. Blaudeck, S. Sujecki, A. J. Blake, C. Wilson, *Angew. Chem., Int. Ed. Engl.* **2008**, *47*, 6033-6036.

[109] H. Ma, J. Okuda, *Macromolecules* **2005**, *38*, 2665-2673.

[110] A. Amgoune, C. M. Thomas, T. Roisnel, J.-F. Carpentier, *Chem. Eur. J.* **2006**, *12*, 169-179.

[111] M. Bouyahi, N. Ajellal, E. Kirillov, C. M. Thomas, J.-F. Carpentier, *Chem. Eur. J.* **2011**, *17*, 1872-1883.

[112] D. Patel, S. T. Liddle, S. A. Mungur, M. Rodden, A. J. Blake, P. L. Arnold, *Chem. Commun.* **2006**, *3*, 1124–1126.

[113] R. H. Platel, A. J. P. White, C. K. Williams, *Inorg. Chem.* **2011**, *50*, 7718-7728.

[114] T. M. Ovitt, G. W. Coates, *J. Am. Chem. Soc.* **2002**, *124*, 1316-1326.

[115] W. M. Stevels, M. J. K. Ankoné, P. J. Dijkstra, J. Feijen, *Macromolecules*, **1996**, *29*, 6132-6138.

[116] Y. Luo, X. Wang, J. Chen, C. Luo, Y. Zhang, Y. Yao, *J. Organomet. Chem.* **2009**, *694*, 1289-1296.

[117] Y. Luo, W. Li, D. Lin, Y. Yao, Y. Zhang, Q. Shen, *Organometallics* **2010**, *29*, 3507-3517.

[118] W. Zhao, D. Cui, X. Liu, X. Chen, *Macromolecules* **2010**, *43*, 6678-6684.

[119] L. M. Broomfield, J. A. Wright, M. Bochmann, *Dalton Trans.* **2009**, 8269-8279.

[120] T.-P.-A. Cao, A. Buchard, X. Le Goff, A. Auffrant, C. K. Williams, *Inorg. Chem.* **2012**, *51*, 2157-2169.

[121] A. Dumitrescu, B. Martin-Vaca, H. Gornitzka, J.-B. Cazaux, D. Bourissou, G. Bertrand, *Eur. J. Inorg. Chem.* **2002**, 1948-1951.

[122] R. Jiao, M. Xue, X. Shen, Y. Zhang, Y. Yao, Q. Shen, *Eur. J. Inorg. Chem*. **2010**, 2523–2529.

[123] M. A. Sinenkov, G. K. Fukin, A. V. Cherkasov, N. Ajellal, T. Roisnel, F. M. Kerton, J.-F. Carpentier, A. A. Trifonov, *New. J. Chem.* **2011**, *35*, 204-212.

[124] M. Save, M. Schappacher, A. Soum, *Macromol. Chem. Phys.* **2002**, *203*, 889-899.

[125] A. Otero, A. Lara-Sánchez, J. Fernanández-Baeza, C. Alonso-Moreno, I. Márquez-Segovia, L. F. Sánchez-Barba, J. A. Castro-Osma, A. M. Rodríguez, *Dalton Trans.* **2011**, *40*, 4687-4696.

[126] A. Buchard, R. H. Platel, A. Auffrant, X. F. Le Goff, P. Le Floch, C. K. Williams, *Organometallics* **2010**, *29*, 2892-2900.

[127] H. E. Dyer, S. Huijser, N. Susperregui, F. Bonnet, A. D. Schwarz, R. Duchateau. L. Maron, P. Mountford, *Organometallics*, **2010**, *29*, 3602-3621.

[128] R. R. Gowda, D. Chakraborty, V. Ramkumar, *Inorg. Chem. Commun.* **2011**, *14*, 1777-1782.

[129] D. Deivasagayam, F. Peruch, *Polymer* **2011**, *52*, 4686-4693.

[130] S. L. Hancock, M. F. Mahon, M. D. Jones, *Dalton Trans.* **2011**, *40*, 2033-2037.

[131] A. D. Schwarz, K. R. Herbert, C. Paniagua, P. Mountford, *Organometallics* **2010**, *29*, 4171-4188.

[132] E. L. Whitelaw, M. D. Jones, M. F. Mahon, *Inorg. Chem.* **2010**, *49*, 7176-7181.

[133] E. Sergeeva, J. Kopilov, I. Goldberg, M. Kol, *Inorg. Chem.* **2010**, *49*, 3977-3979.

[134] C. Romain, L. Brelot, S. Bellemin-Laponnaz, S. Dagorne, *Organometallics* **2010**, *29*, 1191-1198.

[135] M. D. Jones, M. G. Davidson, G. Kociok-Kohn, *Polyhedron* **2010**, *29*, 697-700.

[136] A. L. Zelikoff, J. Kopilov, I. Goldberg, G. W. Coates, M. Kol, *Chem. Commun*. **2009**, 6804-6806.

[137] E. L. Whitelaw, M. D. Jones, M. F. Mahon, G. Kociok-Kohn, *Dalton Trans.* **2009**, 9020-9025.

[138] R. H. Howard, C. Alonso-Moreno, L. M. Broomfield, D. L. Hughes, J. A. Wright, M. Bochmann, *Dalton Trans.* **2009**, 8667-8682.

[139] A. D. Schwarz, A. L. Thompson, P. Mountford, *Inorg, Chem.* **2009**, *48*, 10442-10454.

[140] K. Krauzy-Dziedzic, J. Ejfler, S. Szafert, P. Sobota, *Dalton Trans*. **2008**, *19*, 2620-2626.

[141] A. J. Chmura, M. G. Davidson, C. J. Frankis, M. D. Jones, M. D. Lunn, *Chem. Commun*. **2008**, 1293-1295.

[142] A. J. Chmura, D. M. Cousins, M. G. Davidson, M. D. Jones, M. D. Lunn, M. F. Mahon, *Dalton Trans.* **2008**, 1437-1443.

[143] F. Gornshtein, M. Kapon, M. Botoshansky, M. S. Eisen, *Organometallics* **2007**, *26*, 497-507.

[144] R. C. J. Atkinson, K. Gerry, V. C. Gibson, N. J. Long, E. L. Marshall, L. J. West, *Organometallics* **2007**, *26*, 316-320.

[145] C. K. A. Gregson, I. J. Blackmore, V. C. Gibson, N. J. Long, E. L. Marshall, A. J. P. White, *Dalton Trans*. **2006**, 3134-3140.

[146] C. K. A. Gregson, V. C. Gibson, N. J. Long, E. L. Marshall, P. J. Oxford, A. J. P. White, *J. Am. Chem. Soc.* **2006**, *128*, 7410-7411.

[147] S. Gendler, S. Segal, I. Goldberg, Z. Goldschmidt, M. Kol, *Inorg. Chem.* **2006**, *45*, 4783-4790.

[148] S. K. Russel, C. L. Gamble, K. J. Gibbins, K. C. S. Juhl, W. S. Mitchell, III, A. J. Tumas, G. E. Hofmeister, *Macromolecules* **2005**, *38*, 10336-10340.

[149] Y. Kim, G. K. Jnaneshwara, J. G. Verkade, *Inorg. Chem.* **2003**, *42*, 1437-1447.

[150] Y. Takashima, Y. Nakayama, K. Watanabe, T. Itono, N. Ueyama, A. Nakamura, H. Yasude, A. Harada, *Macromolecules* **2002**, *35*, 7538-7544.

[151] Y. Kim, P. N. Kapoor, J. G. Verkade, *Inorg. Chem.* **2002**, *41*, 4834-4838.

[152] Y. Kim, J. G. Verkade, *Organometallics* **2002**, *21*, 2395-2399.

[153] J.-C. Buffet, J. Okuda, *Chem. Commun.* **2011**, *47*, 4796-4798.

[154] M. H. Chisholm, C.-C. Lin, J. C. Gallucci, B.-T. Ko, *Dalton Trans.* **2003**, 406-412.

[155] E. L. Whitelaw, M. G. Davidson, M. D. Jones, *Chem. Commun.* **2011**, *47*, 10004-10006.

[156] A. Sauer, J.-C. Buffet, T. P. Spaniol, H. Nagae, K. Mashima, J. Okuda, *Inorg. Chem.* **2012**, *51*, 5764-5770.

[157] C. Romain, B. Heinrich, S. Bellamin Laponnaz, S. Dagorne, *Chem Commun*. **2012**, *48*, 2213-2215.

[158] A. Stopper, J. Okuda, M. Kol, *Macromolecules* **2012**, 698-704.

[159] S. L. Hancock, M. F. Mahon, G. Kociok-Kohn, M. D. Jones, *Eur. J. Inorg. Chem.* **2011**, 4596-4602.

[160] A. Stopper, I. Goldberg, M. Kol, *Inorg. Chem. Commun.* **2011**, *14*, 715-718.

[161] T. K. Saha, V. Ramkumar, D. Chakraborty, *Inorg. Chem.* **2011**, *50*, 2720-2722.

[162] T. K. Saha, B. Rajashekhar, R. R. Gowda, V. Ramkumar, D. Chakraborty, *Dalton Trans.* **2010**, *39*, 5091-5093.

[163] M. Hu, M. Wang, H. Zhu, L. Zhu, H. Zhang, L. Sun, *Dalton Trans.* **2010**, *39*, 4440-4446.

[164] Y. Ning, Y. Zhang, A. Rodriguez-Delgado, E. Y.-X. Chen, *Organometallics* **2008**, *27*, 5632-5640.

[165] K.-C. Hsieh, W.-Y. Lee, L.-F. Hsueh, H. M. Lee, J.-H. Huang, *Eur. J. Inorg. Chem.* **2006**, 2306-2312.

[166] J. L. Gorczynski, J. Chen, C. L. Fraser, *J. Am. Chem. Soc.* **2005**, *127*, 14956-14957.

[167] D. S. McGuinness, E. L. Marshall, V. C. Gibson, J. W. Steed, *J. Polym. Sci., Polym. Chem.* **2003**, *41*, 3798-3803.

[168] V. C. Gibson, E. L. Marshall, D. Navarro-Llobet, A. J. P. White, D. J. Williams, *J. Chem. Soc., Dalton Trans.* **2002**, 4321-4322.

[169] B. J. O'Keefe, L. E. Breyfogle, M. A. Hillmyer, W. B. Tolman, *J. Am. Chem. Soc.* **2002**, *124*, 4384-4393.

[170] B. J. O'Keefe, S. M. Monnier, M. A. Hillmyer, W. B. Tolman, *J. Am. Chem. Soc.* **2001**, *123*, 339-340.

[171] M. Stolt, A. Södergard, *Macromolecules* **1999**, *32*, 6412-6417.

[172] A. John, V. Katiyar, K. Pang, M. M. Shaikh, H. Nanacati, G. Hemant, P. Ghosh, *Polyhedron* **2007**, *26*, 4033-4044.

[173] R. R. Gowda, D. Chakraborty, *J. Mol. Catal. A, Chem.* **2011**, *349*, 86-93.

[174] C. C. Roberts, B. R. Barnett, D. B. Green, J. M. Fritsch, *Organometallics*, **2012**, *31*, 4133-4141.

[175] H. Sun, J. S. Ritch, P. G. Hayes, *Dalton Trans.*, **2012**, *41*, 3701-3713.

[176] S. Song, X. Zhang, H. Ma, Y. Yang, *Dalton Trans.* **2012**, *41*, 3266-3277.

[177] C. A. Wheaton, P. G. Hayes, *J. Organomet. Chem.* **2012**, *704*, 65-69.

[178] S. Nayab, H. Lee, J. H. Jeong, *Polyhedron*, **2012**, *31*, 682-687.

[179] L. Yao, L. Wang, J. Zhang, N. Tang, J. Wu, *J. Molec. Catal. A., Chemical*, **2012**, *352*, 57-62.

[180] M. Pastusiak, P. Dobrzynski, B. Kaczmarczyk, J. Kasperczyk, A. Smola, *Polymer* **2011**, *52*, 5255-5261.

[181] J. Börner, I. dos Santos Vieira, M. D. Jones, A. Döring, D. Kuckling, U. Flörke, S. Herres-Pawlis, *Eur. J. Inorg. Chem.* **2011**, 4441-4456.

[182] H. Sun, J. S. Ritch, P. G. Hayes, *Inorg. Chem.* **2011**, *50*, 8063-8072.

[183] W.-A. Ma, Z.-X. Wang, *Organometallics* **2011**, *30*, 4364-4373.

[184] I. dos Santos Vieira, A. Pawlis, A. Döring, D. Kuckling, S. Herres-Pawlis, *Chem. Eur. J.* **2011**, *17*, 4507-4512.

[185] C. A. Wheaton, P. G. Hayes, *Chem. Commun.* **2010**, *46*, 8404-8406.

[186] D. J. Darensbourg, O. Karroonnirun, *Macromolecules* **2010**, *43*, 8880-8886.

[187] C. Di Iulio, M. D. Jones, M. F. Mahon, D. C. Apperley, *Inorg. Chem.* **2010**, *49*, 10232-10234.

[188] Z. Liu, W. Gao, J. Zhang, D. Cui, Q. Wu, Y. Mu, *Organometallics* **2010**, *29*, 5783-5790.

[189] L. Wang, H. Ma, *Dalton Trans.* **2010**, *39*, 7897-7910.

[190] F. Drouin, P. O. Oguadinma, T. J. J. Whitethorne, R. E. Prud'homme, F. Schaper, *Organometallics* **2010**, *29*, 2139-2147.

[191] C. A. Wheaton, P. G. Hayes, *Dalton Trans.* **2010**, *39*, 3861-3869.

[192] J. Börner, U. Flörke, A. Döring, D. Kuckling, M. D. Jones, M. Steiner, M. Breuning, S. Herres-Pawlis, *Inorg. Chem. Commun.* **2010**, *13*, 369-371.

[193] D. J. Darensbourg, O. Karroonnirun, *Inorg. Chem.* **2010**, *43*, 2360-2371.

[194] M. D. Jones, C. G. Keir, A. L. Johnson, M. F. Mahon, *Polyhedron* **2010**, *29*, 312-316.

[195] J. Börner, U. Flörke, A. Döring, D. Kuckling, M. D. Jones, S. Herres-Pawlis, *Sustainability* **2009**, *1*, 1226-1239.

[196] C. N. Ayala, M. H. Chisholm, J. C. Gallucci, C. Krempner, *Dalton Trans.* **2009**, 9237-9245.

[197] E. Grunova, T. Roisnel, J.-F. Carpentier, *Dalton Trans.* **2009**, 9010-9019.

[198] J. Börner, U. Flörke, K. Huber, A. Döring, D. Kuckling, S. Herres-Pawlis, *Chem. Eur. J.* **2009**, *15*, 2362-2376.

[199] M. D. Jones, M. G. Davidson, C. K. Keir, L. M. Hughes, M. F. Mahon, D. C. Apperley, *Eur. J. Inorg. Chem.* **2009**, 635-342.

[200] C. A. Wheaton, B. J. Ireland, P. G Hayes, *Organometallics* **2009**, *28*, 1282-1285.

[201] G. Labourdette, D. J. Lee, B. O. Patrick, M. B. Ezhova, P. Mehrkhodavandi, *Organometallics* **2009**, *28*, 1309-1319.

[202] J. Ejfler, S. Szafert, K. Mierzwicki, L. B. Jerzykiewicz, P. Sobota, *Dalton Trans.* **2008**, 6556-6562.

[203] C. Zhang, Z.-X. Wang, *J. Organomet. Chem.* **2008**, *693*, 3151-3158.

[204] J. Börner, S. Herres-Pawlis, U. Flörke, K. Huber, *Eur. J. Inorg. Chem.* **2007**, *36*, 5645-5651

[205] S. D. Bunge, J. M. Lance, J. A. Bertke, *Organometallics* **2007**, *26*, 6320-6328.

[206] B. Lian, C. M. Thomas, O. L. Casagrande Jr, C. W. Lehmann, T. Roisnel, J.-F. Carpentier, *Inorg. Chem.* **2007**, *46*, 328-340.

[207] T. R. Jensen, C. P. Schaller, M. A. Hillmyer, W. B. Tolman, *J. Organomet. Chem.* **2005**, 5881-5891.

[208] T. R. Jensen, L. E. Breyfogle, M. A. Hillmyer, W. B. Tolman, *Chem. Commun.* **2004**, 2504-2505.

[209] M. P. Coles, P. B. Hitchcock, *Eur. J. Inorg. Chem.* **2004**, 2662-2672.

[210] C. K. Williams, L. E. Breyfogle, S. K. Choi, W. Nam, V. G. Young Jr., M. A. Hillmyer, W. B. Tolman, *J. Am. Chem. Soc.* **2003**, *125*, 11350-11359.

[211] D. Chakraborty, E. Y.-X. Chen, *Organometallics* **2003**, *22*, 769-774.

[212] M. S. Hill, P. B. Hitchcock, *J. Chem. Soc., Dalton Trans.* **2002**, 4694-4702.

[213] C. K. Williams, N. R. Brooks, M. A. Hillmyer, W. B. Tolman, *Chem. Commun.* **2002**, 2132-2133.

[214] M. H. Chisholm, J. C. Gallucci, H. Zhen, *Inorg. Chem.* **2001**, *40*, 5051-5054.

[215] M. Cheng, A. B. Attygalle, E. B. Lobkovsky, G. W. Coates, *J. Am. Chem. Soc.* **1999**, *121*, 11583-11584.

[216] G. Schwach, J. Coudane, R. Engel, M. Vert, *Polymer International* **1998**, *46*, 177-182.

[217] N. Ikpo, L. N. Saunders, J. L. Walsh, J. M. B. Smith, L. N. Dawe, F. M. Kerton, *Eur. J. Inorg. Chem.* **2011**, *35*, 5347-5359.

[218] L. E. N. Allan, J. A. Bélanger, L. M. Callaghan, D. J. A. Cameron, A. Decken, M. P. Shaver, *J. Organomet. Chem.* **2012**, 106-112.

[219] H.-J. Chuang, Y.-C. Su, B.-T. Ko, C.-C. Lin, *Inorg. Chem. Commun.* **2012**, *18*, 38-42.

[220] H.-L. Chen, S. Dutta, P.-Y. Huang, C.-C. Lin, *Organometallics* **2012**, *31*, 2016-2025.

[221] M. Bouyahyi, T. Roisnel, J.-F. Carpentier, *Organometallics* **2012**, *31*, 1458-1466.

[222] E. L. Whitelaw, G. Loraine, M. F. Mahon, M. D. Jones, *Dalton Trans.* **2011**, *40*, 11469-11473.

[223] D. J. Darensbourg, O. Karroonnirun, S. J. Wilson, *Inorg. Chem.* **2011**, *50*, 6775-6787.

[224] J. Koller, R. G. Bergman, *Organometallics* **2011**, *30*, 3217-3224.

[225] A. Otero, A. Lara-Sánchez, J. Fernández-Baeza, C. Alonso-Moreno, J. A. Castro-Osma, I. Márquez-Osma, I. Márquez-Segovia, L. F. Sánchez-Barba, A. M. Rodríguez, J. C. Garcia-Martinez, *Organometallics* **2011**, *30*, 1507-1522.

[226] C.-Y. Li, C.-Y Tsai, C.-H. Lin, B.-T. Ko, *Dalton Trans.* **2011**, *40*, 1880-1887.

[227] F. Qian, K. Liu, H. Ma, *Dalton Trans.* **2010**, *39*, 8071-8083.

[228] D. J. Darensbourgm O. Karroonnirun, *Organometallics* **2010**, *29*, 5627-5634.

[229] M.-H. Thibault, F.-G. Fontaine, *Dalton Trans.* **2010**, *39*, 5688-5697.

[230] A. D. Schwarz, Z. Chu, P. Mountford, *Organometallics* **2010**, *29*, 1246-1260.

[231] M. Bouyahyi, T. Roisnel, J.-F. Carpentier, *Organometallics* **2010**, *29*, 491-500.

[232] F. Hild, P. Haquette, L. Brelot, S. Dagorne, *Dalton Trans.* **2010**, *39*, 533-540.

[233] B. Lian, H. Ma, T. P. Spaniol, J. Okuda, *Dalton Trans.* **2009**, 9033-9042.

[234] H. Du, A. H. Velders, P. J. Dijkstra, J. Sun, Z. Zhong, X. Chen, J. Feijen, *Chem. Eur. J.* **2009**, *15*, 9836-9845.

[235] A. L. Johnson, M. G. Davidson, Y. Pérez, M. D. Jones, N. Merle, P. R. Raithby, S. P. Richards, *Dalton Trans.* **2009**, 5551-5558.

[236] C.-T. Chen, H.-J. Weng, M.-T. Chen, C.-A. Huang, K.-F. Peng, *Eur. J. Inorg. Chem.* **2009**, 2129-2135.

[237] H. Du, A. H. Velders, P. J. Dijkstra, Z. Zhong, X. Chen, J. Feijen, *Macromolecules* **2009**, *42*, 1058-1066.

[238] M. Bouyahyi, E. Grunova, N. Marquet, E. Kirillov, C. M. Thomas, T. Roisnel, J.-F. Carpentier, *Organometallics* **2008**, *27*, 5815-5825.

[239] S. Gong, H. Ma, *Dalton Trans.* **2008**, 3345-3357.

[240] X. Pang, H. Du, X. Chen, X. Wang, X. Jing, *Chem. Eur. J.* **2008**, *14*, 3126-3136.

[241] M. H. Chisholm, J. C. Gallucci, K. T. Queisenberry, Z. Zhou, *Inorg. Chem.* **2008**, *47*, 2613-2624.

[242] C. R. Wade, B. J. Lamprecht, V. W. Day, J. A. Belot, *Polyhedron* **2007**, *26*, 3286-3290.

[243] N. Nomura, R. Ishii, Y. Yamamoto, T. Kondo, *Chem. Eur. J.* **2007**, *13*, 4433-4451.

[244] S. Dagorne, F. Le Bideau, R. Welter, S. Bellamin-Laponnaz, A. Maisse-Francois, *Chem. Eur. J.*, **2007**, *13*, 3202-3217.

[245] J. Zhao, H. Song, C. Cui, *Organometallics* **2007**, *26*, 1947-1954.

[246] H. Du, X. Pang, H. Yu, X. Zhuang, X. Chen, D. Cui, X. Wang, X. Jing, *Macromolecules* **2007**, *40*, 1904-1913.

[247] J. Lewinski, P. Horeglad, K. Wójcik, I. Justyniak, *Organometallics* **2005**, *24*, 4588-4593.

[248] H. Ma, G. Melillo, L. Oliva, T. P. Spaniol, U. Englert, J. Okuda, *Dalton Trans.* **2005**, 721-727.

[249] M. H. Chisholm, N. J. Patmore, Z. Zhou, *Chem. Commun.* **2005**, 127-129.

[250] S. Doherty, R. J. Errington, N. Housley, W. Clegg, *Organometallics* **2004**, *23*, 2382-2388.

[251] H. Li, C. Wang, F. Bai, J. Yue, H.-G. Woo, *Organometallics* **2004**, *23*, 1411-1415.

[252] P. Hormnirun, E. L. Marshall, V. C. Gibson, A. J. P. White, D. J. Williams, *J. Am. Chem. Soc.* **2004**, *126*, 2688-2689.

[253] K. Majerska, A. Duda, *J. Am. Chem. Soc.* **2004**, *126*, 1026-1027.

[254] Z. Zhong, P. J. Dijkstra, J. Feijen, *J. Am Chem Soc.* **2003**, *125*, 11291-11298.

[255] Z. Zhong, P. J. Dijkstra, J. Feijen, *Angew. Chem. Int. Ed.* **2002**, *41*, 4510-4513.

[256] N. Nomura, R. Ishii, M. Akakura, K. Aoi, *J. Am. Chem. Soc.* **2002**, *124*, 5938-5939.

[257] T. M. Ovitt, G. W. Coates, *J. Am. Chem. Soc*. **2002**, *124*, 1316-1326.

[258] C.-H. Huang, F.-C. Wang, B.-T. Ko, T.-L. Yu, C.-C. Lin, *Macromolecules* **2001**, *34*, 356-361.

[259] T. M. Ovitt, G. W. Coates, *J. Polym. Sci., Polym. Chem.* **2000**, *38*, 4686-4692.

[260] C. P. Radano, G. L. Baker, M. R. Smith, *J. Am. Chem. Soc.* **2000**, *122*, 1552-1553.

[261] P. A. Cameron, D, Jhurry, V. C. Gibson, A. J. P. White, D. J. Williams, S. Williams, *Macromol. Rapid Commun.* **1999**, *20*, 616-618.

[262] J. L. Eguiburu, M. J. Fernandez-Berridi, F. P. Cossio, J. San Román, *Macromolecules* **1999**, *32*, 8252-8258.

[263] T. M. Ovitt, G. Coates, *J. Am. Chem. Soc.* **1999**, *121*, 4072-4073,

[264] N. Ernig, H. Nguyen, H. Krautscheid, R. Réau, J.-B. Cazaux, G. Bertrand, *Organometallics* **1998**, *17*, 3599-3608.

[265] A. Kowalski, A. Duda, S. Penczek, *Macromolecules* **1998**, *31*, 2114-2122.

[266] P. Degée, P. Dubois, R. Jérôme, *Macromol. Chem. Phys.* **1997**, *198*, 1985-1995.

[267] M. Wisniewski, A. Le Borgne, N. Spassky, *Macromol. Chem. Phys.* **1997**, *198*, 1227-1238.

[268] N. Spassky, M. Wisniewski, C. Pluta, A. Le Borgne, *Macromol. Chem. Phys.* **1996**, *197*, 2627-2637,

[269] N. Ropson, Ph. Dubois, R. Jérômw, Ph. Teyssié, *Macromolecules* **1995**, *28*, 7589-7598.

[270] P. Horeglad, P. Kruk, J. Pécaut, *Organometallics* **2010**, *29*, 3729-3734.

[271] P. Horeglad, G. Sczepaniak, M. Dranka, J. Zachara, *Chem. Commun.* **2012**, *48*, 1171-1173.

[272] M. Normand, E. Kirillov, T. Roisnel, J.-F. Carpentier, *Organometallics* **2012**, *31*, 1448-1457.

[273] M. P. Blake, A. D. Schwarz, P. Mountford, *Organometallics* **2011**, *30*, 1202-1214.

[274] A. Pietrangelo, S. C. Knight, A. K. Gupta, L. J. Yao, M. A. Hillmyer, W. B. Tolman, *J. Am. Chem. Soc.* **2010**, *132*, 11649-11657.

[275] M. Hu, M. Wang, P. Zhang, L. Wang, F. Zhu, L. Sun, *Inorg. Chem.Commun.* **2010**, *13*, 968-971.

[276] J.-C. Buffet, J. Okuda, P. L. Arnold, *Inorg. Chem.* **2010**, *49*, 419-426.

[277] I. Peckermann, A. Kapelski, T. P. Spaniol, J. Okuda, *Inorg. Chem.* **2009**, *48*, 5526-5534.

[278] A. Pietrangelo, M. A. Hillmyer, W. B. Tolman, *Chem. Commun.* **2009**, *19*, 2736-2737.

[279] A. F. Douglas, B. O. Patrick, P. Merkhodavandi, *Angew. Chem. Int. Ed.* **2008**, *47*, 2290-2293.

[280] I. Yu, A. Acosta-Ramirez, P. Mehrkhodavandi, *J. Am, Chem. Soc.* **2012**, *134*, 12758-12773.

# Chapter II

# OSSO-Type Bis(phenols): A Class of Proligands for Complexes in the Post-Metallocene Age



Parts of this chapter have already been published:

A. Kapelski, J.-C. Buffet, T. P. Spaniol, J. Okuda, *Chem. Asian J.* **2012**, *7*, 1320-1330.

# II. OSSO-Type Bis(phenols): A Class of Proligands for Complexes in the Post-Metallocene Age

## II.1. Introduction

### II.1.1. Tetradentate Bis(phenols)

The design of ligands for chiral nonmetallocene complexes is challenging.[1] Over the last two decades, post-metallocene transition metal complexes showed astounding potential in activity and selectivity in catalysis.[2-5]

Bis(phenolate) based ligands have been used as chelates for a plethora of different metals. The general structure of bis(phenols) is drawn in Scheme 2.1. Two 2,4-disubstituted phenols are connected by a bridge. This bridge can comprise heteroatoms with donor qualities (Do). Substituents in *ortho*-position ($R_1$,$R_3$) define the steric bulk around the metal centers, controlling the selectivity of the catalyzed reaction. Substituents in *para*-position ($R_2$,$R_4$) have an electronic effect on the ligand.

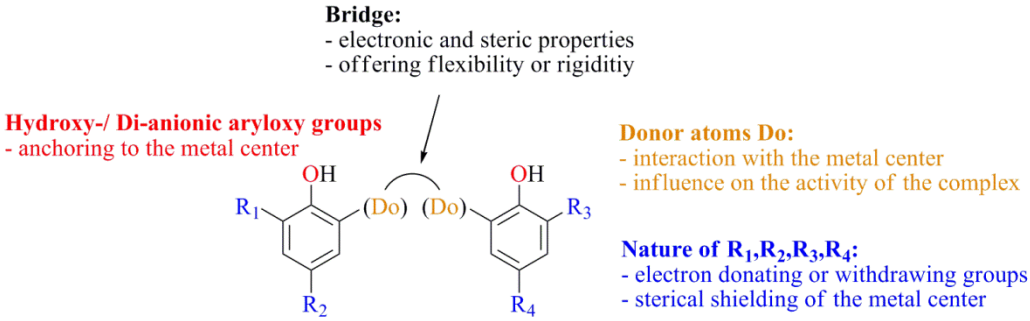


**Scheme 2.1.** General structure of a bis(phenol).

Complexes of tetradentate $C_2$ symmetric bis(phenolate) ligands of the ONNO-type with nitrogen donors are well known for their catalytic properties. Complexes of Salan ligands consisting of a diamine bis(phenolate) structure (Scheme 2.2. **A**)[6], Salen ligands with a diimine bis(phenolate) backbone (Scheme 2.2. **B**)[7] and Salalen ligands with a mixed amine-imine donating system (Scheme 2.2 **C**)[8] are known to polymerize $\alpha$-olefins and lactides.

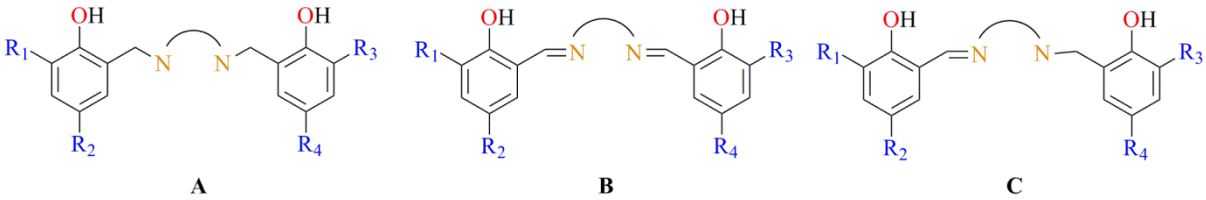


**Scheme 2.2** Salan- (**A**), Salen- (**B**) and Salalen-type (**C**) proligands.

Compared to the hard-donor nitrogen in ONNO-type ligands, sulfur is relatively soft. The weaker interaction of sulfur with a hard early transition metal cation offers increased activity in catalysis.[9-14]

## II.1.2. Syntheses of OSSO-Type Bis(phenols)

Bis(phenolate) ligands are classified concerning their chelation ring size.[9] Okuda firstly reported preparation of 5-5-5 chelating bis(phenols) $H_2\mathbf{L}^1$ - $H_2\mathbf{L}^9$ by a three step reaction in 2003 (Scheme 2.3.).[1,15]

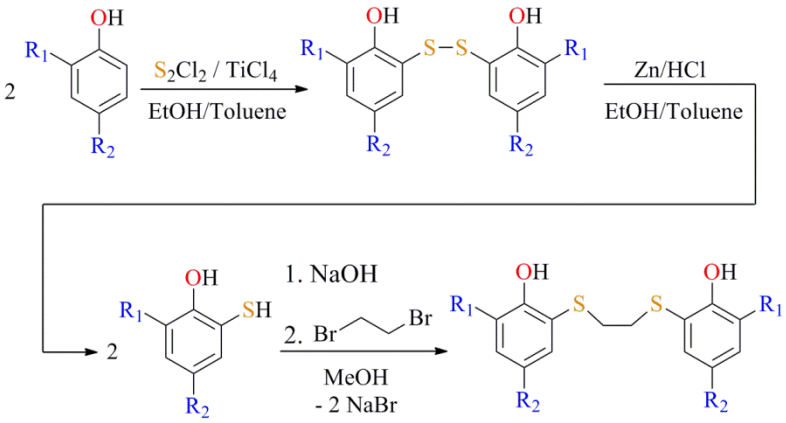


| Bis(phenol) | $R_1$ | $R_2$ | Ref |
|---|---|---|---|
| $H_2\mathbf{L}^1$ | H | H | 1 |
| $H_2\mathbf{L}^2$ | H | Me | 1 |
| $H_2\mathbf{L}^3$ | Me | Me | 1 |
| $H_2\mathbf{L}^4$ | $^i$Pr | $^t$Bu | 1 |
| $H_2\mathbf{L}^5$ | $^t$Bu | Me | 1 |
| $H_2\mathbf{L}^6$ | $^t$Bu | $^t$Bu | 15 |
| $H_2\mathbf{L}^7$ | $^t$Bu | OMe | 1 |
| $H_2\mathbf{L}^8$ | $CMe_2Ph$ | Me | 1 |
| $H_2\mathbf{L}^9$ | $CMe_2Ph$ | $CMe_2Ph$ | 1 |

**Scheme 2.3.** Syntheses of 5-5-5 chelating OSSO-type bis(phenols) $H_2\mathbf{L}^1$- $H_2\mathbf{L}^9$.

Following a procedure by Pastor and Denney,[16] reaction of 2,4-disubstituted phenols with $S_2Cl_2$ in presence of $TiCl_4$ gives analytically pure disulfides that are reduced using a mixture of Zn/HCl forming 3,5-disubstituted 2-hydroxybenzenethiols. Nucleophilic substitution at 1,2-dibromoethane leads to 1,4-dithiabutanediyl-linked OSSO-type bis(phenols).

Preparation of *trans*-1,2-dithiocyclohexanediyl-bridged bis(phenols) is possible by reaction of 3,5-disubstituted 2-hydroxybenzenethiols with cyclohexene oxide followed by subsequent chlorination with thionyl chloride. In the third reaction step, the chlorinated intermediate is treated with a second equivalent of 3,5-disubstituted 2-hydroxybenzenethiol in presence of a base, forming exlusively *trans*-configured racemic proligands (Scheme 2.4.).

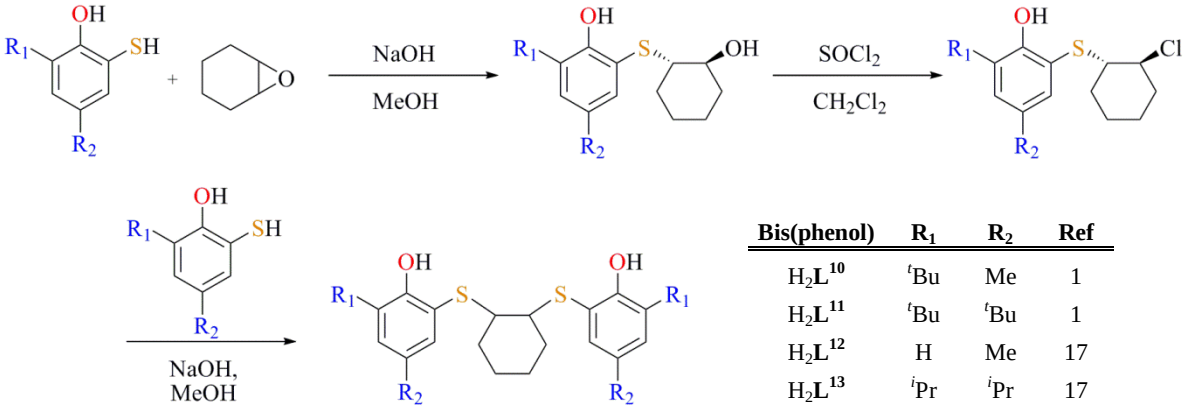


| Bis(phenol) | $R_1$ | $R_2$ | Ref |
|---|---|---|---|
| $H_2L^{10}$ | $^t$Bu | Me | 1 |
| $H_2L^{11}$ | $^t$Bu | $^t$Bu | 1 |
| $H_2L^{12}$ | H | Me | 17 |
| $H_2L^{13}$ | $^i$Pr | $^i$Pr | 17 |

**Scheme 2.4.** Syntheses of 5-5-5-chelating OSSO-type bis(phenols) *rac*-$H_2$**L**$^{10}$-*rac*-$H_2$**L**$^{13}$.[18]

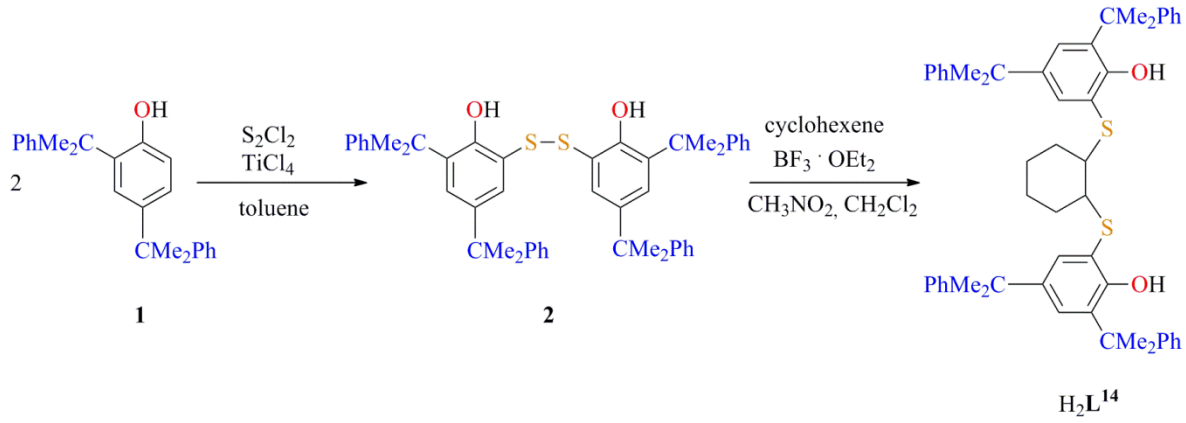


**Scheme 2.5.** Synthesis of OSSO-type racemic bis(phenol) $H_2$**L**$^{14}$.[18]

The synthesis of bulky 2,4-dicumyl substituted *trans*-1,2-dithiocyclohexanediyl-bridged 5-5-5 chelating bis(phenol) $H_2$**L**$^{14}$ using a simple two step method was reported by Doye *et al.* Reaction of 2,4-di(2-phenylpropan-2-yl)phenol **1** with $S_2Cl_2$ in presence of $TiCl_4$ formed disulfide **2**, that was further treated with cyclohexene and $BF_3{\cdot}OEt_2$ to give racemic bis(phenol) $H_2$**L**$^{14}$ after recrystallization from a mixture of acetonitrile and acetone (Scheme 2.5.).[18]

By treatment of lithiated racemic bis(phenol) $Li_2\mathbf{L}^{14}$ with (1*S*)-camphorsulfonyl chloride, diastereomers are formed. After separation by preparative HPLC and subsequent cleavage of camphorsulfonate residues from the diastereomers, enantiopure (+)-(*S*,*S*)-$H_2\mathbf{L}^{14}$ and (-)-(*R*,*R*)-$H_2\mathbf{L}^{14}$ are isolated.[19]

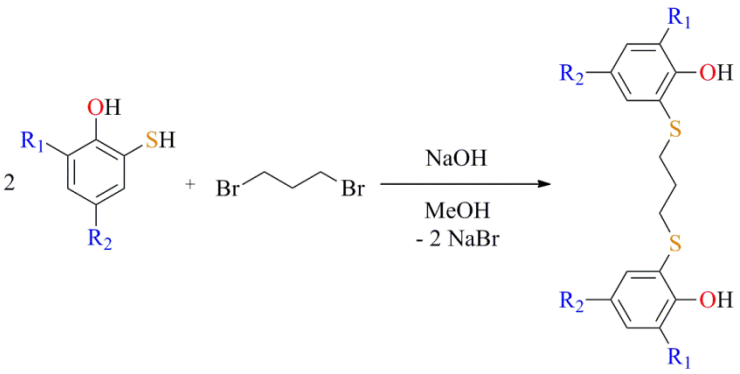


| Bis(phenol) | $R_1$ | $R_2$ | Ref |
|---|---|---|---|
| $H_2\mathbf{L}^{15}$ | $^t$Bu | Me | 1 |
| $H_2\mathbf{L}^{16}$ | $^t$Bu | $^t$Bu | 15 |
| $H_2\mathbf{L}^{17}$ | $^t$Bu | OMe | 1 |

**Scheme 2.6.** Syntheses of 5-6-5 chelating OSSO-type bis(phenols) $H_2\mathbf{L}^{15}$-$H_2\mathbf{L}^{17}$.

Preparation of 5-6-5 chelating OSSO-type bis(phenols) was reported by Okuda *et al.* using a similar method as used for the synthesis of 5-5-5-chelating bis(phenols). 1,3-Dibromopropane reacts with 3,5-disubstituted 2-hydroxybenzenethiols in presence of NaOH to form 1,5-dithiapentanediyl-linked bis(4,6-disubstituted) bis(phenols) (Scheme 2.6.).[1,15]

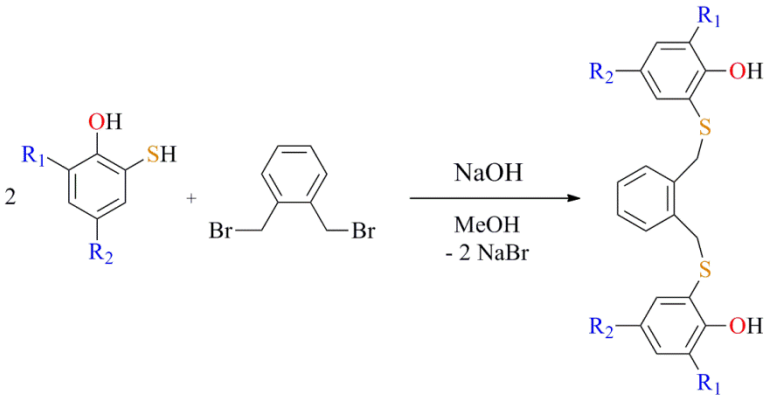


| Bis(phenol) | $R_1$ | $R_2$ | Ref |
|---|---|---|---|
| $H_2\mathbf{L}^{18}$ | $^t$Bu | Me | 20 |
| $H_2\mathbf{L}^{19}$ | $CMe_2Ph$ | $CMe_2Ph$ | 19 |
| $H_2\mathbf{L}^{20}$ | Ada | Me | 21 |

**Scheme 2.7.** Syntheses of 5-7-5 chelating OSSO-type bis(phenols) $H_2\mathbf{L}^{18}$-$H_2\mathbf{L}^{20}$.

Reaction of 3,5-disubstituted 2-hydroxybenzenethiols with 1,2-bis(dibromomethyl)benzene in presence of NaOH afforded bis(phenols) $H_2\mathbf{L}^{18}$-$H_2\mathbf{L}^{20}$ (Scheme 2.7.) that build 5-7-5 chelates around coordinated metal centers.[20-22]

Next to achiral 5-7-5 chelating OSSO-type bis(phenols), racemic 5-7-5 chelating proligand $H_2$**L**$^{21}$ was prepared by reaction of 4-methyl-6-*tert*-butyl thiophenol with *trans*-1,2-bis(hydroxymethyl)cyclohexane in presence of $K_2CO_3$ (Scheme 2.8.).[22]

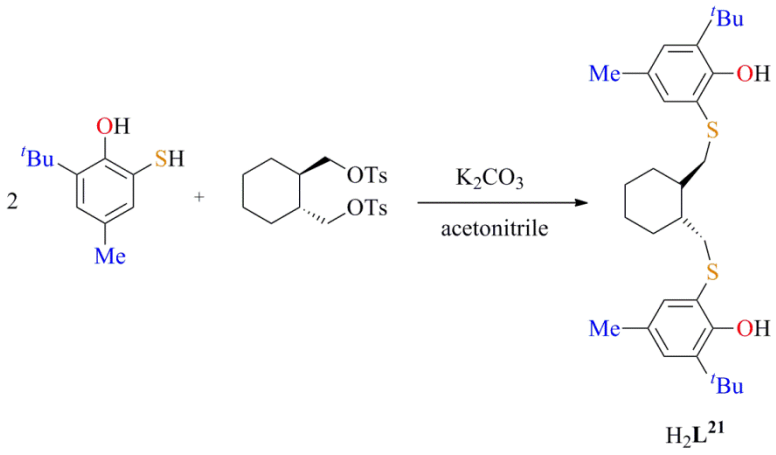


**Scheme 2.8.** Synthesis of racemic 5-7-5 chelating OSSO-type bis(phenol) $H_2$**L**$^{21}$.[22]

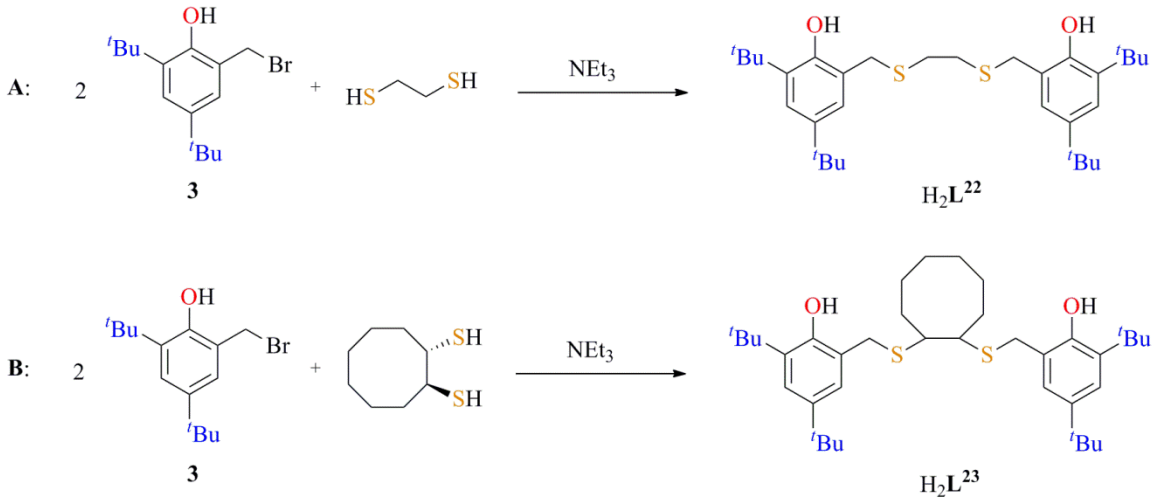


**Scheme 2.9.** Syntheses of 6-5-6 chelating OSSO-type bis(phenol) $H_2$**L**$^{22}$ and $H_2$**L**$^{23}$.[23,24]

OSSO-type bis(phenols) leading to 6-5-6-chelate arrays around metal cations have been reported by Kol *et al.* and Ishii *et al.* These ligands are sulfur analogues to Salen ligands **A** (Scheme 2.2.) and were prepared by reacting 2-(bromomethyl)-4,6-di-*tert*-butylphenol **3** with either ethanedithiol in presence of $NEt_3$ to yield bis(phenol) $H_2$**L**$^{22}$ (Scheme 2.9. **A**) or with *trans*-cyclooctane-1,2-diyl in presence of $NEt_3$ to give racemic bis(phenol) $H_2$**L**$^{23}$ (Scheme 2.9. **B**).[23-24]

# II.2. Results and Discussion

The first part of this chapter describes the preparation of 5-4-5 and 5-5-5 chelating bis(phenols) of the OSSO-type. Next to well known *tert*-butyl and cumyl functionalized bis(phenols), the first bis(phenols) with a 1-methylcyclohexyl group in *ortho*-position of the phenolate moiety are reported. Furthermore, syntheses of 2,4-disubstituted phenols that can potentially be used as starting materials for the snthesis of new bis(phenols) will be discussed

## II.2.1. Syntheses of New 5-4-5 Chelating OSSO-Type Bis(phenols)

For metal cations with small atomic radii, ligands with a short backbone promise to form stable organometallic complexes. 5-4-5 chelating OSSO-type bis(phenol) $H_2\mathbf{L}^{24}$ with *tert*-butyl groups in *ortho* and *para* positions was prepared by adapting the typical literature procedure for syntheses of 5-5-5 chelating OSSO-type bis(phenols).[1,15]

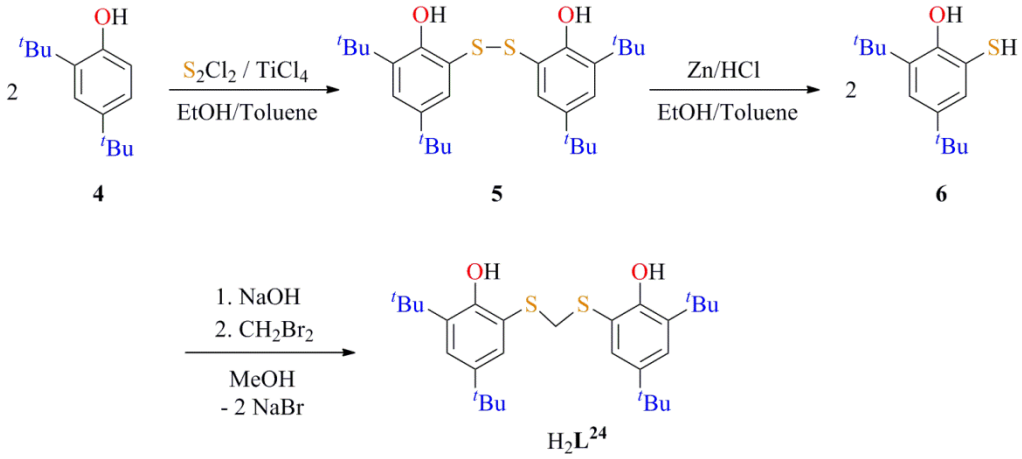


**Scheme 2.10.** Synthesis of bis(phenol) $H_2\mathbf{L}^{24}$.

Increasing the steric demand of OSSO-type bis(phenols) is accomplished by starting from disulfide **2**. Reduction of disulfide **2** using Zn/HCl in adaption of a literature procedure gave analytically pure 2-mercapto-4,6-bis(2-phenylpropan-2-yl)phenol **7**.[16] However, the standard protocol for the synthesis of OSSO-type bis(phenols)[1,15] with NaOH and $CH_2Br_2$ as methylene precursor did not result in formation of the desired product. Although the precipitate formed during the reaction was identified as NaBr,[25] $^1$H NMR spectroscopic

analyses did not show characteristic signals for the 1,3-dithiapropanediyl-bridge.[24] Instead, use of NaOMe as a base in an ethanol/methanol mixture and refluxing for 16 h successfully yielded bis(phenol) $H_2$**L**[25] (Scheme 2.11.).

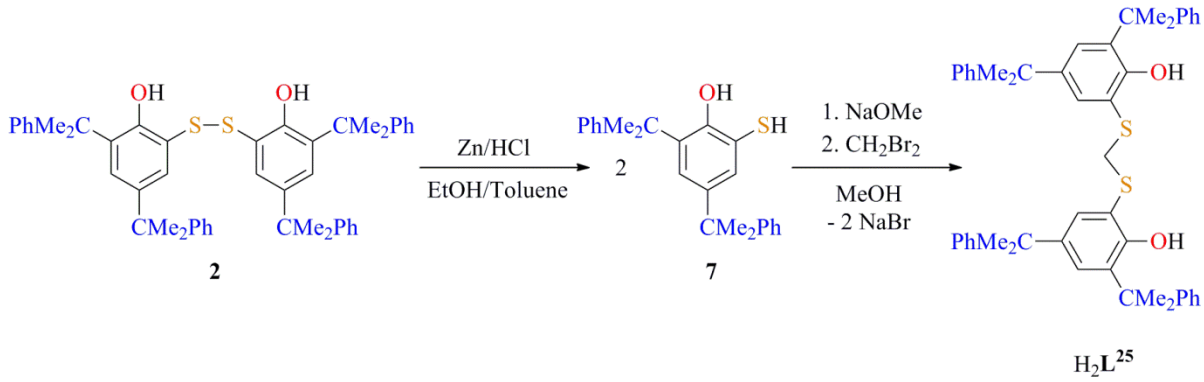


**Scheme 2.11.** Synthesis of bis(phenol) $H_2$**L**[25].

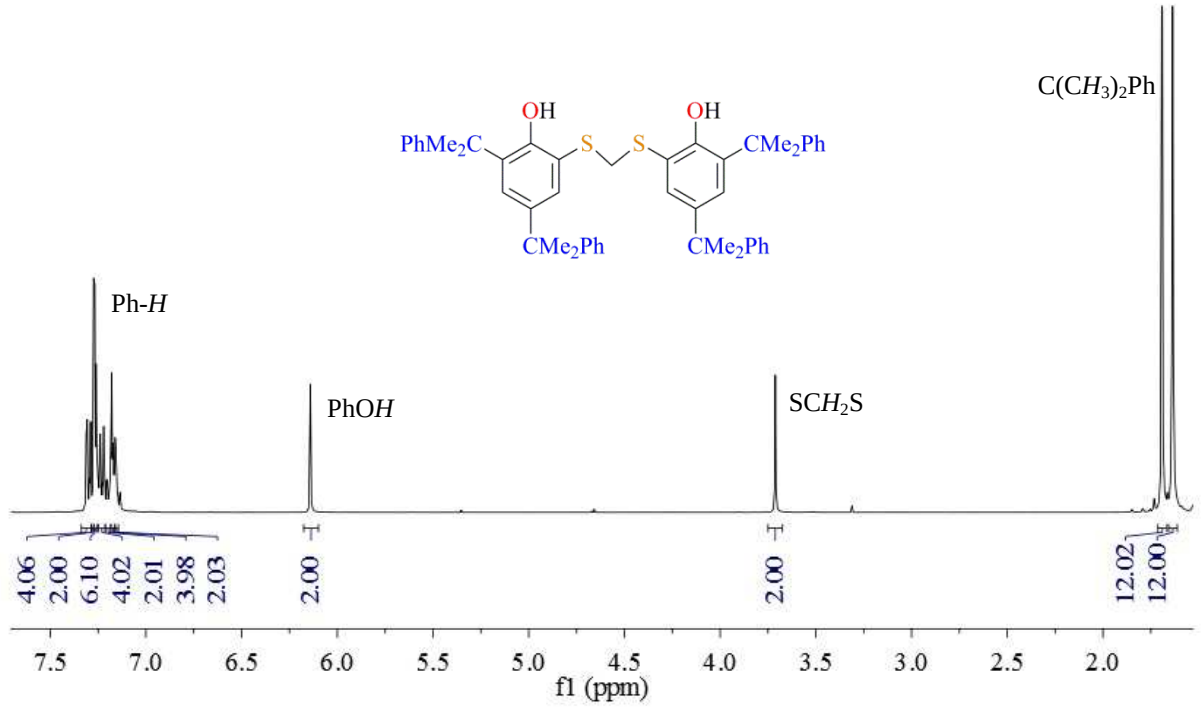


**Figure 2.1.** $^1$H NMR spectrum of $H_2$**L**[25] in $CDCl_3$ at 25 °C.

The $^1$H NMR spectrum of $H_2$**L**[25] (Figure 2.1.) shows the methyl groups of the cumyl substituents as two doublets at 1.65 and 1.70 ppm. A signal at 3.72 appm arises for the methylene protons. The OH groups are identified as two singlets at 6.15 ppm. All aromatic

protons can be found in the expected region between 7.14 and 7.32 ppm. Elemental analysis is consistent with theoretical values.

To explore the steric effects of different *ortho*-substituents on activity and selectivity in the ROP of lactide, the *ortho*-substituent was varied. 4-Methyl-2-(1-methylcyclohexyl)phenol **8** was prepared following a literature procedure for the synthesis of 4-methyl-2-adamantyl-phenol[26] starting from *p*-cresol and 1-methylcyclohexanol under acidic conditions to give **8** as a dark solid. Using **8** as starting material for the preparation of new bis(phenols) affords proligands with a 1-methylcyclohexyl group in *ortho* and a methyl group in *para* position.

Reaction of **8** with $S_2Cl_2$ catalyzed by $TiCl_4$ yielded disulfide **9**. Treatment of **9** with Zn/ HCl gave 2-mercapto-4-methyl-6-(1-methylcyclohexyl)phenol **10**. Finally, reaction of **10** with $CH_2Br_2$ in presence of NaOMe successfully formed $H_2\mathbf{L}^{26}$ in an isolated yield of 57% (Scheme 2.12.).

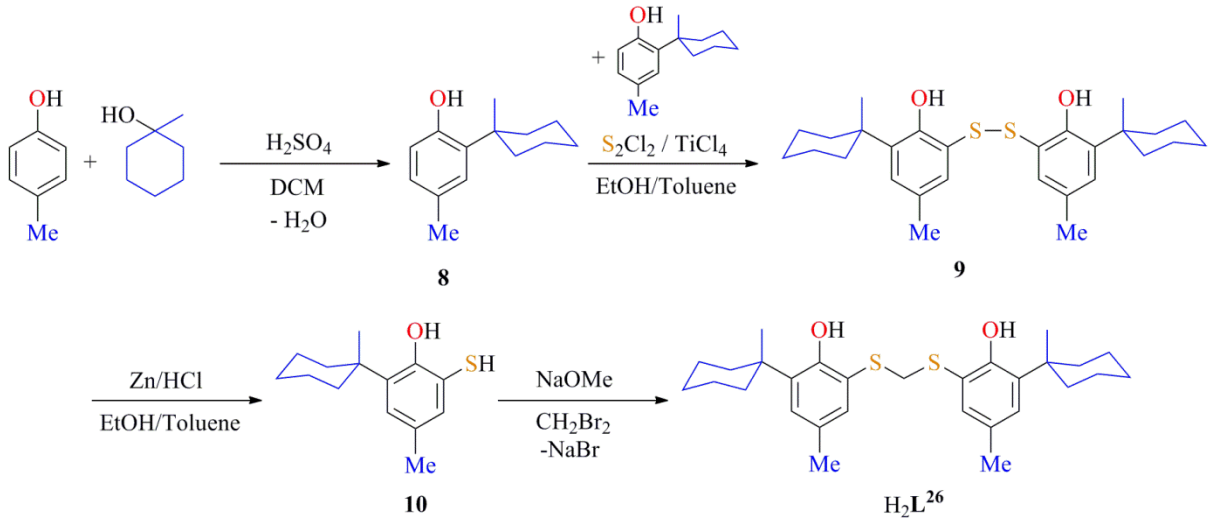


**Scheme 2.12.** Synthesis of bis(phenol) $H_2\mathbf{L}^{26}$.

NMR spectroscopic measurements and elemental analyses verified formation of $H_2\mathbf{L}^{26}$. The methylene protons form a broad signal at 3.90 ppm. The 1-methylcyclohexyl group gives several broad and overlapping signals between 1.41 and 2.15 ppm for the protons on the cyclohexyl ring and one sharp singulet at 1.30 for the methyl group. Signals for the Ph$CH_3$ protons (2.25 ppm), the OH-groups (6.76 ppm) and the aromatic protons (7.09 and 7.12 ppm) are found in expexted regions.

## II.2.2. Syntheses of New 5-5-5 Chelating OSSO-Type Bis(phenols)

Following the literature route for the synthesis of 5-5-5 chelating OSSO-type bis(phenols),[1,15] reaction of **10** with 1,2-dibromoethane in presence of NaOH afforded bis(phenol) $H_2$**L**$^{27}$ in 15% yield (Scheme 2.13.).

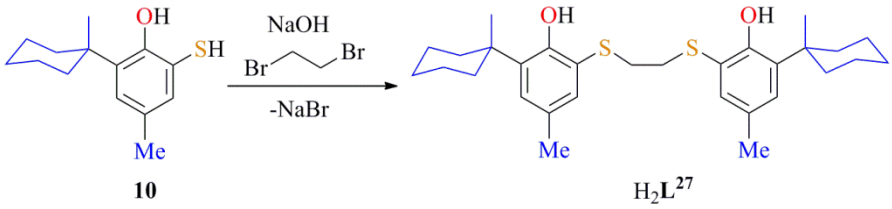


**10** $H_2$**L**$^{27}$

**Scheme 2.13.** Synthesis of bis(phenol) $H_2$**L**$^{27}$.

The $^1$H NMR spectrum of $H_2$**L**$^{27}$ looks similar to that measured for $H_2$**L**$^{26}$. A different chemical shift appears for the resonance of the 1,4-dithiabutanediyl-bridge (2.77 ppm). In this region, the resonances of the bridge commonly appear as for $H_2$**L**$^{1}$ and $H_2$**L**$^{2}$ (2.80 ppm), $H_2$**L**$^{3}$ (2.79 ppm)[1] or $H_2$**L**$^{8}$ (2.78 ppm).[15] Additionally, elemental analysis of $H_2$**L**$^{26}$ (C: 71.43, H: 8.84) is consistent with theoretical values (C: 71.85, H: 8.32).

As introduced by Doye *et al.*, synthesis of racemic 5-5-5-chelating OSSO-type bis(phenol) $H_2$**L**$^{14}$ is accomplished by treating disulfide **2** with cyclohexene in presence of $BF_3 \cdot OEt_2$.[18] Replacing cyclohexene with cyclopentene or cyclooctene allows extension of the series of chiral racemic bis(phenols) by $H_2$**L**$^{28}$ and $H_2$**L**$^{29}$ (Scheme 2.14.).

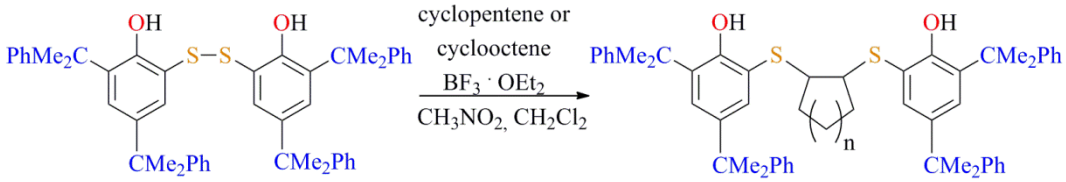


**2**

$H_2$**L**$^{28}$ ; n = 1
$H_2$**L**$^{29}$ ; n = 3

**Scheme 2.14.** Syntheses of bis(phenols) $H_2$**L**$^{28}$ and $H_2$**L**$^{29}$.

The $^1$H NMR spectrum of $H_2$**L**$^{29}$ is depicted in Figure 2.2. As a result of the nearly identical structure of $H_2$**L**$^{29}$, $H_2$**L**$^{28}$ and $H_2$**L**$^{14}$, the NMR-spectra of the bis(phenols) look quite similar.

The resonances for the cycloalkyl backbone are found between 1.08 and 1.74 ppm as several broad signals, indicating flexibility of the backbone. The C*Me*$_2$Ph protons form three signals at 1.73, 1.83 and 1.84 ppm representing 12 and 2 x 6 protons for $H_2$**L**$^{29}$. Similar patterns are observed for $H_2$**L**$^{28}$. The S(C*H*)$_2$S protons form one signal at 2.90 ppm for $H_2$**L**$^{29}$ and 2.79 ppm for $H_2$**L**$^{28}$. The aromatic protons appear at their expected chemical shifts.

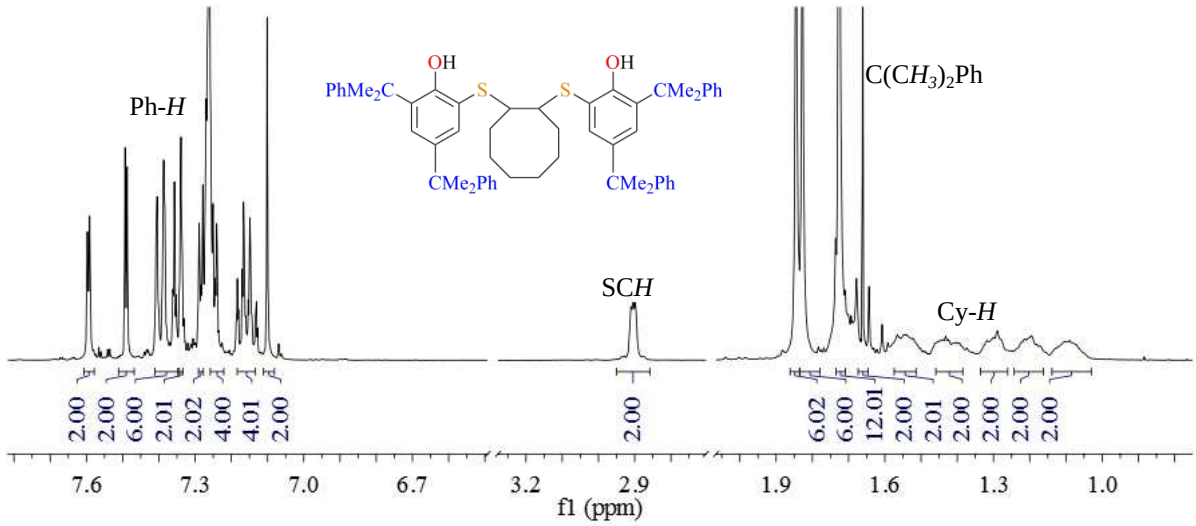


**Figure 2.2.** $^1$H NMR spectrum of $H_2$**L**$^{28}$ in $C_6D_6$ at 25 °C.

Similar to bis(phenols) $H_2$**L**$^{14}$, $H_2$**L**$^{24}$, $H_2$**L**$^{25}$ and $H_2$**L**$^{26}$, elemental analyses for $H_2$**L**$^{28}$ and $H_2$**L**$^{29}$ are in good agreement with theoretical values.

## II.2.3. Syntheses of 2,4-Disubstituted Phenols as Starting Materials for New Bis(phenols).

The syntheses of bulky cumyl containing bis(phenols) require use of commercially available phenol **1**, bearing cumyl groups in *ortho* and *para* position. 4-methyl-2-(2-phenylpropan-2-yl)phenol **11** was targeted as a possible starting molecule for the synthesis of bis(phenols) by reaction of *p*-cresol and *α*-methylstyrene catalyzed by *p*-toluenesulfonic acid monohydrate (Scheme 2.15.).[27] **11** only bears large cumyl groups in *ortho* position and was isolated as a colorless viscous oil in 49% yield.

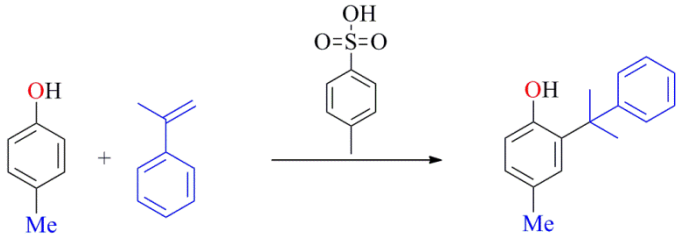


**11**

**Scheme 2.15.** Synthesis of 4-methyl-2-(2-phenylpropan-2-yl)phenol **11**.

Following the literature protocol for preparation of OSSO-type bis(phenols), reaction of **11** with $S_2Cl_2$ catalyzed by $TiCl_4$ formed disulfide **12** (Scheme 2.16.).

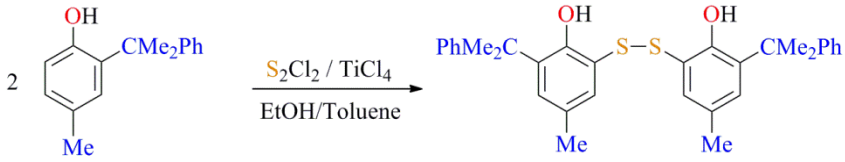


**11** **12**

**Scheme 2.16.** Synthesis of disulfide **12**.

Formation of **12** was confirmed by $^1$H NMR spectroscopic analysis of the crude product. However, recrystallization of **12** did not yield a clean product. Next to disulfide **12**, phenol **11** was still present and signals of several other unidentified aromatic products were observed. Selective distillation of **11** from the mixture lead to partial decomposition of **12** due to harsh distillation conditions.[27] Extended reaction times and variation of the solvent used for crystallization (acetonitrile to acetone, *n*-pentane, diethylether, toluene and several mixtures of these solvents) did also not give analytically pure **12**.

Reduction of crude **12** with Zn/HCl in an ethanol/methanol mixture gave the crude thiophenol, but purification by crystallization was not possible because of multiple impurities that could not be separated by crystallization or extraction.

To explore the possibility of introducing aromatic groups in *ortho*-position of the phenol, 5-methyl-(1,1'-biphenyl)-2-ol **16** was targeted. These class of substituted phenols offer the chance to synthesize bis(phenols) with rigid aromatic groups. Synthesis of **16** is possible by using a multi step reaction including Suzuki coupling as essential step (Scheme 2.17.)

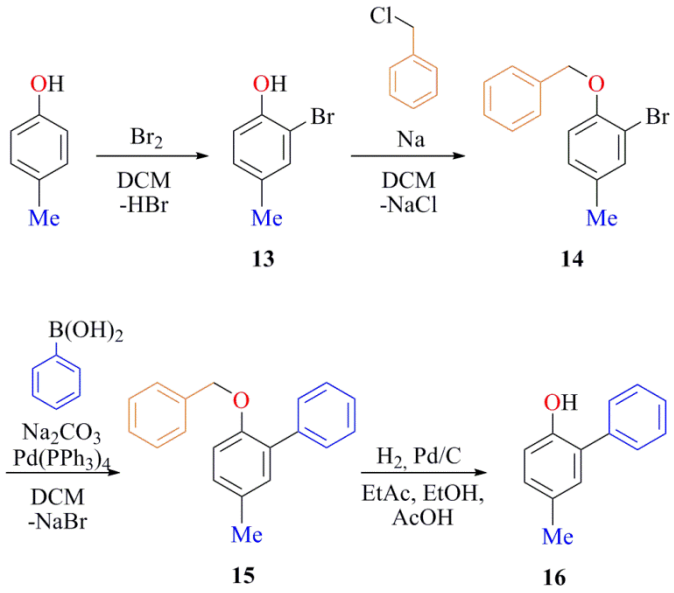


**Scheme 2.17.** Synthesis of **16** via benzyl protection of the phenol.

*p*-Cresol was treated with bromine to give 2-bromo-4-methylphenol **13**.[28] Protection of the hydroxy group with benzylchloride in presence of sodium formed 1-(benzyloxy)-2-bromo-4-methylbenzene **14**.[29] Suzuki coupling with phenylboronic acid catalyzed by [$Pd(PPh_3)_4$] followed by deprotection with $H_2$ over Pd/C and purification via column chromatography gave **16** in an overall yield of 13%.[28]

For preparation of bis(phenols) of the OSSO-type, a relatively large amount of 2,4-disubstituted phenol is needed to generate corresponding disulfides. Through this reaction and the following reduction with Zn/HCl, up to 75% of the deployed starting compound is lost.[16] Consequently, a large amount of **16** is needed to isolate a useful amount of the corresponding thiophenol. The scale of the coupling reaction from **14** to **15** is a limiting step.

To avoid deprotection *via* hydrogenation, THP-protected phenol **17** was synthesized from **13** and 3,4-dihydro-2*H*-pyran catalyzed by PPTS. Suzuki coupling with phenylboronic acid formed phenol **18** that was directly deprotected by heating in a mixture of MeOH and $HCl_{(aq.)}$ to give **16** in an overall yield of 18% (Scheme 2.18.).[30]

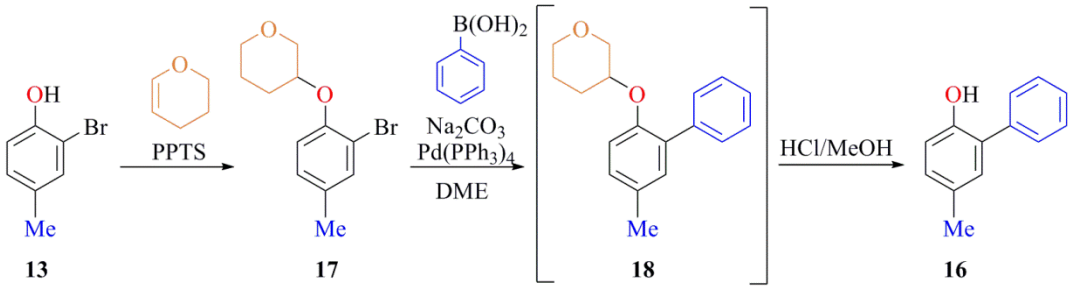


**Scheme 2.18.** Synthesis of **16** via THP protected intermediate **17**.

Higher activity than [$Pd(PPh_3)_4$] in coupling reaction catalysis show Pd-NHC based complexes. In this thesis, (1,3-bis{2,6-diisopropylphenyl}imidazolidene)(3-chloropyridyl)palladium(II)dichloride (Pd-PEPPSI**)** (Scheme 2.19.) was used as catalyst for coupling of **13** and **17** with phenylboronic acid.

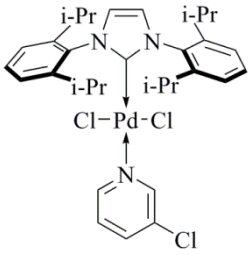


**Scheme 2.19.** Pd-PEPPSI

While coupling with [$Pd(PPh_3)_4$] was performed over several days, coupling mediated by 5 mol % Pd-PEPPSI gave high conversions within less than 5 h. Unfortunately, after 2.5 h the reaction mixture turns slowly dark-brown indicating decomposition of the declaredly highly moisture and air sensitive Pd-catalyst.[31] However, isolated yields of **15** and **18** were strongly dependent on the reaction scale. With increasing amount of starting material, yield dropped from 50% to 25%.

## II.3. Summary

A series of new 5-4-5 ($H_2$**L**$^{24}$, $H_2$**L**$^{25}$ and $H_2$**L**$^{26}$) and 5-5-5 ($H_2$**L**$^{27}$, $H_2$**L**$^{28}$ and $H_2$**L**$^{29}$) chelating OSSO-type bis(phenols) were prepared by adapting standard literature procedures. $H_2$**L**$^{26}$ and $H_2$**L**$^{27}$ are the first bis(phenols) bearing a 1-methylcyclohexyl group in the *ortho* position. All bis(phenols) are air and moisture stable powders that were isolated in moderate to good yields. 4-Methyl-2-(2-phenylpropan-2-yl)phenol (**11**) and 5-methyl-(1,1'-biphenyl)-2-ol (**16**) were synthesized and tested as starting compounds for the synthesis of OSSO-type bis(phenols). **11** reacted with $S_2Cl_2$ and $TiCl_4$ to give disulfide **12** that could not be isolated analytically pure. **16** was prepared by Suzuki-coupling using different Pd complexes and can be used as precursor for the synthesis of new bis(phenols) of the OSSO-type.

## II.4. Experimental Section

**6,6'-Disulfanediylbis(2,4-bis(2-phenylpropan-2-yl)phenol) (2)**

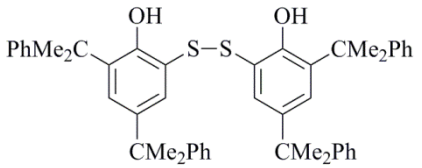


**2**
$C_{48}H_{50}O_2S_2$
723.04

Disulfide **2** was prepared adapting a literature procedure for the synthesis of 2,2'-dithiobis(4,6-di-*tert*-butylphenol) (**5**).[16] 82.62 g of **1** (250 mmol, 1 equiv.) were dissolved in 180 mL of toluene. After addition of 0.3 mL $TiCl_4$ the solution was cooled to 0 °C. 10 mL of $S_2Cl_2$ were introduced and the solution was stirred at 0 °C for 3 h and for additional 3 d at 25 °C. The solution was washed two times with 200 mL of a 19% HCl solution, saturated aqueous $Na_2CO_3$ solution (3 x 150 mL) and $H_2O$ (3 x 100 mL). After removal of toluene under vacuum and recrystallization of the orange residue in 1 L acetonitrile, **2** was isolated in a yield of 57% as an orange powder (51.5 g, 71 mmol). **$^1$H NMR** ($CDCl_3$, 25 °C, 400 MHz), δ (ppm): 1.57 (s, 12 H, C(C*H*$_3$)$_2$Ph), 1.63 (s, 12 H, C(C*H*$_3$)$_2$Ph), 5.91 (br, 2 H, PhO*H*), 7.07-7.29 (m, 24 H, Ph-*H*), **$^{13}$C{$^1$H} NMR** ($CDCl_3$, 25 °C, 100.1 MHz), δ (ppm): 29.5 (C(*C*H$_3$)$_2$Ph), 31.0 (C(*C*H$_3$)$_2$Ph), 42.6 (*C*(CH$_3$)$_2$Ph), 42.8 (*C*(CH$_3$)$_2$Ph), 120.6 (Ph-*C*2), 125.7 (Ph-*C*), 125.8 (Ph-*C*3), 126.8 (Ph-C*5*), 128.2 (Ph-*C*), 129.4 (Ph-*C*), 131.0 (Ph-C*6*), 135.5 (Ph-

*C*), 142.3 (Ph-C*4*), 150.0 (Ph-*C*), 152.7 (Ph-*C*1). **Elemental analysis**, calculated for $C_{48}H_{50}O_2S_2$ (723.04 g/mol) (%): C 79.73, H 6.97; found: C 79.61, H 6.85.

---

**6,6'-Disulfanediylbis(2,4-di-tert-butylphenol)**[16] **(5)**

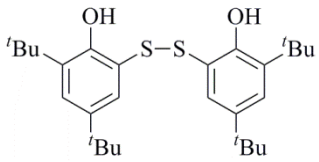


**5**
$C_{28}H_{42}O_2S_2$
474.76

Disulfide **5** was prepared following a literature procedure starting from 206.33 g of **4** (1.0 mol) in a yield of 43% (109.7 g, 0.216 mol). **$^1$H NMR** ($CDCl_3$, 25 °C, 400 MHz), δ (ppm): 1.22 (s, 18 H, C(C*H*$_3$)$_3$), 1.38 (s, 18 H, C(C*H*$_3$)$_3$), 6.58 (br, 2 H, PhO*H*), 7.17 (d, $^4J_{HH}$ = 2.5 Hz, 2 H, Ph-*H*5), 7.34 (d, $^4J_{HH}$ = 2.5 Hz, 2 H, Ph-*H*3).

---

**2,4-Di-tert-butyl-6-mercaptophenol**[16] **(6)**

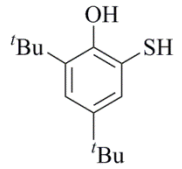


**6**
$C_{14}H_{22}OS$
238.39

**6** was prepared following a literature procedure starting from 109.5 g of **5** (216.4 mmol) in a yield of 58% (128.0 mmol, 45.9 g). **$^1$H NMR** ($CDCl_3$, 25 °C, 400 MHz), δ (ppm): 1.33 (s, 9 H, C(C*H*$_3$)$_3$), 1.45 (s, 9 H, C(C*H*$_3$)$_3$), 2.87 (t, 1 H, $^4J_{HH}$ = 1.1 Hz, PhS*H*), 6.68 (br, 1 H, PhO*H*), 7.35 (dd, 1 H, $^4J_{HH}$ = 2.5 Hz, Ph-*H*5), 7.43 (dd, 1 H, $^4J_{HH}$ = 2.5 Hz, Ph-*H*3), **$^{13}$C{$^1$H} NMR** ($CDCl_3$, 25 °C, 100.1 MHz), δ (ppm): 29.7 (C(*C*H$_3$)$_3$), 31.6 (C(*C*H$_3$)$_3$), 34.4 (*C*(CH$_3$)$_3$), 35.4 (*C*(CH$_3$)$_2$), 110.9 (Ph-*C*-SH), 125.5 (Ph-*C3*), 130.8 (Ph-*C*5), 135.6 (Ph-*C*6), 142.5 (Ph-*C*3), 153.2 (Ph-*C*1).

**1,3-Dithiapropanediyl-2,2´-bis(4,6-di-*tert*-butylphenol)**[32] ($H_2$**L**$^{24}$)

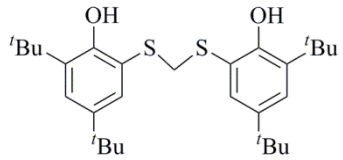


$H_2$**L**$^{24}$
$C_{29}H_{44}O_2S_2$
488.79

10.0 g of **6** (41.9 mmol, 2 equiv.), 1.68 g of NaOH (41.9 mmol, 2 equiv.) and 1.47 mL of $CH_2Br_2$ (3.65 g, 21.0 mmol) were refluxed in methanol for 4 h. Water (200 mL) was added and the mixture was extracted three times with 100 mL of $Et_2O$. The organic phase was separated, dried over anhydrous $MgSO_4$, filtered and evaporated to give a colorless powder. Recrystallization from *n*-pentane afforded colorless crystals of $H_2$**L**$^{24}$ in 90% yield (9.20 g, 18.8 mmol). **$^1$H NMR** ($CDCl_3$, 25 °C, 400 MHz), δ (ppm): 1.33 (s, 18 H, C(C*H*$_3$)$_3$), 1.42 (s, 18 H, C(C*H*$_3$)$_3$), 3.93 (s, 2 H, SC*H*$_2$S), 6.79 (s, 2 H, PhO*H*), 7.38 (d, $^4J_{HH}$ = 3.8 Hz, 2 H, Ph-*H*3), 7.42 (d, $^4J_{HH}$ = 3.8 Hz, 2 H, Ph-*H*5); **$^{13}$C{$^1$H} NMR** ($CDCl_3$, 25 °C, 100.1 MHz), δ (ppm): 29.5 (*p*-C(*C*H$_3$)$_3$), 31.5 (*o*-C(*C*H$_3$)$_3$), 34.3 (*o*-*C*(CH$_3$)$_3$), 35.3 (*p*-*C*(CH$_3$)$_3$), 44.5 (S*C*H$_2$S), 117.8 (Ph-*C*2), 126.6 (Ph-*C*3), 130.3 (Ph-*C*5), 135.7 (Ph-*C*4), 142.4 (Ph-*C*6), 153.0 (Ph-*C*1).

---

**2-Mercapto-4,6-bis(2-phenylpropan-2-yl)phenol**[16] **(7)**

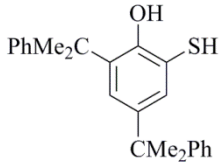


**7**
$C_{24}H_{26}OS$
362,53

**7** was prepared adapting a literature procedure. 50 g of **2** (69 mmol) was solved in a mixture of 150 mL EtOH and 150 mL toluene. Over a period of 5 d, 150 mL of aqueous 30% hydrochloric acid and 25 g zinc metal powder were introduced stepwise. After filtration, the organic phase was separated and the $H_2O$-phase was extracted two times with 100 mL toluene. The collected organic phase was dried over $Na_2SO_4$, filtered and reduced under vacuum to give a pale yellow oil. After recrystallization from 500 mL of a 1:1 mixture of acetone and acetonitrile, white crystals of **7** were formed in a yield of 43% (21.3 g, 58.65 mmol). **$^1$H NMR** ($CDCl_3$, 25 °C, 400 MHz), δ (ppm): 1.61 (s, 6 H, C(C*H*$_3$)$_2$Ph), 1.70 (s, 6 H, C(C*H*$_3$)$_2$Ph), 3.07 (s, 1 H, PhS*H*), 6.56 (s, 1 H, PhO*H*), 7.14 (br, 1 H, Ph-*H*3), 7.36 (br, 1 H,

Ph-*H*). **$^{13}C\{^{1}H\}$ NMR** ($CDCl_3$, 25 °C, 100.1 MHz), δ (ppm): 29.4 (C(*C*$H_3$)$_2$Ph), 30.9 (C(*C*$H_3$)$_2$Ph), 42.3 (*C*(CH$_3$)$_2$Ph), 42.6 (*C*(CH$_3$)$_2$), 125.2 (Ph-*C2*), 125.7 (Ph-*C3*), 125.8 (Ph-C4), 126.2 (Cum-C2), 126.7 (Cum-*C4*), 128.0 (Ph-*C*5), 129.8 (Ph-*C*6), 149.9 (Cum-*C1*), 151.0 (Ph-*C*1). **Elemental analysis**, calculated for $C_{24}H_{26}OS$ (362.53 g/mol) (%): C 79.51, H 7.23; Found: C 80.39, H 7.23.

---

**1,3-Dithiapropanediyl-2,2´-bis(4,6-di{2-phenylpropan-2-yl}phenol)** $H_2$**L**$^{25}$

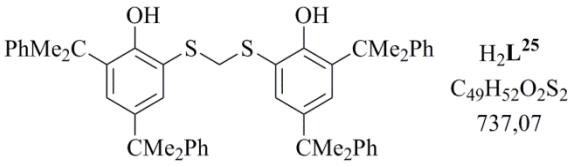


$H_2$**L**$^{25}$
$C_{49}H_{52}O_2S_2$
737,07

To a solution of 36.00 g of **7** (99 mmol, 2 equiv.) in 100 mL of MeOH and 100 mL of EtOH, 5.35 g of NaOMe (99 mmol, 2 equiv.) was added and refluxed until all NaOMe was dissolved. The mixture was cooled to 25 °C and 3.21 mL of $CH_2Br_2$ (46 mmol, 1 equiv.) were added dropwise. The mixture was refluxed for 16 h and the solvents were evaporated under vacuum. Water (200 mL) was added and the mixture was extracted three times with 100 mL $Et_2O$. The organic phase was separated, dried over anhydrous $MgSO_4$, filtered and evaporated to give a colorless foam. Recrystallization from *n*-pentane afforded colorless crystals of $H_2$**L**$^{25}$ in 15% yield (5.35 g, 7.26 mmol). **$^{1}$H NMR** ($CDCl_3$, 25 °C, 400 MHz), δ (ppm): 1.65 (s, 12 H, C(C*H*$_3$)$_2$Ph), 1.70 (s, 12 H, C(C*H*$_3$)$_2$Ph), 3.72 (s, 2 H, SC*H*$_2$S), 6.15 (s, 2 H, PhO*H*), 7.14-7.18 (m, 4 H, Ph-*H*), 7.22-7.25 (m, 4 H, Ph-*H*), 7.26-7.27 (m, 2 H, Ph-*H*), 7.28-7.29 (m, 6 H, Ph-*H*), 7.30 (m, 2 H, Ph-*H*), 7.32 (m, 2 H, Ph-*H*). **$^{13}C\{^{1}H\}$ NMR** ($CDCl_3$, 25 °C, 100.1 MHz), δ (ppm): 29.5 (*p*-C(*C*$H_3$)$_2$Ph), 31.1 (*o*-C(*C*$H_3$)$_2$Ph), 42.5 (S*C*H$_2$S), 42.6 (*o*-*C*(CH$_3$)$_2$Ph), 42.7 (*p*-*C*(CH$_3$)$_2$Ph), 118.3 (Ph-*C*2), 125.6 (Ph-*C*3), 125.7 (Ph-*C*), 126.8 (Ph-*C*), 128.1 (Ph-*C*), 128.2 (Ph-*C*), 132.0 (Ph-*C*), 135.1 (Ph-*C*), 142.2 (Ph-*C*), 150.2 (Ph-*C*), 150.6 (Ph-*C*), 152.9 (Ph-*C*). **Elemental analysis**, calculated for $C_{49}H_{52}O_2S_2$ (737.07 g/mol) (%): C 79.85, H 7.11; found: C 80.46, H 7.19.

**4-Methyl-2-(1-methylcyclohexyl)phenol (8)**

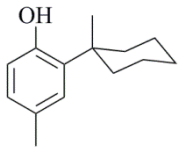


**8**
$C_{14}H_{20}O$
204,31

A solution of 6 mL 20% aqueous $H_2SO_4$ in 45 mL of DCM has been added over 20 minutes into a mixture of 11.4 g *p*-Cresol (108.7 mmol, 1 equiv.) and 12.4 g of 1-methylcyclohexanol (108.7 mmol, 1.03 equiv.) in 45 mL DCM at 0 °C. The biphasic mixture was stirred for 16 h. After addition of 120 mL $H_2O$, the mixture was neutralized slowly to pH = 9 by adding 2 M aqueous NaOH solution. The mixture was extracted three times with 100 mL DCM. The collected organic phase was washed with brine, dried over $Na_2SO_4$, filtered and concentrated. After additing 100 mL of MeOH, the mixture was heated to reflux. After cooling to 25 °C and filtration, the mother liquor was concentrated to give a dark oil that solidified over night to give **8** in a yield of 61% as a black solid. (13.1 g, 64.1 mmol). **$^1$H NMR** ($CDCl_3$, 25 °C, 400 MHz), δ (ppm): 1.33 (s, 3 H, CyC*H*$_3$), 1.50-1.56 (m, 6 H, Cy-*H*), 1.66-1.75 (m, 2 H, Cy-*H*), 2.07-2.16 (m, 2 H, Cy-*H*), 2.29 (s, 3 H, Ph-C*H*$_3$), 4.61 (s, 1 H, Ph-O*H*), 6.56 (d, 1 H, $^3J_{HH}$ = 8.0 Hz, Ph-*H*6), 6.87 (dd, 1 H, $^4J_{HH}$ = 2.1 Hz, $^3J_{HH}$ = 8.0 Hz, Ph-*H*5), 7.09 (d, $^4J_{HH}$ = 2.1 Hz, Ph-*H*3). **$^{13}$C{$^1$H} NMR** ($CDCl_3$, 25 °C, 100.1 MHz), δ (ppm): 21.0 (Ph*C*H$_3$), 22.9 (*C*H$_3$), 23.0 (Cy-*C*), 25.8 (Cy-*C*), 26.8 (Cy-*C*), 37.1 (Cy-*C*), 37.8 (Cy-*C*), 38.0 (Cy-*C*), 116.9 (Ph-*C*6), 127.1 (Ph-*C*5), 128.9 (Ph-*C*4), 129.6 (Ph-*C*3), 135.3 (Ph-*C*2), 152.2 (Ph-*C*1). **Elemental analysis**, calculated for $C_{14}H_{20}O$ (204.31 g/mol) (%): C 82.30, H 9.87; found: C 81.64; H 10.26.

---

**6,6'-Disulfanediylbis(4-methyl-2-{1-methylcyclohexyl}phenol) (9)**

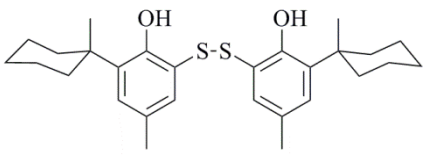


**9**
$C_{28}H_{38}O_2S_2$
470,23

To a stirred solution of 16.5 g of **8** (80.8 mmol, 2 equiv.) and 0.1 mL of $TiCl_4$ (0.8 mmol, 2.0 mol %) in 60 mL toluene, 3.22 mL of $S_2Cl_2$ (40.4 mmol, 1 equiv.) were added dropwise at 5 °C. The reaction mixture was stirred for five days at 25 °C and extracted sequentially with hydrochloric acid (2 x 100 mL, *c* = 19%), 200 mL of saturated aqueous $Na_2CO_3$ solution and

200 mL water. The organic layer was dried over anhydrous $MgSO_4$ and concentrated under vacuum. The residue was recrystallized from a mixture of 200 mL acetonitrile and 200 mL acetone to give **9** as an orange powder in a yield of 71% (13.5 g, 28.7 mmol). **$^1$H NMR** ($CDCl_3$, 25 °C, 400 MHz), δ (ppm): 1.32 (s, 3 H, Cy-C*H*$_3$), 1.35 (s, 3 H, Cy-C*H*$_3$), 1.40-1.55 (br, 8 H, Cy-*H*), 1.55-1.65 (br, 6 H, Cy-*H*), 1.65-1.80 (br. 6 H, Cy-*H*), 2.08-2.18 (br, 2 H, Cy-*H*), 2.19 (s, 6 H, PhC*H*$_3$), 6.59 (s, 2 H, PhO*H*), 7.01 (d, 2 H, $^4J_{HH}$ = 2.0 Hz, Ph-*H*5), 7.17 (d, 2 H, $^4J_{HH}$ = 2.0 Hz, Ph-*H*3). **$^{13}$C{$^1$H} NMR** ($CDCl_3$, 25 °C, 100.1 MHz), δ (ppm): 20.7 (Cy-*C*), 22.9 (Cy-*C*), 26.7 (Cy-*C*), 31.0 (Cy*C*H$_3$), 36.8 (Cy-*C*), 38.6 (Cy-*C*), 38.7 (Cy-*C*), 120.3 (Ph-*C*2), 120.9 (Ph-*C*2'), 129.4 (Ph-*C*3), 129.5 (Ph-*C*3'), 132.6 (Ph-*C*4), 132.9 (Ph-*C*4'), 133.8 (Ph-*C*5), 133.9 (Ph-*C*5'), 135.7 (Ph-*C*6), 136.2 (Ph-*C*6'), 153.4 (Ph-*C*1), 153.7 (Ph-*C*1).

---

**2-Mercapto-4-methyl-6-(1-methylcyclohexyl)phenol** (**10**)

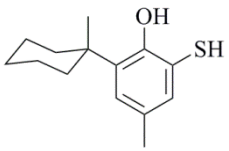


**10**
$C_{14}H_{20}OS$
236,37

13.5 g of **9** (28.7 mmol, 1 equiv.) were dissolved in a mixture of 150 mL of EtOH and 150 mL of toluene. Over a period of seven days, 100 mL of 30% aqueous hydrochloric acid and 15 g zinc metal powder were added stepwise. After filtration, the organic phase was separated and the $H_2O$-phase was extracted two times with 100 mL toluene. The collected organic phase was dried over $Na_2SO_4$, filtered and reduced under vacuum to give **10** as a pale yellow oil in a yield of 45% (6.2 g, 26.1 mmol). **$^1$H NMR** ($CDCl_3$, 25 °C, 400 MHz), δ (ppm): 1.34 (s, 3 H, Cy-C*H*$_3$), 1.45-1.55 (m, 4 H, Cy-*H*), 1.55-1.63 (m, 2 H, Cy-*H*), 1.67-1.75 (m, 2 H, Cy-*H*), 2.12-2.20 (m, 2 H, Cy-*H*), 2.28 (s, 3 H, PhC*H*$_3$), 2.84 (s, 1 H, S*H*), 6.66 (s, 1H, O*H*), 7.11 (br, 1 H, Ph-*H*5), 7.22 (br, 1 H, Ph-3). **$^{13}$C{$^1$H} NMR** ($CDCl_3$, 25 °C, 100.1 MHz), δ (ppm): 20.8 (PhC*H*$_3$), 23.0 (Cy-*C*), 25.4 (Cy-C*H*$_3$), 26.8 (Cy-*C*), 36.8 (Cy-*C*), 38.4 (Cy-*C*), 111.5 (Ph-*C*2), 125.4 (Ph-*C*4), 128.4 (Ph-*C*3), 130.5 (Ph-*C*5), 134.0 (Ph-*C*6), 153.3 (Ph-*C*1).

**1,3-Dithiapropanediyl-2,2´-bis(4-methyl-6-{1-methylcyclohexyl}phenol)** ($H_2$**L**$^{26}$)

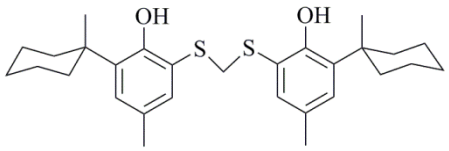


$H_2$**L**$^{26}$
$C_{29}H_{40}O_2S_2$
484,76

To a solution of 2.50 g of **10** (12.2 mmol, 2 equiv.) in 25 mL MeOH, 0.66 g of NaOMe (12.2 mmol, 2 equiv.) were added and the mixture heated to reflux until all NaOMe dissolved. After cooling to 0 °C, 0.43 mL of $CH_2Br_2$ (6.1 mmol, 1 equiv.) were added slowly with a syringe and the mixture refluxed for 1 h. After removal of the solvent under vacuum, 100 mL of water were added to dissolve NaBr. After addition of 100 mL of $Et_2O$, the organic phase was separated, the aqueous phase extracted twice with 50 mL of $Et_2O$ and the combined organic phases dried over $Na_2SO_4$. The crude product was recrystallized from *n*-pentane to give $H_2$**L**$^{26}$ in a yield of 38% (1.13 g, 2.33 mmol) as a yellow powder. **$^1$H NMR** ($CDCl_3$, 25 °C, 400 MHz), δ (ppm): 1.30 (s, 6 H, CyC*H*$_3$), 1.41-1.45 (m, 6 H, Cy-*H*), 1.46-1.50 (m, 8 H, Cy-*H*), 1.54-1.56 (m, 4 H, Cy-*H*), 1.66-1.71 (m, 4 H, Cy-*H*), 2.08-2.15 (m, 4 H, Cy-*H*), 2.25 (s, 6 H, PhC*H*$_3$), 2.26 (m, 2 H, Ph-Cy-*H*), 3.90 (s, 2 H, SC*H*$_2$), 6.76 (s, 2 H, O*H*), 7.09 (d, 2 H, $^4J_{HH}$ = 2.2 Hz, Ph-*H*5), 7.12 (d, 2 H, $^4J_{HH}$ = 2.2 Hz, Ph-*H*3). **$^{13}$C{$^1$H} NMR** ($CDCl_3$, 25 °C,100.1 MHz), δ (ppm): 20.8 (Ph-*C*H$_3$), 22.9 (Cy-*C*H$_3$), 25.4 (Cy-*C*), 26.8 (Cy-*C*), 36.8 (Cy-*C*), 38.5 (Cy-*C*), 45.0 (S*C*H$_2$), 118.5 (Ph-*C*2), 129.1 (Ph-*C*3), 131.4 (Ph-*C*4), 133.4 (Ph-*C*5), 135.6 (Ph-*C*6), 153.4 (Ph-*C*1). **Elemental analysis**, calculated for $C_{29}H_{40}O_2S_2$ (484,76 g/mol) (%): C: 71.85, H: 8.32; found: C: 71.43, H: 8.84.

---

**1,4-Dithiabutanediyl-2,2´-bis(4-methyl-6-{1-methylcyclohexyl}phenol)** ($H_2$**L**$^{27}$)

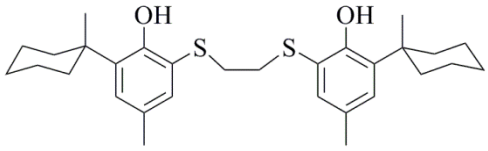


**$H_2$L$^{27}$**
$C_{30}H_{42}O_2S_2$
498,78

To a solution of 5.0 g of **10** (21.2 mmol, 2 equiv.) in 50 mL of MeOH, 0.85 g of NaOH (21,2 mmol, 2 equiv.) were added and the mixture was heated to reflux until all NaOH dissolved. After cooling to 0 °C, 0.92 mL of 1,2-dibromoethane (10.6 mmol, 1 equiv.) were added slowly with a syringe and the mixture was refluxed for 1 h. After removal of the solvent under

vacuum, 100 mL of water were added to dissolve NaBr. After addition of 200 mL of $Et_2O$ the organic phase was separated, the aqueous phase extracted twice with 100 mL od $Et_2O$ and the combined organic phases dried over $Na_2SO_4$. After filtration and removal of the solvent under vacuum, the crude product was recrystallized from *n*-pentane to give 0.81 g (1.63 mmol, 15%) of $H_2$**L**[27] as a brownish powder. **$^1$H NMR** ($CDCl_3$, 25 °C, 400 MHz), δ (ppm): 1.31 (s, 6 H, Cy-C*H*$_3$), 1.42-1.49 (m, 8 H, Cy-*H*), 1.54-1.60 (m, 4 H, Cy-*H*), 1.66-1.74 (m, 4 H, Cy-*H*), 2.08-2.16 (m, 4 H, Cy-*H*), 2.24 (s, 6 H, PhC*H*$_3$), 2.77 (s, 4 H, SC*H*$_2$), 7.08 (s, 2 H, O*H*), 7.10 (br, 2 H, Ph-*H*5), 7.12 (br, 2 H, Ph-*H*3). **$^{13}$C{$^1$H} NMR** ($CDCl_3$, 25 °C, 100 MHz), δ (ppm): 20.9 (Ph*C*H$_3$), 22.9 (Cy-*C*), 25.4 (Cy-*C*), 26.8 (Cy-*C*), 36.3 (S*C*H$_2$), 36.8 (Cy-*C*), 38.5 (Cy*C*CH$_3$), 118.2 (Ph-*C*2), 129.0 (Ph-*C*3), 131.0 (Ph-*C*4), 133.6 (Ph-*C*5), 135.4 (Ph-*C*6), 153.6 (Ph-*C*1). **Elemental analysis**, calculated for $C_{30}H_{42}O_2S_2$ (498.8 g/mol) (%): C 72.24, H 8.49; Found: C 72.25, H 8.76.

---

***rac*-(2,3-*trans*-Propanediyl-1,4-dithiabutanediyl)-2,2´-bis(4,6-di{2-phenylpropan-2-yl}phenol)** ($H_2$**L**[28])

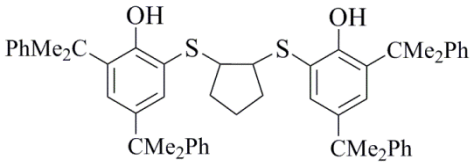


$H_2$**L**[28]
$C_{53}H_{58}O_2S_2$
791,16

1.24 mL of cyclopentene (14 mmol, 1 equiv.) and 0.25 mL of a solution of $BF_3 \cdot OEt_2$ were added to a solution of 10.0 g of $S_2Cl_2$ (14 mmol, 1 equiv.) in a mixture of 8 mL of nitromethane and 8 mL of $CH_2Cl_2$ at -10 °C. The resulting mixture was stirred at –10 °C for 3 h and at 25 °C for additional 72 h. The resulting mixture was washed with aqueous $NaHCO_3$ solution, the organic layer was dried over $MgSO_4$, filtered and concentrated under vacuum. Crystallization from a mixture of acetonitrile:acetone (4:1, 200 mL) gave pure $H_2$**L**[28] in 74% yield (8.24 g, 10.4 mmol). **$^1$H NMR** ($CDCl_3$, 25 °C, 400 MHz), δ (ppm): 1.34 (m, 2 H, Cy-*H*), 1.44 (m, 2 H, Cy-*H*), 1.65 (s, 6 H, C(C*H*$_3$)$_2$Ph), 1.66 (s, 6 H, C(C*H*$_3$)$_2$Ph), 1.70 (s, 12 H, C(C*H*$_3$)$_2$Ph), 1.76 (m, 2 H, Cy-*H*), 2.79 (br, 2 H, SC*H*), 6.64 (s, 2 H, PhO*H*) 7.11-7.16 (m, 4 H, Ph-*H*), 7.16-7.18 (m, 4 H, Ph-*H*), 7.19 (d, 2 H, $^3J_{HH}$ = 2.2 Hz, Ph-*H*), 7.20-7.25 (m, 6 H, Ph-*H*), 7.26 (m, 4 H, Ph-*H*), 7.26-7.30 (m, 4 H, Ph-*H*), 7.35 (d, 2 H, $^3J_{HH}$ = 2.2 Hz, Ph-*H*). **$^{13}$C{$^1$H} NMR** ($CDCl_3$, 25 °C, 100.1 MHz), δ (ppm): 24.9 (Cy-*C*), 25.8 (Cy-*C*), 26.2 (Cy-*C*),

27.5 (Cy-*C*), 29.6 (C(*C*H$_3$)$_2$Ph), 29.7 (C(*C*H$_3$)$_2$Ph), 30.2 (Cy-*C*), 31.1 (Cy-*C*), 42.8 (*C*(CH$_3$)$_2$Ph), 42.9 (*C*(C*H*$_3$)$_2$Ph), 54.9 (S*C*H$_2$), 119.1 (Ph-*C*2), 125.6 (Ph-*C*), 126.0 (Ph-*C*), 126.2 (Ph-*C*), 127.0 (Ph-*C*), 128.0 (Ph-*C*), 128.3 (Ph-*C*3), 128.9 (Ph-*C*4), 133.7 (Ph-*C*5), 135.4 (Ph-*C*), 142.0 (Ph-*C*), 150.8 (Ph-*C*), 151.1 (Ph-*C*), 154.1 (Ph-*C*1). **Elemental analysis**, calculated for $C_{53}H_{58}O_2S_2$ (791.67 g/mol) (%): C 80.46, H 7.39; found C 80.32, H 7.22.

---

***rac*-(2,3-*trans*-Hexanediyl-1,4-dithiabutanediyl)-2,2´-bis(4,6-di{2-phenylpropan-2-yl}phenol) (**$H_2$**L**$^{29}$**)**

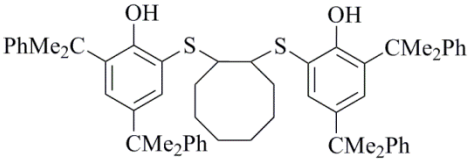


$H_2$**L**$^{29}$
$C_{56}H_{64}O_2S_2$
833.24

7.40 mL of cyclooctene (56 mmol, 2 equiv.) and 0.25 mL of a solution of $BF_3 \cdot OEt_2$ were added to a solution of 20.0 g of $S_2Cl_2$ (28 mmol, 1 equiv.) in a mixture of 15 mL of nitromethane and 15 mL of DCM at –10 °C. The resulting mixture was stirred at –10 °C for 3 h and at 25 °C for additional 72 h. The mixture was washed with saturated aqueous $NaHCO_3$ solution. The organic layer was dried over $MgSO_4$, filtered and concentrated under vacuum. Crystallization from a mixture of acetonitrile:acetone (4:1, 200 mL) gave pure bis(phenol) $H_2$**L**$^{29}$ in 15% yield (3.6 g, 4.3 mmol). **$^1$H NMR** ($C_6D_6$, 25 °C, 400 MHz), δ (ppm): 1.09 (m, 2 H, Cy-*H*), 1.20 (m, 2 H, Cy-*H*), 1.29 (m, 2 H, Cy-*H*), 1.43 (m, 2 H, Cy-*H*), 1.55 (m, 2 H, Cy-*H*), 1.73 (s, 12 H, C(C*H*$_3$)$_2$Ph), 1.83 (s, 6 H, C(C*H*$_3$)$_2$Ph), 1.84 (s, 6 H, C(C*H*$_3$)$_2$Ph), 2.90 (br, 2 H, SC*H*), 7.10 (s, 2 H, Ph-*H*), 7.13-7.19 (m, 2 H, Ph-*H*), 7.22-7.26 (m, 2 H, Ph-*H*), 7.28 (d, 2 H, $^4J_{HH}$ = 2.8 Hz, Ph-*H2*), 7.34 (d, 2 H, $^4J_{HH}$ = 2.8 Hz, Ph-*H*5), 7.35-7.41 (m, 6 H, Ph-*H*), 7.49 (d, 2 H, $^4J_{HH}$ = 2.8 Hz, Ph-*H*), 7.60 (d, 2 H, $^3J_{HH}$ = 2.3 Hz, Ph-*H*). **$^{13}$C{$^1$H} NMR** ($C_6D_6$, 25 °C, 100.1 MHz), δ (ppm): 25.8 (Cy-*C*), 26.2 (Cy-*C*), 29.6 (C(*C*H$_3$)$_2$Ph), 29.7 (C(*C*H$_3$)$_2$Ph), 30.2 (Cy-*C*), 31.1 (Cy-*C*), 42.8 (*C*(CH$_3$)$_2$Ph), 42.9 (*C*(C*H*$_3$)$_2$Ph), 54.8 (S*C*H$_2$), 119.1 (Ph-*C*), 125.6 (Ph-*C*), 126.0 (Ph-*C*), 126.2 (Ph-*C*), 127.0 (Ph-*C*), 128.0 (Ph-*C*), 128.3 (Ph-*C*), 128.9 (Ph-*C*), 133.7 (Ph-*C*), 135.4 (Ph-*C*), 142.0 (Ph-*C*), 150.8 (Ph-*C*), 151.1 (Ph-*C*), 154.1 (Ph-*C*). **Elemental analysis**, calculated for $C_{56}H_{64}O_2S_2$ (832.25 g/mol) (%): C 80.72, H 7.74; found: C 79.58, H 7.71.

**4-Methyl-2-(2-phenylpropan-2-yl)phenol**[27] **(11)**

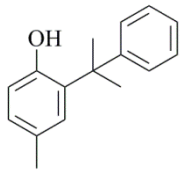


**11**
$C_{16}H_{18}O$
226,31

**11** was prepared adapting a literature procedure. 47.6 g of *p*-cresol (0.44 mol, 1.1 equiv.) were stirred in a 250 mL three-neck-flask at 50 °C. 0.76 g of *p*-toluenesulfonic acid monohydrate (0.04 mol, 0.004 equiv.) were added slowly while stirring. After adding 52.0 mL of α-methylstyene (0.4 mol, 1 equiv.) the mixture was stirred at 50 °C for 1.5 h. The solution was poured onto ice, extracted with 400 mL of diethyl ether and the organic phase was dried over $MgSO_4$. Ether was removed at 45 °C and the crude oily product was distilled to give 47.8 g (211 mmol, 49%) of **11** as a colorless oil. **$^1$H NMR** ($CDCl_3$, 25 °C, 400 MHz), δ (ppm): 1.59 (s, 6 H, C(C*H*$_3$)$_2$Ph), 2.27 (s, 3 H, Ph-C*H*$_3$), 6.56 (d, $^3J_{HH}$ = 8.0 Hz, 1 H, Ph-*H*6), 6.90 (dd, $^3J_{HH}$ = 8.0 Hz, $^4J_{HH}$ = 1.6 Hz, 1 H, Ph-*H*5), 7.15, (m, 1 H, Ph-*H*), 7.19 (d, $^4J_{HH}$ = 1.6 Hz, 1 H, Ph-*H*3), 7.25 (d, $^3J$ = 2.9 Hz, 2 H, Ph-*H*), 7.27 (m, 2 H, Ph-*H*). **$^{13}$C{$^1$H} NMR** ($CDCl_3$, 25 °C, 100.1 MHz), δ (ppm): 20.9 (Ph*C*H$_3$), 29.5 (C(*C*H$_3$)$_2$Ph, 41.6 (*C*(CH$_3$)$_2$Ph), 117.6 (Ph-*C*5), 126.0 (Ph-C*3*), 128.2 (Ph-*C*), 128.5 (Ph-*C*5), 129.2 (Ph-*C*), 135.0 (Ph-*C*2), 138.8 (Ph-C*4*), 148.5 (Ph-*C*), 151.6 (Ph-*C*1). **Elemental analysis**, calculated for $C_{16}H_{18}O$ (226.31 g/mol) (%): C 84.91, H 8.02; Found: C 86.48, H 7.68.

---

**2-Bromo-4-methylphenol**[28] (**13**)

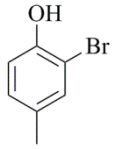


**13**
$C_7H_7BrO$
187,03

**13** was prepared following a literature procedure. A solution of bromine (40 g, 251 mmol, 1 equiv.) in 100 mL of $CH_2Cl_2$ was added dropwise to a stirred solution of *p*-cresol (27.2 g, 251 mmol, 1 equiv.) in 500 mL $CH_2Cl_2$ at 0 °C. Dry argon was bubbled through the reaction mixture to remove HBr. Once the addition was complete, the ice bath was removed and the solution stirred for 2 hours. After quenching with 300 mL $H_2O$, the organic layer was dried with $MgSO_4$ and filtered. The solvent was removed by rotary evaporator and the product was purified by vacuum distillation to give a colorless oil in 46% yield (21.8 g, 117 mmol).

**$^{1}$H NMR** ($CDCl_3$, 25 °C, 400 MHz), δ (ppm): 2.27 (s, 3 H, PhC*H*$_3$), 5.44 (s, 1 H, O*H*), 6.92 (d, 1 H, $^{3}J_{HH}$ = 8.4 Hz, Ph-*H*6), 7.02 (dd, 1 H, $^{3}J_{HH}$ = 8.4 Hz, $^{4}J_{HH}$ = 2.0 Hz, Ph-*H*5), 7.29 (m, 1 H, Ph-*H*6). **$^{13}$C{$^{1}$H} NMR** ($CDCl_3$, 25 °C, 100 MHz), δ (ppm): 20.3 (Ph*C*H$_3$), 110.0 (Ph-*C*2), 115.9 (Ph-*C*6), 129.9 (Ph-*C*5), 131.6 (Ph-*C*4), 132.2 (Ph-*C*3), 150.1 (Ph-*C*1).

---

**1-(Benzyloxy)-2-bromo-4-methylbenzene**[29] (**14**)

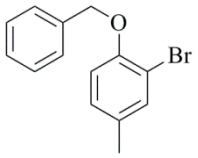


**14**
$C_{14}H_{13}BrO$
277,16

**14** was prepared following a standard procedure for protection of phenols. 2.46 g of Na (107 mmol, 1 equiv.) were dissolved in 125 mL of dry EtOH. A solution of 20 g of **13** (12.9 mL, 107 mmol, 1 equiv.) in 30 mL of dry EtOH was added and the solution refluxed for 14 h. EtOH was removed by destillation and 40 mL of an aqueous 5% NaOH solution was added. After threefold extraction with 100 mL $Et_2O$, the organic phases were dried over $MgSO_4$. After evaporation of $Et_2O$, a yellow oil was obtained that was further dissolved in 150 mL of EtOH and stored in a fridge. After 3 d white crystals were obtained. These crystals were filtered and dried under vacuum to give 16.96 g (61 mmol, 57%) of analytically pure **14**. **$^{1}$H NMR** ($CDCl_3$, 25 °C, 400 MHz), δ (ppm): 2.30 (s, 3 H, PhC*H*$_3$), 5.14 (s, 2 H, PhOC*H*$_2$Ph), 6.85 (d, 1 H, $^{3}J_{HH}$ = 8.3 Hz, Ph-*H*6), 7.04 (dd, 1 H, $^{3}J_{HH}$ = 8.3 Hz, $^{4}J_{HH}$ = 2.1 Hz , Ph-*H*5), 7.29-7.38 (m, 1 H, Ph-*H*3), 7.38-7.46 (m, 3 H, Ph-*H*), 7.51 (m, 2 H, Ph-*H*). **$^{13}$C{$^{1}$H} NMR** ($CDCl_3$, 25 °C, 100 MHz), δ (ppm): 20.3 (Ph*C*H$_3$), 71.1 (PhO*C*H$_2$Ph), 112.4 (Ph-*C*), 114.1 (Ph-*C*), 127.1 (Ph-*C*), 128.0 (Ph-*C*), 128.6 (Ph-*C*3), 129.0 (Ph-*C*4), 132.0 (Ph-*C*), 133.9 (Ph-*C*5), 136.9 (Ph-*C*6), 153.0 (Ph-*C*1). **Elemental analysis**, calculated for $C_{14}H_{13}BrO$ (277.16 g/mol) (%): C 60.67, H 4.73; Found: C 60.62, H 4,70.

---

**2-(benzyloxy)-5-methylbiphenyl**[28] (**15**)

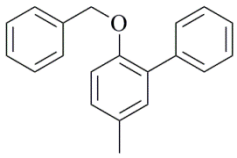


**15**
$C_{20}H_{18}O$
274,36

**15** was prepared following a literature procedure. 11.3 g of **14** (41 mmol, 1 equiv.), phenylboronic acid (5.0 g, 41 mmol, 1 equiv.), 30 mL of a 2 M solution of $Na_2CO_3$ in water and 250 mL of dimethoxyethane were added into an 500 mL three neck round bottom flask at 25 °C. The solution was degassed with two freeze-pump-thaw cycles and the system was placed under argon. [$Pd(PPh_3)_4$] (2.3 g, 2 mmol) was added to the solution. The reaction was heated to 90 °C, stirred and refluxed for 72 hours. The reaction was quenched with ethyl acetate (100 mL) and extracted three times with $H_2O$ and brine. The organic layer was dried over $MgSO_4$, filtered and the solvent removed under vacuum. Column chromatography using a 10:1 mixture of *n*-hexane and ethyl acetate yielded **15** as a colorless oil in 65% yield (7.3 g, 26.6 mmol). **$^1$H NMR** ($CDCl_3$, 25 °C, 400 MHz), δ (ppm): 2.35 (s, 3 H, PhC*H*$_3$), 5.05 (s, 2 H, PhOC*H*$_2$Ph), 6.94 (d, 1 H, $^3J_{HH}$ = 8.3 Hz, Ph-*H*6), 7.09 (dd, 1 H, $^3J_{HH}$ = 8.3 Hz, $^4J_{HH}$ = 2.3 Hz, Ph-*H*5), 7.19 (d, 1 H, $^4J_{HH}$ = 2.3 Hz, Ph-*H*3), 7.30-7.38 (m, 5 H, Ph-*H*), 7.41 (m, 2 H, Ph-*H*), 7.59 (dt, 2 H, Ph-*H*). **$^{13}$C{$^1$H} NMR** ($CDCl_3$, 25 °C, 100 MHz), δ (ppm): 20.7 (Ph*C*H$_3$), 70.9 (PhO*C*H$_2$Ph), 113.9 (Ph-*C*), 126,9 (Ph-*C*3), 127.0 (Ph-*C*), 127.7 (Ph-*C*2), 128.0 (Ph-*C*), 128.5 (Ph-*C*5), 129.0 (Ph-*C*), 129.8 (Ph-*C*), 130.8 (Ph-*C*), 131.4 (Ph-*C*), 131.8 (Ph-*C*4), 137.6 (Ph-*C*6), 138.8 (Ph-*C*), 153.7 (Ph-*C*1).

---

**5-Methyl-(1,1'-biphenyl)-2-ol** (**16**)

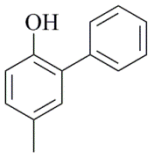


**16**
$C_{13}H_{12}O$
184,23

*Method A*[28]: 2.34 g (8.5 mmol) of **15**, 1g Pd/C (10%), acetic acid (10 drops), ethyl acetate (15 mL) and ethanol (15 mL) were added to a stainless steel reactor equipped with a stirbar. The flask was pressured with 6 bar $H_2$ (g), heated to 70 °C and stirred for 5 d. The mixture was cooled to 25 °C and filtered through celite; the filtrate was dried *in vacuo* and recrystallized from *n*-pentane to yield colorless crystals in a yield of 76% (1.20 g, 6.5 mmol).

*Method B*[30]: An oven dried, Schlenk-adapted tube was charged with 3.90 g of **17** (14.4 mmol, 1 equiv.) and [$Pd(PPh_3)_4$] (0.83 g, 0.72 mmol) in anhydrous DME (15 mL) under Ar. The solution was degassed and transferred into a flask containing a degassed solution of

phenylboronic acid (2.11 g, 17.3 mmol) and 2.0 M aqueous $Na_2CO_3$ (14.4 mL, 28.8 mmol) in DME (15 mL). Under an active Ar purge, the solution was heated to reflux and stirred under Ar for 16 h. After cooling, 30 mL of ethyl acetate were added and the solution was dried over $Na_2SO_4$. After filtration and removal of the solvent under vacuum, a dark and highly viscous residue was obtained. HCl (0.3 mL) in 2 mL of a 1:1 mixture of methanol/ethyl acetate were added and the solution stirred at 40 °C for 4 hours. After cooling, the solvent was removed under vacuum and the crude product was purified by flash chromatography (hexanes/ethyl acetate 20:1) to yield a colorless oil that solidified upon drying under vacuum in a yield of 38% (1.0 g, 5.43 mmol). **$^1$H NMR** ($CDCl_3$, 25 °C, 400 MHz), δ (ppm): 2.34 (s, 3 H, PhC*H*$_3$), 4.91 (br.,1 H, O*H*), 6.90 (d, 1 H, $^3J_{HH}$ = 8.7 Hz, Ph-*H*6), 7.08 (d, 2 H, $^3J_{HH}$ = 5.8 Hz, Ph-*H*5), 7.41 (m, 1 H, Ph-*H*3), 7.48 (s, 2 H, Ph-*H*), 7.49 (d, 2 H, $^4J_{HH}$ = 2.7 Hz). **$^{13}$C{$^1$H} NMR** ($CDCl_3$, 25 °C, 100 MHz), δ (ppm): 20.6 (Ph*C*H$_3$), 115.8 (Ph-*C*6), 127.2 (Ph-*C*3), 128.0 (Ph-*C*), 129.2 (Ph-*C*), 129.3 (Ph-*C*5), 129.6 (Ph-*C*), 130.0 (Ph-*C*4), 130.1 (Ph-*C*), 130.8 (Ph-*C*), 137.5 (Ph-*C*2), 150.3 (Ph-*C*1). **Elemental analysis**, calculated for $C_{13}H_{12}O$ (277.16 g/mol) (%): C 84.75, H 6.57; Found: C 84.48, H 6.59.

---

**Reaction of 14 and 17 with phenylboronic acid catalyzed by Pd-PEPPSI**

Coupling reactions were performed in the same way than described above for the coupling reactions with [Pd($PPh_3$)$_4$]. Starting with 300 mg of **14**, 90% yield of **15** were isolated. These yields dropped to 50% starting with 1.0 g of **14** and to 25% with 2.0 g of the starting compound. Reactions performed with **17** achieved similar yields.

---

**Pyridinium 4-methylbenzenesulfonate**[33] (**PPTS**)

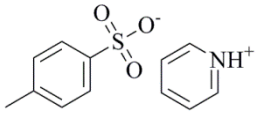


**PPTS**
$C_{12}H_{13}NO_3S$
251,30

**PPTS** was prepared following a literature procedure. *p*-Toluenesulfonic acid monohydrate **(**11.51 g, 66 mmol) was added to pyridine (100 mL) at 25 °C. After stirring for 3 h, excess pyridine was removed under vacuum on a water bath at approximately 60 °C to afford 14.5 g

(58 mmol, 88%) of **PPTS** as a colorless powder that was further dried under vacuum. **$^1$H NMR** ($CDCl_3$, 25 °C, 400 MHz), δ (ppm): 2.33 (s, 3 H, PhC*H*$_3$), 7.15 (m, 2 H, Ph-*H*), 7.79 (m, 2 H, Ph-*H*), 7.93 (m, 2 H, Py-*H*), 8.40 (tt, 1 H, $^3J_{HH}$ = 7.8 Hz, $^4J_{HH}$ = 1.6 Hz, Py-*H*), 8.95-9.03 (m, 2 H, Py-*H*).

---

**3-(2-bromo-4-methylphenoxy)tetrahydro-2H-pyran**[30] (**17**)

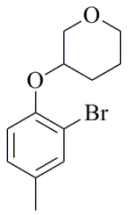

**17**
$C_{12}H_{15}BrO_2$
271,15

An oven-dried, Schlenk tube was charged with 16.2 mL of **13** (134 mmol, 1 equiv.), 3,4-dihydro-2*H*-pyran (16.5 mL, 180 mmol, 1.34 equiv.), PPTS (3.4 g, 13.4 mmol, 10 mol%) and DCM (170 mL) under Ar. The reaction was stirred overnight at 25 °C. Brine (120 mL) was added and the organic phase was separated, dried over $Na_2SO_4$, filtered and the solvent removed under vacuum to yield **17** as a colorless oil in 89% yield (32,2 g, 119 mmol). **$^1$H NMR** ($CDCl_3$, 25 °C, 400 MHz), δ (ppm): 1.14-1.23 (m, 1 H, ArOTHP-*H*), 1.28-1.43 (m, 2 H, ArOTHP-*H*), 1.48-1.58 (m, 1 H, ArOTHP-*H*), 1.73-1.82 (m, 1 H, ArOTHP-*H*), 1.91 (s, 3 H, Ar-C*H*$_3$), 1.95-2,08 (m, 1 H, ArOTHP-*H*), 3.31-3,38 (m, 1 H, ArOTHP-*H*), 3.74-3,83 (m, 1 H, ArOTHP-*H*), 5.27 (t, 1 H, $^3J_{HH}$ = 2.5 Hz, ArOC*H*), 6.77 (dd, 1 H, $^3J_{HH}$ = 8.5 Hz, $^4J_{HH}$ = 1.5 Hz, Ar-*H*5), 7.06 (d, 1 H, $^3J_{HH}$ = 8.5 Hz, Ar-*H*6), 7.27 (d, 1 H, $^4J_{HH}$ = 1.5 Hz, Ar-*H*3). **$^{13}$C{$^1$H} NMR** ($CDCl_3$, 25 °C, 100 MHz), δ (ppm): 18.6 (ArOTHP-*C)*, 20.1 (Ar*C*H$_3$), 25.5 (ArOTHP-*C*), 30.5 (ArTHP-*C*), 61.4 (ArOTHP-*C*), 96.9 (ArO*C*H), 113.28 (Ar-*C*2), 116.9 (Ar-*C*6), 129.9 (Ar-*C*5), 132.5 (Ar-*C*4), 134.0 (Ar-*C*3), 152.0 (Ar-*C*1). **Elemental analysis**, calculated for $C_{12}H_{15}BrO_2$ (271.15 g/mol) (%): C 53.15, H 5.58; Found: C 51.66, H 5.75.

# II.5. References


1 C. Capacchione, R. Manivannan, M. Barone, K. Beckerle, R. Centore, L. Oliva, A. Proto, A. Tuzi, T. P. Spaniol, J. Okuda, *Organometallics* **2005**, *24*, 2971-2982.

2 L. S. Baugh, J.-A. Canich, *Stereoselective Polymerization with Single-Site Catalysts*, CRC Press, Boca Raton, FL, **2008**.

[3] G. J. P. Britovsek, V. C. Gibson, D. F. Wass, *Angew. Chem. Int. Ed.* **1999**, *38*, 428-447.

[4] V. C. Gibson, S. K. Spitzmesser, *Chem. Rev.* **2003**, *103*, 283-316.

[5] V. C. Gibson, C. Redshaw, G. A. Solan, *Chem. Rev.* **2007**, *107*, 1745-1776.

[6] Selected exampled on catalysts with Salan-type ligands for ROP of lactide monomers: a) H. Du, A. H. Velders, P. J. Dijkstra, J. Sun, Z. Zhong, X. Chen, J. Feijen, *Chem. Eur. J.* **2009**, *15*, 9836-9845; b) S. Gendler, S. Segal, I. Goldberg, Z. Goldschmidt, M. Kol, *Inorg. Chem.* **2006**, *45*, 4783-4790; c) S. H. Kim, J. Lee, D. J. Kim, J. H. Moon, S. Yoon, H. J. Oh, Y. Do, Y. S. Ko, J.-H. Yim, Y. Kim, *J. Organomet. Chem.* **2009**, *694*, 3409-3417; d) M. D. Jones, M. G. Davidson, G. Kociok-Köhn, *Polyhedron* **2010**, *29*, 697-700; e) D. C. Bradley, R. C. Mehrotra, I. P. Rothwell, A..Singh, *Alkoxo and Aryloxo Derivatives of Metals*; Academic: San Diego, CA, **2001**, f) E. L. Marshall, V. C. Gibson, H. S. Rzepa, *J. Am. Chem. Soc.* **2005**, *127*, 6048-6051.

[7] Selected examples on catalysts with Salen-type ligands for ROP of lactide monomers: a) N. Spassky, M. Wisniewski, C. Pluta, A. Le Borgne, *Macromol. Chem. Phys.* **1996**, *197*, 2627-2637; b) M. Wisniewski, A. Le Borgne N. Spassky, *Macromol. Chem. Phys.* **1997**, *198*, 1227-1238; c) P. A. Cameron, D. Jhurry, V. C. Gibson, A. J. P. White, D. J. Williams, S. Williams, *Macromol. Rapid Commun.* **1999**, *20*, 616-618; d) T. M. Ovitt, G. W. Coates, *J. Am. Chem. Soc.* **1999**, *121*, 4072-4073; e) T. M. Ovitt, G. W. Coates, *J. Polym. Sci. A – Polym. Chem.* **2000**, *38*, 4686-4692; f) C. P. Radano, G. L. Baker, M. R. Smith III, *J. Am. Chem. Soc.* **2000**, *122*, 1552-1553; g) T. M. Ovitt, G. W. Coates, *J. Am. Chem. Soc.* **2002**, *124*, 1316-1326; h) Z. Zhong, P. J. Dijkstra, J. Feijen, *Angew. Chem. Int. Ed.* **2002**, *41*, 4510-4513; i) N. Nomura, R. Ishii, M. Akakura, K. Aoi, *J. Am. Chem. Soc.* **2002**, *124*, 5938-5939; j) Z. Zhong, P. J. Dijkstra, J. Feijen, *J. Am. Chem. Soc.* **2003**, *125*, 11291-11298; k) Z. Tang, X. Chen, X. Pang, Y. Yang, X. Zhang, X. Jing, *Biomacromolecules*, **2004**, *5*, 965-970; l) K. Majerska, A. Duda, *J. Am. Chem. Soc.* **2004**, *126*, 1026-1027; m) P. Hormnirun, E. L. Marshall, V. C. Gibson, A. J. P. White, D. J. Williams, *J. Am. Chem. Soc.* **2004**, *126*, 2688-2689; n) N. Nomura, R. Ishii, Y. Yamamoto, T. Kondo, *Chem Eur. J.* **2007**, *13*, 4433-4451; o) H. Du, X. Pang, H- Yu, X. Zhuang, X. Chen, D. Cui, X. Wang, X. Jing, *Macromolecules* **2007**, *40*, 1904-1913; p) M. H. Chisholm, J. C. Gallucci, K. T. Queisenberry, Z. Zhou, *Inorg. Chem.* **2008**, *47*, 2613-2624; q) A. Alaaeddine, C. M. Thomas, T. Roisnel, J.-F. Carpentier, *Organometallics* **2009**, *28*, 1469-1475; r) H.-L. Chen, S. Dutta, P.-Y. Huang, C.-C. Lin, *Organometallics*, **2012**, *31*, 2016-2025, s) C. K. A. Gregson, I. J. Blackmore, V. C. Gibson, N. J. Long, E. L. Marshall, A. J. P. White, *Dalton Trans.* **2006**, 3134-3140.

[8] Selected examples on Catalysts with SALALEN-type ligands for ROP of lactide monomers: a) E. L. Whitelaw, G. Loraine, M. F. Mahon, M. D. Jones, *Dalton Trans*. **2011**, *40*, 11469-11473; b) E. L. Whitelaw, M. D. Jones, M. F. Mahon, *Inorg. Chem.* **2010**, *49*, 3977-3979; c) E. L. Whitelaw, M. G. Davidson, M. D. Jones, *Chem. Commun.* **2011**, *47*, 10004-10006.

[9] N. Nakata, T. Toda, A. Ishii, *Polym. Rev.* **2011**, *2*, 1597-1610.

[10] T. Miyatake, K. Mizunuma, Y. Seki, M. Kakugo, *Makromol. Chem., Rapid Commun.* **1989**, *10*, 349-352.

[11] T. Miyatake, K. Mizunuma, M. Kakugo, *Makromol. Chem., Makromol. Symp.* **1993**, *66*, 203-214.

[12] J. Schaverien, A. J. van der Linden, A. G. Orpen, *J. Am. Chem. Soc.* **1995**, *117*, 3008-3021.

[13] R. D. Froese, D. G. Musaev, K. Morokuma, *J. Am. Chem. Soc.* **1997**, *119*, 7190-7196.

[14] R. D. Froese, D. G. Musaev, K. Morokuma, *Organometallics* **1999**, *18*, 373-379.

[15] C. Capacchione, A. Proto, H. Ebeling, R. Mülhaupt, K. Möller, T. P. Spaniol, J. Okuda, *J. Am. Chem. Soc.* **2003**, *125*, 4964-4965.

[16] S. D. Pastor, D. Z. Denney, *J. Heterocycl. Chem.* **1988**, *25*, 681–683.

[17] G.-J. Meppelder, K. Beckerle, R. Manivannan, B. Lian, G. Raabe, T. P. Spaniol, J. Okuda, *Chem Asian. J.* **2008**, *3*, 1312-1323.

[18] K. Marcsekova, C. Loos, F. Rominger, S. Doye, *Synlett* **2007**, *16*, 2564 – 2568.

[19] C. Hohberger, *Observation of Main Chain Chirality in Isotactic Polystyrene*, Dissertation, RWTH Aachen University, **2010**

[20] H. Ma, T. P. Spaniol, J. Okuda, *Inorg. Chem.* **2008**, *47*, 3328-3339.

[21] H. Ma, G. Melillo, L. Oliva, T. P. Spaniol, U. Englert, J. Okuda, *Dalton Trans.* **2005**, 721-727.

[22] H. Ma, T. P. Spaniol, J. Okuda, *Angew. Chem. Int. Ed.* **2006**, *45*, 7218-7821.

[23] A. Cohen, A. Yeori, I. Goldberg, M. Kol, *Inorg. Chem.* **2007**, *46*, 8114-8116.

[24] A. Ishii, T. Toda, N. Nakata, T. Matsuo, *J. Am. Chem. Soc.* **2009**, *131*, 13566-13567.

[25] E. Gerdes, *Qualitative Anorganische Analyse*, Springer Verlag Berlin, 2. Auflage, **2001**.

[26] K. Gademann; D. E. Chavez; E. N. Jacobsen, *Angew. Chem. Int. Ed.* **2002**, *41*, 3059-3061.

[27] J. Rosevear; J. F. K. Wilshire, *Aust. J. Chem.* **1985**, *38*, 1163-1176.

[28] E. T. Kiesewetter, S. Randoll, M. Radlaur, R. M. Waymouth, *J. Am. Chem. Soc.* **2010**, 132, 5566-5567.

[29] Organikum, 22. Auflage, *Wiley VCH*, Weinheim 2004

[30] J. B. Edson, Z. Wang, E. J. Kramer, G. W. Coates, *J. Am. Chem. Soc* **2008**, *130*, 4968 – 4977.

[31] E. A. B. Kantchev, C. J. O'Brien, M. G. Organ *Angew. Chem.* **2007**, *119*, 2824-2870.

[32] B. Lian, K. Beckerle, J. Okuda, unpublished results.

[33] F. Freeman, D. S. H. L. Kim, E. Rodriguez, *J. Org. Chem.* **1992**, *57*, 1722-1727.

# Chapter III

## Rare Earth Metal Silylamide Complexes with an OSSO-Type Bis(phenolate) Ligand

Parts of this chapter have already been published:

J.-C. Buffet, A. Kapelski, J. Okuda, *Macromolecules* **2010**, *43*, 10201-10203.

A. Kapelski, J.-C. Buffet, T. P. Spaniol, J. Okuda, *Chem. Asian J.* **2012**, *7*, 1320-1330.

# III. Rare Earth Metal Silylamide Complexes with an OSSO-Type Bis(phenolate) Ligand

## III.1. Introduction

Inspired by the syntheses of OSSO-type bis(phenolate) complexes of group 4 metals Zr, Ti and Hf by Okuda *et al.* in 2002,[1,2] bis(phenolate) complexes of rare earth metal alkyls,[3] –allyls,[6] –hydrides[3,4,7] and –silylamides[8-12] have been prepared. Rare earth metal bis(phenolate) complexes are highly air and moisture sensitive and have to be handled under careful exclusion of oxygen and moisture.

Rare earth metal bis(phenolate) alkyl complexes are typically prepared by treatment of metal tris(alkyl) precursors with one equivalent of an OSSO-type bis(phenol) (Scheme 3.1.). Almost exclusively tris(trimethylsilyl) metal precursors are used. Formation of readily volatile tetramethylsilane is the driving force of these reactions. NMR-spectroscopic analyses as well as X-ray diffraction studies confirmed monomeric structures of these complexes in solution and in the solid state with octahedral or distorted octahedral coordination around the metal centers.[3-5]

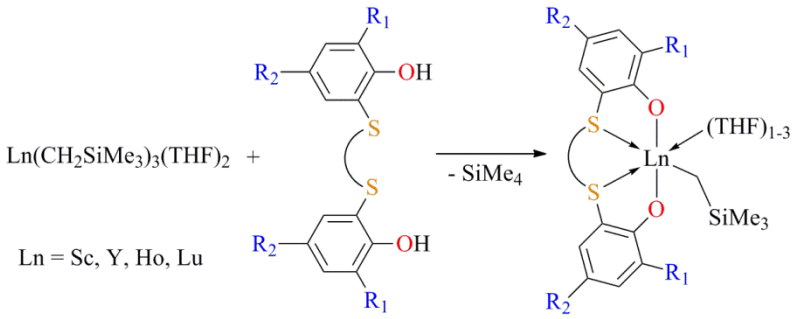


**Scheme 3.1.** Syntheses of rare earth metal alkyl complexes supported by an OSSO-type ligand.

Dimeric hydride complexes [Ho**L**$^5$($\mu$-H)THF]$_2$ and [Lu**L**$^5$($\mu$-H)THF]$_2$ were synthesized by treatment of [Ho**L**$^5$($CH_2SiMe_3$)$THF_{1-2}$] and [Lu**L**$^5$($CH_2SiMe_3$)$THF_{1-2}$] with phenylsilane, (Scheme 3.2.). These hydride species react with pyridin, olefins, $CO_2$, phenylacetylene or benzophenone via insertion into the Ln-H bond.[3-4]

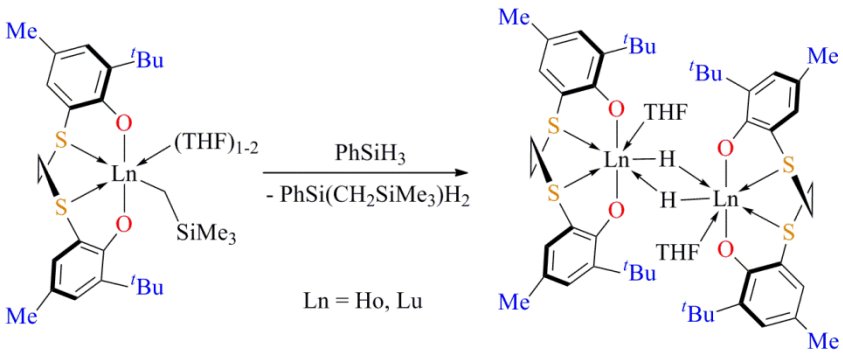


**Scheme 3.2.** Formation of dimeric holmium and lutetium bis(phenolate) hydride complexes.

Rare earth metal bis(phenolate) allyl complexes are prepared by propene elimination reactions at tris(allyl) metal precursors after addition of bis(phenols) (Scheme 3.3.). These complexes show remarkable activity in hydrosilylation of olefins.[6]

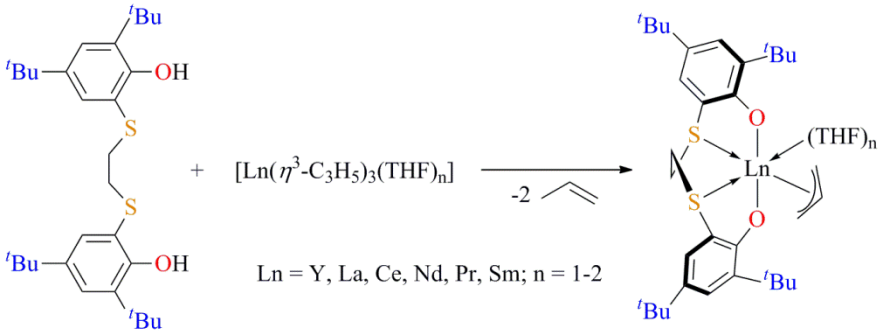


**Scheme 3.3.** Preparation of rare earth metal bis(phenolate) allyl complexes.

Silylamide complexes [Ln**L**$^{x}${N(SiMe$_2$H)$_2$}(THF)] are synthesized by amine elimination reaction from rare earth metal tris(silylamide) precursors [Ln{N(SiMe$_2$H)$_2$}$_3$(THF)$_x$] (Ln = Sc, x = 1; Ln = Y, Lu, La, Sm, x = 2) by one equivalent of bis(phenol) under slightly varying conditions.[9-11] Table 3.1. gives an overview about reported rare earth metal silylamide bis(phenolate) compounds.

Silylamide complexes of Sc, Y and Lu bearing a 5–5–5 chelating OSSO-type ligand are prepared by amine elimination reaction at rare earth metal tris(silylamide) precursors with one equivalent of 5-5-5 chelating bis(phenol) in toluene, *n*-pentane or benzene (Scheme 3.4.).

**Table 3.1.** Rare earth metal bis(phenolate) silylamide complexes.

| Chelate | Bridge | | Metal | $R_1$ | $R_2$ | Complex | Ref. |
|---|---|---|---|---|---|---|---|
| 5–5–5 | $C_2$ | $(CH_2)_2$ | Sc | $^t$Bu | Me | [Sc**L**$^5${N(SiMe$_2$H)$_2$}(THF)] | 9-11 |
| | | | Y | $^t$Bu | Me | [Y**L**$^5${N(SiMe$_2$H)$_2$}(THF)] | 9-11 |
| | | | Lu | $^t$Bu | Me | [Lu**L**$^5${N(SiMe$_2$H)$_2$}(THF)] | 9-11 |
| | | | Sc | $^t$Bu | $^t$Bu | [Sc**L**$^6${N(SiMe$_2$H)$_2$}(THF)] | 9 |
| | | | Lu | $^t$Bu | $^t$Bu | [Lu**L**$^6${N(SiMe$_2$H)$_2$}(THF)] | 9 |
| | | | Sc | CMe$_2$Ph | CMe$_2$Ph | [Sc**L**$^9${N(SiMe$_2$H)$_2$}(THF)] | 10-11 |
| | | | Y | CMe$_2$Ph | CMe$_2$Ph | [Y**L**$^9${N(SiMe$_2$H)$_2$}(THF)] | 11 |
| | |  | Sc | $^t$Bu | Me | [Sc**L**$^{10}${N(SiMe$_2$H)$_2$}(THF)] | 10-11 |
| | | | Y | $^t$Bu | Me | [Y**L**$^{10}${N(SiMe$_2$H)$_2$}(THF)] | 11 |
| | | | Lu | $^t$Bu | Me | [Lu**L**$^{10}${N(SiMe$_2$H)$_2$}(THF)] | 11 |
| 5–6–5 | $C_3$ | $(CH_2)_3$ | Sc | $^t$Bu | Me | [Sc**L**$^{15}${N(SiMe$_2$H)$_2$}(THF)] | 9-11 |
| | | | Lu | $^t$Bu | Me | [Lu**L**$^{15}${N(SiMe$_2$H)$_2$}(THF)] | 9 |
| | | | Y | $^t$Bu | $^t$Bu | [Y**L**$^{16}${N(SiMe$_2$H)$_2$}(THF)] | 9,11,13 |
| | | | Lu | $^t$Bu | $^t$Bu | [Lu**L**$^{16}${N(SiMe$_2$H)$_2$}(THF)] | 9 |
| 5–7–5 | $C_4$ |  | Sc | $^t$Bu | Me | [Sc**L**$^{18}${N(SiMe$_2$H)$_2$}(THF)] | 10-11 |
| | | | Y | $^t$Bu | Me | [Y**L**$^{18}${N(SiMe$_2$H)$_2$}(THF)] | 11 |
| | | | Lu | $^t$Bu | Me | [Lu**L**$^{18}${N(SiMe$_2$H)$_2$}(THF)] | 11 |
| | | | Y | CMe$_2$Ph | CMe$_2$Ph | [Y**L**$^{19}${N(SiMe$_2$H)$_2$}(THF)] | 11 |
| | | | Sc | ada | Me | [Sc**L**$^{20}${N(SiMe$_2$H)$_2$}(THF)] | 10-11 |
| | |  | Sc | $^t$Bu | Me | [Sc**L**$^{21}${N(SiMe$_2$H)$_2$}(THF)] | 10-11 |
| | | | Y | $^t$Bu | Me | [Y**L**$^{21}${N(SiMe$_2$H)$_2$}(THF)] | 11 |

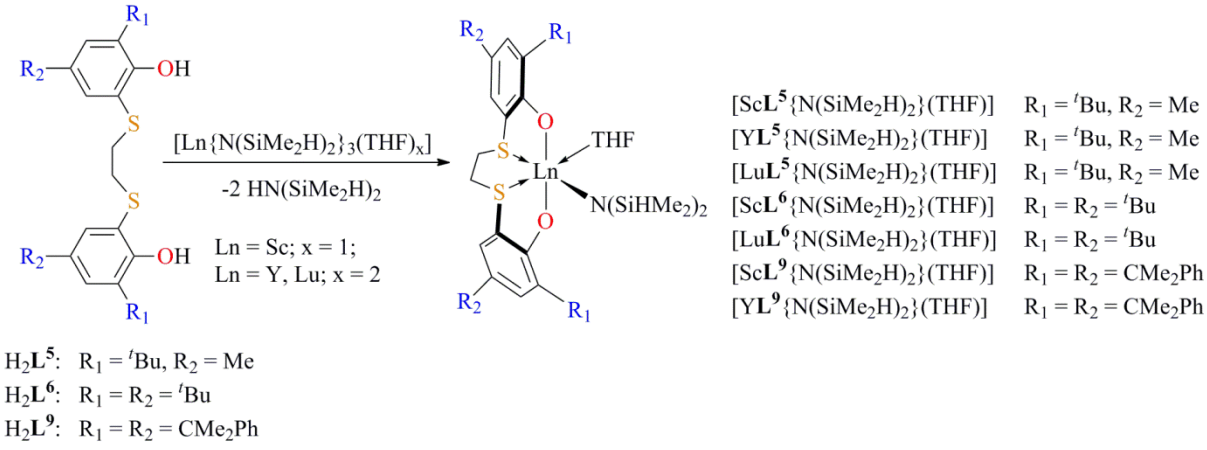


**Scheme 3.4.** Syntheses of rare earth metal silylamide complexes ligated by a 5-5-5 chelating OSSO-type bis(phenolate) ligands.

All complexes show fluxional behavior in solution. Commonly, the THF dissociation on the NMR time scale is fast and leads to pseudo-five coordinated metal centers with either a trigonal bipyramidal $C_2$ or square pyramidal $C_s$-symmetry. In lutetium complexes [Lu**L**$^5${N(SiMe$_2$H)$_2$}(THF)] and [Lu**L**$^6${N(SiMe$_2$H)$_2$}(THF)], THF dissociation seems to occur easier than in analogous Sc- or Y-complexes.[9]

In terms of fluxionality, yttrium complexes [Y**L**$^5${N(SiMe$_2$H)$_2$}(THF)] and [Y**L**$^9${N(SiMe$_2$H)$_2$}(THF)] are more fluxional in solution than their scandium analogues as indicated by broadening of $^1$H NMR resonances for the protons of the ethylene bridge and of the *ortho*-groups.[9,11]

After the reaction of Sc{N(SiHMe$_2$)$_2$}$_3${LiN(SiHMe$_2$)$_2$(THF)}] and H$_2$**L**$^5$, three different products, [Sc**L**$^5${N(SiMe$_2$H)$_2$}(THF)], [Sc**L**$^5${N(SiMe$_2$H)$_2$}][Li(THF)] and lithiated bis(phenol) Li$_2$**L**$^5$ were developed (Scheme 3.5.).[9]

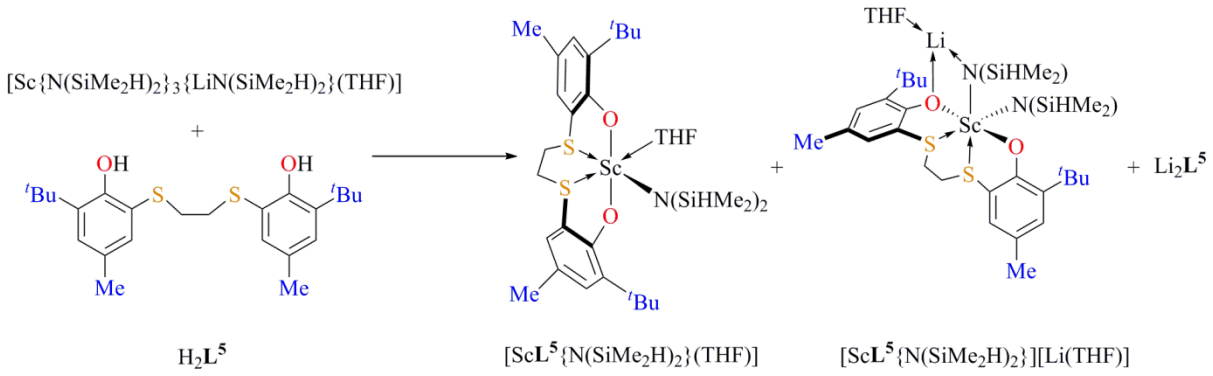


**Scheme 3.5.** Reaction of [Sc{N(SiMe$_2$H)$_2$}$_3${LiN(SiMe$_2$H)$_2$(THF)}] with H$_2$**L**$^5$.

Reaction of racemic 5–5–5 chelating OSSO-type bis(phenol) H$_2$**L**$^{10}$ with silylamide precursors affords corresponding silylamide bis(phenolate) complexes (Scheme 3.6.). [Sc**L**$^{10}${N(SiMe$_2$H)$_2$}(THF)] shows rigid $C_1$ symmetry while [Y**L**$^{10}${N(SiMe$_2$H)$_2$}(THF)] and [Lu**L**$^{10}${N(SiMe$_2$H)$_2$}(THF)] possesses higher symmetry in solution ($C_2$ (trigonal bipyramidal) and $C_s$ symmetry (square pyramidal)).[10-11]

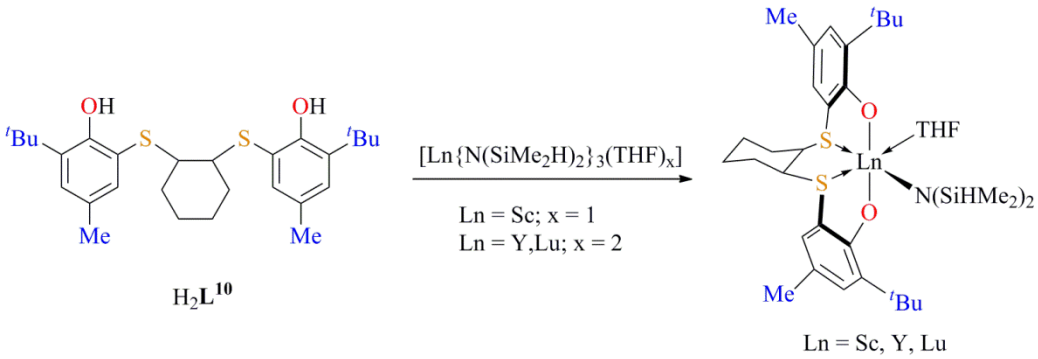


**Scheme 3.6.** Syntheses of Sc-, Y- and Lu-silylamide complexes with a racemic 5–5–5 chelating OSSO-type ligand.

Rare earth metal silylamide complexes bearing a 5–6–5 chelating OSSO-type ligand (Scheme 3.7.) shows fluxional behavior in solution, due to the flexible backbone and commonly reversible THF dissociation on NMR time scale.[9] While Sc**L**$^{15}${N(SiMe$_2$H)$_2$}(THF)] adopts a distorted octahedral geometry with the silylamide group ligated *cis* to THF and *trans* to one of the sulfur donors of the bis(phenolate) ligand,[9] the yttrium center in [Y**L**$^{16}${N(SiMe$_2$H)$_2$}(THF)] adopts a distorted trigonal prismatic geometry. The two oxygen donors of the bis(phenolate) ligand are *cis* coordinated.

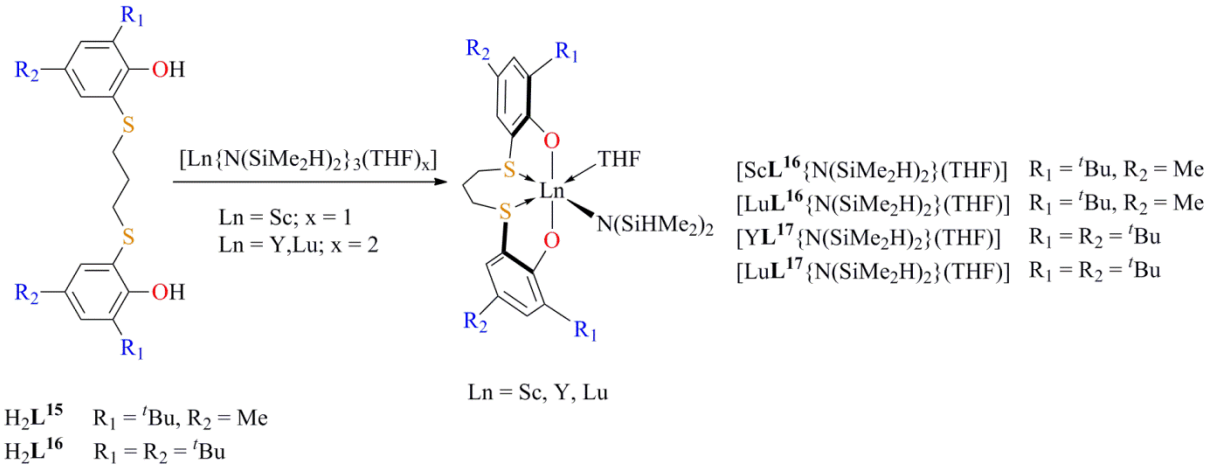


**Scheme 3.7.** Syntheses of rare earth metal silylamide complexes with a 5–6–5 chelating OSSO-type ligand.

Sc-, Y- and Lu-silylamide complexes bearing 5–7–5 chelating OSSO-type ligands are accessible by amine elimination reaction at silylamide precursors in toluene or *n*-hexane (Scheme 3.8.).

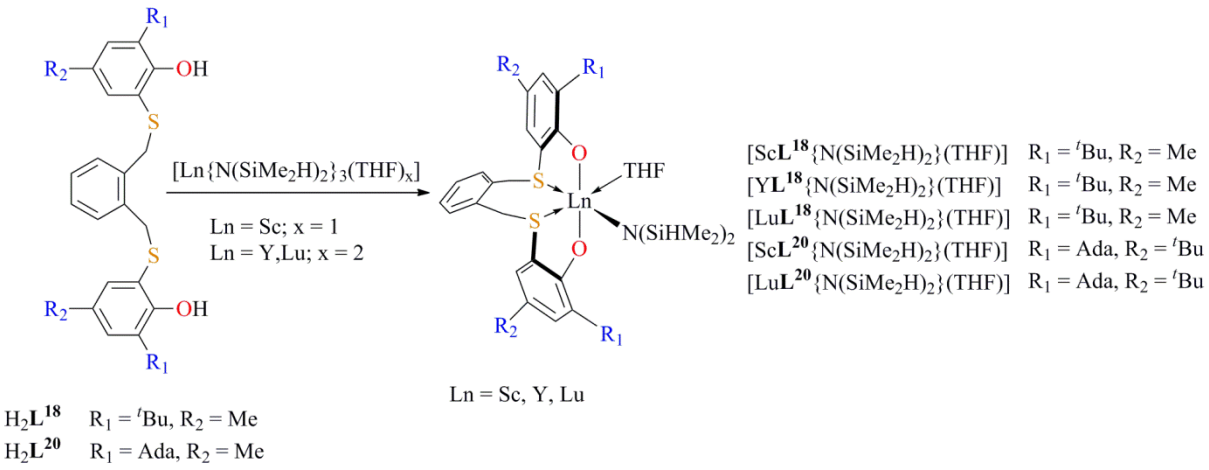


**Scheme 3.8.** Reaction of rare earth metal silylamide precursors with 5–7–5 chelating OSSO-type bis(phenols) $H_2\mathbf{L}^{18}$ and $H_2\mathbf{L}^{20}$.

X-ray diffraction analysis of [Y$\mathbf{L}^{18}${$N(SiMe_2H)_2$}(THF)] confirmed that both enantiomers have a distorted octahedral $C_1$-symmetric structure with the silylamide group ligated *cis* to THF and *trans* to one of the sulfur atoms with slightly decreased angles, due to the larger metal radius.[10-11] The Sc-complexes showed either $C_2$ or $C_s$-symmetry, similar to already reported findings.[9-11,14]

Reaction of [Sc{$N(SiHMe_2)_2$}$_3$(THF)] with 5-7-5 chelating bis(phenols) $H_2\mathbf{L}^{18}$ and $H_2\mathbf{L}^{20}$ afforded two THF-free Sc-complexes [Sc$\mathbf{L}^{18}${$N(SiMe_2H)_2$}] and [Sc$\mathbf{L}^{20}${$N(SiMe_2H)_2$}]. They were isolated after prolonged drying of the THF containing compounds.[10-11]

Reaction of [Sm{$N(SiHMe_2)_2$}$_3$$(THF)_2$] with $H_2\mathbf{L}^{18}$ afforded the expected product [Sm$\mathbf{L}^{18}${$N(SiHMe_2)_2$}(THF)]. Similar reaction of [La{$N(SiHMe_2)_2$}$_3$$(THF)_2$] afforded crystals of dinuclear $C_1$-symmetric [$La_2(\mathbf{L}^{18})_3$]. NMR spectroscopic data and X-ray diffraction analysis showed a complex consisting of a cationic fragment **[**La$\mathbf{L}^{18}$**]**$^+$ as well as an anionic fragment **[**La$(\mathbf{L}^{18})_2$**]**$^-$.[11] No THF or silylamide group is attached to the metal center.[11]

Treatment of [$La_2(\mathbf{L}^{18})_3$] with [La{$N(SiMe_2H)_2$}$_3$$THF_2$] in $C_6D_6$ led to monomeric [La$\mathbf{L}^{18}${$N(SiMe_2H)_2$}THF], but presence of $HN(SiHMe_2)_2$ in the NMR spectra indicated significant decomposition.[11]

Syntheses of [Sc$\mathbf{L}^{21}${$N(SiMe_2H)_2$}(THF)] and [Y$\mathbf{L}^{21}${$N(SiMe_2H)_2$}THF] bearing a racemic 5–7–5 chelating OSSO-type ligand were accomplished by treating [M{$N(SiMe_2H)_2$}$_3$$(THF)_x$] with one equivalent of $H_2\mathbf{L}^{21}$ in *n*-pentane (Scheme 3.9.).[10]

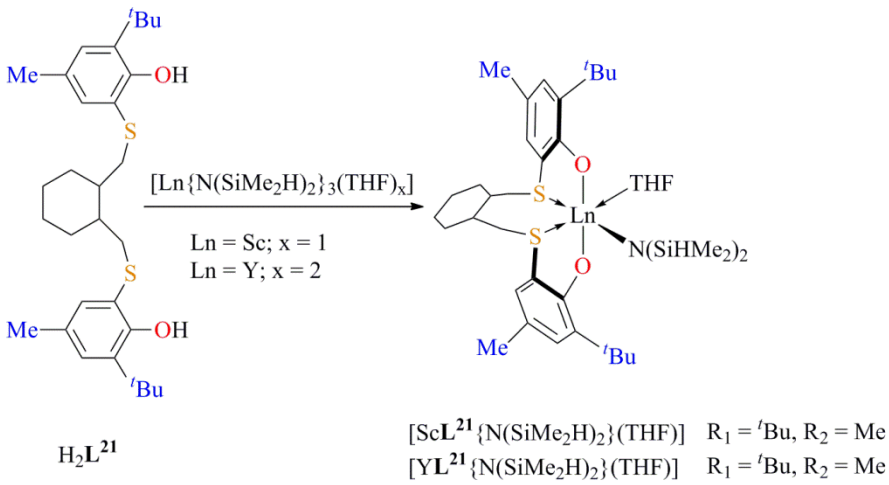


**Scheme 3.9.** Syntheses of [Sc$\mathbf{L}^{21}${$N(SiMe_2H)_2$}THF] and [Y$\mathbf{L}^{21}${$N(SiMe_2H)_2$}THF].

The silylamide group in these complexes can easily be removed by a *β*-diketonato or alkoxy group indicating the applicability of these complexes as initiators for ROP of lactide.[9-11,14]

## III.2. Results and Discussion

The bis(phenols) reported in chapter II are treated with rare earth metal silylamide precursors to give monomeric complexes [Ln$\mathbf{L}^{x}${$N(SiMe_2H)_2$}(THF)]. The monomeric structure of these complexes is shown by NMR spectroscopic analysis, elemental analysis and X-ray diffraction analysis.

### III.2.1. Syntheses of Rare Earth Metal Silylamide Precursors

Following literature procedures, H{$N(SiMe_2H)_2$} was lithiated with *n*-BuLi to give Li{$N(SiMe_2H)_2$} (**18**) in nearly quantitative yield. Subsequent reaction of **18** with $ScCl_3$ or $YCl_3$ in THF results in formation of [Sc{$N(SiMe_2H)_2$}$_3$(THF)] (**19**) or [Y{$N(SiMe_2H)_2$}$_3$(THF)] (**20**) in yields close to literature data (Scheme 3.10.).[15,16,24]

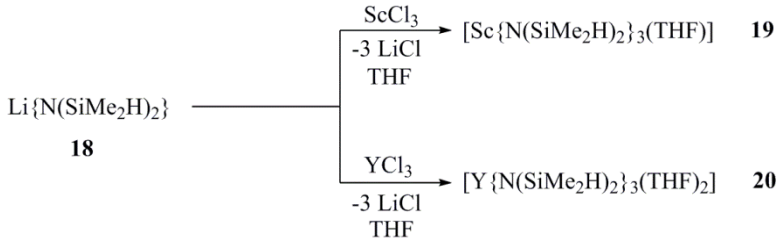


**Scheme 3.10.** Syntheses of [Sc{N(SiMe$_2$H)$_2$}$_3$(THF)] (**19**) and [Y{N(SiMe$_2$H)$_2$}(THF)$_2$] (**20**).

## III.2.2. Syntheses of Rare Earth Metal Bis(phenolate) Silylamide Complexes

### III.2.2.1 Syntheses of Rare Earth Metal Silylamide Complexes Bearing a 5-4-5 Chelating OSSO-Type Bis(phenolate) Ligand.

Following the well established amine elimination pathway,[9-11,13] **19** and **20** were treated with bis(phenols) H$_2$**L**$^{24\text{-}26}$ resulting in formation of bis(phenolate) silylamide complexes [Sc**L**$^{24\text{-}26}${N(SiMe$_2$H)$_2$}(THF)] and [Y**L**$^{24\text{-}26}${N(SiMe$_2$H)$_2$}(THF)] (Scheme 3.11.).

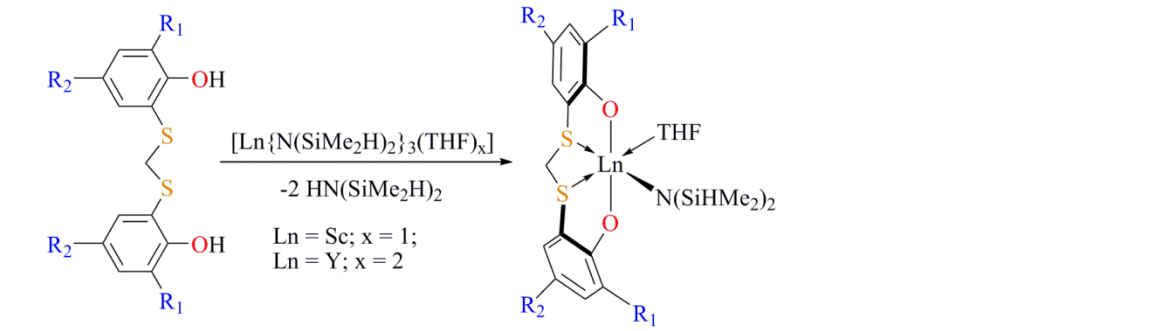


H$_2$**L**$^{24}$: $R_1 = R_2 = {}^t$Bu
H$_2$**L**$^{25}$: $R_1 = R_2 = CMe_2Ph$
H$_2$**L**$^{26}$: $R_1$ = 1-Methylcyclohexyl, $R_2$ = Me

[Sc**L**$^{24}${N(SiMe$_2$H)$_2$}(THF)] $R_1 = R_2 = {}^t$Bu
[Y**L**$^{24}${N(SiMe$_2$H)$_2$}(THF)] $R_1 = R_2 = {}^t$Bu
[Sc**L**$^{25}${N(SiMe$_2$H)$_2$}(THF)] $R_1 = R_2 = CMe_2Ph$
[Y**L**$^{25}${N(SiMe$_2$H)$_2$}(THF)] $R_1 = R_2 = CMe_2Ph$
[Sc**L**$^{26}${N(SiMe$_2$H)$_2$}(THF)] $R_1$ = 1-Methylcyclohexyl $R_2$ = Me
[Y**L**$^{26}${N(SiMe$_2$H)$_2$}(THF)] $R_1$ = 1-Methylcyclohexyl $R_2$ = Me

**Scheme 3.11.** Syntheses of Sc- and Y-bis(phenolate) silylamide complexes bearing 5–4–5 chelating OSSO-type ligands.

All complexes were isolated as oxygen and moisture sensitive, light yellow or colorless powders in moderate yields ([Sc**L**$^{24}${N(SiMe$_2$H)$_2$}(THF)] 42%; [Y**L**$^{24}${N(SiMe$_2$H)$_2$}(THF)] 54%; [Sc**L**$^{25}${N(SiMe$_2$H)$_2$}(THF)] 63%; [Y**L**$^{25}${N(SiMe$_2$H)$_2$}(THF)] 57%; [Sc**L**$^{26}${N(SiMe$_2$H)$_2$}(THF)] 57%; [Y**L**$^{26}${N(SiMe$_2$H)$_2$}THF] 62%). NMR spectroscopic and elemental analyses of most of the complexes show one silylamide group, one OSSO-type bis(phenolate) ligand and one THF molecule attached to the metal center. Due to incomplete combustion, elemental analysis of some complexes deviate from their theoretical values.

Figure 3.1. shows the $^1$H NMR spectrum of [Y**L**$^{24}${N(SiMe$_2$H)$_2$}(THF)] in $C_6D_6$ at 25 °C to illustrate the characteristic signals for these complexes.

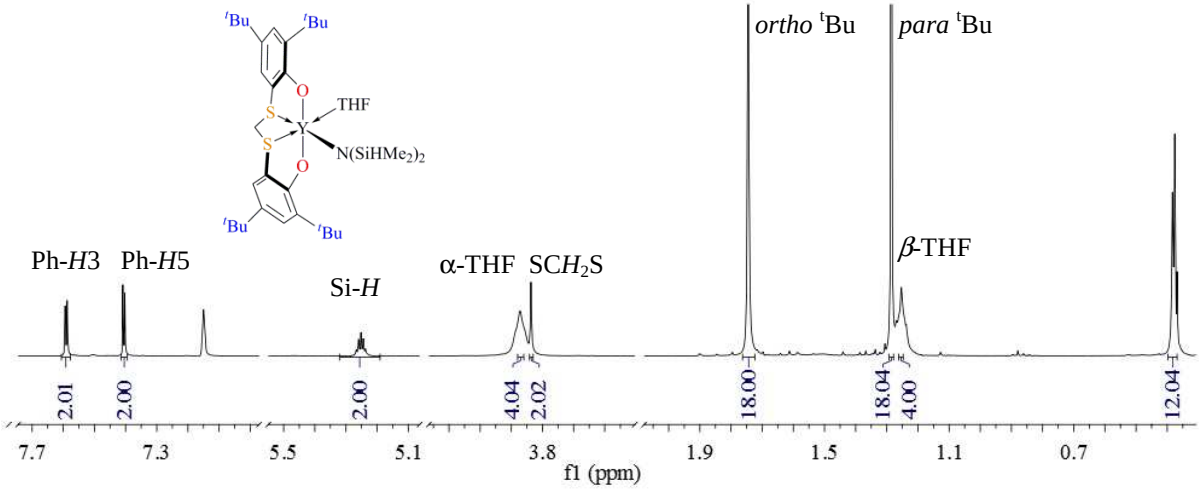


**Figure 3.1.** $^1$H NMR spectrum of [Y**L**$^{24}${N(SiMe$_2$H)$_2$}(THF)] in $C_6D_6$ at 25 °C.

For the silylamide group a doublet at 0.38 ppm represents the methyl groups coupling with the Si*H*-proton giving a septet at 5.18 ppm. Broad signals at 1.20 and 3.81 show the coordination of one THF molecule to yttrium. The $^t$Bu groups in *ortho* and *para*-position of the phenolate moieties give two signals at 1.29 and 1.75 ppm. The signal for the SC*H*$_2$S protons appears at a chemical shift of 3.80 ppm differing marginally from the corresponding signals of proligand H$_2$**L**$^{24}$ (3.93 ppm). Another typical signal for OSSO-type bis(phenolate) complexes arises at around 160 ppm in the $^{13}$C{$^1$H} NMR spectrum representing the *ipso* carbon of the phenolate moieties.[9-12] For [Y**L**$^{24}${N(SiMe$_2$H)$_2$}(THF)] this resonance arises at 165.6 ppm. For H$_2$**L**$^{24}$ the *ipso* carbon signal arises at 153.0 ppm. [Sc**L**$^{24}${N(SiMe$_2$H)$_2$}THF] shows similar signals. Resulting from the rigid geometry around the scandium center in

[Sc**L**$^{25}${N(SiMe$_2$H)$_2$}(THF)], SC*H*$_2$S protons are diastereotopic as indicated by two broad signals at 3.50 and 3.64 ppm. Two broad resonances at 1.0-1.5 ppm and 3.0-4.1 ppm show a THF attached to the metal center. The broad signals indicate expected reversible THF dissociation on the NMR time scale. A septet at 5.1 ppm is assigned to the Si*H*Me$_2$ protons and a doublet at ca. 0.5 ppm is assigned to Si*Me*$_2$H of the amide ligand. The coupling constant $^1J_{SiH}$ = 170-180 Hz indicates a weak *β*-Si-H interaction with the metal.[15,16] The $^{13}C\{^1H\}$ NMR spectrum shows the resonance of the *ipso* carbon at 151.8 ppm. While [Y**L**$^{25}${N(SiMe$_2$H)$_2$}(THF)] displays basically the same sets of signals at similar chemical shifts as [Sc**L**$^{25}${N(SiMe$_2$H)$_2$}(THF)], signals are broader due to lower rigidity as a consequence of the larger ionic radius of Y. This observation is typical for the comparison of Sc and Y-complex and estimates the Sc complexes to be more selective in the ROP of lactide.

For [Sc**L**$^{26}${N(SiMe$_2$H)$_2$}(THF)] and [Y**L**$^{26}${N(SiMe$_2$H)$_2$}(THF)], signals for the 1-methylcyclohexyl groups between 1.00 and 2.10 ppm are relatively broad, indicating fluxionality of the 1-methylcyclohexyl groups at 25 °C. The short 1,3-dithiaalkanediyl bridge effects a close vicinity of the 1-methylcyclohexyl groups where both groups avoid close contact in solution.[8] All other signals of [Ln**L**$^{26}${N(SiMe$_2$H)$_2$}(THF)] (Ln = Sc, Y) are similar to the signals for [Ln**L**$^{24\text{-}25}${N(SiMe$_2$H)$_2$}(THF)].

### III.2.2.2. Syntheses of Rare Earth Metal Silylamide Complexes Bearing a 5-5-5 Chelating OSSO-Type Bis(phenolate) ligand.

Amine elimination reaction from **19** and **20** with 5-5-5 chelating bis(phenol) H$_2$**L**$^{27}$ gave bis(phenolate) silylamide complexes [Sc**L**$^{27}${N(SiMe$_2$H)$_2$}(THF)] and [Y**L**$^{27}${N(SiMe$_2$H)$_2$}(THF)] (Scheme 3.12.).

[Sc**L**$^{27}${N(SiMe$_2$H)$_2$}(THF)] and [Y**L**$^{27}${N(SiMe$_2$H)$_2$}(THF)] were characterized by NMR spectroscopy. The $^1$H NMR spectrum of [Y**L**$^{27}${N(SiMe$_2$H)$_2$}(THF)] (Figure 3.2.) shows the aromatic protons as two doublets and the Si-*H* protons as a septet. Two broad signals arise for one THF molecule attached to the metal center. The methyl groups in *para* position at the phenolate moiety form one sharp signal at 2.18 ppm while the 1-methylcyclohexyl groups form broad signals for the C*H*$_2$ protons between 1.88-1.97, 1.70-1.74 and 1.53-1.68 ppm. At 1.69 ppm, a signal for the CyC*H*$_3$ protons arises and a doublet at 0.43 ppm represents the N(Si*Me*$_2$H)$_2$ groups.

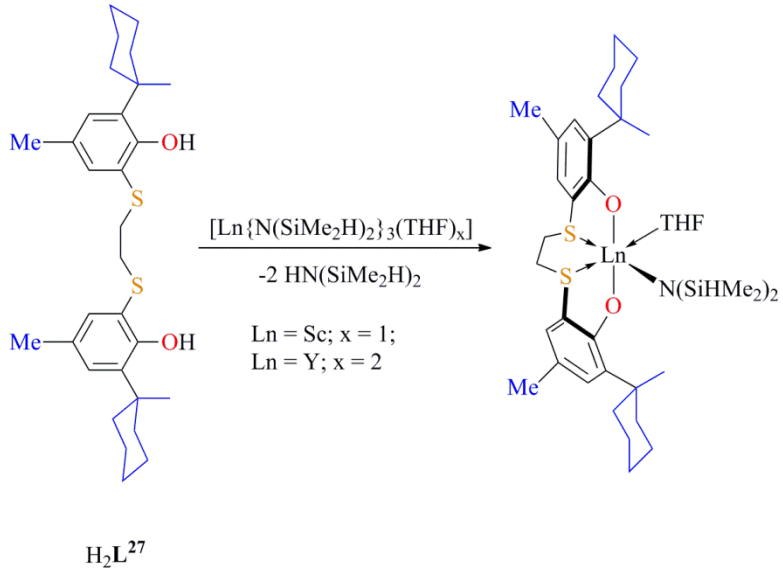


$H_2\mathbf{L}^{27}$

**Scheme 3.12.** Syntheses of [Sc$\mathbf{L}^{27}${N(SiMe$_2$H)$_2$}(THF)] and [Y$\mathbf{L}^{27}${N(SiMe$_2$H)$_2$}(THF)].

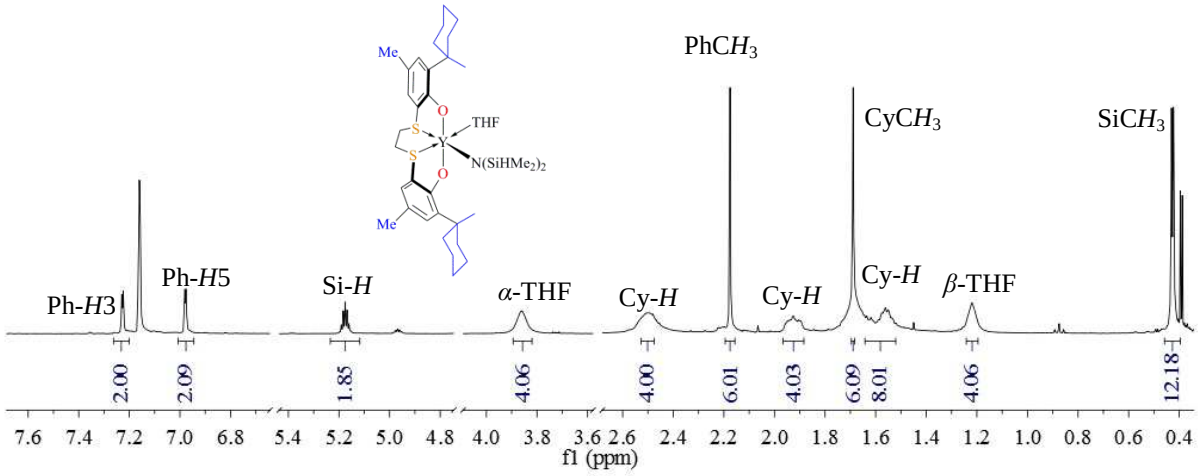


**Figure 3.2.** $^1$H NMR spectrum of [Y$\mathbf{L}^{27}${N(SiMe$_2$H)$_2$}(THF)] in $C_6D_6$ at 25 °C.

The $^1$H NMR spectrum of [Sc$\mathbf{L}^{27}${N(SiMe$_2$H)$_2$}(THF)] deviates from the spectrum of [Y$\mathbf{L}^{27}${N(SiMe$_2$H)$_2$}(THF)]. The signals of the aromatic protons split into 4 signals due to $C_1$ symmetry of the complex. The signal for the protons in $\alpha$ position at the attached THF molecule is splitted. Splitting of the signal for α-THF protons was observed previously for [Sc$\mathbf{L}^{5}${N(SiMe$_2$H)$_2$}(THF)][9], [Sc$\mathbf{L}^{6}${N(SiMe$_2$H)$_2$}(THF)][9] and [Sc$\mathbf{L}^{10}${N(SiMe$_2$H)$_2$}(THF)].[10]

[Sc$\mathbf{L}^{14,28\text{-}29}${N(SiMe$_2$H)$_2$}(THF)] and [Y$\mathbf{L}^{14,28\text{-}29}${N(SiMe$_2$H)$_2$}(THF)] were also synthesized by amine elimination. One equivalent of proligands $\mathbf{H_2L}^{14,28\text{-}29}$ was added slowly to a solution of **19** or **20** in benzene and reacted at 70 °C for 24 h. After work-up, colorless solids were

obtained in good yields ([Sc**L**$^{14}${N(SiMe$_2$H)$_2$}(THF)] 90%; [Sc**L**$^{28}${N(SiMe$_2$H)$_2$}(THF)] 67%; [Y**L**$^{14}${N(SiMe$_2$H)$_2$}(THF)] 54%; [Y**L**$^{28}${N(SiMe$_2$H)$_2$}(THF)] 61%; [Sc**L**$^{29}${N(SiMe$_2$H)$_2$}(THF)] 71% and [Y**L**$^{29}${N(SiMe$_2$H)$_2$}(THF)] 65%) (Scheme 3.13.). NMR spectra of all six complexes look similar. All these complexes bear two large cumyl groups on the phenolate moiety. The phenolate moieties are bridged by 1,2-dithiocycloalkanediyl bridges with varying ring sizes. The $^1$H NMR spectrum shows the SC*H* protons of the bridges as multiplet signals from 2.60-2.70 ppm. The amide group of [Ln**L**$^{28}${N(SiMe$_2$H)$_2$}(THF)] exhibits septet resonances at 5.10-5.20 ppm and a doublet around 0.30-0.50 ppm for the Si*Me*$_2$H-groups. For [Ln**L**$^{29}${N(SiMe$_2$H)$_2$}(THF)] broad multiplets indicate increased fluxionality within the backbone. Aromatic protons Ph-*H*3 und Ph-*H*5 are observed as two doublets around 7.5-7.7 ppm. The $^{13}$C{$^1$H} NMR spectra of [Ln**L**$^{14,28,29}${N(SiMe$_2$H)$_2$}(THF)] show resonances for the S*C*H carbon atoms at 50.0 ppm for [Ln**L**$^{28}${N(SiMe$_2$H)$_2$}(THF)]; at 52.5 ppm for [Ln**L**$^{14}${N(SiMe$_2$H)$_2$}(THF)] and at 55.0 ppm for [Ln**L**$^{29}${N(SiMe$_2$H)$_2$}(THF)]. An increasing ring size effects a minimal increase in the chemical shift. The *ipso*-carbon signals appear around 165-168 ppm.

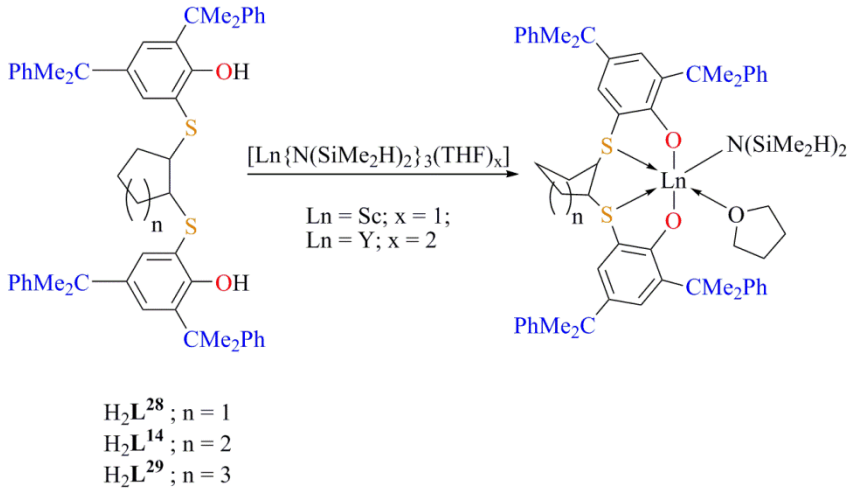


**Scheme 3.13.** Syntheses of [Sc**L**$^{14,28\text{-}29}${N(SiMe$_2$H)$_2$}(THF)] and [Y**L**$^{14,28\text{-}29}${N(SiMe$_2$H)$_2$}(THF)].

Single crystals of [Y**L**$^{14}${N(SiMe$_2$H)$_2$}(THF)] suitable for X-ray diffraction analysis were obtained by cooling a saturated *n*-pentane solution. The molecular structure is depicted in Figure 3.3. (Table A1, Appendix).

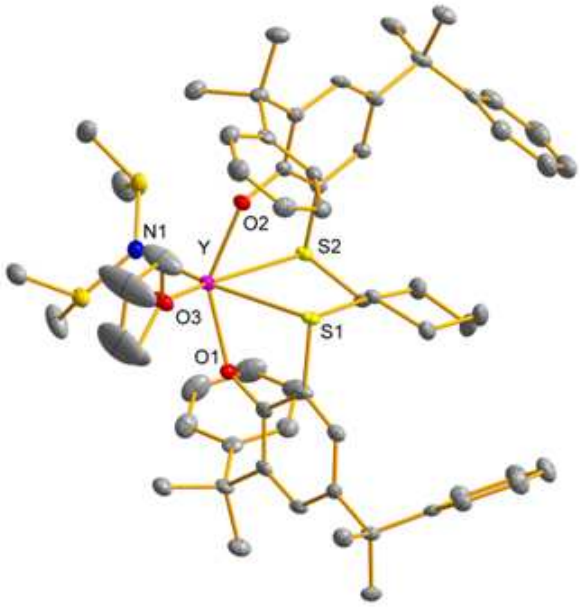


**Figure 3.3.** Molecular structure of [Y**L**$^{14}${N(SiMe$_2$H)$_2$}(THF)]. Hydrogen atoms are omitted for clarity. Selected bond lengths (Å) and angles (°): Y-O1 2.147(2), Y-O2 2.147(2), Y-O3 2.317(2), Y-S1 2.9641(8) Y-S2 2.8502(8), Y-N1 2.242(3); O1-Y-O2 143.64(8), S1-Y-S2 121.30(3), N1-Y-S1 173.74(7), N1-Y-O3 103.16(9), O3-Y-S2 153.58(6) and S1-Y-N1 173.74(7).

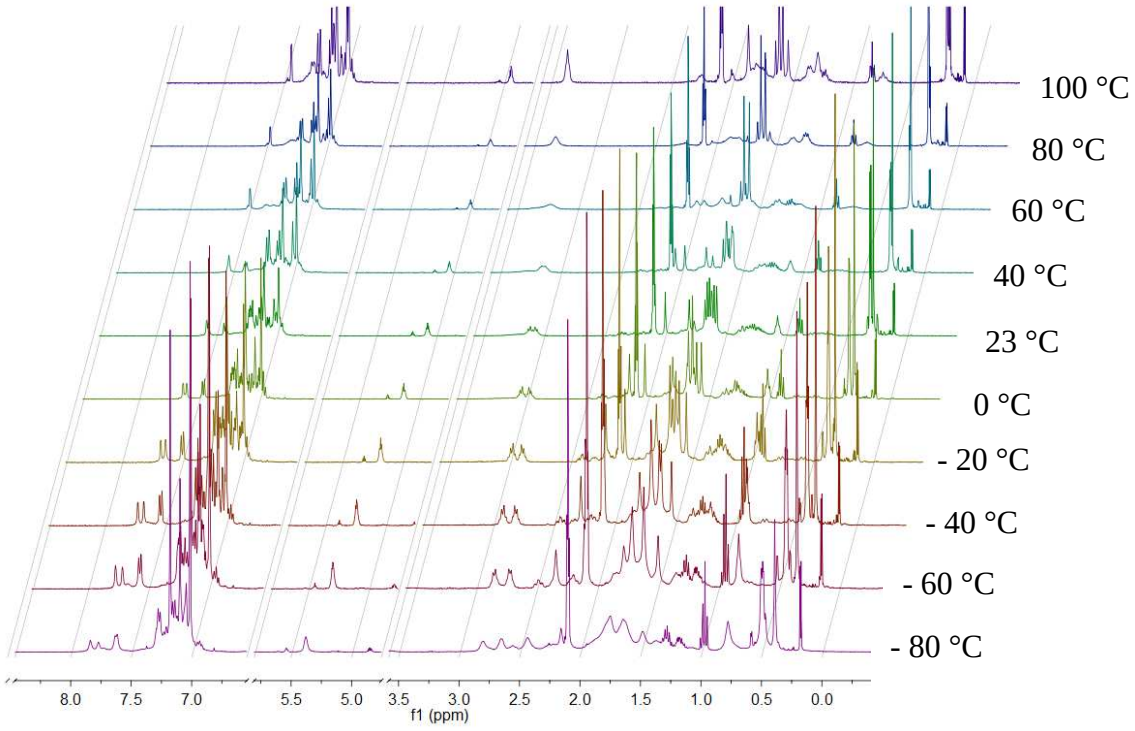


**Figure 3.4.** VT-NMR spectra of [Sc**L**$^{14}${N(SiMe$_2$H)$_2$}(THF)].

The yttrium center in [Y**L**$^{14}${N(SiMe$_2$H)$_2$}(THF)] is six-coordinate with a distorted octahedral geometry, bonded to the tetradentate bis(phenolate) ligand, the silylamide group and one THF ligand. This is a typical structure motif for rare earth metal silylamide bis(phenolate) complexes.[9-11]

Both enantiomers of the $C_1$-symmetric molecule are found in the centrosymmetric crystal. The two oxygen donors of the bis(phenolate) ligand are arranged *trans* to each other. The average Y-O(phenolate) bond lengths (2.147(2) Å in [Y**L**$^{14}${N(SiMe$_2$H)$_2$}(THF)]) are within the range of Y-O bond lengths in literature (2.104-2.177 Å).[17-19] The Y-N bond length of 2.242(3) Å is close to values found for yttrium amide precursors (2.229(4)-2.276(4) Å).[15]

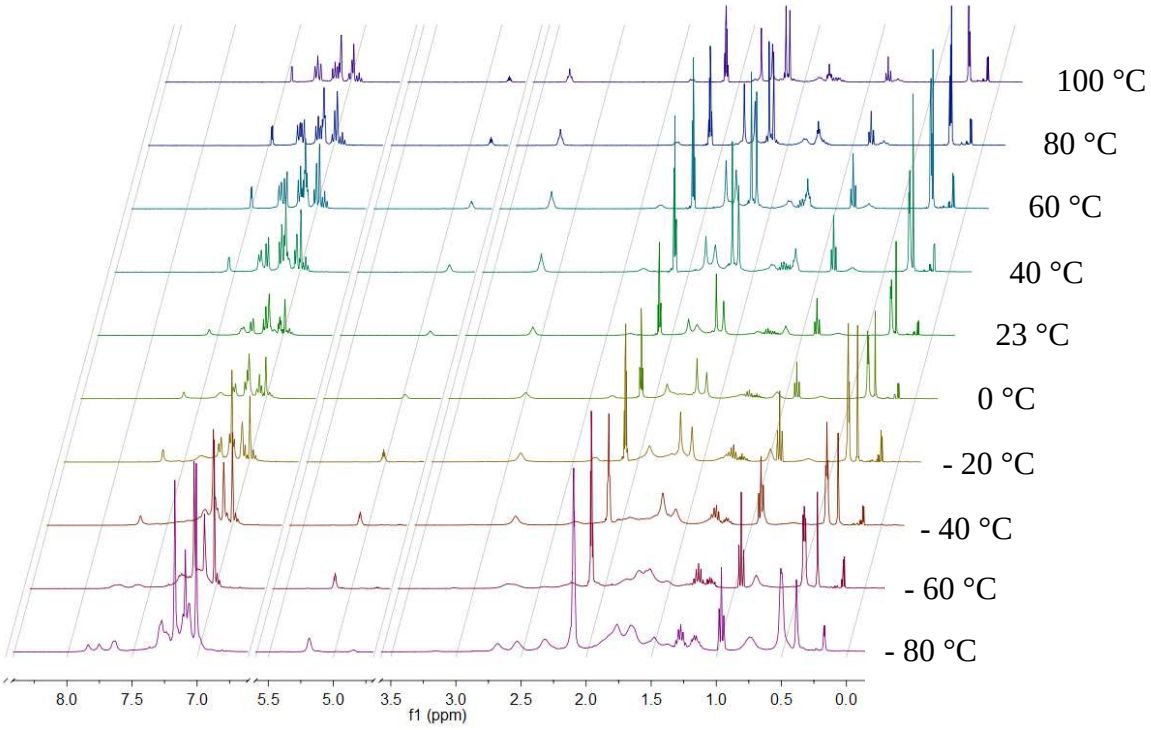


**Figure 3.5** VT-NMR spectra of [Y**L**$^{14}${N(SiMe$_2$H)$_2$}(THF)].

Variable temperature NMR spectroscopy[20-22] of [Sc**L**$^{14}${N(SiMe$_2$H)$_2$}(THF)] and [Y**L**$^{14}${N(SiMe$_2$H)$_2$}(THF)] shows both complexes to be fluxional in solution despite the stabilising influence of large *ortho*-substituents (Figures 3.4. and 3.5.).[23] Reversible THF-dissociation is suggested to origin this fluxionality. Dissociation of THF leads to a pseudo-five coordinated geometry with either trigonal bipyramidal $C_2$ or square pyramidal $C_s$ symmetry.[9] The signals of both complexes become sharper at higher temperatures showing

fast exchange of the protons. At a coalescence temperature $T_c$ = 303 K the signals coalesce with a corresponding rate constant of $k_{303}$ = 140 $s^{-1}$ for [Sc**L**$^{14}${N(SiMe$_2$H)$_2$}(THF)]. For [Y**L**$^{14}${N(SiMe$_2$H)$_2$}(THF)], $T_c$ = 203 and $k_{203}$ = 132 $s^{-1}$ were determined, indicating the Y-complex being more fluxional in solution than the Sc-complex. This derives the Sc-complex being more selective in catalytic applications than the corresponding Y-complex. At low temperature, the proton exchange slows down which can be seen from the signals of the $\alpha$-protons of THF splitting into two multiplets of equal intensity.

Similar fluxional behavior can be inferred for the other complexes presented in this chapter.

Treatment of **19** with enantipure (+)-(*S*,*S*)-H$_2$**L**$^{14}$ and (-)-(*R*,*R*)-H$_2$**L**$^{14}$ afforded enantiopure (*S*,*S*)-[Sc**L**$^{14}${N(SiMe$_2$H)$_2$}THF] and (*R*,*R*)-[Sc**L**$^{14}${N(SiMe$_2$H)$_2$}THF] (Scheme 3.14.).

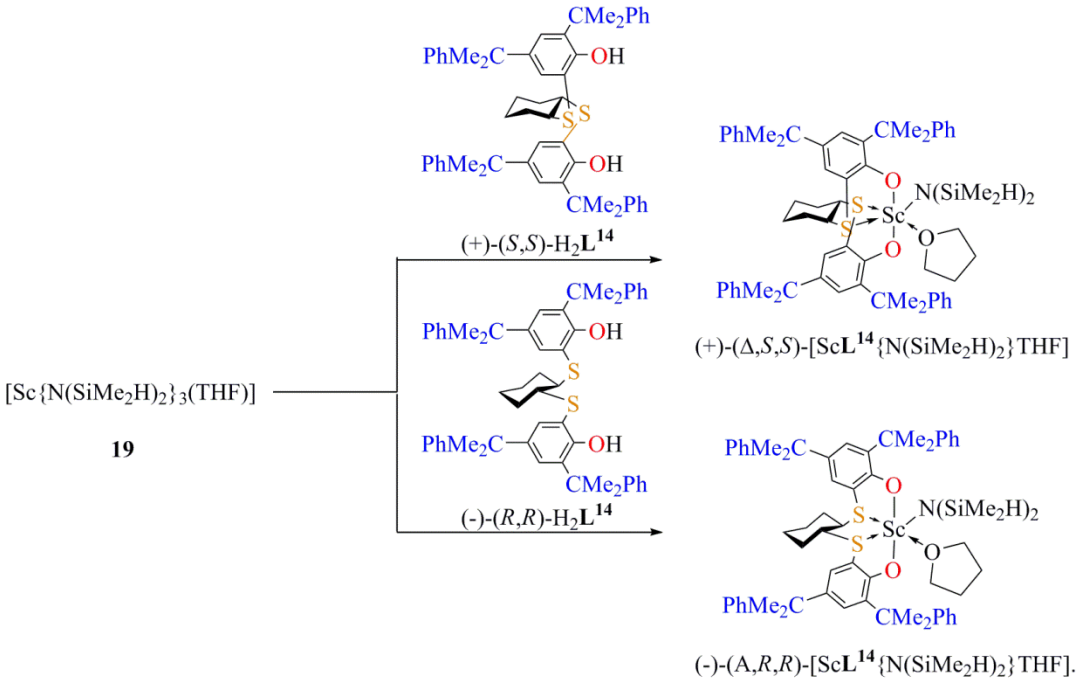


**Scheme 3.14.** Syntheses of (+)-(Δ,*S*,*S*)-[Sc**L**$^{14}${N(SiMe$_2$H)$_2$}(THF)] and (-)-(Λ,*R*,*R*)-[Sc**L**$^{14}${N(SiMe$_2$H)$_2$}(THF)].

## III.3. Summary

Reaction of 5-4-5 chelating OSSO-type bis(phenols) (H$_2$**L**$^{24}$, H$_2$**L**$^{25}$ and H$_2$**L**$^{26}$) and 5-5-5 chelating OSSO-type bis(phenols) (H$_2$**L**$^{14}$, (+)-(*S*,*S*)-H$_2$**L**$^{14}$, (-)-(*R*,*R*)-H$_2$**L**$^{14}$, H$_2$**L**$^{27}$, H$_2$**L**$^{28}$ and H$_2$**L**$^{29}$) with Sc- and Y-silylamide precursors **19** and **20** led to new monomeric

bis(phenolate) silylamide complexes [Ln**L**$^{x}${N(SiMe$_2$H)$_2$}(THF)] with Ln = Sc, Y. The complexes are air and moisture sensitive powders and were characterized by NMR spectroscopy, elemental analysis and X-ray diffraction of [Y**L**$^{14}${N(SiMe$_2$H)$_2$}(THF)]. Variable temperature NMR measurements of [Ln**L**$^{14}${N(SiMe$_2$H)$_2$}(THF)] were performed to proof fluxional behaviour in solution.

# III.4. Experimental Section

**Li{N(SiMe$_2$H)$_2$}**[16,24] (**18**)

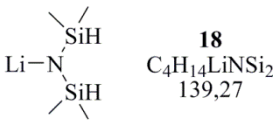

**18**
$C_4H_{14}LiNSi_2$
139,27

18.5 mL of a 2.5 M solution of *n*-BuLi in *n*-hexane was added slowly to a solution of 8.2 mL H{N(SiMe$_2$H)$_2$} (46.3 mmol, 1 equiv.) in 20 mL *n*-hexane at 0 °C. After stirring for 3 h at ambient temperature the solvent was removed under vacuum leaving a colorless powder that was further dried under vacuum for several hours. **18** was isolated as a colorless powder in a yield of 96% (6.2 g, 44.5 mmol). **$^1$H NMR** ($C_6D_6$, 25 °C, 400 MHz), δ (ppm): 0.22 (d, 12 H, $^3J_{HH}$ = 3.0 Hz, Si*Me*$_2$H), 4.63 (m, 2 H, SiMe$_2$*H*). **$^{13}$C{$^1$H} NMR** ($C_6D_6$, 25 °C, 100.1 MHz), δ (ppm): 4.20 (Si*Me*$_2$H).

---

**[Sc{N(SiMe$_2$H)$_2$}$_3$(THF)]**[15] (**19**)

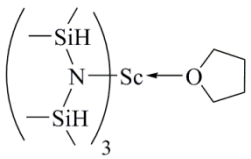

**19**
$C_{16}H_{50}ScN_3Si_6O$
514.06

2.09 g of **18** (15.2 mmol, 2.8 equiv.) were added slowly to a suspension of 2.0 g [$ScCl_3(THF)_3$] (5.4 mmol, 1 equiv.) in 50 mL *n*-hexane. After stirring for 18 h at ambient temperature, the reaction mixture was filtered and the white residue washed with 10 mL of *n*-hexane. The phases were combined and the product crystallized in the fridge for 3 days at

-30 °C to give **19** in a yield of 35% (1.38 g, 2.31 mmol). **$^{1}$H NMR** ($C_6D_6$, 25 °C, 400 MHz), δ (ppm): 0.38 (d, 36 H, $^{3}J_{HH}$ = 3.1 Hz, SiC*H*$_3$), 1.30 (m, 12 H, *β*-THF), 4.0 (m, 12 H, *α*-THF), 5.09 (m, 6 H, Si*H*). **$^{13}$C{$^{1}$H} NMR** ($C_6D_6$, 25 °C, 100.1 MHz), δ (ppm): 3.0 (Si*C*H$_3$), 25.1 (*β*-THF), 72.7 (*α*-THF).

---

**[Y{N(SiMe$_2$H)$_2$}$_3$(THF)$_2$]**[24] (**20**)

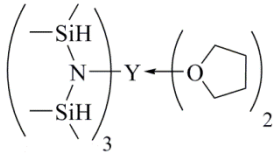

**20**
$C_{20}H_{58}YN_3Si_6O_2$
630.11

To a solution of 6.30 g (43.5 mmol, 2.8 equiv.) of **18** in 30 mL THF, 3.00 g (15.3 mmol, 1 equiv.) $YCl_3$ were added. The reaction mixture was stirred for 12 h at 25 °C. After removing the solvent under vacuum, the precipitate was dissolved in 10 mL *n*-hexane and recrystallized at −30 °C. The colorless crystals were dried under vacuum to give analytically pure **20** in a yield of 55% (5.30 g, 8.45 mol). **$^{1}$H NMR** ($C_6D_6$, 25 °C, 400 MHz), δ (ppm): 0.37 (d, 36 H, $^{3}J_{HH}$ = 3.1 Hz, SiC*H*$_3$), 1.36 (m, 8 H, *α*-THF), 3.86 (s, 8 H, *β*-THF), 4.99 (sept, 6 H, $^{3}J_{HH}$ = 3.0 Hz, Si*H*). **$^{13}$C{$^{1}$H} NMR** ($C_6D_6$, 25 °C, 100.1 MHz), δ (ppm): 3.4 (Si*C*H$_3$), 25.4 (*β*-THF), 70.9 (*α*-THF).

---

**[ScL$^{24}${N(SiMe$_2$H)$_2$}(THF)]**

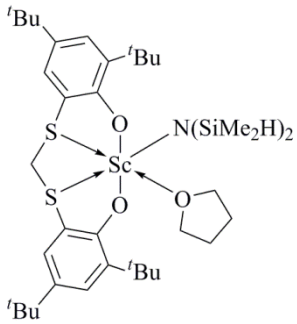

**[ScL$^{24}${N(SiMe$_2$H)$_2$(THF)]**
$C_{37}H_{64}NO_3S_2ScSi_2$
736.14

0.20 g of **19** (0.4 mmol, 1 equiv.) and 0.19 g of $H_2$**L**$^{24}$ (0.4 mmol, 1 equiv.) were dissolved in 2.5 mL of benzene and the solution was stirred for 24 h at 70 °C. After removing the solvent under vacuum, the colorless solid was recrystallized from *n*-pentane at −30 °C.

[Sc**L**$^{24}${N(SiMe$_2$H)$_2$}(THF)] was isolated as a colorless powder in 42% yield (0.12 g, 0.16 mmol). **$^1$H NMR** ($C_6D_6$, 25 °C, 400 MHz), δ (ppm): 0.49 ppm (d, $^3J_{HH}$ = 3.1 Hz, 12 H, Si(C*H*$_3$)$_2$), 1.24 (m, 4 H, *β*-THF), 1.37 (s, 18 H, C(C*H*$_3$)$_3$), 1.83 (s, 18 H, C(C*H*$_3$)$_3$), 3.71 (s, 2 H, SC*H*$_2$S), 4.10 (s, 4 H, *α*-THF), 5.40 (sept, $^3J_{HH}$ = 3.1 Hz, 2 H, Si*H*), 7.51 (d, $^4J_{HH}$ = 2.6 Hz, 2 H, Ph-*H*3), 7.71 (d, $^4J_{HH}$ = 2.6 Hz, 2 H, Ph-*H*5). **$^{13}$C{$^1$H} NMR** ($C_6D_6$, 25 °C, 100.1 MHz), δ (ppm): 3.3 (Si(*C*H$_3$)$_2$), 24.9 (*β*-THF), 30.0 (4-C(*C*H$_3$)$_3$), 31.7 (6-C(*C*H$_3$)$_3$), 34.2 (*C*(CH$_3$)$_3$), 35.4 (*C*(CH$_3$)$_3$), 50.8 (S*C*H$_2$S), 71.9 (*α*-THF), 123.8 (Ph-*C*2), 127.0 (Ph-*C*5), 129.0 (Ph-*C*3), 137.4 (Ph-*C*4), 139.2 (Ph-*C*6), 157.9 (Ph-*C*1). **Elemental analysis**, calculated for $C_{37}H_{64}NO_3S_2ScSi_2$ (736.2 g/mol) (%): C 60.37, H 8.76, N 1.90; Found: C 57.13, H 8.39, N 1.78.

---

**[YL$^{24}${N(SiMe$_2$H)$_2$}(THF)]**

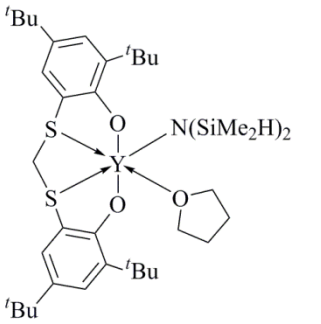


**[YL$^{24}${N(SiMe$_2$H)$_2$}(THF)]**
$C_{37}H_{64}NO_3S_2YSi_2$
780.10

0.20 g of **20** (0.4 mmol, 1 equiv.) and 0.20 g of H$_2$**L**$^{24}$ (0.4 mmol, 1 equiv.) were dissolved in 2.5 mL of benzene and the solution was stirred for 24 h at 70 °C. After removing the solvent under vacuum, the colorless precipitate was recrystallized from *n*-pentane at −30 °C. [Y**L**$^{24}${N(SiMe$_2$H)$_2$}(THF)] was isolated as a colorless powder in 54% yield (0.18 g, 0.22 mmol). **$^1$H NMR** ($C_6D_6$, 25 °C, 400 MHz), δ (ppm): 0.38 (d, $^3J_{HH}$ = 3.0 Hz, 12 H, Si(C*H*$_3$)$_2$), 1.20 (m, 4 H, *β*-THF), 1.29 (s, 18 H, C(C*H*$_3$)$_3$), 1.75 (s, 18 H, C(C*H*$_3$)$_3$), 3.81 (s, 2 H, SC*H*$_2$S), 3.86 (s, 4 H, *α*-THF), 5.18 (sept, $^3J_{HH}$ = 3.5 Hz, 2 H, Si*H*), 7.39 (d, $^4J_{HH}$ = 2.7 Hz, 2 H, Ph-*H*3), 7.61 (d, $^4J_{HH}$ = 2.7 Hz, 2H, Ph-*H*5). **$^{13}$C{$^1$H} NMR** ($C_6D_6$, 25 °C, 100.1 MHz), δ (ppm): 1.4 (Si(*C*H$_3$)$_2$), 24.1 (*β*-THF), 30.0 (4-C(*C*H$_3$)$_3$), 31.9 (6-C(*C*H$_3$)$_3$), 34.2 (4-*C*(CH$_3$)$_3$), 36.0 (6-*C*(CH$_3$)$_3$), 49.7 (S*C*H$_2$S), 69.9 (*α*-THF), 123.2 (Ph-*C*2), 127.2 (Ph-*C*5), 129.8 (Ph-*C*3), 138.1 (Ph-*C*4), 138.7 (Ph-*C*6), 165.6 (Ph-*C*1). **Elemental analysis**, calculated for $C_{37}H_{64}NO_3S_2YSi_2$ (780.1 g/mol) (%): C 56.97, H 8.27, N 1.80; Found: C 55.54, H 8.19, N 1.22.

**[ScL$^{25}${N(SiMe$_2$H)$_2$}(THF)]**

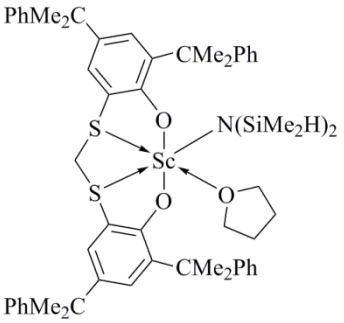


**[ScL$^{25}${N(SiMe$_2$H)$_2$(THF)]**
$C_{57}H_{72}NO_3S_2ScSi_2$
984.44

A solution of 0.10 g of $H_2$**L$^{25}$** (0.14 mmol, 1 equiv.) in 1 mL of benzene was added slowly to a solution of 0.07 g of **19** (0.14 mmol, 1 equiv.) in 1 mL of benzene at 25 °C. The resulting orange solution was stirred at 70 °C for 24 h. Removal of the solvent under vacuum afforded a colorless powder that was dissolved in 2 mL of *n*-pentane, filtered and stored at −30 °C for two weeks. After crystallization, [Sc**L$^{25}${N(SiMe$_2$H)$_2$}(THF)] was isolated in 64% yield (0.085 g, 0.09 mmol). **$^1$H NMR** ($C_6D_6$, 25 °C, 400 MHz), δ (ppm): 0.34 (d, $^3J_{HH}$ = 3.0 Hz, 6 H, Si(C*H*$_3$)$_2$), 0.39 (d, $^3J_{HH}$ = 3.0 Hz, 6 H, Si(C*H*$_3$)$_2$), 0.91 (br, 4 H, *β*-THF), 1.4-2.1 (br, 24 H, C(C*H*$_3$)$_2$Ph), 2.94 (br, 4 H, *α*-THF), 3.50 (br, 1H, SC*H*$_2$S), 3.67 (br, 1H, SC*H*$_2$S), 5.11 (sept, $^3J_{HH}$ = 3.0 Hz, 2 H, Si*H*), 6.93 (m, 2 H, Ph-*H*), 7.00-7.13 (m, 6 H, Ph-*H*), 7.15 (s, 2 H, Ph-*H*), 7.16-7.21 (m, 4 H, Ph-*H*), 7.29 (d, $^3J_{HH}$ = 7.7 Hz, 4 H, Ph-*H*), 7.32 (d, $^3J_{HH}$ = 2.6 Hz, 2 H, Ph-*H*3), 7.46 (br, 2 H, Ph-*H*5). **$^{13}$C{$^1$H} NMR** ($C_6D_6$, 25 °C, 100.1 MHz), δ (ppm): 3.0 (Si(*C*H$_3$)$_2$), 3.7 (Si(*C*H$_3$)$_2$), 25.0 (*β*-THF), 31.2 (C(*C*H$_3$)$_2$Ph), 31.5 (C(*C*H$_3$)$_2$Ph), 42.7 (*C*(CH$_3$)$_2$), 43.3 (*C*(CH$_3$)$_2$), 52.4 (S*C*H$_2$S), 71.2 (*α*-THF), 125.7 (Ph-*C*2), 125.9 (Ph-*C*5), 127.1 (Ph-*C*), 127.9 (Ph-*C*), 128.2 (Ph-*C*3), 128.4 (Ph-*C*), 130.2 (Ph-*C*), 131.0 (Ph-*C*4), 138.8 (Ph-*C*6), 151.8 (Ph-*C*1). **Elemental analysis**, calculated for $C_{57}H_{72}NO_3S_2ScSi_2$ (984.44 g/mol) (%): C 69.54, H 7.37, N 1.42; Found: C 66.22, H 7.20, N 1.65.

---

**[YL$^{25}${N(SiMe$_2$H)$_2$}(THF)]**

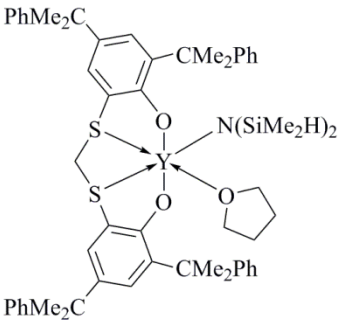


**[YL$^{25}${N(SiMe$_2$H)$_2$(THF)]**
$C_{57}H_{72}NO_3S_2YSi_2$
1028.39

A solution of 0.10 g of $H_2$**L**$^{25}$ (0.14 mmol, 1 equiv.) in 1 mL of benzene was added slowly to a solution of 0.09 g of **20** (0.14 mmol, 1 equiv.) in 1 mL of benzene at 25 °C. The orange solution was stirred at 70 °C for 24 h. The solvent was removed under vacuum to afford a colorless powder that was dissolved in 2 mL of *n*-pentane, filtered and stored at -30 °C for 2 weeks. After crystallization, [Y**L**$^{25}${N(SiMe$_2$H)$_2$}(THF)] was isolated as a colorless powder in 57% yield (0.08 g, 0.08 mmol). **$^1$H NMR** ($C_6D_6$, 25 °C, 400 MHz), δ (ppm): 0.36 (br, 6 H, SiC*H*$_3$), 0.39 (br, 6 H, SiC*H*$_3$), 1.07 (br, 4 H, *β*-THF), 1.64 (s, 12 H, C(C*H*$_3$)$_2$Ph), 1.80 (s, 12 H, C(C*H*$_3$)$_2$Ph), 3.14 (br, 4 H, *α*-THF), 3.64 (s, 2 H, SC*H*$_2$S), 4.98 (m, 2 H, Si*H*), 6.87 (m, 6 H, Ph-*H*), 7.07 (m, 6 H, Ph-*H*), 7.18 (m, 4 H, Ph-*H*), 7.31 (m, 8 H, Ph-*H*), 7.35 (d, $^4J_{HH}$ = 2.6 Hz, 2 H, Ph-*H*3), 7.50 (d, $^4J_{HH}$ = 2.6 Hz, 2 H, Ph-*H*5). **$^{13}$C{$^1$H} NMR** ($C_6D_6$, 25 °C, 100.1 MHz), δ (ppm): 3.2 (Si(*C*H$_3$)$_2$), 3.7 (Si(*C*H$_3$)$_2$), 25.2 (*β*-THF), 30.2 (C(*C*H$_3$)$_2$Ph), 31.3 (C(*C*H$_3$)$_2$Ph), 42.7 (*C*(CH$_3$)$_2$Ph), 43.2 (*C*(CH$_3$)$_2$), 51.7 (S*C*H$_2$S), 70.1 (*α*-THF), 121.1 (Ph-*C*2), 124.8 (Ph-*C*), 125.9 (Ph-*C*), 126.6 (Ph-*C*), 127.1 (Ph-*C*5), 127.9 (Ph-*C*), 128.4 (Ph-*C*), 129.8 (Ph-*C*), 131.5 (Ph-*C*3), 137.3 (Ph-*C*4), 138.1 (Ph-*C*6), 151.5 (Ph-*C*), 152.1 (Ph-*C*), 165.1 (Ph-*C*1). **Elemental analysis**, calculated for $C_{57}H_{72}NO_3S_2YSi_2$ (1028.39 g/mol) (%): C 66.57, H 7.06, N 1.36; Found: C 65.93, H 6.77, N 1.34.

---

**[ScL$^{26}${N(SiMe$_2$H)$_2$}(THF)]**

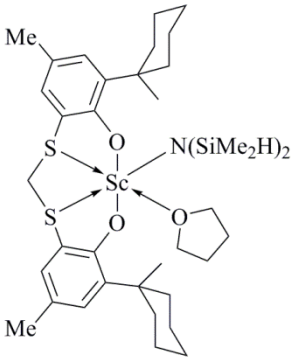


**[ScL$^{26}${N(SiMe$_2$H)$_2$}(THF)]**
$C_{37}H_{60}NO_3S_2ScSi_2$
732.13

A solution of 0.10 g of $H_2$**L**$^{26}$ (0.21 mmol, 1 equiv.) in 1 mL benzene was added slowly to a solution of 0.11 g of **19** (0.39 mmol) in 3 mL of benzene. The yellow solution was stirred at 80 °C for 5 d. The solvent was removed under vacuum to give a yellow powder that was dissolved in 3 mL of *n*-pentane, filtered and stored at −30 °C for 3 d. After drying, [Sc**L**$^{26}${N(SiMe$_2$H)$_2$}(THF)] was isolated as a yellow powder in a 57% yield (90 mg, 0.12 mmol). **$^1$H NMR** ($C_6D_6$, 25 °C, 400 MHz), δ (ppm): 0.39 ppm (d, $^3J_{HH}$ = 3.0 Hz, 12 H,

Si(C$H_3$)$_2$), 1.23-1.31 (br, 4 H, *β*-THF), 1.43-1.71 (br, 16 H, cyclohexyl-*H*), 1.50 (s, 6 H, cyclohexyl-C$H_3$), 2.16 (s, 3 H, Ph-C$H_3$), 2.30-2.53 (br, 4 H, cyclohexyl-*H*), 3.90-4.14 (br, 4 H, *α*-THF), 3.94 (br, 2 H, SC$H_2$), 5.10 (sept, $^3J_{HH}$ = 3.0 Hz, 2 H, Si*H*), 6.90-7.06 (br, 2 H, Ph-*H*3), 7.20-7.30 (s, 2 H, Ph-*H*5). **$^{13}$C{$^1$H} NMR** ($C_6D_6$, 25 °C, 100.1 MHz), δ (ppm): 3.02 (Si(*C*$H_3$)$_2$), 20.8 (Ph-*C*$H_3$), 23.5 (cyclohexyl-*C*), 25.2 (*β*-THF), 27.4 (cyclohexyl-*C*$H_3$), 37.4 (S*C*$H_2$), 38.9 (cyclohexyl-*C*), 51.5 (cyclohexyl-*C*(C$H_3$)), 72.1 (*α*-THF), 125.8 (Ph-*C*3), 127.4 (Ph-*C*4), 128.6 (Ph-*C*5), 132.1 (Ph-*C*2), 132.6 (Ph-*C*6), 164.4 (Ph-*C*1).

---

**[YL$^{26}${N(SiMe$_2$H)$_2$}(THF)]**

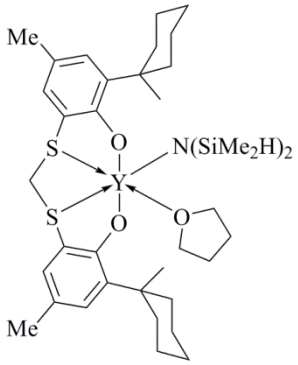


**[YL$^{26}${N(SiMe$_2$H)$_2$}(THF)]**
$C_{37}H_{60}NO_3S_2YSi_2$
776.08

A solution of 0.10 g of $H_2$**L$^{26}$** (0.21 mmol, 1 equiv.) in benzene (1 mL) was slowly added to a solution of 0.13 g of **20** (0.39 mmol, 1 equiv.) in 3 mL of benzene. The yellow solution was stirred at 80 °C for 5 d. The solvent was removed under vaccum to give a yellow powder that was dissolved in 3 mL of *n*-pentane, filtered and stored at −30 °C for 3 d. After drying, [Y**L$^{26}$**{N(SiMe$_2$H)$_2$}(THF)] was isolated as a yellow powder in a yield of 62% (98 mg, 0.13 mmol). **$^1$H NMR** ($C_6D_6$, 25 °C, 400 MHz), δ (ppm): 0.39 (d, $^3J_{HH}$ = 3.0 Hz, 12 H, Si(C$H_3$)$_2$), 1.28 (br, 4 H, *β*-THF), 1.43-1.60 (br, 16 H, cyclohexyl-*H*), 1.68 (s, 6H, cyclohexyl-C$H_3$), 1.90-2.10 (br, 4 H, cyclohexyl-*H*), 2.17 (s, 6 H, Ph-C$H_3$), 3.77 (s, 2 H, SC$H_2$), 3.83 (br, 4 H, *α*-THF), 4.97 (sept, $^3J_{HH}$ = 3.0 Hz, 2 H, Si*H*), 7.04 (d, $^4J_{HH}$ = 2.4 Hz, 2 H, Ph-*H*3), 7.26 (d, $^4J_{HH}$ = 2.4 Hz, 2 H, Ph-*H*5). **$^{13}$C{$^1$H} NMR** ($C_6D_6$, 25 °C, 100.1 MHz), δ (ppm): 3.20 (Si(*C*$H_3$)$_2$), 20.8 (Ph-*C*$H_3$), 23.5 (cyclohexyl-*C*), 25.3 (*β*-THF), 27.4 (cyclohexyl-*C*$H_3$), 37.2 (S*C*H), 39.0 (cyclohexyl-*C*), 51.7 (cyclohexyl-*C*(C$H_3$)), 71.1 (*α*-THF), 125.0 (Ph-*C*3), 127.9 (Ph-*C*4), 128.2 (Ph-*C*5), 132.1 (Ph-*C*2), 133.1 (Ph-*C*6), 165.8 (Ph-*C*1).

**[ScL$^{27}${N(SiMe$_2$H)$_2$}(THF)]**

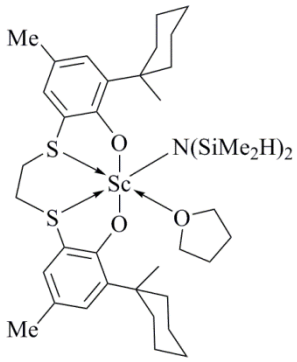


**[ScL$^{27}${N(SiMe$_2$H)$_2$}(THF)]**
$C_{38}H_{62}NO_3S_2ScSi_2$
746.16

A solution of 0.19 g of $H_2$**L$^{27}$** (0.38 mmol, 1 equiv.) in benzene (1 mL) was added slowly to a solution of 0.10 g of **19** (0.39 mmol, 1 equiv.) in *n*-pentane (4 mL). The yellow solution was stirred at 25 °C for 48 h. The solvent was removed under vacuum to give a yellow powder that was dissolved in 3 mL *n*-pentane filtered and stored at −30 °C for 3 d. After drying, [Sc**L$^{27}$**{N(SiMe$_2$H)$_2$}(THF)] was isolated as a yellow powder in a yield of 72% (209 mg, 0.28 mmol). **$^1$H NMR** ($C_6D_6$, 25 °C, 400 MHz), δ (ppm): 0.39 (d, $^3J_{HH}$ = 3.1 Hz, 6 H, SiC*H*$_3$), 0.46 (d, $^3J_{HH}$ = 3.1 Hz, 6 H, Si(C*H*$_3$)$_2$), 1.23 (br, 4 H, *β*-THF), 1.48-1.63 (br, 10 H, cyclohexyl-*H*), 1.65 (s, 3 H, cyclohexyl-C*H*$_3$), 1.67-1.73 (br, 6 H, cyclohexyl-*H*), 1.77 (s, 3 H, cyclohexyl-C*H*$_3$), 1.93-2.08 (br, 4 H, cyclohexyl-*H*), 2.16 (s, 3 H, Ph-C*H*$_3$), 2.17 (s, 3 H, Ph-C*H*$_3$), 2.35-2.50 (br, 4 H, SC*H*), 3.93-4.04 (m, 2 H, *α*-THF), 4.10-4.20 (br, 2 H, *α*-THF), 5.24 (sept, 1 H, $^3J_{HH}$ = 3.1 Hz, Si*H*), 6.88 (s, 1 H, Ph-*H*3), 7.04 (s, 1 H, Ph-*H*3'), 7.22 (s, 1 H, Ph-*H*5), 7.24 (s, 1H, Ph-*H*5'). **$^{13}$C{$^1$H} NMR** ($C_6D_6$, 25 °C, 100.1 MHz), δ (ppm): 3.6 (Si*C*H$_3$), 3.8 (Si*C*H$_3$), 20.9 (Ph-*C*H$_3$), 23.6 (Cy-*C*), 25.2 (*β*-THF), 26.5 (cyclohexyl-*C*H$_3$), 27.5 (cyclohexyl-*C*), 37.0 (cyclohexyl-*C*), 37.3 (S*C*H$_2$), 37.5 (cyclohexyl-*C*), 37.8 (cyclohexyl-*C*), 38.8 (cyclohexyl-*C*), 39.0 (cyclohexyl-*C*(CH$_3$)), 72.3 (*α*-THF), 118.6 (Ph-*C*3), 119.2 (Ph-*C*3'), 125.4 (Ph-*C*4), 126.2 (Ph-*C*4'), 131.5 (Ph-*C*5), 131.6 (Ph-*C*5'), 131.8 (Ph-*C*2), 132.0 (Ph-*C*2'), 136.3 (Ph-*C*6), 137.3 (Ph-*C*6'), 166.8 (Ph-*C*1), 167.3 (Ph-*C*1'). **Elemental analysis**, calculated for $C_{38}H_{62}NO_3S_2ScSi_2$ (746.16 g/mol) (%): C 61.17, H 8.38, N 1.88; Found: C 56.02, H 7.53, N 1.19.

**[YL$^{27}${N(SiMe$_2$H)$_2$}(THF)]**

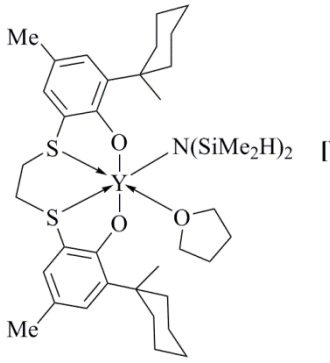


**[YL$^{27}${N(SiMe$_2$H)$_2$}(THF)]**
$C_{38}H_{62}NO_3S_2YSi_2$
782.11

A solution of 0.16 g of $H_2$**L$^{27}$** (0.16 g, 0.32 mmol) in 1 mL of *n*-pentane was slowly added to a solution of 0.20 g of **20** (0.32 mmol, 1 equiv.) in 4 mL of *n*-pentane. The yellow solution was stirred at 25 °C for 48 h. The solvent was removed under vacuum to give a yellow powder that was dissolved in 3 mL of *n*-pentane, filtered and stored at −30 °C for 3 d. After drying, [Y**L$^{27}${N(SiMe$_2$H)$_2$}(THF)] was isolated as a yellow powder in a yield of 76% (0.19 g, 0.24 mmol). **$^1$H NMR** ($C_6D_6$, 25 °C, 400 MHz), δ (ppm): 0.43 (d, $^3J_{HH}$ = 3.0 Hz, 12 H, Si(C*H*$_3$)$_2$), 1.22 (br, 4 H, *β*-THF), 1.53-1.68 (br, 12 H, cyclohexyl-*H*), 1.69 (s, 6 H, cyclohexyl-C*H*$_3$), 1.70-1.74 (br, 4 H, cyclohexyl-*H*), 1.88-1.97 (br, 4 H, cyclohexyl-*H*), 2.18 (s, 6 H, Ph-C*H*$_3$), 2.47-2.56 (br, 4 H, SC*H*$_2$), 3.85 (br, 4 H, *β*-THF), 5.18 (m, 2 H, Si*H*), 6.98 (d, $^4J_{HH}$ = 2.2 Hz, 2 H, Ph-*H*5), 7.23 (d, $^4J_{HH}$ = 2.2 Hz, 2 H, Ph-*H*5). **$^{13}$C{$^1$H} NMR** ($C_6D_6$, 25 °C, 100.1 MHz), δ (ppm): 3.7 (Si(*C*H$_3$)$_2$), 20.9 (*β*-THF), 23.6 (cyclohexyl-*C*H$_3$), 25.1 (cyclohexyl-*C*), 26.2 (cyclohexyl-*C*(CH$_3$)), 27.5 (cyclohexyl-*C*), 37.0 (cyclohexyl-*C*), 39.0 (cyclohexyl-*C*), 71.0 (*α*-THF), 118.8 (Ph-*C*3), 125.3 (Ph-*C*4), 131.5 (Ph-*C*5), 132.2 (Ph-*C*2), 137.3 (Ph-*C*4), 167.3 (Ph-*C*1).

---

**[ScL$^{14}${N(SiMe$_2$H)$_2$}(THF)]**

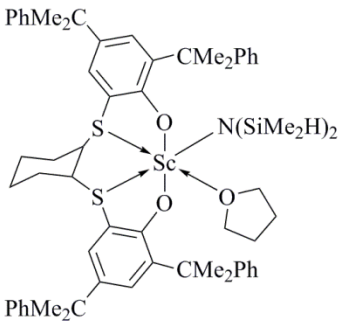


**[ScL$^{14}${N(SiMe$_2$H)$_2$}(THF)]**
$C_{62}H_{80}NO_3S_2ScSi_2$
1052,56

0.31 g of $H_2$**L**$^{14}$ (0.39 mmol) were slowly added to a solution of 0.20 g of **19** (0.39 mmol, 1 equiv.) in 5 mL of benzene at 25 °C. The orange solution was stirred at 70 °C for 5 d. The solvent was removed under vacuum to give a white powder that was dissolved in 5 mL of *n*-pentane, filtered and stored at –30 °C for 3 d. After crystallization and drying under vacuum, [Sc**L**$^{14}${N(SiMe$_2$H)$_2$}(THF)] was isolated as a colorless powder in 74% yield (0.31 g, 0.29 mmol). **$^1$H NMR** ($C_6D_6$, 25 °C, 400 MHz), δ (ppm): 0.33 (d, 6 H, $^3J_{HH}$ = 3.4 Hz, SiC*H*$_3$), 0.34 (d, 6 H, $^3J_{HH}$ = 3.4 Hz, SiC*H*$_3$), 0.60 (m, 1 H, Cy-*H*), 0.77 (m, 1 H, Cy-*H*), 1.02 (m, 4 H, *β*-THF), 1.27 (m, 2 H, Cy-*H*), 1.36 (m, 2 H, Cy-*H*), 1.58 (s, 3 H, C(C*H*$_3$)$_2$Ph), 1.61 (s, 3 H, C(C*H*$_3$)$_2$Ph), 1.64 (s, 3 H, C(C*H*$_3$)$_2$Ph), 1.65 (s, 3 H, C(C*H*$_3$)$_2$Ph), 1.67 (s, 3 H, C(C*H*$_3$)$_2$Ph), 1.74 (m, 2 H, Cy-*H*), 1.83 (s, 3 H, C(C*H*$_3$)$_2$Ph), 2.04 (s, 3 H, C(C*H*$_3$)$_2$Ph), 2.14 (s, 3 H, C(C*H*$_3$)$_2$Ph), 2.23 (m, 1 H, SC*H*), 2.41 (m, 1 H, SC*H*), 3.10 (m, 4 H, *α*-THF), 5.13 (sept, 2 H, $^3J_{HH}$ = 3.4 Hz, Si*H*), 6.99 (d, 2 H, $^3J_{HH}$ = 6.8 Hz, Ph-*H*), 7.03 (d, 2 H, $^3J_{HH}$ = 6.8 Hz, Ph-*H*), 7.09 (d, 2 H, $^3J_{HH}$ = 9.2 Hz, Ph-*H*), 7.14 (d, 4 H, $^3J_{HH}$ = 6.6 Hz, Ph-*H*), 7.18 (m, 4 H, Ph-*H*), 7.25 (m, 6 H, Ph-*H*), 7.47 (d, 2 H, $^3J_{HH}$ = 9.2 Hz), 7.62 (m, 2 H, Ph-*H*). **$^{13}$C{$^1$H} NMR** ($C_6D_6$, 25 °C, 100.1 MHz), δ (ppm): 3.8 (Si(*C*H$_3$)), 24.9 (*β*-THF), 25.8 (Cy-*C*), 26.2 (Cy-*C*), 27.5 (C(*C*H$_3$)$_2$Ph), 28.2 (C(*C*H$_3$)$_2$Ph), 30.8 (C(*C*H$_3$)$_2$Ph), 30.9 (C(*C*H$_3$)$_2$Ph), 31.2 (C(*C*H$_3$)$_2$Ph), 31.5 (C(*C*H$_3$)$_2$Ph), 33.3 (Cy-*C*), 33.5 (C(*C*H$_3$)$_2$Ph), 33.9 (C(*C*H$_3$)$_2$Ph), 34.4 (Cy-*C*), 42.5 (*C*(CH$_3$)$_2$Ph), 42.6 (*C*(CH$_3$)$_2$Ph), 42.9 (*C*(CH$_3$)$_2$Ph), 43.1 (*C*(CH$_3$)$_2$Ph), 51.2 (*C*(CH$_3$)$_2$Ph), 53.7 (S*C*H), 71.3 (α-THF), 115.8 (Ph-*C*2), 116.2 (Ph-*C*2'), 125.0 (Ph-*C*), 125.6 (Ph-*C*), 125.7 (Ph-*C*), 126.1 (Ph-*C*), 127.01 (Ph-*C*), 127.06 (Ph-*C*), 127.09 (Ph-*C*), 123.9 (Ph-*C*), 128.2 (Ph-*C*), 134.38 (Ph-*C*3), 134.41 (Ph-*C*3'), 135.7 (Ph-*C*4), 136.9 (Ph-*C*4'), 137.1 (Ph-*C*6), 137.3 (Ph-*C*6'), 151.8 (Ph-*C*), 152.1 (Ph-*C*), 152.3 (Ph-*C*), 166.4 (Ph-*C*1), 166.9 (Ph-*C*1'). **Elemental analysis**, calculated for $C_{62}H_{80}NO_3S_2ScSi_2$ (1052,56 g/mol): C 70.75, H 7.66, N 1.33; Found: C 69.85, H 7.62, N 1.05.

(+)-(Δ,*S*,*S*)-[Sc**L**$^{14}${N(SiMe$_2$H)$_2$}THF] and (-)-(Λ,*R*,*R*)-[Sc**L**$^{14}${N(SiMe$_2$H)$_2$}THF] were prepared in a similar manner starting from **19** and (+)-(Δ,*S*,*S*)-$H_2$**L**$^{14}$ or (-)-(Λ,*R*,*R*)-$H_2$**L**$^{14}$ in comparable yields showing identical NMR resonances.

**[YL$^{14}${N(SiMe$_2$H)$_2$}(THF)]**

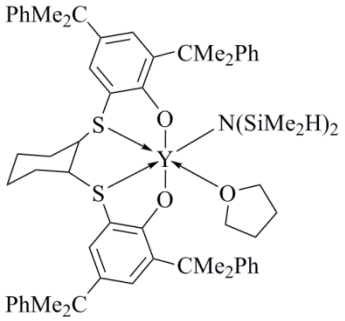


**[YL$^{14}${N(SiMe$_2$H)$_2$}(THF)]**
$C_{62}H_{80}NO_3S_2YSi_2$
1096.42

0.26 g of $H_2$**L$^{14}$** (0.32 mmol, 1 equiv.) were slowly added to a solution of 0.20 g of **20** (0.32 mmol, 1 equiv.) in 10 mL of benzene at 25 °C. The orange solution was stirred at 70 °C for 1 d. The solvent was removed under vacuum to give a white powder that was dissolved in 5 mL *n*-pentane, filtered and stored at –30 °C for 3 d to give colorless crystals of [Y**L$^{14}$**{N(SiMe$_2$H)$_2$}(THF)] in a yield of 56% (196 mg, 0.178 mmol). **$^1$H NMR** ($C_6D_6$, 25 °C, 400 MHz), δ (ppm): 0.36 (d, 12 H, $^3J_{HH}$ = 3.0 Hz, SiC*H*$_3$), 0.69 (br, 2 H, Cy-*H*), 1.05 (m, 4 H, *β*-THF), 1.43 (br, 2 H, Cy-*H*), 1.62 (s, 6 H, C(C*H*$_3$)$_2$Ph), 1.67 (s, 6 H, C(C*H*$_3$)$_2$Ph), 1.70 (br, 2 H, Cy-*H*), 1.81 (br, 2 H, Cy-H), 1.84 (s, 6 H, C(C*H*$_3$)$_2$Ph), 1.91 (s, 6 H, C(C*H*$_3$)$_2$Ph), 2.39 (br, 2 H, SC*H*), 3.06 (m, 4 H, *α*-THF), 4.99 (sept, 2 H, $^3J_{HH}$ = 3.0 Hz, Si*H*), 6.97 (tr., 2 H, $^3J_{HH}$ = 7.2 Hz, Ph-*H*), 7.05 (m 2 H, $^3J_{HH}$ = 6.8 Hz, Ph-*H*), 7.13 (m, 6 H, Ph-*H*), 7.17 (m, 4 H, Ph-*H*), 7.28 (m, 4 H, Ph-*H*), 7.37 (d, 2 H, $^3J_{HH}$ = 7.2 Hz), 7.62(br., 2 H, Ph-*H*). **$^{13}$C{$^1$H} NMR** ($C_6D_6$, 25 °C, 100.1 MHz), δ (ppm): 3.7 (Si(*C*H$_3$)), 3.8 (Si(*C*H$_3$)), 25.0 (*β*-THF), 26.0 (Cy-*C*), 30.9 (C(*C*H$_3$)$_2$Ph), 31.2 (C(*C*H$_3$)$_2$Ph), 31.5 (C(*C*H$_3$)$_2$Ph), 33.9 (C(*C*H$_3$)$_2$Ph), 34.1 (Cy-*C*), 34.4 (C(*C*H$_3$)$_2$Ph), 42.5 (*C*(CH$_3$)$_2$Ph), 42.6 (*C*(CH$_3$)$_2$Ph), 43.1 (*C*(CH$_3$)$_2$Ph), 52.5 (S*C*H), 70.3 (*α*-THF), 115.8 (Ph-*C*2), 124.8 (Ph-*C*), 125.6 (Ph-*C*), 126.5 (Ph-*C*), 127.1 (Ph-*C*), 128.2 (Ph-*C*), 134.9 (Ph-*C*3), 136.6 (Ph-*C*3'), 136.9 (Ph-*C*4), 137.1 (Ph-*C*6), 152.0 (Ph -*C*), 152.3 (Ph-*C*), 166.8 (Ph-*C*1), 166.9 (Ph-*C*1'). **Elemental analysis**, calculated for $C_{62}H_{80}NO_3S_2YSi_2$ (1096.42 g/mol) (%): C 67.91, H 7.35, N 1.28; Found: C 67.05, H 7.44, N 1.16.

**[ScL$^{28}${N(SiMe$_2$H)$_2$}(THF)]**

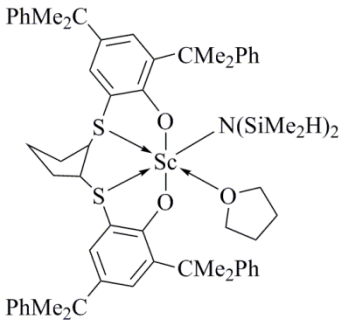


**[ScL$^{28}${N(SiMe$_2$H)$_2$}(THF)]**
$C_{61}H_{78}NO_3S_2ScSi_2$
1038,53

A solution of 0.15 g $H_2$**L**$^{28}$ (0.19 mmol, 1 equiv.) in 1 mL of benzene was added dropwise to a solution of 0.10 g of **19** (0.10 g, 0.19 mmol, 1 equiv.) in 1 mL of benzene at 25 °C. The orange solution was stirred at 70 °C for 24 h. The solvent was removed under vacuum to afford an orange oil which was dissolved in 3 mL of a *n*-pentane/THF mixture, filtered and stored at −30 °C for 3 d. After crystallization, [Sc**L**$^{28}${N(SiMe$_2$H)$_2$}(THF)] was isolated as a colorless powder in 67% yield (0.13 g, 0.13 mmol). **$^1$H NMR** ($C_6D_6$, 25 °C, 400 MHz), δ (ppm): 0.42 ppm (d, $^3J_{HH}$ = 3.1 Hz, 6 H, SiC*H*$_3$), 0.45 (d, $^3J_{HH}$ = 3.1 Hz, 6 H, SiC*H*$_3$), 1.11 (m, 4 H, *α*-THF), 1.47 (br, 2 H, Cy-*H*), 1.59 (m, 2 H, Cy-*H*), 1.70 (s, 6 H, C(C*H*$_3$)$_2$Ph), 1.73 (s, 6 H, C(C*H*$_3$)$_2$Ph), 1.77 (m, 2 H, Cy-*H*), 1.96 (s, 6 H, C(C*H*$_3$)$_2$Ph), 2.10 (s, 3 H, C(C*H*$_3$)$_2$Ph), 2.19 (s, 3 H C(C*H*$_3$)$_2$Ph), 2.69 (m, 2 H, SC*H*), 3.25 (m, 4 H, *α*-THF), 5.18 (m, 2 H, Si*H*), 7.11 (m, 4 H, Ph-*H*), 7.22 (m, 6 H, Ph-*H*), 7.31 (br, 10 H, Ph-*H*), 7.55 (d, $^3J_{HH}$ = 7.5 Hz, 2 H, Ph-*H*3), 7.68 (d, $^4J_{HH}$ = 5.4 Hz, 2 H, Ph-*H*5). **$^{13}$C{$^1$H} NMR** ($C_6D_6$, 25 °C, 100.1 MHz), δ (ppm): 3.7 (Si(*C*H$_3$)$_2$), 22.0 (Cy-*C*), 24.3 (*β*-THF), 27.0 (C(*C*H$_3$)$_2$Ph), 28.2 (C(*C*H$_3$)$_2$Ph), 28.8 (Cy-*C*), 29.2 (Cy-*C*), 30.3 (C(*C*H$_3$)$_2$Ph), 30.4 (C(*C*H$_3$)$_2$Ph), 30.7 (C(*C*H$_3$)$_2$Ph), 33.1 (Cy-*C*), 41.9 (*C*(CH$_3$)$_2$Ph), 42.4 (*C*(CH$_3$)$_2$Ph), 42.6 (*C*(CH$_3$)$_2$Ph), 43.2 (*C*(CH$_3$)$_2$Ph), 50.4 (S*C*H), 53.0 (S*C*H), 70.8 (*α*-THF), 115.7 (Ph-*C*2), 124.4 (Ph-*C*), 124.5 (Ph-*C*), 125.1 (Ph-*C*), 125.2 (Ph-*C*), 125.6 (Ph-*C*), 126.3 (Ph-*C*), 126.4 (Ph-*C*), 127.3 (Ph-*C*), 128.0 (Ph-*C*3), 128.2 (Ph-*C*3'), 133.1 (Ph-*C*4), 133.3 (Ph-*C*4'), 135.2 (Ph-*C*), 137.0 (Ph-*C*6), 137.3 (Ph-*C*6'), 151.0 (Ph-*C*), 151.1 (PH-*C*), 151.3 (Ph-*C*), 151.5 (Ph-*C*), 165.9 (Ph-*C*1), 166.5 (Ph-*C*1'). **Elemental analysis**, calculated for $C_{61}H_{78}NO_3S_2ScSi_2$ (1038.53 g/mol) (%): C 70.55, H 7.48, N 1.36; Found: C 68.90, H 7.49, N 0.98.

**[YL$^{28}${N(SiMe$_2$H)$_2$}(THF)]**

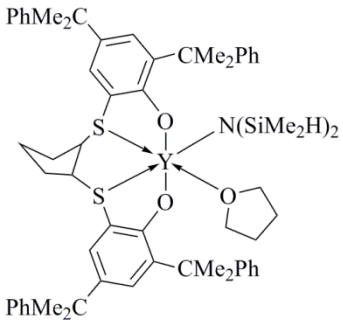


**[YL$^{28}${N(SiMe$_2$H)$_2$}(THF)]**
$C_{61}H_{78}NO_3S_2ScSi_2$
1082.48

A solution of 0.12 g of $H_2$**L$^{28}$** (0.16 mmol, 1 equiv.) in 1 mL benzene was added dropwise to a solution of 0.10 g of **20** (0.16 mmol) in 1 mL of benzene at 25 °C. The orange solution was stirred at 70 °C for 24 h. The solvent was removed under vacuum to afford an orange oil which was dissolved in 3 mL of an *n*-pentane/THF mixture, filtered and stored at −30 °C for 3 d. [Y**L$^{28}$**{N(SiMe$_2$H)$_2$}(THF)] was isolated as a colorless powder in 61% yield (0.13 g, 0.12 mmol). **$^1$H NMR** ($C_6D_6$, 25 °C, 400 MHz), δ (ppm): 0.33 ppm (d, $^3J_{HH}$ = 3.0 Hz, 6 H, SiC*H*$_3$), 0.36 (d, $^3J_{HH}$ = 3.0 Hz, 6 H, SiC*H*$_3$), 1.29 (m, 4 H, *β*-THF), 1.60 (s, 6 H, C(C*H*$_3$)$_2$Ph), 1.61 (br, 2 H, Cy-*H*), 1.63 (s, 6 H, C(C*H*$_3$)$_2$Ph), 1.66 (m, 4 H, Cy-*H*), 1.78 (s, 6 H, C(C*H*$_3$)$_2$Ph), 1.92 (s, 6 H, C(C*H*$_3$)$_2$Ph), 2.62 (m, 2 H, SC*H*), 3.40 (m, 4 H, *α*-THF), 4.97 (sept, $^3J_{HH}$ = 3.0 Hz, 2 H, Si*H*), 7.04 (m, 4 H, Ph-*H*), 7.13 (m, 6 H, Ph-*H*), 7.17 (d, $^3J_{HH}$ = 5.2 Hz, 2 H, Ph-*H*), 7.21 (d, $^4J_{HH}$ = 2.5 Hz, 2 H, Ph-*H*), 7.25 (dt, $^3J_{HH}$ = 3.1 Hz, $^4J_{HH}$ = 1.8 Hz, 2 H, Ph-*H*), 7.34 (d, $^3J_{HH}$ = 7.2 Hz, 4 H, Ph-*H*3), 7.59 (d, $^3J_{HH}$ = 2.5 Hz, 2 H, Ph-*H*5). **$^{13}$C{$^1$H} NMR** ($C_6D_6$, 25 °C, 100.1 MHz), δ (ppm): 3.8 ppm (Si*C*H$_3$), 3.9 (Si*C*H$_3$), 23.2 (Cy-*C*), 25.6 (*β*-THF), 28.4 (C(*C*H$_3$)$_2$Ph), 31.0 (Cy-*C*), 31.1 (C(*C*H$_3$)$_2$Ph), 31.2 (Cy-*C*), 42.6 (*C*(CH$_3$)$_2$Ph), 43.1 (*C*(CH$_3$)$_2$Ph), 51.9 (S*C*H), 68.8 (*α*-THF), 116.4 (Ph-*C*2), 124.9 (Ph-*C*), 125.8 (Ph-*C*), 126.4 (Ph-*C*), 127.1 (Ph-*C*), 127.9 (Ph-*C*3), 128.2 (Ph-*C*3'), 128.4 (Ph-*C*4), 134.2 (PH-*C*), 137.2 (Ph-*C*6), 137.3 (Ph-*C*6'), 167.1 (Ph-*C*1). **Elemental analysis**, calculated for $C_{61}H_{78}NO_3S_2YSi_2$ (1082.48 g/mol) (%):C 67.68, H 7.26, N 1.29; Found: C 67.08, H 6.78, N 1.10.

**[ScL$^{29}${N(SiMe$_2$H)$_2$}(THF)]**

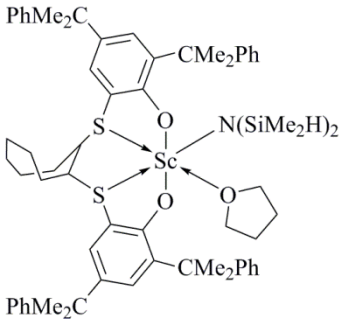


**[ScL$^{29}${N(SiMe$_2$H)$_2$}(THF)]**
$C_{64}H_{84}NO_3S_2ScSi_2$
1080.61

A solution of 0.16 g of $H_2$**L**$^{29}$ (0.19 mmol, 1 equiv.) in 1 mL of benzene was added dropwise to a solution of 0.10 g **19** (0.19 mmol, 1 equiv) in 1 mL benzene at 25 °C. The orange solution was stirred at 70 °C for 24 h. The solvent was removed under vacuum to afford an orange oil which was dissolved in 3 mL of a *n*-pentane/THF mixture, filtered and stored at –30 °C for 3 d. After crystallization, [Sc**L**$^{29}${N(SiMe$_2$H)$_2$}(THF)] was isolated as an orange powder in 71% yield (0.15 g, 0.14 mmol). **$^1$H NMR** ($C_6D_6$, 25 °C, 400 MHz), δ (ppm): 0.33 ppm (br, 12 H, Si(C*H*$_3$)$_2$), 1.01 (m, 4 H, *β*-THF), 1.36 (br, 4 H, Cy-*H*), 1.59 (br, 6 H, C(C*H*$_3$)$_2$Ph), 1.63 (s, 6 H, C(C*H*$_3$)$_2$Ph), 1.67 (s, 6 H, C(C*H*$_3$)$_2$Ph), 1.72 (br, 3 H, C(C*H*$_3$)$_2$Ph), 1.82 (br, 3H, C(C*H*$_3$)$_2$Ph), 2.03-2.09 (br, 6 H, Cy-*H*), 2.21 (s, 1 H, Cy-*H*), 2.36 (s, 1 H, Cy-*H*), 2.73 (s, 1 H, SC*H*), 2.83 (s, 1 H, SC*H*), 3.10 (m, 4 H, *α*-THF), 5.10 (br, 2 H, Si*H*), 6.90-7.10 (br, 6 H, Ph-*H*), 7.13 (br, 2 H, Ph-*H*), 7.18 (br, 6 H, Ph-*H*), 7.28 (m, 8 H, Ph-*H*), 7.44 (br, 2 H, Ph-*H*3), 7.60 (br, 2H, Ph-*H*5). **$^{13}$C{$^1$H} NMR** ($C_6D_6$, 25 °C, 100.1 MHz), δ (ppm): 3.9 (Si(*C*H$_3$)$_2$), 25.0 (*β*-THF), 25.7 (Cy-*C*), 26.1 (Cy-*C*), 26.9 (Cy-*C*), 27.2 (Cy-*C*), 27.4 (Cy-*C*), 27.7 (Cy-*C*), 28.5 (Cy-*C*), 31.1 (C(*C*H$_3$)$_2$Ph), 31.3 (C(*C*H$_3$)$_2$Ph), 34.1 (C(*C*H$_3$)$_2$Ph), 34.3 (C(*C*H$_3$)$_2$Ph), 34.5 (*C*(CH$_3$)$_2$Ph), 35.3 (*C*(CH$_3$)$_2$Ph), 42.6 (*C*(CH$_3$)$_2$Ph), 43.2 (*C*(CH$_3$)$_2$Ph), 53.9 (S*C*H), 56.3 (S*C*H), 71.4 (*α*-THF), 116.3 (Ph-*C*2), 117.2 (Ph-*C*2'), 125.0 (Ph-*C*), 125.8 (Ph-*C*), 126.1 (Ph-*C*), 126.8 (Ph-*C*), 127.1 (Ph-*C*), 127.9 (Ph-*C*), 128.8 (Ph-*C*), 132.6 (Ph-*C*3), 133.3 (Ph-*C*3'), 135.9 (Ph-*C*4), 137.1 (Ph-*C*6), 137.3 (Ph-*C*6'), 137.3 (Ph-*C*4'), 151.9 (Ph-*C*), 166.5 (Ph-*C*1), 167.4 (Ph-*C*1'). **Elemental analysis**, calculated for $C_{64}H_{84}NO_3S_2ScSi_2$ (1080.61 g/mol) (%): C 71.13, H 7.84, N 1.30; Found: C 69.35, H 7.91, N 1.21.

**[YL$^{29}${N(SiMe$_2$H)$_2$}(THF)]**

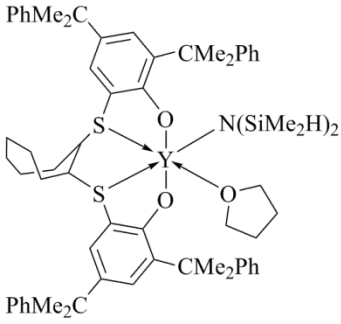


**[YL$^{29}${N(SiMe$_2$H)$_2$}(THF)]**
$C_{64}H_{84}NO_3S_2YSi_2$
1124.56

A solution 0.27 g of $H_2$**L$^{29}$** (0.32 mmol, 1 equiv.) in 1 mL of benzene was added dropwise to a solution of 0.20 g of **19** (0.32 mmol, 1 equiv.) in 1 mL of benzene at 25 °C. The solution was stirred for 3 d at 25 °C. The solvent was removed under vacuum to afford an orange powder that was dissolved in 5 mL *n*-pentane/THF, filtered and stored at −30 °C for 5 d. After crystallization, [Y**L$^{29}$**{N(SiMe$_2$H)$_2$}(THF)] was isolated as an orange powder in 75% yield (0.27 g, 0.24). **$^1$H NMR** ($C_6D_6$, 25 °C, 400 MHz), δ (ppm): 0.33 (d, $^3J_{HH}$ = 3.0 Hz, 6 H, SiC*H*$_3$), 0.35 (d, $^3J_{HH}$ = 3.0 Hz, 6 H, SiC*H*$_3$), 0.99 (br, 6 H, Cy-*H*), 1.20 (br, 4 H, *β*-THF), 1.42 (br, 4 H, Cy-*H*), 1.67 (s, 6 H, C(C*H*$_3$)$_2$Ph), 1.68 (s, 6 H, C(C*H*$_3$)$_2$Ph), 1.75 (br, 2 H, Cy-*H*), 1.82 (br, 6 H, C(C*H*$_3$)$_2$Ph), 2.66 (s, 2 H, SC*H*), 3.26 (m, 4 H, *α*-THF), 5.00 (br, 2 H, Si*H*), 6.95 (t, $^3J_{HH}$ = 7.3 Hz, 2 H, Ph-*H*), 7.06 (m, 4 H, Ph-*H*), 7.11 (br, 4 H, Ph-*H*), 7.19 (m, 4H, Ph-*H*), 7.28 (br, 2H, Ph-*H*3), 7.32 (m, 6 H, Ph-*H*), 7.57 (d, $^4J_{HH}$ = 2.5 Hz, 2 H, Ph-*H*5). **$^{13}$C{$^1$H} NMR** ($C_6D_6$, 25 °C, 100.1 MHz), δ (ppm): 3.7 (Si(*C*H$_3$)$_2$), 25.3 (*β*-THF), 25.9 (Cy-*C*), 27.5 (Cy-*C*), 30.1 (Cy-*C*), 30.6 (Cy-*C*), 31.2 (C(*C*H$_3$)$_2$Ph), 31.3 (*C*(CH$_3$)$_2$Ph), 42.6 (*C*(CH$_3$)$_2$Ph), 43.2 (*C*(CH$_3$)$_2$Ph), 58.8 (S*C*H), 69.6 (*α*-THF), 124.9 (Ph-*C*2), 125.3 (Ph-*C*), 126.6 (Ph-*C*), 127.2 (Ph-*C*), 127.9 (Ph-*C*), 128.2 (Ph-*C*5), 132.8 (Ph-*C*3), 136.8 (Ph-*C*4), 136.9 (Ph-*C*6), 151.8 (PH-*C*), 165.0 (Ph-*C*1). **Elemental analysis**, calculated for $C_{64}H_{84}NO_3S_2YSi_2$ (1124.56 g/mol) (%): C 68.35, H 7.53, N 1.25; Found: C 68.34, H 7.43, N 0.99.

## III.5. References


1 C. Capacchione, A. Proto, H. Ebeling, R. Mülhaupt, K. Möller, T. P. Spaniol, J. Okuda, *J. Am. Chem. Soc.* **2003**, *125*, 4964-4965.

2 N. Nakata, T. Toda, A. Ishii, *Polym. Chem.* **2011**, *2*, 1597-1610.

3 M. Konkol, T. P.Spaniol, M. Kondracka, J. Okuda, *Dalton Trans.* **2007**, 4095-4102.

4 M. Konkol, M. Kondracka, P. Voth, T. P. Spaniol, J. Okuda, *Organometallics* **2008**, *27*, 3774-3784.

[5] S.-Y. Lee, I. Peckermann, E. Abinet, J. Okuda, G. Henze, A. Prokop, *Med. Oncol.* **2012**, *29*, 235-242.

[6] E. Abinet, T. P.Spaniol, J. Okuda, *Chem. Asian J.* **2011**, *2*, 389-391.

[7] M. Konkol, J. Okuda, *Coord. Chem. Rev.* **2008**, *252*, 1577-1591.

[8] A. Kapelski, J.-C. Buffet, T. P.Spaniol, J. Okuda, *Chem. Asian J.* **2012**, *7*, 1320-1330.

[9] H. Ma, T. P. Spaniol, J. Okuda, *Dalton Trans* **2003**, 4770-4780.

[10] H. Ma, T. P. Spaniol, J. Okuda, *Angew. Chem.*, **2006**, *118*, 7982-7985.

[11] H. Ma, T. P. Spaniol, J. Okuda, *Inorg. Chem.* **2008**, *47*, 3328-3339.

[12] J.-C. Buffet, A. Kapelski, J. Okuda, *Macromolecules* **2010**, *43*, 10201-10203.

[13] H. Ma, J. Okuda, *Macromolecules*, **2005**, *38*, 2665-2673.

[14] H. Ma, G. Melillo, L. Oliva, T. P.Spaniol, U. Englert, J. Okuda, *Dalton Trans*. **2005**, 721-727.

[15] R. Anwander, O. Runte, J. Eppinger, G. Gerstberger, E. Herdtweck, M. Spiegler, *J. Chem. Soc., Dalton Trans.*, **1998**, 847-858.

[16] a) J. Eppinger, M. Spiegler, W. Hieringer, W. A. Herrmann, R. Anwander, *J. Am. Chem. Soc.* **2000**, *122*, 3080-3096; b) R. Anwander, J. Eppinger, I. Nagl. W. Scherer, M. Tafipolsky, P. Stirsch, *Inorg. Chem.* **2000**, *39*, 4713-4720.

[17] a) O. Runte, T. Priermeier, R. Anwander,. *Chem. Commun.* **1996**, 1385-1386; b) A. Lara-Sanchez, A. Rodriguez, D. L. Hughes, M. Schormann, M. Bochmann, *J. Organomet. Chem.* **2002**, *663*, 63-69 ; c) D. J. H. Emslie, W. E. Piers, M. Parvez, R. McDonal, *Organometallics* **2002**, *21*, 4226-4240; d) C. L. Boyd, T. Toupance, B. R. Tyrrell, B. D. Ward, C. R. Wilson, A. R. Cowley, P. Mountford, *Organometallics* **2005**, *24*, 309-330; e) S. C. Marinescu, T. Agapie, M. Day, J. E. Bercaw, *Organometallics* **2007**, *26*, 1178-1190.

[18] K. B. Aubrecht, K. Chang, M. A. Hillmyer, W. B. Tolman, *J. Polym. Sci. Part A: Polym. Chem.* **2001**, *39*, 284-293.

[19] I. Westmoreland, J. Arnold, *Dalton Trans.* **2006**, 4155-4163.

[20] L. M. Jackman, F. A. Cotton (Eds.): *Dynamic Nuclear Magnetic Resonance Spectroscopy*. New York: Academic Press, **1975**

[21] M. Oki (Ed.): *Applications of Dynamic NMR Spectroscopy to Organic Chemistry*, Deerfield Beach: VCH Publishers, **1985**.

[22] J. Sandström: *Dynamic NMR Spectroscopy. New York*: Academic Press. **1982**.

[23] C. Capaccione, R. Manivannan, M. Barone, K. Beckerle, R. Centore, L. Oliva, A. Proto, A. Tuzi, T. P. Spaniol, J. Okuda, *Organometallics* **2005**, *24*, 2971-2982.

[24] W. A. Herrmann, J. Eppinger, M. Spiegler, O. Runte, R. Anwander, *Organometallics*, **1997**, *16*, 1813-1815.

# Chapter IV

# Rare Earth Metal Initiators with an OSSO-Type Bis(phenolate) Ligand for the Stereoselective Polymerization of Lactide Monomers

Parts of this chapter have already been published:

J.-C. Buffet, A. Kapelski, J. Okuda, *Macromolecules* **2010**, *43*, 10201-10203.

A. Kapelski, J.-C. Buffet, T. P. Spaniol, J. Okuda, *Chem. Asian J.* **2012**, *7*, 1320-1330.

# IV. Rare Earth Metal Silylamide Initiators with an OSSO-Type Bis(phenolate) Ligand for the Stereoselective Polymerization of Lactide Monomers

## IV.1. Introduction

### IV.1.1. Rare Earth Metal Initiators for the ROP of Lactide Monomers

Inspired by results about the ROP of lactide monomers achieved by aluminum initiators, complexes of trivalent rare earth metal cations were considered as possible initiators for ROP of lactide monomers.[1-2]

Feijen *et al.* reported, that yttrium alkoxide cluster $Y_5(\mu\text{-O})(O^iPr)_{13}$ showed remarkable activity in ROP of L-lactide. A non-linear relationship between propagation rate and initial initiator concentration indicated aggregation of propagating polymer chains in solution.[3] Typical for initiators with a cluster structure, control over molecular weight and polydispersity is not effective because of more than one potential initiating group. Over the years, numerous studies about structurally characterized initiators based on rare earth metal cations have been carried out.[4-37] In addition to excellent activities, many complexes showed good stereoselectivities and produced narrowly distributed PLAs with high molecular weights.

Prominent rare earth metal complexes used for heteroselective ROP of lactide monomers are amine bis(phenolate) complexes by Carpentier *et al.* (Scheme 4.1., **VII** and **VIII**).[8,15]

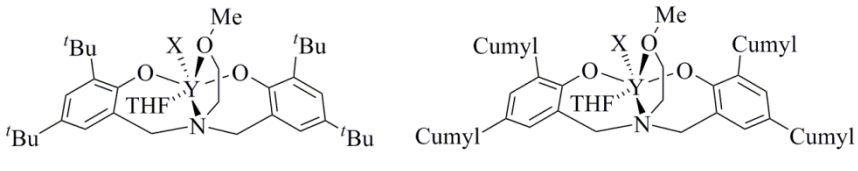


**VII** **VIII**

X = $N(SiMe_2H)_2$

**Scheme 4.1.** Yttrium complexes by Carpentier (**VII**, **VIII**).[8,15]

These initiators polymerized *rac*-lactide to heterotactic poly(*rac*-lactide) with $P_r$ up to 0.90. Stereoselectivity can be improved by subtle modification of the ligand framework and by changing the donor group on the pendant arm. *meso*-Lactide was polymerized to syndiotactically enriched poly(*meso*-lactide) within 0.5 h at 20 °C.[8,15] Theoretical calculations corroborate that effect as a rare example of electronic contributions to the stereoselective ROP of a cyclic ester.[21]

Highly heteroselective ROP of *rac*-lactide was also observed for lanthanide mono(alkyl) complexes supported by ONNO-type tetradentate diamine ligands reported by Cui *et al.*[7] (Scheme 4.2., **X**). Polymers with a heterotacticity up to $P_r = 0.99$ have been isolated. **X** retained its structure in solution upon monomer coordination and subsequent insertion. Cui *et al.* report that the sterical environment at the propagating sites favors the coordination of a monomer of opposite configuration to decrease the energy of the transition state.

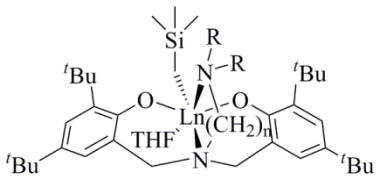


**X**

**Scheme 4.2.** Lanthanide initiators **X** by Cui *et al.*[7]

Yttrium silylamide complexes ligated by bis(phosphinic)diamido ancillary ligands (Scheme 4.3., **XI**) were reported to initiate the ROP of *rac*-LA with high rates (Williams *et al.*, 2011).[23] Heterotactic PLAs were formed ($P_r = 0.85$).

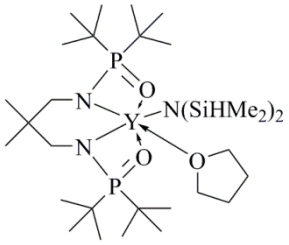


**XI**

**Scheme 4.3.** Yttrium bis(diphosphinic)amido silylamide initiator **XI** by Williams *et al.*[23]

High polymerization rates have also been reported recently by Williams *et al.* for phosphasalen yttrium complexes (Scheme 4.4., **XII**). With an initial monomer:initiator:alcohol ratio of 1000:1:1, 80% conversion was achieved within just one minute giving narrowly distributed, highly heterotactic poly(rac-lactides).[37]

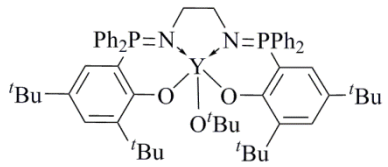


**XII**

**Scheme 4.4.** Yttrium phosphasalen complex by Williams *et al.*[37]

Isoselective ROP of *rac*-LA was reported by Arnold *et al.*[19] Applying $C_3$-symmetric lanthanide tris(alkoxide) complexes (Scheme 4.5., **XIII**) at -5 °C led to narrowly distributed poly(*rac*-lactides) with $P_i$ = 0.83. Retention of stereochemical control is given even for high monomer conversions. High molecular weights demonstrate, that there is no neccessity for using a single-site initiator with only one monodentate initiating group attached to the metal center to achieve excellent control over the ROP.

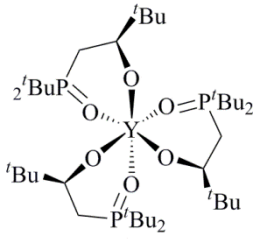


**XIII**

**Scheme 4.5.** Yttrium tris(alkoxide) complex **XIII** by Arnold *et al.*[19]

Scandium amide complexes containing cyclen-derived [NNNN]-type proligands $Me_2$TACD (**XIV**) and $Me_3$TACD (**XV**) ligand recently reported by Okuda *et al.* polymerized *meso*-lactide with full conversion at 25 °C in less than 0.5 h resulting in syndiotactic poly(*meso*-lactides) ($P_s$ = 0.73). (Scheme 4.6.).[36]

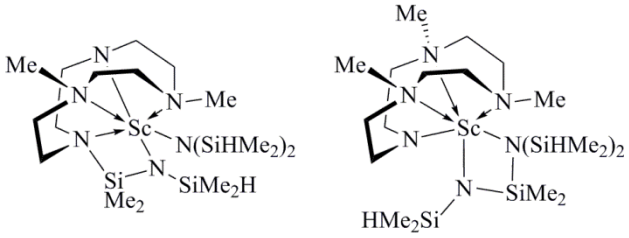


**XIV** **XV**

**Scheme 4.6.** Scandium amide complexes supported by tetradentate $Me_2$TACD (**XIV**) and $Me_3$TACD-ligand (**XV**).[36]

## IV.1.2. Rare Earth Metal Initiators with an OSSO-Type Bis(phenolate) Ligand in the ROP of Lactide Monomers

### IV.1.2.1. ROP of L-lactide

Rare earth metal bis(phenolate) silylamide complexes [Ln$\mathbf{L}^{\mathbf{x}}${$N(SiMe_2H)_2$}(THF)] collated in Table 4.1. have already been studied in the ROP of L- or *rac*-lactide by Okuda *et al.*[38-40]

Some reported results on the ROP of L-lactide are collated in Table 4.2. L-lactide is polymerized in a controlled fashion to highly isotactic PLAs with high molecular weights and relatively broad PDIs. With a given ligand, lutetium initiators [Lu$\mathbf{L}^{\mathbf{x}}${$N(SiMe_2H)_2$}(THF)] were reported to show slightly higher activity than yttrium initiators [Y$\mathbf{L}^{\mathbf{x}}${$N(SiMe_2H)_2$}(THF)]. Lu and Y complexes are much more active than scandium initiators [Sc$\mathbf{L}^{\mathbf{x}}${$N(SiMe_2H)_2$}(THF)] due to the larger coordination sphere around the metal center.[42] The complexes show higher activity when ROP is performed in THF than in $CH_2Cl_2$ or toluene; exemplarily demonstrated for [Y$\mathbf{L}^{\mathbf{5}}${$N(SiMe_2H)_2$}(THF)] by entries 4a-c in Table 4.2 (THF, 0.17 h, > 99% conversion; $CH_2Cl_2$, 1 h, 67% conversion; toluene, 1 h, 76% conversion).[38,41]

Coordinated THF increases the nucleophilicity of the active end group, enhancing the polymerization rate.[41,43] In addition, excess THF accelerates reversible dissociation of the six-coordinated complex, giving a pseudo five coordinated complex in solution. This alleviates monomer coordination to the metal center. Detailed kinetic studies demonstrate the polymerization to occur first order in monomer concentration as well as in initiator concentration when the monomer conversion stays low.[41] Studies on the mechanism confirm

the silylamide group as initiating group. The bis(phenolate) ligand is not involved in the polymerization as no resonances of ligand fragments could be observed in the $^1$H NMR spectrum of the polymers. Formation of purely isotactic poly(L-Lactide) also shows that no epimerization of L-lactide takes place.

With a given metal, complexes bearing a $C_2$ bridged ligand are more active than analogous complexes bearing a $C_3$ bridged ligand.

**Table 4.1.** Rare earth metal silylamide initiators bearing 5–5–5, 5–6–5 and 5–7–5 chelating OSSO-type ligands.[38-40]

| Chelate | Bridge | | Metal | $R_1$ | $R_2$ | [Ln$\mathbf{L}^x${N(SiMe$_2$H)$_2$}THF] | Ref. |
|---|---|---|---|---|---|---|---|
| 5–5–5 | $C_2$ | $(CH_2)_2$ | Sc | $^t$Bu | Me | Ln = Sc, x = 5 | 38-40 |
| | | | Y | $^t$Bu | Me | Ln = Y, x = 5 | 38-40 |
| | | | Lu | $^t$Bu | Me | Ln = Lu, x = 5 | 38-40 |
| | | | Sc | $^t$Bu | $^t$Bu | Ln = Sc, x = 6 | 38 |
| | | | Lu | $^t$Bu | $^t$Bu | Ln = Lu, x = 6 | 38 |
| | | | Sc | CMe$_2$Ph | CMe$_2$Ph | Ln = Sc, x = 9 | 39-40 |
| | | | Y | CMe$_2$Ph | CMe$_2$Ph | Ln = Y, x = 9 | 40 |
| | |  | Sc | $^t$Bu | Me | Ln = Sc, x = 10 | 39-40 |
| | | | Y | $^t$Bu | Me | Ln = Y, x = 10 | 40 |
| | | | Lu | $^t$Bu | Me | Ln = Lu, x = 10 | 40 |
| 5–6–5 | $C_3$ | $(CH_2)_3$ | Sc | $^t$Bu | Me | Ln = Sc, x = 15 | 38-40 |
| | | | Lu | $^t$Bu | Me | Ln = Lu, x = 15 | 38 |
| | | | Y | $^t$Bu | $^t$Bu | Ln = Y, x = 16 | 38-40 |
| | | | Lu | $^t$Bu | $^t$Bu | Ln = Lu, x = 16 | 38 |
| 5–7–5 | $C_4$ |  | Sc | $^t$Bu | Me | Ln = Sc, x = 18 | 39-40 |
| | | | Y | $^t$Bu | Me | Ln = Y, x = 18 | 40 |
| | | | Lu | $^t$Bu | Me | Ln = Lu, x = 18 | 40 |
| | | | Y | CMe$_2$Ph | CMe$_2$Ph | Ln = Y, x = 19 | 40 |
| | |  | Sc | Ada | Me | Ln = Sc, x = 20 | 39-40 |
| | | | Sc | $^t$Bu | Me | Ln = Sc, x = 21 | 39-40 |
| | | | Y | $^t$Bu | Me | Ln = Y, x = 21 | 40 |

ROP of L-lactide initiated by *in situ* generated rare earth metal alkoxide bis(phenolate) systems were compared to the results achieved by [Y$\mathbf{L}^5${N(SiMe$_2$H)$_2$}(THF)], [Y$\mathbf{L}^{16}${N(SiMe$_2$H)$_2$}(THF)] and [Lu$\mathbf{L}^{18}${N(SiMe$_2$H)$_2$}(THF)].[41] Addition of isopropanol results in formation of dimeric species. ROP of L-Lactide with an isopropanol:initiator ratio of 2:1 ran faster than polymerizations where a 1:1 ratio was used. This alkoxide generated *in situ* initiated living ROP of L-lactide to afford linear PLAs with isopropoxide end groups. ROP is

first-order in monomer and initiator concentration. Over the entire conversion range, no aggregation or deactivation of the active site was observed. Thus, the initiating group has a strong influence on the polymerization process, in particular during initiation.[40,41]

**Table 4.2.** ROP of L-lactide initiated by rare earth metal bis(phenolate) silylamide complexes [Ln**L**$^{x}${N(SiMe$_2$H)$_2$}(THF)]. [a] [38-40]

| Entry | Initiator | $[Ln]_0/[LA]_0$ | $t$ (h) | Conv. (%)[b] | $M_c$(g·mol$^{-1}$) (×10$^{-4}$)[c] | $M_n$(g·mol$^{-1}$) (×10$^{-4}$)[d] | $M_w/M_n$[d] |
|---|---|---|---|---|---|---|---|
| 1 | Ln = Sc, x = 5 | 300 | 4 | 66 | 2.85 | 2.95 | 1.37 |
| 2 | Ln = Sc, x = 6 | 300 | 20 | 98 | 4.23 | 5.40 | 1.20 |
| 3 | Ln = Sc, x = 15 | 300 | 24 | 42 | 1.82 | 2.79 | 1.41 |
| 4a | Ln = Y, x = 5 | 300 | 0.17 | 99 | 4.28 | 4.99 | 1.17 |
| 4b[e] | | 300 | 1 | 67 | 2.90 | 4.08 | 1.97 |
| 4c[f] | | 300 | 1 | 76 | 3.29 | 3.87 | 1.49 |
| 5 | Ln = Y, x = 9 | 300 | 0.15 | 94 | 4.06 | 11.9 | 1.58 |
| 6 | Ln = Y, x = 10 | 300 | 0.17 | 80 | 3.46 | 8.97 | 1.74 |
| 7 | Ln = Y, x = 16 | 300 | 24 | 97 | 4.19 | 4.20 | 1.15 |
| 8 | Ln = Y, x = 18 | 300 | 2 | 93 | 4.02 | 6.29 | 1.31 |
| 9 | Ln = Y, x = 19 | 300 | 2.5 | 66 | 2.85 | 5.67 | 1.19 |
| 10 | Ln = Y, x = 21 | 300 | 2 | 80 | 3.46 | 5.77 | 1.28 |
| 11 | Ln = Lu, x = 5 | 300 | 0.1 | 97 | 4.19 | 5.76 | 1.17 |
| 12 | Ln = Lu, x = 6 | 300 | 0.5 | 93 | 4.02 | 2.38 | 1.24 |
| 13 | Ln = Lu, x = 10 | 300 | 0.1 | 63 | 2.72 | 18.6 | 1.43 |
| 14 | Ln = Lu, x = 15 | 300 | 47 | 49 | 2.10 | 2.42 | 1.31 |
| 15 | Ln = Lu, x = 16 | 300 | 48 | 60 | 2.59 | 3.41 | 1.18 |
| 16 | Ln = Lu, x = 18 | 300 | 2 | 81 | 3.50 | 9.04 | 1.43 |

[a][Ln] = 2.9 mmol·L$^{-1}$, THF (1 mL), 25 °C; [b]determined by integration ratio of the methine protons of the monomer and polymer in the $^1$H NMR spectrum; [c]$M_c$ = ([M]/[Ln]) × 144.13 × conv.%; [d] determined by GPC; [e] [Ln] = 2.9 mmol·L$^{-1}$, $CH_2Cl_2$ (1 mL); [f] [Ln] = 2.9 mmol·L$^{-1}$, toluene (1 mL), T = 60 °C.

### IV.1.2.2. ROP of *rac*-Lactide

Table 4.3. collates published results on the ROP of *rac*-LA initiated by rare earth metal bis(phenolate) silylamide complexes.[39,40]

Not surprisingly, activity showed trends, similar to the ROP of L-lactide.[38-40] High monomer conversion was observed within 1 h. Even with initial monomer:initiator ratio higher than 300, high conversions were reached within a few hours by using Y- or Lu-initiators.[39,40] Generally, initiators with a 1,4-dithiabutanediyl bridge were more active than identically substituted complexes with other bridges. This might result from a blocked coordination

sphere around the metal centers given by complexes bearing bis(phenolate) ligands with larger bridges. PDIs of the polymers are relatively narrow, not exceeding values of 2.0. This indicates the complexes acting as single-site initiators. Broadening of the PDI was observed by increasing the initial monomer:initiator ratio.

**Table 4.3.** ROP of *rac*-lactide initiated by rare earth metal bis(phenolate) silylamide initiators [Ln**L**$^{x}${N(SiMe$_2$H)$_2$}(THF)]. [a] [39-40]

| Entry | Initiator | $[Ln]_0/[LA]_0$ | *t* (h) | Conv. (%)[b] | $M_c$(g·mol$^{-1}$) (×10$^{-4}$)[c] | $M_n$(g·mol$^{-1}$) (×10$^{-4}$)[d] | $M_w/M_n$[d] | $P_r$[e] |
|---|---|---|---|---|---|---|---|---|
| 1 | Ln = Sc, x = 5 | 300 | 9 | 82 | 3.55 | 17.8 | 1.89 | 0.78 |
| 2 | Ln = Sc, x = 9 | 300 | 8 | 85 | 3.68 | 25.9 | 1.66 | 0.80 |
| 3 | Ln = Sc, x = 10 | 300 | 9 | 79 | 3.42 | 23.8 | 1.88 | 0.82 |
| 4 | Ln = Sc, x = 15 | 300 | 8 | 81 | 3.50 | 12.6 | 1.85 | 0.95 |
| 5 | Ln = Sc, x = 18 | 300 | 8 | 84 | 3.63 | 9.30 | 1.84 | 0.93 |
| 6 | Ln = Sc, x = 20 | 300 | 5 | 75 | 3.25 | 28.5 | 1.60 | 0.94 |
| 7 | Ln = Sc, x = 21 | 300 | 21 | 89 | 3.85 | 14.3 | 1.88 | 0.94 |
| 8 | Ln = Y, x = 5 | 300 | 1 | 94 | 4.06 | 5.41 | 1.66 | 0.67 |
| 9 | Ln = Y, x = 9 | 300 | 0.15 | 95 | 4.11 | 8.78 | 1.62 | 0.71 |
| 10 | Ln = Y, x = 10 | 300 | 0.17 | 90 | 3.89 | 6.40 | 1.60 | 0.71 |
| 11 | Ln = Y, x = 16 | 300 | 2 | 90 | 3.89 | 6.08 | 1.52 | 0.82 |
| 12 | Ln = Y, x = 18 | 300 | 0.5 | 85 | 3.68 | 8.74 | 1.32 | 0.89 |
| 13 | Ln = Y, x = 19 | 300 | 0.75 | 89 | 3.85 | 5.29 | 1.74 | 0.88 |
| 14 | Ln = Y, x = 21 | 300 | 0.5 | 81 | 3.50 | 7.88 | 1.57 | 0.90 |
| 15 | Ln = Lu, x = 5 | 300 | 0.2 | 92 | 3.98 | 15.6 | 1.89 | 0.64 |
| 16 | Ln = Lu, x = 10 | 300 | 0.5 | 91 | 3.93 | 12.0 | 1.81 | 0.68 |
| 17 | Ln = Lu, x = 18 | 300 | 2 | 94 | 4.06 | 6.59 | 1.90 | 0.83 |

[a] $[Ln]_0$ = 2.9 mmol·L$^{-1}$, THF (1 mL), rt; [b] monomer conversion determined by $^1$H NMR spectroscopy; [c] $M_c$ = ([LA]/[Ln] × conv.% × 144.13); [d] determined by GPC; [e] probability of forming a new *r*-dyad determined by homonuclear decoupled $^1$H NMR spectroscopy.

Isolated poly(*rac*-lactides) showed heterotacticity due to a dynamic monomer recognition.[39-40] Treatment of [Sc**L**$^{21}${N(SiMe$_2$H)$_2$}(THF)] with (*R*)-*tert*-butyl lactate resulted in a dimeric lactate complex.[39] Because of the structural relationship between (*R*)-*tert*-butyl lactate and lactide, a similar transition state occurs during monomer coordination. The configuration of the lactate and resulting steric repulsion induces *Λ*–conformation of the bis(phenolate) ligand.[39] Polymerization of *rac*-lactide initiated by this dimeric lactate complex formes highly heterotactic poly(*rac*-lactides).

As a result of high heteroselectivity given by 1,5-dithiapentanediyl bridged complexes [Sc**L**$^{15}${N(SiMe$_2$H)$_2$}(THF)], [Lu**L**$^{15}${N(SiMe$_2$H)$_2$}(THF)], [Y**L**$^{16}${N(SiMe$_2$H)$_2$}(THF)] and

[Lu**L**$^{16}${N(SiMe$_2$H)$_2$}(THF)], dynamic monomer-recognition takes place in which incoming lactide monomers induce either *Λ*-configuration (D-lactide) or *Δ*-configuration (L-lactide) of the resulting intermediate. Steric repulsion prefers one enantiomer coordinates to the metal center. After ring-opening of the coordinated monomer, repulsion of the α-methyl groups and the *ortho*-substituents induce change of conformation.[39]

Use of THF has a significant impact in preparation of heterotactic polymers.[8] Generally, [Sc**L**$^{x}${N(SiMe$_2$H)$_2$}(THF)] showes higher heteroselectivity, due to the smaller metal center and larger steric hindrance around the metal center. Highest $P_r$ values were found for poly(*rac*-lactides) formed by [Sc**L**$^{15}${N(SiMe$_2$H)$_2$}(THF)] ($P_r$ = 0.95, entry 4), [Sc**L**$^{18}${N(SiMe$_2$H)$_2$}(THF)] ($P_r$ = 0.93, entry 5), [Sc**L**$^{20}${N(SiMe$_2$H)$_2$}(THF)] ($P_r$ = 0.94, entry 6), [Sc**L**$^{21}${N(SiMe$_2$H)$_2$}(THF)] ($P_r$ = 0.94, entry 7), and [Y**L**$^{21}${N(SiMe$_2$H)$_2$(THF)] ($P_r$ = 0.90, entry 14a). Modification of the bis(phenolate) ligand influenced the stereoselectivity. Greatest effects were achieved by extending the bridge from $C_2$ to $C_4$ ([Y**L**$^{5}${N(SiMe$_2$H)$_2$}(THF)], $P_r$ = 0.67, entry 8a; [Y**L**$^{21}${N(SiMe$_2$H)$_2$}(THF)], $P_r$ = 0.90, entry 14a).

## IV.2. Results and Discussion

This chapter describes ROP of *rac*- and *meso*-lactide initiated by rare earth metal bis(phenolate) silylamide complexes introduced in Chapter III as well as application of already reported bis(phenolate) initiators in *meso*-lactide polymerization. Based on the results presented in the first part of this chapter, the second part concentrates on the analysis of the microstructure of produced PLAs to identify the origin of stereoerrors along the polymer chain.

## IV.2.1. Rare Earth Metal Bis(phenolate) Silylamide Complexes as Initiators for the ROP of Lactide Monomers.

### IV.2.1.1. ROP of *rac*-Lactide

Rare earth metal bis(phenolate) silylamide initiators [Ln**L**$^{x}${N(SiMe$_2$H)$_2$(THF)] (Ln = Sc,Y and x = 14, 24-29) were tested in the ROP of *rac*-lactide (Scheme 4.7., Table 4.4)

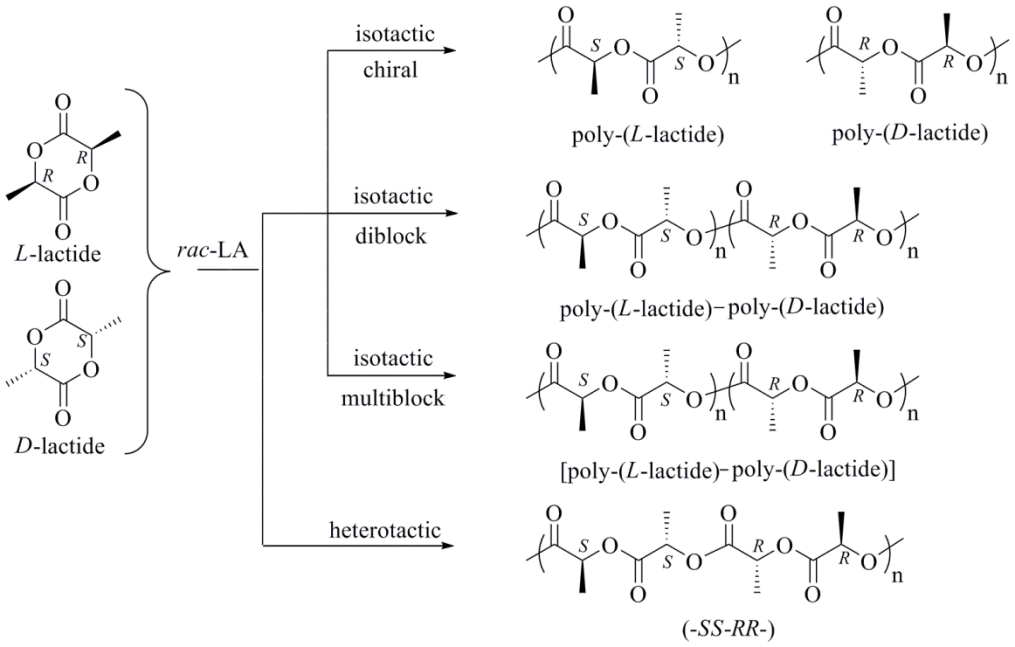


**Scheme 4.7.** ROP of *rac*-lactide and resulting microstructures of poly(*rac*-lactides).

Most of the polymerizations in THF proceeded fast with high monomer conversions in less than 3 h. Scandium initiators [Sc**L**$^{x}${N(SiMe$_2$H)$_2$}(THF)] (x = 24-26) with a rigid 5-4-5 chelate array, polymerized *rac*-lactide with low conversions between 21 and 35% giving atactic poly(*rac*-lactides) (entries 1-3). This indicates, that a highly rigid system lowers the polymerization rate. The coordination sphere around the metal center is blocked. In addition, bis(dimethylsilylamide) groups that are less nucleophilic than alkoxides, lead to slower initiation of the ROP. With [Y**L**$^{x}${N(SiMe$_2$H)$_2$}(THF)] (x = 24-26), conversions of 81%, 93% and 97% were achieved, giving slightly heterotactic enriched poly(*rac*-lactides). In accordance with reported results, yttrium initiators were more active than scandium initiators.[40] However, [Y**L**$^{27}${N(SiMe$_2$H)$_2$}(THF)] with a 5-5-5 chelate array was less active

than [Sc**L**$^{27}${N(SiMe$_2$H)$_2$}(THF)]. This might result from the fluxionality of the 1-methylcyclohexyl groups.

**Table 4.4.** ROP of *rac*-lactide initiated by rare earth metal bis(phenolate) silylamide complexes [Ln**L**$^{x}${N(SiMe$_2$H)$_2$}(THF)]. [a]

| Entry | Initiator | [Ln]$_0$/ [LA]$_0$ | Conv. (%)[b] | $M_c$(g·mol$^{-1}$) (×10$^{-4}$) | $M_n$(g·mol$^{-1}$) (×10$^{-4}$)[c] | $M_w$/ $M_n$[c] | $P_r$[d] |
|---|---|---|---|---|---|---|---|
| 1 | Ln = Sc, x = 24 | 100 | 26 | 0.38 | 0.6 | 1.89 | 0.49 |
| 2 | Ln = Sc, x = 25 | 100 | 35 | 0.50 | 1.20 | 1.19 | 0.50 |
| 3 | Ln = Sc, x = 26 | 100 | 21 | 0.30 | 2.20 | 1.24 | 0.50 |
| 4 | Ln = Sc, x = 27 | 100 | 94 | 1.35 | 2.38 | 1.61 | 0.71 |
| 5 | Ln = Sc, x = 28 | 100 | 80 | 1.15 | 2.40 | 1.11 | 0.85 |
| 6 | Ln = Sc, x = 14 | 100 | 98 | 1.41 | 1.13 | 1.09 | 0.74 |
| 7 | Ln = Sc, x = 29 | 100 | 86 | 1.24 | 1.83 | 1.65 | 0.64 |
| 8 | Ln = Y, x = 24 | 100 | 81 | 1.17 | 0.83 | 1.05 | 0.59 |
| 9 | Ln = Y, x = 25 | 100 | 93 | 1.34 | 1.83 | 1.65 | 0.61 |
| 10 | Ln = Y, x = 26 | 100 | 97 | 1.40 | 2.00 | 1.45 | 0.57 |
| 11 | Ln = Y, x = 27 | 100 | 98 | 1.41 | 1.22 | 1.66 | 0.54 |
| 12 | Ln = Y, x = 28 | 100 | 55 | 0.79 | 1.25 | 1.10 | 0.68 |
| 13 | Ln = Y, x = 14 | 100 | 98 | 1.44 | 2.08 | 1.15 | 0.68 |
| 14 | Ln = Y, x = 29 | 100 | 98 | 1.41 | 1.70 | 1.42 | 0.63 |

[a] Polymerization conditions: [LA]$_0$/[Init]$_0$ = 100, 3 h, THF, 1 mL, 25 °C. [b] conversion of monomer (([LA]$_0$ – [LA]$_t$)/[LA]$_0$); [c] measured by GPC, calibrated with PS standards in THF[32]; [d] determined by homonuclear decoupled $^1$H NMR, $P_r$ is the probability to obtain *isi* or *sis* tetrad.[2]

In contrast to published results, yttrium initiators [Y**L**$^{x}${N(SiMe$_2$H)$_2$}(THF)] (x = 24-26) based on 5-4-5 chelating ligands showed higher heterotacticity than scandium initiators [Sc**L**$^{x}${N(SiMe$_2$H)$_2$}(THF)] (x = 24-26). This is a rare example for rare earth metal bis(phenolate) complexes, where the yttrium initiator is both more active and selective than homologous scandium initiators in lactide polymerization.

When [Ln**L**$^{x}${N(SiMe$_2$H)$_2$}(THF)] (Ln = Sc,Y; x = 14, 28-29) based on racemic 5-5-5 chelating OSSO-type ligands but differing in the cycloalkane ring size are compared, heterotacticity decreased with increase in ring size for the scandium initiators ($P_r$ = 0.74, [Sc**L**$^{14}${N(SiMe$_2$H)$_2$}(THF)]; $P_r$ = 0.85, [Sc**L**$^{28}${N(SiMe$_2$H)$_2$}(THF)] (Figure 4.1), $P_r$ = 0.61, [Sc**L**$^{28}${N(SiMe$_2$H)$_2$}(THF)]). More rigid 1,2-cycloalkanediyl backbones led to higher heterotacticity. Previous results show an increased size of the *ortho*-substituent on the aromatic rings resulting in a higher heterotacticity of the poly(*rac*-lactides).[39]

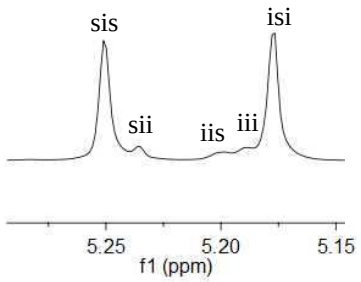


**Figure 4.1.** $^{1}H\{^{1}H\}$ NMR spectrum of poly(*rac*-lactide) synthesized using [Sc**L**$^{28}${N(SiMe$_2$H)$_2$}(THF)] (Table 4.3., Entry 5).

When [Ln**L**$^{27}${N(SiMe$_2$H)$_2$}(THF)] (Ln = Sc,Y) with a 1-methylcyclohexyl group in the *ortho*-position of the 5-5-5 chelating ligand were used, heterotacticity of the polymers was lower ($P_r$ = 0.71 for [Sc**L**$^{27}${N(SiMe$_2$H)$_2$}(THF)] vs. $P_r$ = 0.54 for [Y**L**$^{27}${N(SiMe$_2$H)$_2$}(THF)]) than observed for initiators with $^{t}$Bu groups in *ortho*-position ($P_r$ = 0.78 for Sc and $P_r$ = 0.68 for Y).[39] A similar trend was also observed for heterotacticity of the polymers generated by [Ln**L**$^{24}${N(SiMe$_2$H)$_2$}(THF)] (entries 1 and 8) and [Ln**L**$^{26}${N(SiMe$_2$H)$_2$}(THF)] with a 5-4-5 chelate array (entries 3 and 10). Initiators [Ln**L**$^{26}${N(SiMe$_2$H)$_2$}(THF)] and [Ln**L**$^{27}${N(SiMe$_2$H)$_2$}(THF)] were not as active and selective than initiators bearing a cumyl group (cumyl = 2-phenyl-2-propyl) in *ortho*-position.[39] This is in accordance with published results. The large cumyl groups in *ortho*-position block the coordination sphere, controlling the coordination of lactide more efficiently. In addition, electron-withdrawing properties of cumyl groups increase the lewis-acidity of the metal center. This leads to an increase in activity.[39,40]

### IV.2.1.2. ROP of *meso*-lactide

The mechanism of the ROP of *meso*-lactide suggested by Coates and Ovitt is based on the control at one chiral site of the monomer. An initiator that polymerizes *rac*-lactide to give highly heterotactic PLA should also polymerize *meso*-lactide syndioselectively, providing the initiator's dynamic properties. This means, that one of the two diastereotopic sites in *meso*-lactide is favored to undergo acyl-bond cleavage.[24,46] Heteroselective rare earth metal bis(phenolate) silylamide initiators [Ln**L**$^{x}${N(SiMe$_2$H)$_2$(THF)] with Ln = Sc,Y and x = 14, 24-29 were tested in the ROP of *meso*-lactide (Scheme 4.8., Table 4.5.)

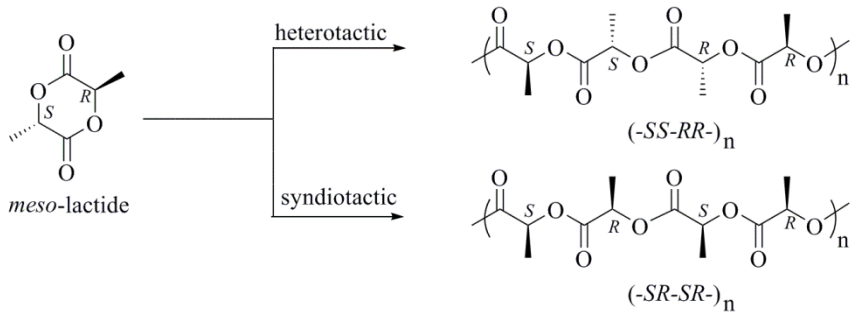


**Scheme 4.8.** ROP of *meso*-lactide and resulting microstructures of poly(*meso*-lactides).

**Table 4.5.** ROP of *meso*-lactide initiated by rare earth metal bis(phenolate) silylamide complexes [Ln**L**$^{x}${N(SiMe$_2$H)$_2$}(THF)]. [a]

| Entry | Initiator | [Ln]$_0$/ [LA]$_0$ | Conv. (%)[b] | $M_c$(g·molˉ$^1$) (×10$^{-4}$) | $M_n$(g·molˉ$^1$) (×10$^{-4}$)[c] | $M_w$/ $M_n$[c] | $P_s$[d] |
|---|---|---|---|---|---|---|---|
| 1 | Ln = Sc, x = 24 | 100 | 96 | 1.38 | 2.95 | 1.23 | 0.66 |
| 2 | Ln = Sc, x = 25 | 100 | 76 | 1.09 | 2.10 | 1.94 | 0.87 |
| 3 | Ln = Sc, x = 26 | 100 | 82 | 1.18 | 3.38 | 1.80 | 0.84 |
| 4 | Ln = Sc, x = 27 | 100 | 95 | 1.37 | 2.32 | 2.18 | 0.89 |
| 5 | Ln = Sc, x = 28 | 100 | 93 | 1.34 | 4.33 | 2.19 | 0.91 |
| 6 | Ln = Sc, x = 14 | 100 | > 99 | 1.41 | 3.23 | 1.80 | 0.92 |
| 7 | Ln = Sc, x = 29 | 100 | > 99 | 1.44 | 3.83 | 1.67 | 0.87 |
| 8 | Ln = Y, x = 24 | 100 | > 99 | 1.44 | 1.93 | 1.88 | 0.82 |
| 9 | Ln = Y, x = 25 | 100 | > 99 | 1.44 | 1.43 | 1.99 | 0.83 |
| 10 | Ln = Y, x = 26 | 100 | > 99 | 1.44 | 1.23 | 1.19 | 0.74 |
| 11 | Ln = Y, x = 27 | 100 | > 99 | 1.44 | 0.01 | 14.7 | 0.70 |
| 12 | Ln = Y, x = 28 | 100 | 26 | 0.37 | 1.83 | 1.52 | 0.80 |
| 13 | Ln = Y, x = 14 | 100 | 79 | 1.14 | 0.48 | 1.94 | 0.71 |
| 14 | Ln = Y, x = 29 | 100 | > 99 | 1.44 | 0.01 | 7,51 | 0.76 |

[a] Polymerization conditions: [LA]$_0$/[Init]$_0$ = 100, 0.5 h, toluene, 1 mL, 25 °C. [b] conversion of monomer (([LA]$_0$ - [LA]$_t$) /[LA]$_0$); [c] measured by GPC with PS standards in THF,[32] [d]determined by homonuclear decoupled $^1$H NMR, $P_s$ is the probability of forming a new *s* dyad.[44]

In contrast to ROP of *rac*-lactide, 1,3-dithiapropanediyl-bridged bis(phenolate) complexes [Sc**L**$^{24\text{-}26}${N(SiMe$_2$H)$_2$}(THF)] polymerize *meso*-lactide efficiently, reaching high conversions within 0.5 h. *meso*-Lactide is polymerized faster because of its higher ring strain.[35]

ROP of *meso*-lactide using initiators [Sc**L**$^{14,25\text{-}29}${N(SiMe$_2$H)$_2$}(THF))] afforded highly syndiotactic PLA ($P_s$ > 0.84) with $P_s$ = 0.92 as a maximum observed for [Sc**L**$^{14}${N(SiMe$_2$H)$_2$}(THF)] (Figure 4.2.).

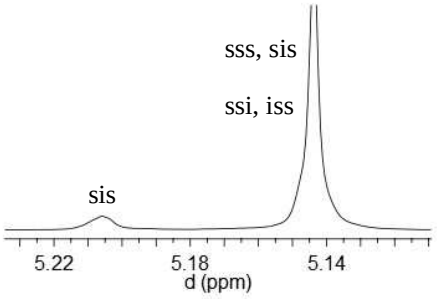


**Figure 4.2.** $^{1}H\{^{1}H\}$ NMR spectrum of poly(*meso*-lactide) synthesized using [Sc**L**$^{14}${$N(SiMe_2H)_2$}(THF)] (Table 4.4., Entry 6).

Syndiotacticity of poly(*meso*-lactides) decreased with an increase of the metal radius, as all yttrium initiators led to lower syndiotacticity ($0.70 \leq P_s \leq 0.83$). However [Sc**L**$^{24}${$N(SiMe_2H)_2$}(THF)], based on a rigid 5-4-5 OSSO-type ligand, showed a relatively low syndioselectivity ($P_s = 0.66$), even lower than [Y**L**$^{24}${$N(SiMe_2H)_2$}(THF)] ($P_s = 0.82$).

Polymerization results using [Y**L**$^{24}${$N(SiMe_2H)_2$}(THF)] with variation of the initial monomer:initiator ratio are collated in Table 4.6.

**Table 4.6.** ROP of *meso*-lactide initiated by [Y**L**$^{24}${$N(SiMe_2H)_2$}(THF)].[a]

| Entry | $[Ln]_0/[LA]_0$ | Conv. (%)[b] | $M_c$(g·mol$^{-1}$) (×10$^{-4}$) | $M_n$(g·mol$^{-1}$) (×10$^{-4}$)[c] | $M_w/M_n$[c] | $P_s$[d] |
|---|---|---|---|---|---|---|
| 1 | 100 | > 99 | 1.44 | 1.95 | 1.88 | 0.82 |
| 2 | 200 | > 99 | 2.88 | 2.45 | 1.98 | 0.90 |
| 3 | 300 | > 99 | 4.32 | 4.48 | 1.45 | 0.84 |

[a] Polymerization conditions: 3 h, THF, 1 mL, 25 °C. [b] conversion of monomer ($([LA]_0 - [LA]_t)/[LA]_0$); [c] measured by GPC, $M_n$ calibrated with PS standards in THF corrected with Mark-Houwink parameters,[32] [d] determined by homonuclear decoupled $^{1}H$ NMR, $P_s$ is the probability of a new *s* dyad[44]

An increase from 1:100 to 1:300 results in increasing molecular weights ($M_{n,exp}$ = 19500 - 44800 g/mol) at 25 °C and high syndiotacticity values ($P_s > 0.82$). Carpentier *et al*. reported similar syndiotacticity values using an yttrium alkoxy-amino bis(phenolate) amide complex.[20]

Initiators [Sc**L**$^{25}${$N(SiMe_2H)_2$}(THF)] bearing cumyl groups, give poly(*meso*-lactides) of higher syndiotacticity ($P_s = 0.87$) compared to polymers obtained with the corresponding $^{t}$Bu substituted initiator ($P_s = 0.66$). Syndiotacticity of poly(*meso*-lactides) increases with size of the *ortho* groups.

For [Sc**L**$^{14,28\text{-}29}${N(SiMe$_2$H)$_2$}(THF)] based on chiral 5-5-5 OSSO-type ligands with different cycloalkane ring sizes, high conversion and high syndiotactic preference ($P_s$ > 0.87) is observed.

In contrast to ROP of *rac*-lactide initiated by 1-methylcyclohexyl substituted initiators ([Ln**L**$^{26}${N(SiMe$_2$H)$_2$}(THF)] and [Ln**L**$^{27}${N(SiMe$_2$H)$_2$}(THF)] (Ln = Sc, Y), stereocontrol in *meso*-lactide polymerization is comparable to results for $^t$Bu substituted initiators.[40]

Based on a 5-4-5-chelate, syndiotacticities of $P_s$ = 0.66 [Sc**L**$^{24}${N(SiMe$_2$H)$_2$}(THF)] and 0.82 [Y**L**$^{24}${N(SiMe$_2$H)$_2$}(THF)] were obtained for $^t$Bu substituted initiators while [Sc**L**$^{26}${N(SiMe$_2$H)$_2$}(THF)] and [Y**L**$^{26}${N(SiMe$_2$H)$_2$}(THF)] gave tacticity values of $P_s$ = 0.84 [Sc**L**$^{26}${N(SiMe$_2$H)$_2$}(THF)] and $P_s$ = 0.74 [Y**L**$^{26}${N(SiMe$_2$H)$_2$}(THF)]. $M_w/M_n$ values are high for all poly(*meso*-lactides). Only [Sc**L**$^{24}${N(SiMe$_2$H)$_2$}(THF)] ($M_w/M_n$ = 1.23) and [Y**L**$^{26}${N(SiMe$_2$H)$_2$}(THF)] ($M_w/M_n$ = 1.19) based on a rigid 5-4-5 chelate gave narrowly distributed polymers.

Interestingly, Coates and Ovitt reported that racemic [Al(SalBinap)(OR)] formed heterotactic PLAs from *meso*-lactide.[24] When enantiopure (*S*,*S*)-[Sc**L**$^{14}${N(SiMe$_2$H)$_2$}(THF)] and (*R*,*R*)-[Sc**L**$^{14}${N(SiMe$_2$H)$_2$}(THF)] were explored for ROP of *meso*-lactide, syndiotactic PLA ($P_s$ = 0.93) is formed, demonstrating that use of enantiopure rare earth metal bis(phenolate) initiators has no specific effect on stereoselectivity. (Table 4.7.).

**Table 4.7.** ROP of *meso*-lactide initiated by enantiopure and racemic [Sc**L**$^{14}${N(SiMe$_2$H)$_2$}(THF)]. [a]

| Entry | Catalyst | $[Ln]_0/[LA]_0$ | Conv. (%)[b] | $M_c$(g·mol$^{-1}$) (×10$^{-4}$) | $M_n$(g·mol$^{-1}$) (×10$^{-4}$)[c] | $M_w/M_n$[c] | $P_s$[d] |
|---|---|---|---|---|---|---|---|
| 1 | *S*,*S* | 100 | 98 | 1.42 | 2.05 | 2.09 | 0.93 |
| 2 | *R*,*R* | 100 | > 99 | 1.44 | 5.70 | 2.34 | 0.93 |
| 3 | *rac* | 100 | > 99 | 1.44 | 7.40 | 2.20 | 0.92 |

[a] Polymerization conditions: $[LA]_0/[Init]_0$ = 100, 0.5 h, toluene, 1 mL, 25 °C. [b] conversion of monomer (($[LA]_0$ – $[LA]_t$) /$[LA]_0$); [c] measured by GPC with PS standards in THF,[32] [d] determined by homonuclear decoupled $^1$H NMR, $P_s$ is the probability of forming a new *s* tetrad.[44]

In 1999 Coates and Ovitt reported that enantiopure [Al(SalBinap)(OR)] converted *meso*-lactide into crystalline syndiotactic poly(lactide) with $T_m$ = 150 °C, while the homologous yttrium complex was not active.[46]

In addition to studies on initiators prepared in this thesis, scandium bis(phenolate) silylamide initiators that have already been investigated earlier concerning their heteroselectivity in *rac*-lactide polymerization were explored in ROP of *meso*-lactide. The data are collated in Table 4.8.

**Table 4.8.** ROP of *meso*-lactide initiated by scandium bis(phenolate) silylamide initiators [Sc**L**$^{x}${N(SiMe$_2$H)$_2$}THF]. [a]

| Entry | Catalyst | $[Ln]_0/[LA]_0$ | Conv. (%)[b] | $M_c$(g·mol$^{-1}$) (×10$^{-4}$) | $M_n$(g·mol$^{-1}$) (×10$^{-4}$)[c] | $M_w/M_n$[c] | $P_s$[d] |
|---|---|---|---|---|---|---|---|
| 1 | x = 5 | 100 | > 99 | 1.44 | 1.25 | 1.29 | 0.88 |
| 2 | x = 9 | 100 | 88 | 1.29 | 4.00 | 1.85 | 0.93 |
| 3 | x = 10 | 100 | > 99 | 1.44 | 1.60 | 1.71 | 0.89 |
| 4 | x = 15 | 100 | 95 | 1.37 | 1.33 | 2.15 | 0.90 |
| 5 | x = 18 | 100 | 93 | 1.34 | 1.90 | 1.80 | 0.89 |

[a] Polymerization conditions: 0.5 h, THF, 1 mL, 25 °C. [b] conversion of monomer (($[LA]_0 - [LA]_t$) /$[LA]_0$); [c] measured by GPC, $M_n$ calibrated with PS standards in THF corrected following Mark-Houwink parameters; [d] determined by homonuclear decoupled $^1$H NMR, $P_s$ is the probability of forming a new *s* dyad[44]

ROP is rapid and controlled. Polydispersity values ($M_w/M_n$) of the polymers vary from 1.3-2.1 demonstrating again the influence of different bridges and different *ortho*-groups.

[Sc**L**$^{18}${N(SiMe$_2$H)$_2$}(THF)] has previously been reported to be active in heteroselective ROP of *rac*-lactide ($P_r$ = 0.93).[39] Additional experiments with an initial monomer/initiator ratio of 52 : 1 attained full conversion within 30 min in $C_6D_6$ with $M_n$ = 6500 g/mol, $M_w/M_n$ = 1.22 and $P_s$ = 0.91. An increase in initial initiator/monomer ratio from 1 : 50 to 1 : 200 gave polymers with increased molecular weights between 10 500 g/mol and 34 750 and polydispersities between $M_w/M_n$ = 1.68 - 2.04.

Under similar conditions, 1,3-dithiapropanediyl-bridged complex [Sc**L**$^{15}${N(SiMe$_2$H)$_2$}(THF)] also showed syndioselectivity ($P_s$ = 0.90, Table 4.8., entry 4). This finding is in agreement with previously reported results on ROP of *rac*-lactide ($P_r$ = 0.95).[40] Fast conversion and highest syndiotacticity were achieved by [Sc**L**$^{9}${N(SiMe$_2$H)$_2$}(THF)] ($P_s$ = 0.93) (Table 4.8.).

ROP of *meso*-lactide using [Sc**L**$^{18}${N(SiMe$_2$H)$_2$}(THF)] in THF gave polymers with molecular weights higher than calculated, as opposed to ROP in toluene. Syndiotacticity

values remains at the same level ($P_s$ = 0.86). These findings indicate the Lewis base to block the coordination site (Figure 4.3.)

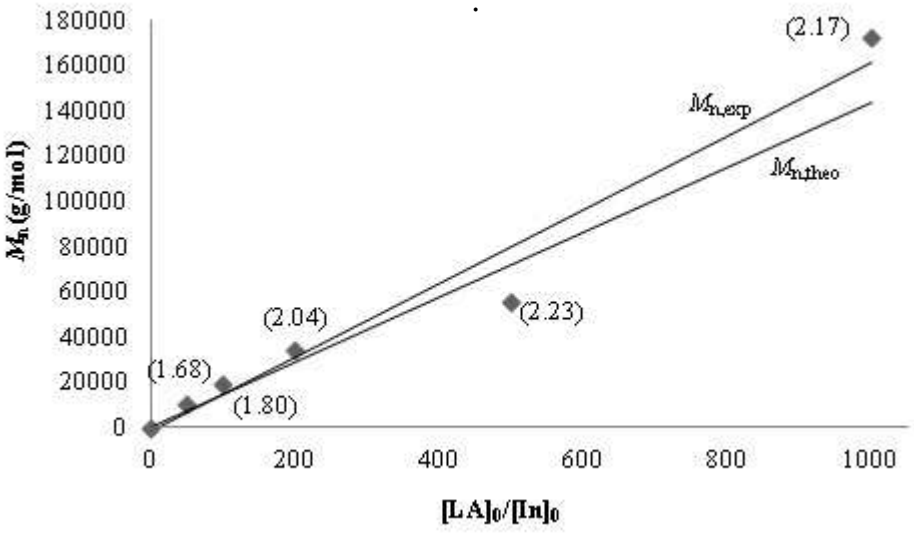


**Figure 4.3.** Polymerization of *meso*-lactide with variation of initial monomer/initiator ratio $[LA]_0/[In]_0$ using [Sc**L**$^{18}${$N(SiMe_2H)_2$}(THF)].

**Table 4.9.** ROP of *meso*-lactide initiated by [Sc**L**$^{18}${$N(SiMe_2H)_2$}(THF)]. [a]

| Entry | T / (°C) | $[Ln]_0/[LA]_0$ | Time / (min) | Conv. (%)[b] | $M_c$(g·mol$^{-1}$) (×10$^{-4}$) | $M_n$(g·mol$^{-1}$) (×10$^{-4}$)[c] | $M_w/M_n$[c] | $P_s$[d] |
|---|---|---|---|---|---|---|---|---|
| 1 | 60 | 200 | 10.2 | 56 | 1.44 | 1.50 | 1.63 | 0.86 |
| 2 | 100 | 200 | 7.2 | 54 | 1.29 | 1.40 | 2.80 | 0.85 |
| 3 | 130 | 200 | 7.2 | 88 | 1.44 | 4.55 | 1.59 | 0.83 |

[a] Melt polymerization; [b] conversion of monomer (($[LA]_0 - [LA]_t$) /$[LA]_0$); [c] measured by GPC, $M_n$ calibrated with PS standards in THF corrected following Mark-Houwink parameters; [d] determined by homonuclear decoupled $^1$H NMR, $P_s$ is the probability of forming a new *s* dyad[44]

ROP of *meso*-lactide in melt using [Sc**L**$^{18}${$N(SiMe_2H)_2$}(THF)] (1 : 200) was rapid (50% monomer conversion <10 min) and controlled (see Table 4.9.). Tacticity ($P_s$ > 0.83) was as high as that observed in solution.

The somewhat broader polydispersities of PLAs obtained with the rare earth metal initiators were ascribed to chain transfer reaction due to their high activity.

### IV.2.2. Analysis of the Microstructure of PLA

The results presented in the previous chapter demonstrate that OSSO-type bis(phenolate) complexes of scandium silylamides initiate syndioselective ROP of *meso*-lactide giving $P_s$ values around 0.92. As described in Chapter I, two general mechanisms for stereocontrol over polymerization are known.

If chain-end control (CEC) occurs, the last monomer inserted at the polymer chain determines the stereochemistry of insertion of the next monomer. When catalytic-site control (CSC) takes place, the initiator ring-opens the monomer preferentially at one of the two enantiotopic sites. CSC was reported by Coates *et al.* to be the origin of selectivity when ROP is performed with [Al(SalBinap)(OR)] as initiator (Scheme 4.8) [24,46]

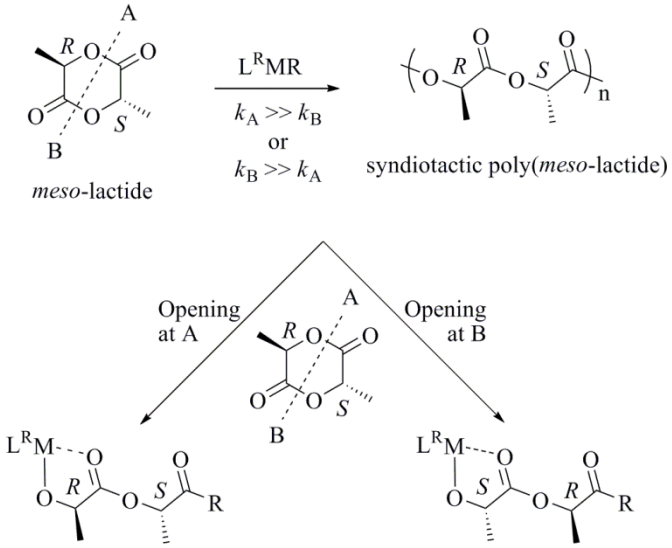


**Scheme 4.8.** Stereoselective ROP of *meso*-lactide by catalytic-site control.

Mechanisms of stereocontrol can be studied by statistical analysis of stereoerrors. (Figure 4.4.) If no misinsertion occurs (Figure 4.4. **A**), lactide is either opened at the A- (*RS*) or the B-site (*SR*). The stereocenters along the polymer chain follow strictly the order *RSRSRS* or *SRSRSR* and no other tetrad than sss tetrads are observed in NMR.

If chain-end control occurs (Figure 4.4. **B**), insertion starts at one enantiotopic site, for example A, forming a syndiotactic stereoblock. If one misinsertion takes place, the incoming monomer is opened at the B site (*SR*). This *SR* configured unit determines opening of the next monomer correctly following CEC mechanism at the B site (*SR*) starting the next syndiotactic

stereoblock. Next to sss tetrads representing syndiotactic stereoblocks, one ssi tetrad, one sis tetrad and one iss tetrad is observed in the $^{13}C\{^{1}H\}$ NMR spectrum of the polymer.

**A**: Insertion sequences for production of syndiotactic poly(*meso*-lactide):

*RSRSRSRSRSRSRSRSRS*

S S S S S S S S S S S S S S S S S S only sss tetrads

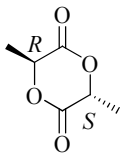


**B**: Insertion sequence for one misinsertion occuring in CEC Mechanism:

*RSRSRSRSRSSRSRSRSRSR*

S S S S S S S S S I S S S S S S S S S ssi, sis and iss tetrad show one misinsertion

**C**: Insertion sequence for one misinsertion occuring in CSC Mechanism:

*RSRSRSRSRSSRRSRSRSRS*

S S S S S S S S S I S I S S S S S S S ssi, 2x sis, isi and iss tetrad show one misinsertion

**Figure 4.4.** Insertion sequences for ROP of *meso*-lactide giving **A**: Syndiotactic PLA without misinsertion; **B**: One misinsertion occuring in CEC mechanism; **C**: One misinsertion occuring in CSC mechanism.

Figure 4.4. **C** shows tetrads that are observed with one stereoerror along the polymer chain with catalytic-site control. After several correct insertions, for example at site A, one monomer is inserted at the "wrong" B site (*SR*). As catalytic-control prefers one site, the next monomer is opened again at the A site (*RS*) which is the preferred site of the catalytic species but inverted in comparison to the last monomer. Next to the sss tetrad, one ssi tetrad, one isi, one iss and two sis tetrads can be found resulting from one misinsertion.

At selectivities around $P_s$ = 0.90 double stereoerrors or even more misinsertions cannot be excluded.

Focussing on the results with rare earth metal bis(phenolate) silylamide systems, [Sc**L**[18]{N(SiMe$_2$H)$_2$}(THF)] showed highest syndioselectivity in ROP of *meso*-lactide ($P_s$ = 0.93) (Figure 4.5.).

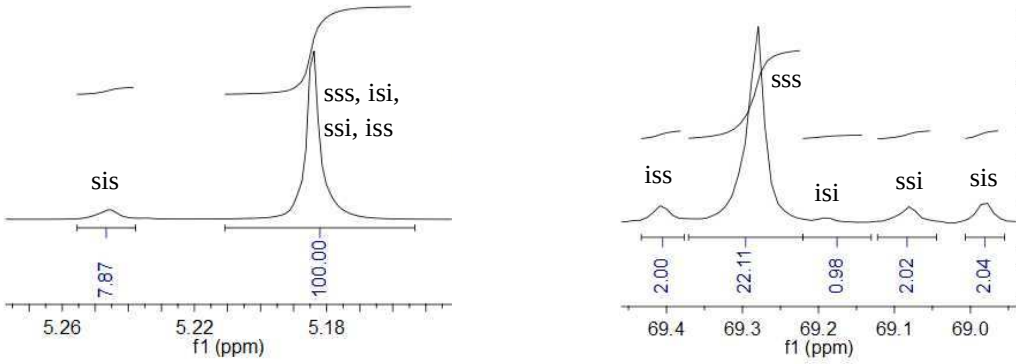


**Figure 4.5.** $^{1}H\{^{1}H\}$ NMR spectrum (left) and $^{13}C\{^{1}H\}$ NMR (right) of poly(*meso*-lactide) produced by [Sc**L**$^{18}${$N(SiMe_2H)_2$}(THF)].

Existence of the isi tetrad in the $^{13}C\{^{1}H\}$ NMR spectrum of poly(*meso*-lactide) (Figure 4.5., right) shows that CSC-mechanism dominates in ROP of *meso*-lactide. ROP runs in a similar way as with initiator systems reported by Coates (Scheme 4.9.).[24,46]

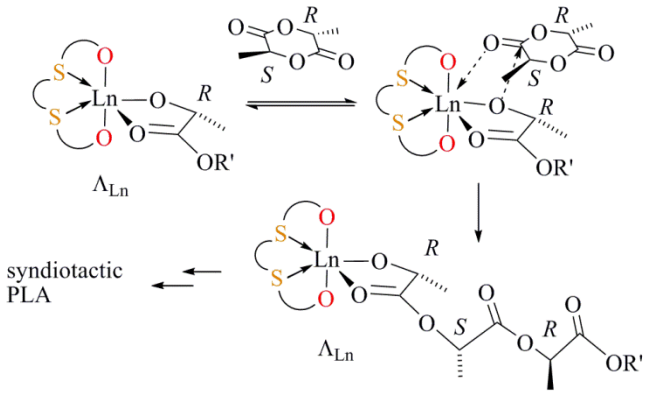


**Scheme 4.9**. Proposed mechanism for ROP of *meso*-lactide

The tetrad integrals in the $^{13}C\{^{1}H\}$ NMR spectra lead to a tetrad ratio iss:sss:isi:ssi:sis of 2:22:1:2:2. Neglecting the integral of the sss tetrad, nearly the same ratio of the other four tetrad integrals can be found for all poly(*meso*-lactides) produced by rare earth metal bis(phenolate) silylamide initiators.

As already shown in Figure 4.4., one misinsertion in the ROP of *meso*-lactide following a CSC-mechanism gives the following ratio of tetrads: 1 x iss, 1 x isi, 1 x ssi, 2 x sis.

Comparing theory with experimental results leaves two tetrads, 1 x iss and 1 x ssi tetrad that do not result from a misinsertion of one monomer. As *meso*-lactide is formed as a side product in preparation of L-lactide, commercially available *meso*-lactide always contains small amounts L-lactide. Hence, purification of *meso*-lactide used for polymerization experiments is mandatory. Typically, purification of *meso*-lactide includes repeated recrystallization from isopropanol or toluene and sublimation. Identification of *RR* and *SS*-lactide next to *meso*-lactide is possible by $^{1}$H NMR spectroscopy. In Figure 4.6. the $^{1}$H NMR spectrum of an equimolar mixture of *meso*- and L-lactide is presented. It can clearly be seen that signals arising for the methine protons of the isomers overlap with each other while resonances for the $CH_3$-groups are separated. If only a small amount of L-lactide soils *meso*-lactide, it should also be possible to identify the diastereomers next to each other.

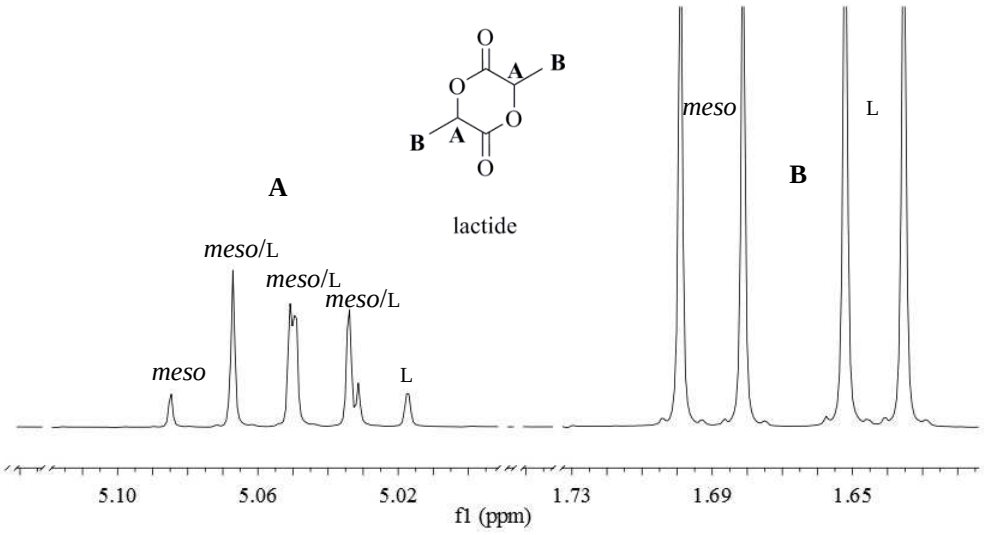


**Figure 4.6.** Part of the $^{1}$H NMR spectrum of a 1:1 mixture of L- and *meso*-lactide in $CDCl_3$ at 25 °C.

After purification of *meso*-lactide by recrystallization and sublimation, no L-lactide can be found in the $^{1}$H NMR spectrum (Figure 4.7.) and after GC/MS analysis. This shows, that there is no detectable amount of L-lactide in *meso*-lactide. Because the silylamide group and THF attached to the metal centers are basic, it was investigated whether these initiators can induce epimerization of lactide as a side reaction of the ROP. Problematically for this analysis, the initiators were demonstrated to be highly active. In the $^{1}$H NMR spectra of quenched reaction mixtures, even after only a few minutes no signals of *rac*-lactide could be found in the region of unconverted monomer. To slow down the polymerization rate, ROP of *meso*-lactide initiated by [Sc**L**$^{18}${N(SiMe$_2$H)$_2$}(THF)] was performed at -70 °C, at -18°C and at 0 °C. At

T < -18 °C neither polymerization nor epimerization occurred. In experiments performed at 0 °C, after 8 h very low conversion of 20% was found. NMR spectroscopic studies and GPC analysis showed the formation of atactic polymers with low molecular weights. No signals of *rac*-lactide could be identified indicating no verifiable epimerization.

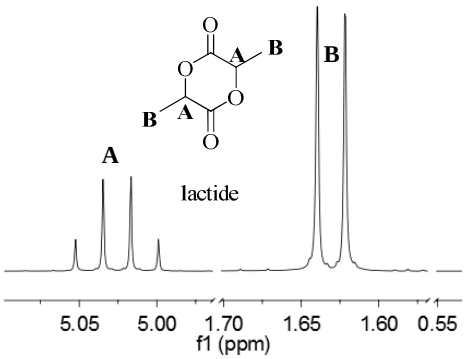


**Figure 4.7.** $^{1}$H NMR spectrum of purified *meso*-lactide measured in $CDCl_3$ at 25 °C.

Finally, **18** and $H\{N(SiMe_2H)_2\}$ were stirred with 100 equiv. of *meso*-lactide in 2 mL toluene and the reaction progress was monitored by $^{1}$H NMR. **18** polymerized *meso*-lactide to atactic polymer with low molecular weights while in the reaction mixture of $H\{N(SiMe_2H)_2\}$ and *meso*-lactide, small signals of the methyl-groups of *rac*-lactide could be found next to signals for *meso*-lactide after 108 h in toluene. No significant polymerization took place (Figure 4.8). This demonstrates that the basic silylamide group attached to the metal centers should possibly be able to epimerize *meso*-lactide into *rac*-lactide.

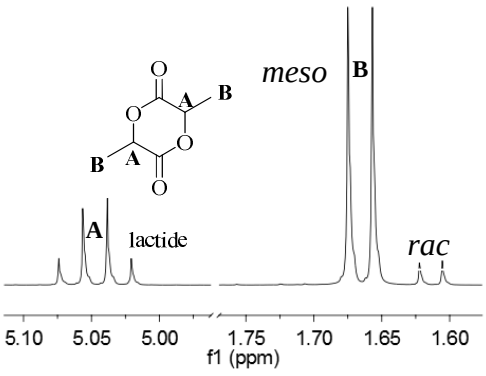


**Figure 4.8.** Part of the $^{1}$H NMR spectrum after reaction of $H\{N(SiMe_2H)_2\}$ with *meso*-lactide for 108 h in $CDCl_3$ at 25 °C.

Figure 4.9. shows the structures of D and *meso*-lactide in the solid state. Theoretical calculations have identified *meso*-lactide having the higher ring strain resulting in an easier cleavage of the acyl bond.[47] Recently, Börner *et al.* reported about epimerization of *meso*-lactide in presence of organic bases.[47] DBU, DABCO or imidazole induce epimerization of *meso*-lactide even at 25 °C resulting in an equimolar mixture of all three isomers.[47] This process occurs without significant polymerization. The authors exclude the possibility, that depolymerization of poly(*meso*-lactides) takes place. As driving force, formation of more stable L- and D-lactide monomers were observed. This should in principle also be possible for the basic silylamide group.

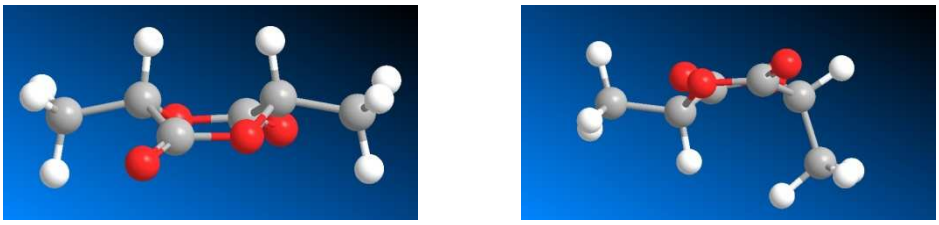

**Figure 4.9.** Solid state structures of D- (left) and *meso*-lactide (right).

From the data collected in the presented study, depolymerization of PLA and subsequent formation of L- or D-lactide cannot be excluded. Inversion of the stereocenters along the polymer chain can be excluded as ROP experiments running for more than 24 h gave the same results than experiments stopped earlier.

If D- or L-lactide formed by epimerization inserts into the polymer chain, the stereocenters can follow for example the order *RSRSRRRSRS* or *SRSRSSSRS*. In that case, sii or iis tetrads occur. Scheme 1.6. (a)-(d) demonstrates, that the iis and sii tetrad signals overlap with diagnostic tetrad signals from poly(*meso*-lactide) influencing the integral area minimally, although only a statistical insertion of L- or D-lactide is likely to occur.

Consequently, [Sc**L**$^{18}${N(SiMe$_2$H)$_2$}(THF)], 100 equiv. of *meso*-lactide and 1 equiv. *rac*-lactide were stirred in THF for 1 h using the standard polymerization procedure. The resulting crude polymer was analyzed by NMR spectroscopy. No signals of *rac*-lactide were found in the $^1$H NMR. Probably, it was also incorporated into the polymer chain. The resulting spectra showed diagnostic resonances of poly(meso-lactide). Diagnostic resonances of insertion of L-

or D-lactide (sii or iis tetrads) were not identified. This demonstrates that, although insertion of L- or D-lactide might be a possible process to produce stereoerrors along the polymer chain, it can not be identified in detail by the analytical methods used here.

Additionally, the effect of THF during the ROP was investigated in more detail. Selectivity decreased dramatically if the reaction was performed only in THF solution.[40] Not surprisingly, when ROP of *meso*-lactide was initiated by [Sc**L**$^{18}${N(SiMe$_2$H)$_2$}(THF)] in a mixture of 0.95 mL toluene and 0.05 mL THF (425 equiv.), syndioselectivity decreases from $P_s$ = 0.90 (Table 4.6., entry 4) to $P_s$ = 0.75. Focussing on the $^{13}C\{^1H\}$ NMR spectrum of the polymer, one can see the ratio of tetrad integrals changing compared to the ratio shown in Figure 4.10.

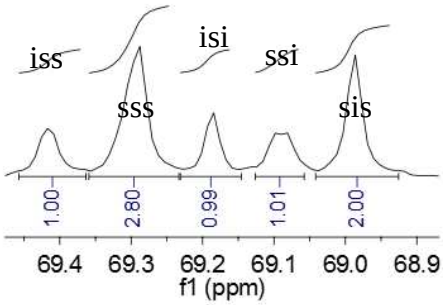


**Figure 4.10.** $^{13}C\{^1H\}$ NMR of poly(*meso*-lactide) produced by [Sc**L**$^{18}${N(SiMe$_2$H)$_2$}(THF)] in a mixture of 0.95 mL toluene and 0.05 mL THF.

Neglecting the sss tetrad, a ratio of iss:isi:ssi:sis of 1:1:1:2 was found. This tetrad ratio fits with the theoretical ratio of misinsertion if CSC mechanism takes place (Figure 4.4.). Based on the results of this analysis and on studies over the last years[38-41] it is obvious, that THF accelerates the reaction. Fast exchange of THF results in formation of a pseudo five-coordinated intermediate leaving a larger coordination sphere for lactide to coordinate to the metal center. Addition of THF results in a loss of selectivity as the coordination and insertion is performed much faster and therefore less controlled. In addition, epimerization does possibly not occur as much as in toluene or $CH_2Cl_2$. The integral ratio of the tetrads from the poly(*meso*-lactides) fits perfectly with the theory of a misinsertion in CSC.

This might result from the effect of THF on the transition state of the initiation process. Polar solvents are known to increase the rate of $S_N1$ reactions. Heterolytic bond-dissociation takes place when the silylamide group attacks on the lactide monomer, followed by acyl bond-

cleavage. The transition state is polar. As a consequence, the polar solvation increases the reaction rate by stabilizing the transition state. Resulting from the increased reaction rate in THF, epimerization is decelerated.

## IV.3. Summary

In summary, *rac*- and *meso*-lactide can be efficiently polymerized by trivalent rare earth metal initiators bearing tetradentate 5-5-5, 5-6-5 or 5-7-5 chelating OSSO-type bis(phenolate) ligands to give heterotactic poly(*rac*-lactides) ($P_r$ = 0.68-0.85) or highly syndiotactic poly(*meso*-lactides) ($P_s$ = 0.88-0.93). Selectivity depends on the length of the 1,$\omega$-dithiaalkanediyl bridge and on the *ortho*-substituents on the phenolate moiety. Refering to the site control mechanism at a chiral stereorigid ligand sphere, highly heteroselective initiators for ROP of *rac*-lactide generally appear to polymerize *meso*-lactide syndiospecifically.

Analysis of the microstructure of poly(*meso*-lactides) shows, that the silylamide group attached to the metal centers possibly induce epimerization of *meso*-lactide into D- and L-lactide. These two monomers can insert into the poly(*meso*-lactide) chains statistically resulting in observed stereoerrors and hindering the production of syndiotactically pure poly(*meso*-lactides).

Furthermore, THF influences the reaction as it increases the reaction rate and probably diminishing the epimerization.

## IV.4. Experimental Section

**General procedure for the ROP of lactide monomers**: 0.5 mL of a 2.9 mmol/L stock solution of the initiator in 0.5 mL toluene or THF was added to a solution of the desired amount of *meso*- or *rac*-lactide (see Tables) which was dissolved in 0.5 mL of toluene or THF. After specified time intervals, each vial was taken out of the glove box and the reaction was quenched with moist *n*-hexane. The polymer was filtered off, washed with diethyl ether, and dried under vacuum. $^{1}$H, $^{1}$H{$^{1}$H} and $^{13}$C{$^{1}$H} NMR spectroscopic analysis of the polymers were performed in $CDCl_3$ at 25 °C.

**Reaction of 18 and *meso*-lactide:** 5 mg (0.036 mmol, 1 equiv) of **18** were dissolved in 5 mL toluene and 100 equiv. of *meso*-lactide were added. After specified time intervals, 0.5 mL of the solution were removed with a syringe and dried under vacuum. The residue was dissolved in 0.6 mL of $CDCl_3$ and analyzed by NMR spectroscopic analysis.

**Reaction of H{N(SiMe$_2$H)$_2$} and *meso*-lactide:** 0.34 mL H{N(SiMe$_2$H)$_2$} (0.036 mmol, 1 equiv) of **18** were dissolved in 5 mL toluene and 100 equiv. of *meso*-lactide have been added. After specified time intervals, 0.5 mL of the solution were removed with a syringe and dried under vacuum. The residue was dissolved in 0.6 mL of $CDCl_3$ and analyzed by NMR.

**Polymerization of *meso*-lactide by** [Sc**L**$^{18}${N(SiMe$_2$H)$_2$}(THF)] **in a mixture of toluene and THF**: 0.5 mL of a 2.9 mmol/L stock solution of the catalyst was added to a solution of the desired amount of *meso*-lactide dissolved in 0.45 mL toluene and 0.05 mL THF. After 0.5 h the polymerization mixture was quenched with drops of moist hexanes and was added slowly to cooled and quickly stirred *n*-hexane. The polymer was filtered over a funnel, washed with diethyl ether, and dried under vacuum. $^1$H, $^1$H{$^1$H} and $^{13}$C{$^1$H} NMR spectroscopic analysis of the polymers were performed in $CDCl_3$ at 25 °C.

# IV.5. References


1 M. J. Sanford, A. P. Dove, *Chem. Soc Rev.* **2010**, *39*, 486-494.

2 J.-C. Buffet, J. Okuda, *Polym. Chem.* **2011**, *2*, 2758-2763.

3 W. M. Stevels, M. J. K. Ankoné, P. J. Dijkstra, J. Feijen, *Macromolecules* **1996**, *29*, 6132-6138.

4 R. H. Platel, A. J. P. White, C. K. Williams, *Chem. Commun.* **2009**, 4115-4117.

5 A. Amgoune, C. M. Thomas, J.-F. Carpentier, *Macromol. Rapid Commun.* **2007**, *28*, 693-697.

6 W. Miao, S. Li, H. Zhang, D. Cui, Y. Wang, B. Huang, *J. Organomet. Chem.* **2007**, *692*, 4828-4834.

7 X. Liu, X. Shang, T. Tang, N. Hu, F. Pei, D. Cui, X. Chen, X. Jing, *Organometallics* **2007**, *26*, 2747-2757.

8 C.-X. Cai, A. Amgoune, C. W. Lehmann, J.-F. Carpentier, *Chem. Commun.* **2004**, 330-331.

9 R. H. Platel, L. M. Hodgson, A. J. P. White, C. K. Williams, *Organometallics* **2007**, *26*, 4955-4963.

10 R. H. Platel, A. J. P. White, C. K. Williams, *Inorg. Chem.* **2008**, *47*, 6840-6849.

11 Y. Yang, S. Li, D. Cui, X. Chen, X. Jing, *Organometallics* **2007**, *26*, 671-678.

12 L. M. Hodgson, A. J. P. White, C. K. Williams, *J. Polym. Sci., Part A: Polym. Chem.* **2006**, *44*, 6646-6651.

13 L. M. Hodgson, R. H. Platel, A. J. P. White, C. K. Williams, *Macromolecules* **2008**, *41*, 8603-8607.

14 A. Alaaeddine, A. Amgoune, C. M. Thomas, S. Dagorne, S. Bellemin-Laponnaz, J.-F. Carpentier, *Eur. J. Inorg. Chem.* **2006**, 3652-3658.

[15] A. Alaaeddine, C. M. Thomas, T. Roisnel, J.-F. Carpentier, *Organometallics* **2009**, *28*, 1469-1475.

[16] I. Westmoreland, J. Arnold, *Dalton Trans.* **2006**, 4155-4163.

[17] G. G. Skvortsov, M. V. Yakovenko, P. M. Castro, G. K. Fukin, A. V. Cherkasov, J.-F. Carpentier, A. A. Trifonov, *Eur. J. Inorg. Chem.* **2007**, 3260-3267.

[18] P. L. Arnold, J.-C. Buffet, R. P. Blaudeck, S. Sujecki, C. Wilson, *Chem. Eur. J.* **2009**, *15*, 8241-8250.

[19] P. L. Arnold, J.-C. Buffet, R. P. Blaudeck, S. Sujecki, A. J. Blake, C. Wilson, *Angew. Chem., Int. Ed. Engl.* **2008**, *47*, 6033-6036.

[20] A. Amgoune, C. M. Thomas, T. Roisnel, J.-F. Carpentier, *Chem. Eur. J.* **2006**, *12*, 169-179.

[21] M. Bouyahi, N. Ajellal, J.-F. Carpentier, *Chem. Eur. J.* **2011**, *17*, 1872-1883.

[22] D. Patel, S. T. Liddle, S. A. Mungur, M. Rodden, A. J. Blake, P. L. Arnold, *Chem. Commun.* **2006**, 1124–1126.

[23] R. H. Platel, A. J. P. White, C. K. Williams, *Inorg. Chem.* **2011**, *50*, 7718-7728.

[24] T. M. Ovitt, G. W. Coates, *J. Am. Chem. Soc.* **2002**, *124*, 1316-1326.

[25] Y. Luo, X. Wang, J. Chen, C. Luo, Y. Zhang, Y. Yao, *J. Organomet. Chem.* **2009**, *694*, 1289-1296.

[26] Y. Luo, W. Li, D. Lin, Y. Yao, Y. Zhang, Q. Shen, *Organometallics* **2010**, *29*, 3507-3517.

[27] W. Zhao, D. Cui, X. Liu, X. Chen, *Macromolecules* **2010**, *43*, 6678–6684.

[28] L. M. Broomfield, J. A. Wright, M. Bochmann, *Dalton Trans.* **2009**, 8289-8279.

[29] A. Dumitrescu, B. Martin-Vaca, H. Gornitzka, J.-B. Cazaux, D. Bourissou, G. Bertrand, *Eur. J. Inorg. Chem.* **2002**, 1948-1951.

[30] R. Jiao, M. Xue, X. Shen, Y. Zhang, Y. Yao, Q. Shen, *Eur. J. Inorg. Chem.* **2010**, 2523–2529.

[31] M. A. Sinenkov, G. K. Fukin, A. V. Cherkasov, N. Ajellal, T. Roisnel, F. M. Kerton, J.-F. Carpentier, A. A. Trifonov, *New. J. Chem.* **2011**, *35*, 204-212.

[32] M. Save, M. Schappacher, A. Soum, *Macromol. Chem. Phys.* **2002**, *203*, 889-899.

[33] A. Otero, A. Lara-Sánchez, J. Fernanández-Baeza, C. Alonso-Moreno, I. Márquez-Segovia, L. F. Sánchez-Barba, J. A. Castro-Osma, A. M. Rodríguez, *Dalton Trans.* **2011**, *40*, 4687-4696.

[34] A. Buchard, R. H. Platel, A. Auffrant, X. F. Le Goff, P. Le Floch, C. K. Williams, *Organometallics* **2010**, *29*, 2892-2900.

[35] H. E. Dyer, S. Huijser, N. Susperregui, F. Bonnet, A. D. Schwarz, R. Duchateau. L. Maron, P. Mountford, *Organometallics* **2010**, *29*, 3602-3621.

[36] J.-C- Buffet, J. Okuda, *Dalton Trans.* **2011**, *40*, 7748-7754.

[37] T.-P.-A. Cao, A. Buchard, X. Le Goff, A. Auffrant, C. K. Williams, Inorg. Chem. **2012**, *51*, 2157-2169.

[38] H. Ma, T. P. Spaniol, J. Okuda, *Dalton Trans.* **2003**, 4770-4780.

[39] H. Ma, T. P. Spaniol, J. Okuda, *Angew. Chem.* **2006**, *118*, 7982-7985.

[40] H. Ma, T. P. Spaniol, J. Okuda, *Inorg. Chem.* **2008**, *47*, 3328-3339.

[41] H. Ma, J. Okuda, *Macromolecules*, **2005**, *38*, 2665-2673.

[42] a) Y. Shen, F. Zhang, Y. Zhang and Z. Shen, *Acta Polymerica Sinica* **1995**, *2*, 222; (b) V. Simic, N. Spassky and L. G. Hubert-Pfalzgraf, *Macromolecules* **1997**, *30*, 7338-7340.

[43] P. Dubois, R. Jerome and P. Theysse, *Polym. Prep.* **1994**, *35*, 536-537.

[44] Probability of tetrad sequences in PLA based on Bernoullian Statistics: [*sss*] = $P_s^2 + P_sP_i/2$, [*sis*] = $(P_i^2 + P_iP_s)/2$, [*ssi*] = [*iss*] =$(P_sP_i)/2$ and [*isi*] = $P_i^2/2$

[45] M. H. Chisholm, N. W. Eilerts, J. C. Huffman, S. S. Iyer, M. Pacold, K. Phomphrai, *J. Am. Chem. Soc.* **2000**, *122*, 11845-11854.

[46] T. M. Ovitt, G. W. Coates, *J. Am. Chem. Soc*. **1999**, *121*, 4072-4073.

[47] I. A. Shuklov, H. Jao, J. Schulze, W. Tietz, K. Kühlein, A. Börner *Tetrahedron Lett.* **2011**, *52*, 1027-1030.

# Chapter V

## Ring-Opening Polymerization of Lactide Monomers Initiated by Indium Bis(phenolate) Complexes

# V. Ring-Opening Polymerization of Lactide Monomers Initiated by Indium Bis(phenolate) Complexes

## V.1. Introduction

As aluminum initiators are prominent for their catalytic activity and selectivity towards the ROP of lactide monomers, complexes of indium were also explored in ROP of cyclic esters. Huang et al. reported series of poly(pyrrolyl) ligated indium complexes (**XVI**, Figure 5.1.); the first molecular indium initiators for ROP of a cyclic ester (ε-caprolactone).[1] In 2008 Merkhodavandi *et al.* introduced dinuclear indium complex [{(NNO)InCl}$_2$(μ-OEt)(μ-Cl)] (**XVII**, Figure 5.1.) as the first indium initiator for ROP of lactide. Slightly isotactic enriched poly(*rac*-lactides) ($P_i$ = 0.53-0.62) with narrow molecular weight distributions ($M_w/M_n$ = 1.20) were formed within 0.5 h at 25 °C in $CH_2Cl_2$.[2]

Tolman *et al.* studied kinetics and coordination-insertion mechanism of the stereoselective ROP of *rac*-lactide initiated by catalysts generated *in situ* from $InCl_3$, $NEt_3$ and BnOH.[3] Highly heterotactic ($P_r$ = 0.97) polymers with narrow PDIs (≤ 1.12) were produced even with 800 equivalents of lactide at 25 °C in one day.

The first bis(phenolate) indium complex that polymerized lactide was reported by Wang and Sun *et al* (**XVIII**, Figure 5.1.). Dinuclear $N_2O_2$-type water-bridged indium complex showed tolerance against alcohols, moisture and air. Narrowly distributed and slightly heterotactic enriched poly(*rac*-lactides) were formed ($P_r \leq 0.69$, PDI ≤ 1.31).[4]

Arnold *et al.* reported, that chiral dialkoxy complex In(O,O')$_2$X (**XIX**, Figure 5.1.) produced atactic or slightly isotactic enriched poly(*rac*-lactides) at 25 °C in THF or $CH_2Cl_2$ starting with high initial monomer/initiator ratios.[5]

Sulfonamide, phenolate and directing ligand-free indium initiators by Mountford *et al.* (**XX**, **XXI** and **XXII**, Figure 5.1.) polymerized *rac*-lactide in toluene solution or in melt to give heterotactic or atactic poly(*rac*-lactides).[6]

Recently, Carpentier *et al.* reported that indium complexes with Salen-like fluorinated dialkoxy-diimino ligands polymerized *rac*-lactide to give slightly heterotactic biased PLAs with relatively broad molecular weight distributions (**XXI**, Scheme 5.1.).[7]

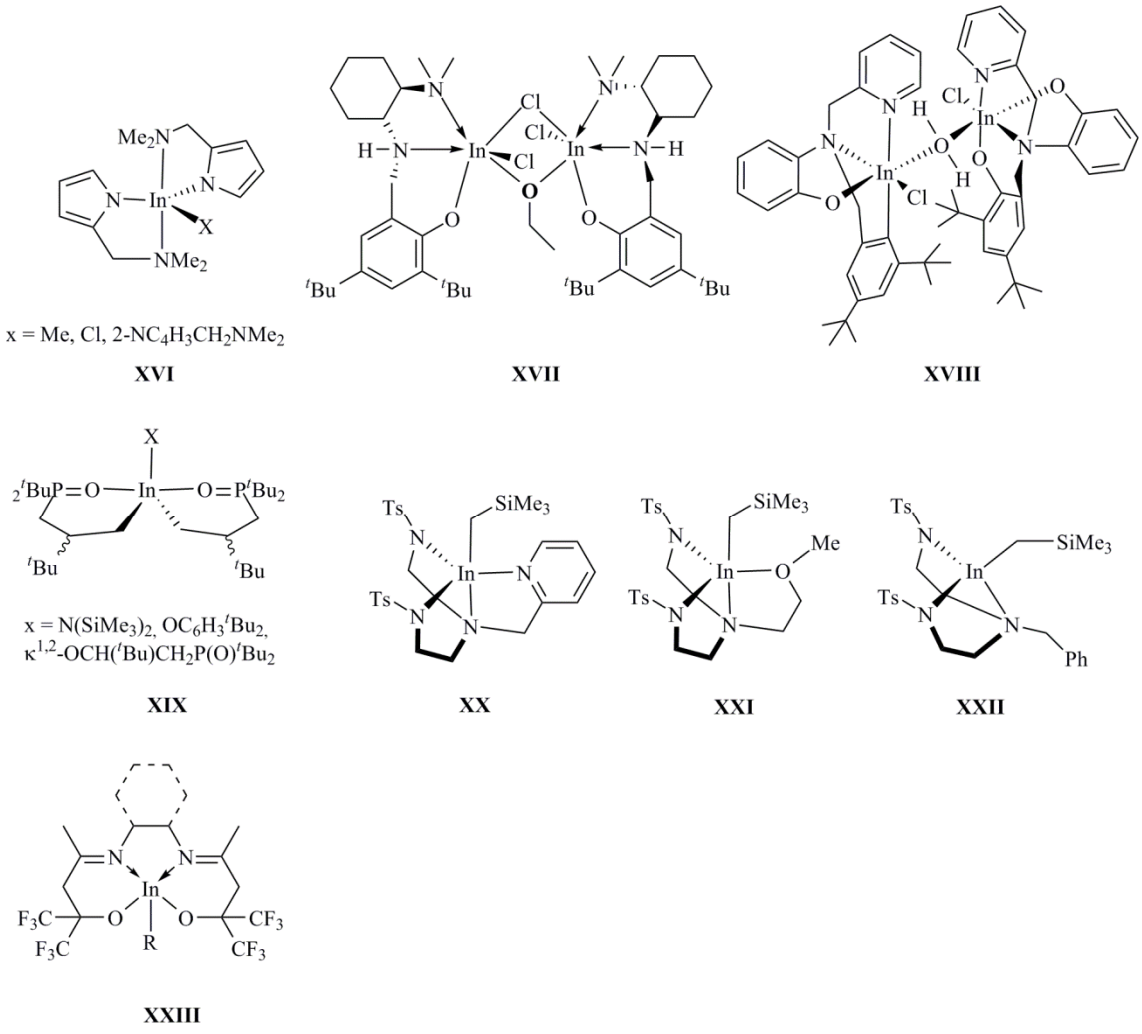


**Scheme 5.1.** Indium initiators for ROP of lactide monomers.

Because bis(phenolate) complexes of trivalent metals showed high activity and selectivity in the ROP of lactide monomers, Okuda *et al.* studied ROP of L-lactide initiated by indium bis(phenolate) isopropoxide complexes [In**L**$^{6}$(O$^{i}$Pr)] and [In**L**$^{9}$(O$^{i}$Pr)] (Scheme 5.2).[8]

The polymerization occured in a controlled fashion giving narrowly distributed poly(L-lactides) ($M_w/M_n$ = 1.03-1.18). As the polymerization appeared slower than with structurally related rare-earth metal bis(phenolate) initiators, a detailed analysis of the polymerization kinetics is possible.

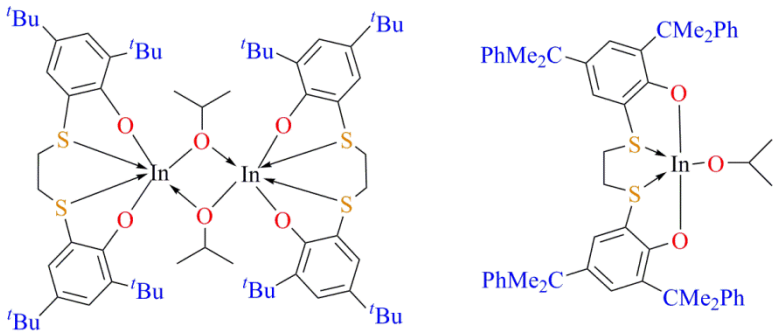


[In**L**$^{6}$(OiPr)] [In**L**$^{9}$(OiPr)]

**Scheme 5.2**. Bis(phenolate) isopropoxide complexes of indium for ROP of lactide monomers.

## V.2. Results And Discussion

Continuing from reported results on the ROP of L-lactide initiated by [In**L**$^{6}$(O$^{i}$Pr)] and [In**L**$^{9}$(O$^{i}$Pr)], ROP of *rac*- and *meso*-lactide initiated by these two complexes is discussed here along with a kinetic study on the activation parameters for ROP of *meso*- as well as *rac*-lactide. Additionally, synthesis and application of a new chiral bis(phenolate) isopropoxide indium complex in ROP of lactide monomers is introduced.

### V.2.1. Syntheses of Indium Bis(phenolate) Isopropoxide complexes

Indium bis(phenolate) isopropoxide complexes [In**L**$^{6}$(O$^{i}$Pr)] and [In**L**$^{9}$(O$^{i}$Pr)] have been synthesized according to alcohol elimination procedures starting from indium isopropoxide In$_5$($\mu_5$-O)($\mu_3$-O$^{i}$Pr)$_4$($\mu_2$-O$^{i}$Pr)$_4$(O$^{i}$Pr)$_5$ ("In(O$^{i}$Pr)$_3$", **21**)[9] and one equivalent of the appropriate bis(phenol).[8]

The new racemic indium bis(phenolate) isopropoxide complex [In**L**$^{14}$(O$^{i}$Pr)] was prepared adapting the literature procedure for the synthesis of [In**L**$^{6}$(O$^{i}$Pr)] and [In**L**$^{9}$(O$^{i}$Pr)].[8] Alcohol elimination at **21** by stoichiometric amounts of bis(phenol) H$_2$**L**$^{14}$ in toluene at 70 °C afforded [In**L**$^{14}$(O$^{i}$Pr)] in 57% yield (Scheme 5.3.).

Spectroscopic data and elemental analysis show one bis(phenolate) ligand and one isopropoxide group attached to the metal center. The $^{1}$H NMR spectrum of [In**L**$^{14}$(O$^{i}$Pr)] shown in Figure 5.1 displays the SC*H* protons as a broad signal between 1.75 and 1.90 ppm. The C*Me*$_2$Ph singlets arise between 1.26 and 1.65 ppm as singlets indicating an unsymmetrical structure of the complex. The isopropoxide group displays one septet at 3.43

ppm and one doublet of doublets at 0.84 ppm, arising from the methyl groups of the isopropoxide. Resonances of the carbon atoms arise at chemical shifts, similar to already reported bis(phenolate) complexes [Sc**L**$^{14}${N(SiMe$_2$H)$_2$}(THF)] and [Y**L**$^{14}${N(SiMe$_2$H)$_2$}(THF)].[9]

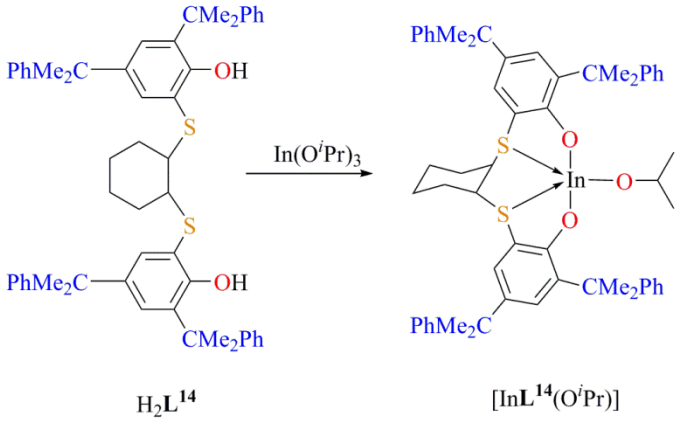


**Scheme 5.3.** Synthesis of indium bis(phenolate) isopropoxide complexes [In**L**$^{14}$(O$^i$Pr)].

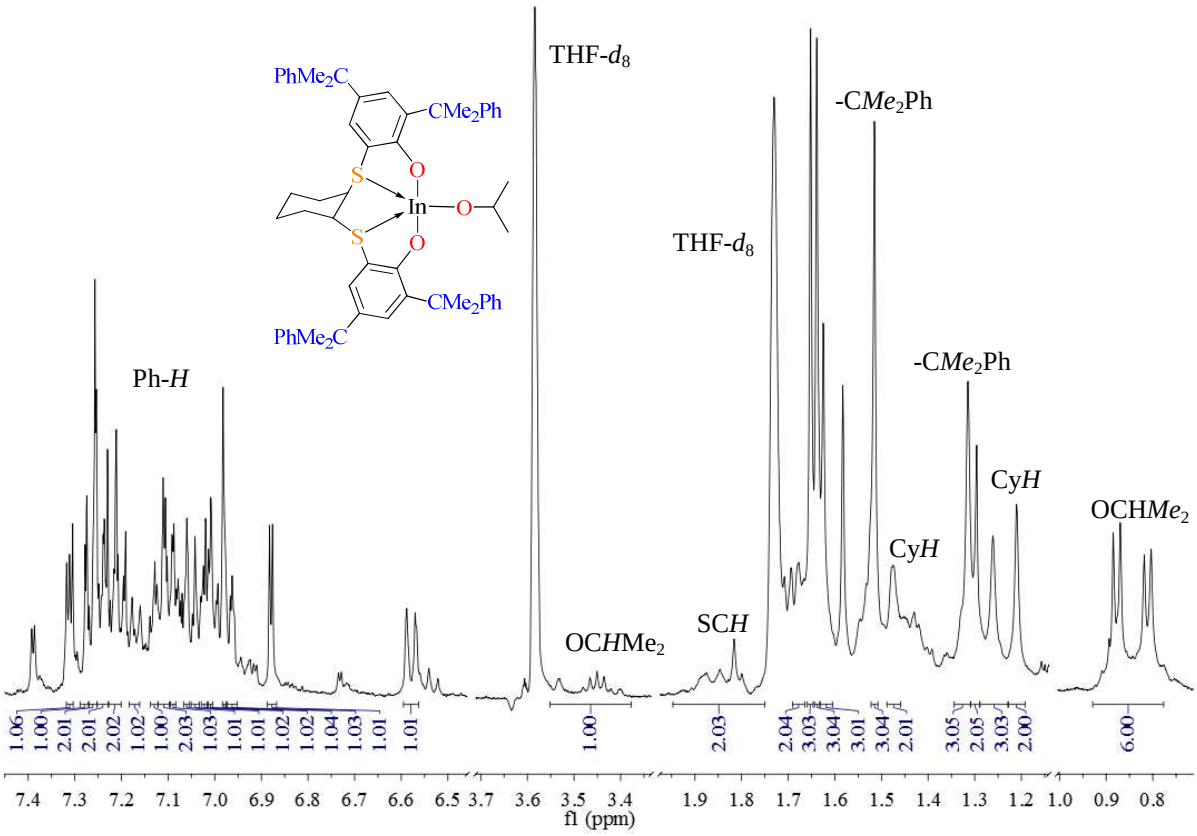


**Figure 5.1.** $^1$H NMR spectrum of [In**L**$^{14}$(O$^i$Pr)] in THF-$d_8$ at 25 °C.

## V.2.2. [In**L**$^{6}$(O$^{i}$Pr)] as Initiator for the ROP of Lactide Monomers.

The structure of [In**L**$^{6}$(O$^{i}$Pr)] in the solid state and in solution has already been studied and discussed.[8] [In**L**$^{6}$(O$^{i}$Pr)] has a dimeric structure consisting of three enantiomers with either a (*ΛΛ*), (*ΔΔ*) or a (*ΛΔ*) configuration giving two signals for the bridging isopropoxide groups and both an ABCD (*ΛΔ*) and an AA'BB' a (*ΛΛ*, *ΔΔ*) spin pattern for the SC*H*$_2$ protons (Scheme 5.4.).[8]

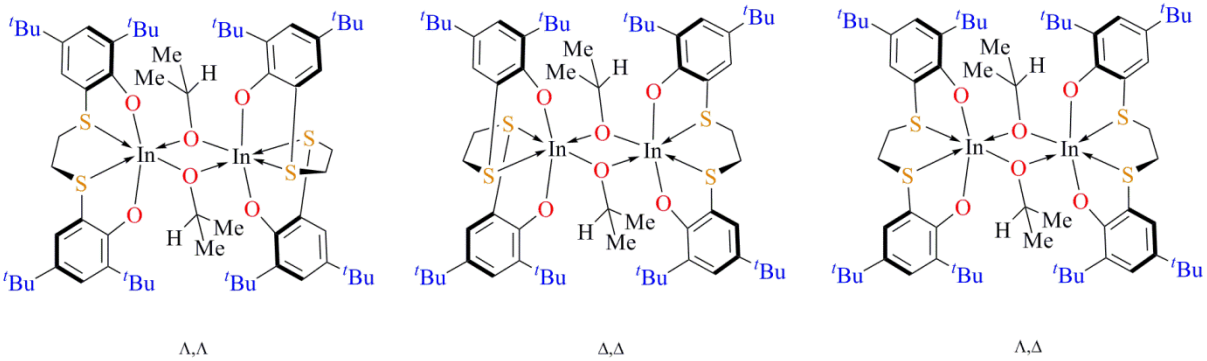


**Scheme 5.4.** Isomers of [In**L**$^{6}$(O$^{i}$Pr)].

To gain insight into the initiation step on the indium centers in [In**L**$^{6}$(O$^{i}$Pr)], one equivalent of *meso*-lactide was mixed with [In**L**$^{6}$(O$^{i}$Pr)] in THF-$d_8$ and the conversion was monitored by $^{1}$H NMR spectroscopy until nearly full conversion of lactide was reached. In the $^{1}$H NMR spectrum, a new signal arose for the methine proton of the isopropoxide end group on the ring-opened monomer at around 5 ppm.[10,11] Corresponding signals for neighboring methyl groups were identified in the expected region of the $^{1}$H NMR spectrum. The spectrum did not longer show characteristic signals for [In**L**$^{6}$(O$^{i}$Pr)], neither the signals of the two bridging isopropoxide groups nor the signals for the AA'BB' pattern of the ethylene bridge protons (Figure 5.2.). In the region of the AA'BB' spin system of dimeric [In**L**$^{6}$(O$^{i}$Pr)], only one signal for the SC*H* protons in the $^{1}$H COSY NMR spectrum was identified. Additionally, overlapping septets at 5.0 ppm arose that were identified by $^{1}$H COSY NMR to consist of one signal for the isopropoxide group (Figure 5.3.) and the resonance of the ring-opened lactide monomer. Coordination of lactide to the metal centers possibly breaks the dimeric structure, forming monomeric intermediates that seem to be more symmetric than the dimer because of the absence of an ABCD spin system. The monomeric intermediate is suggested to be the active single-site initiator for ROP of *rac*- and *meso*-lactide. In contrast, dinuclear complexes reported by Mehrkhodavandi *et al.* do not dissociate during polymerization.[2]

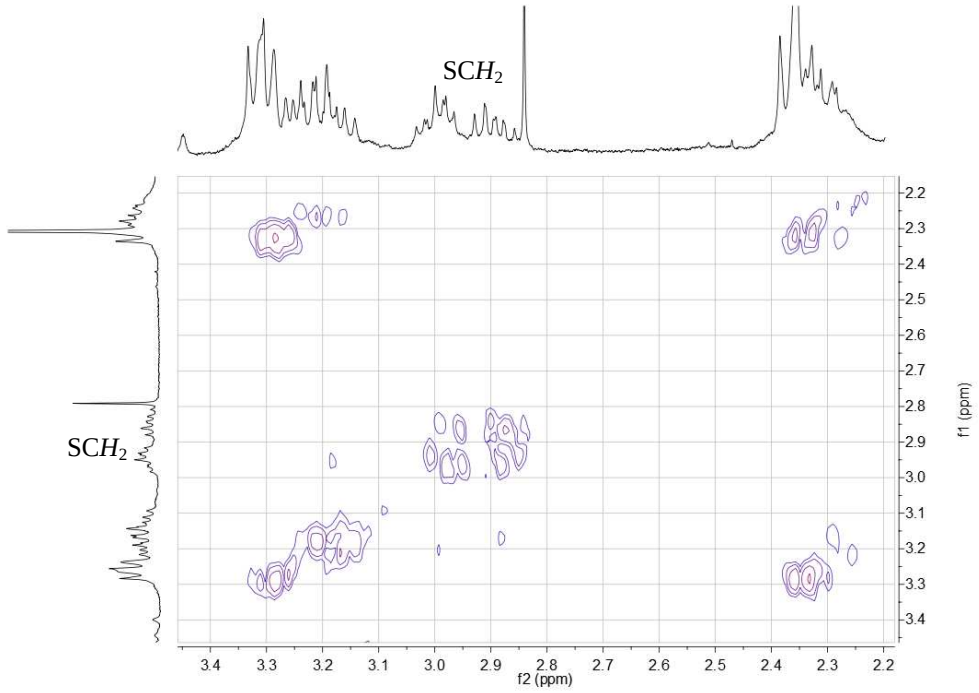


**Figure 5.2.** $^1$H COSY NMR spectrum after reaction of [In**L**$^6$(O$^i$Pr)] with one equivalent of *meso*-lactide in THF-$d_8$ at 25 °C showing coupling between the SC$H_2$ protons and the absence of the ABCD spin system.

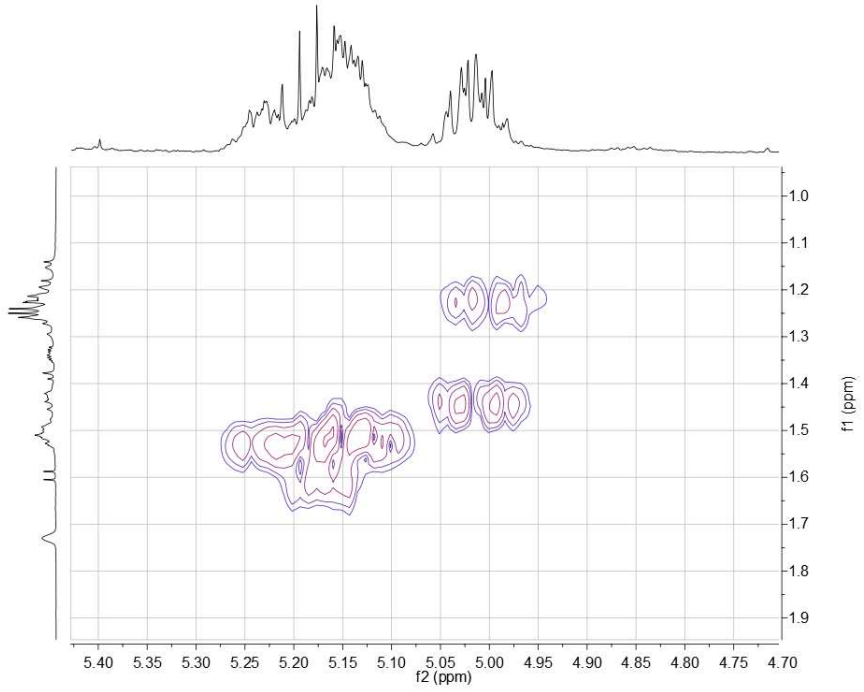


**Figure 5.3.** $^1$H COSY NMR spectrum after full conversion of [In**L**$^6$(O$^i$Pr)] with one equivalent of *meso*-lactide displaying the resonance of the methine proton of the isopropoxide and the first fragment of the polymer chain and their coupling with the methyl groups.

## V.2.3. ROP of *rac*-Lactide

Indium bis(phenolate) isopropoxide complexes [In**L**$^{6}$(O$^{i}$Pr)], [In**L**$^{9}$(O$^{i}$Pr)] and [In**L**$^{14}$(O$^{i}$Pr)] efficiently initiated ROP of *rac*-lactide in THF and $CH_2Cl_2$. The polymerization results are summarized in Table 5.1.

**Table 5.1.** ROP of *rac*-lactide initiated by [In**L**$^{6}$(O$^{i}$Pr)], [In**L**$^{9}$(O$^{i}$Pr)] and [In**L**$^{14}$(O$^{i}$Pr)].[a]

| Initiator | Entry | $[Ln]_0/[LA]_0$ | solvent | $M_n$ (g·mol$^{-1}$) (×10$^{-4}$)[b] | $M_w/M_n$[d] | $P_i$[c] | $P_r$[d] |
|---|---|---|---|---|---|---|---|
| [In**L**$^{6}$(O$^{i}$Pr)]] | 1[e] | 25 | $CH_2Cl_2$ | 0.40 | 1.08 | 0.39 | - |
| | 2[f] | 50 | $CH_2Cl_2$ | 0.77 | 1.04 | 0.48 | - |
| | 3[g] | 100 | $CH_2Cl_2$ | 1.33 | 1.03 | 0.51 | - |
| | 4[h] | 150 | $CH_2Cl_2$ | 1.75 | 1.03 | 0.50 | - |
| | 5[i] | 250 | $CH_2Cl_2$ | 2.65 | 1.02 | 0.50 | - |
| | 6[e] | 25 | THF | 0.40 | 1.02 | - | 0.43 |
| | 7[f] | 50 | THF | 0.69 | 1.24 | - | 0.37 |
| | 8[g] | 100 | THF | 1.10 | 1.14 | - | 0.41 |
| | 9[h] | 150 | THF | 1.42 | 1.18 | - | 0.50 |
| | 10[i] | 250 | THF | 1.76 | 1.22 | - | 0.46 |
| [In**L**$^{9}$(O$^{i}$Pr)] | 11[e] | 50 | $CH_2Cl_2$ | 0.96 | 1.28 | 0.42 | - |
| | 12[f] | 100 | $CH_2Cl_2$ | 1.69 | 1.27 | 0.44 | - |
| | 13[g] | 200 | $CH_2Cl_2$ | 2.46 | 1.29 | 0.41 | - |
| | 14[h] | 300 | $CH_2Cl_2$ | 5.88 | 1.20 | 0.42 | - |
| | 15[i] | 500 | $CH_2Cl_2$ | 8.68 | 1.25 | 0.44 | - |
| | 16[e] | 50 | THF | 0.67 | 1.51 | - | 0.29 |
| | 17[f] | 100 | THF | 2.10 | 1.36 | - | 0.29 |
| | 18[g] | 200 | THF | 1.29 | 1.57 | - | 0.27 |
| | 19[h] | 300 | THF | 1.29 | 1.86 | - | 0.32 |
| | 20[i] | 500 | THF | 1.27 | 2.34 | - | 0.34 |
| [In**L**$^{14}$(O$^{i}$Pr)] | 21 | 100 | THF | 2.17 | 1.06 | - | 0.77 |
| | 22[f] | 100 | THF | 2.25 | 1.13 | - | 0.72 |

[a] T = 25 °C, $[LA]_0$ = 0.30 M, conversion: > 95%, [b]From GPC analyses; corrected using Mark Houwink parameter 0.58;[11] [c] $P_i$ is the probability of forming isotactic tetrads, determined by homonuclear decoupled $^1$H NMR; [d]$P_r$ is the probability of forming heterotactic tetrads, determined by homonuclear decoupled $^1$H NMR; [e] V(Solvent) = 0.5 mL, $[Ln]_0 = 6.06 \cdot 10^{-3}$ M; [f] V(Solvent) = 1 mL, $[Ln]_0 = 3.03 \cdot 10^{-3}$ M; [g] V(Solvent) = 2.0 mL, $[Ln]_0 = 1.50 \cdot 10^{-3}$ M; [h] V(Solvent) = 3.0 mL, $[Ln]_0 = 1.01 \cdot 10^{-3}$ M; [i] V(Solvent) = 5.0 mL, $[Ln]_0 = 6.06 \cdot 10^{-4}$ M.

All polymerization experiments were performed until a monomer conversion of ≥ 95% was reached. Poly(*rac*-lactides) generated by [In**L**$^{6}$(O$^{i}$Pr)], [In**L**$^{9}$(O$^{i}$Pr)] and [In**L**$^{14}$(O$^{i}$Pr)] showed high molecular weights. The PDI values depend minimally on the solvent used for polymerization. While polymerization in $CH_2Cl_2$ resulted in narrowly distributed polymers not exceeding $M_w/M_n$ = 1.08 for [In**L**$^{6}$(O$^{i}$Pr)], $M_w/M_n$ = 1.20 for [In**L**$^{9}$(O$^{i}$Pr)] and $M_w/M_n$ = 1.13 for [In**L**$^{14}$(O$^{i}$Pr)]; in THF PDI values increased slightly ([In**L**$^{6}$(O$^{i}$Pr)]: $M_w/M_n \geq 1.24$,

[In**L**$^{9}$($O^{i}$Pr)]: $M_w/M_n \geq 1.36$). At higher initial monomer/initiator ratio, a broader molecular weight distribution of the polymers was found; possibly resulting from backbiting- or transesterification reactions.[12]

This trend was not observed for polymerizations in $CH_2Cl_2$. [In**L**$^{6}$($O^{i}$Pr)] bearing less bulky $^{t}$Bu groups in *ortho*-position showed a better control over $M_w/M_n$. In $CH_2Cl_2$, $M_w/M_n$ decreased with increasing initial monomer/initiator ratio (Figure 5.4.). In contrast, $M_w/M_n$ of the polymers generated in THF increased with increasing initial monomer/initiator ratio (Figures 5.5. and 5.6.). Control over $M_w/M_n$ of poly(*rac*-lactides) is similar to the control achieved by recently reported bis(phenolate) complex [Y**L**$^{24}${$N(SiMe_2H)_2$}(THF)] ($M_w/M_n$ = 1.05).[13]

Figures 5.4. - 5.6. demonstrate linear dependence of $M_n$ from initial monomer/initiator ratio for ROP of *rac*-lactide in $CH_2Cl_2$ and THF initiated by [In**L**$^{6}$($O^{i}$Pr)] and [In**L**$^{9}$($O^{i}$Pr)] indicating a controlled polymerization. Interestingly, $M_n$ of poly(*rac*-lactides) produced by [In**L**$^{9}$($O^{i}$Pr)] in THF shows a non-linear relation when plotted against the initial monomer/initiator ratio (Figure 5.7.), soon reaching a plateau. This might result from a relatively fast polymerization of *rac*-lactide initiated by [In**L**$^{9}$($O^{i}$Pr)] in THF.

Selectivity is also dependent on the solvent used for polymerization. In $CH_2Cl_2$, complexes [In**L**$^{6}$($O^{i}$Pr)] and [In**L**$^{9}$($O^{i}$Pr)] formed atactic poly(*rac*-lactides) with slight preference for isotactic sequences ([In**L**$^{6}$($O^{i}$Pr)]: $P_i$ = 0.51, [In**L**$^{9}$($O^{i}$Pr)]: $P_i$ = 0.44) with [In**L**$^{6}$($O^{i}$Pr)] showing slightly higher selectivity.

ROP in THF initiated by [In**L**$^{6}$($O^{i}$Pr)] led to heterotactically enriched poly(*rac*-lactides) ($P_r$ = 0.50) and only slightly heterotactically enriched poly(*rac*-lactides) formed by [In**L**$^{9}$($O^{i}$Pr)] ($P_r$ = 0.44). The role of THF in the preparation of heterotactic poly(*rac*-lactides) when complexes of trivalent metals are used as initiators has been discussed in chapter IV.

Arnold's indium amide complexes also generated predominantly atactic poly(*rac*-lactides) with a slight preference for isotactic tetrads in $CH_2Cl_2$.[5]

In THF, chiral complex [In**L**$^{14}$($O^{i}$Pr)] created poly(*rac*-lactides) with preference for heterotactic sequences ($P_r$ = 0.77). This demonstrates the effect of a chiral and rigid bis(phenolate) backbone in indium complexes.

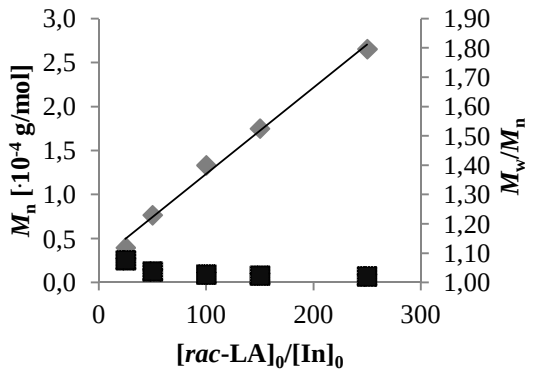


**Figure 5.4.** Dependence of $M_n$ (♦) and $M_w/M_n$ (■) on initial monomer/initiator ratio [*rac*-LA]$_0$/[In]$_0$ for ROP of *rac*-lactide in $CH_2Cl_2$ using [In**L**$^{6}$($O^i$Pr)] as initiator.

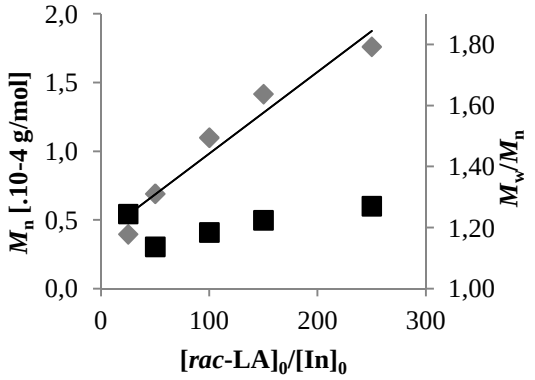


**Figure 5.5.** Dependence of $M_{n,}$ (♦) and $M_w$ /$M_n$ (■) on initial monomer/initiator ratio [*rac*-LA]$_0$/[In]$_0$ for ROP of *rac*-lactide in THF using [In**L**$^{6}$($O^i$Pr)] as initiator.

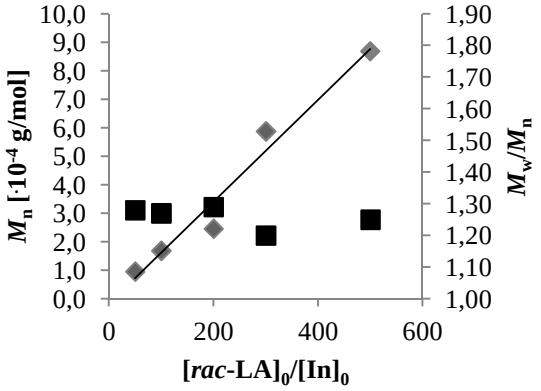


**Figure 5.6.** Dependence of $M_{n,exp}$ (♦) and $M_w$ /$M_n$ (■) on initial monomer/initiator ratio [*rac*-LA]$_0$/[In]$_0$ for ROP of *rac*-lactide in $CH_2Cl_2$ using [In**L**$^{9}$($O^i$Pr)] as initiator.

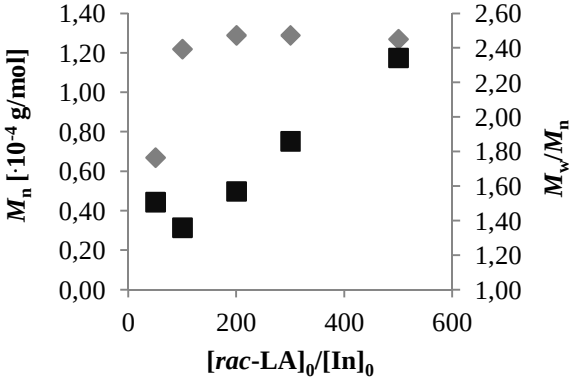


**Figure 5.7.** Dependence of $M_{n,exp}$ (♦) and $M_w/M_n$ (■) on initial monomer/initiator ratio [*rac*-LA]$_0$/[In]$_0$ for ROP of *rac*-lactide in THF using [In**L**$^{9}$($O^i$Pr)] as initiator.

[In**L**$^{14}$($O^i$Pr)] showed higher heteroselectivity than scandium and yttrium analogues reported in chapter IV to create poly(*rac*-lactide) with $P_r$ = 0.74 [Sc**L**$^{14}${$N(SiMe_2H)_2$}(THF)] and $P_r$ = 0.68 [Y**L**$^{14}${$N(SiMe_2H)_2$}(THF)]. [In**L**$^{6}$($O^i$Pr)] and [In**L**$^{9}$($O^i$Pr)] were less active and selective than rare earth metal bis(phenolate) complexes, that generally create heterotactic enriched or highly heterotactic poly(*rac*-lactides) reaching $P_r$ > 0.82 for an 1,2-dithiapropanediyl bridged rare earth metal bis(phenolate) complexes. Mountford's ligand-free Indium initiators were found to be more active and more selective than indium bis(phenolate) isopropoxide

precursors,[6] while Carpentiers fluorinated dialkoxy-diimino Salen based indium complexes were less active and only slightly more selective than [In**L**$^{6}$(O$^{i}$Pr)] and [In**L**$^{9}$(O$^{i}$Pr)] but less selective [In**L**$^{14}$(O$^{i}$Pr)] resulting in a $P_r$ = 0.62.[7] Tolmans system containing $InCl_3$, BnOH and $NEt_3$ is the most selective indium system creating heterotactic poly(*rac*-lactide) ($P_r$ = 0.97).[3] Kinetic studies were carried out at 298.15, 303.15, 308.15 and 313.15 K for complexes [In**L**$^{6}$(O$^{i}$Pr)] and [In**L**$^{9}$(O$^{i}$Pr)] with an initial monomer/initiator concentration of $[LA]_0/[In]_0$ = 100 and $[LA]_0$ = 0.8 M using $CD_2Cl_2$ as solvent. Monomer conversion was monitored by $^{1}$H NMR analyses.

Time/conversion plots for ROP of *rac*-lactide initiated by [In**L**$^{6}$(O$^{i}$Pr)] and [In**L**$^{9}$(O$^{i}$Pr)] are shown in Figures 5.8. - 5.9.

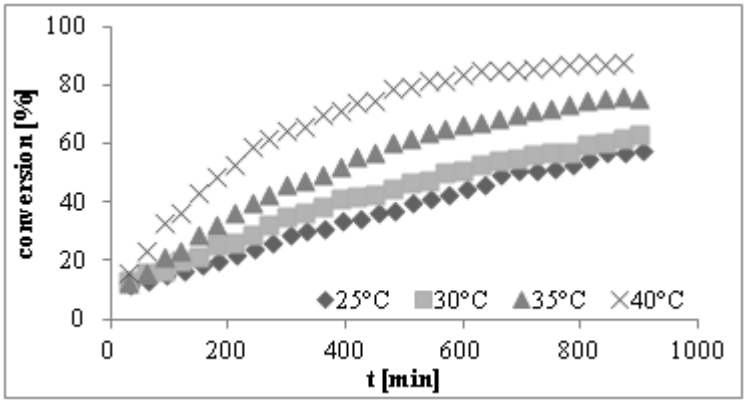


**Figure 5.8.** Time/conversion plots for ROP of *rac*-lactide initiated by [In**L**$^{6}$(O$^{i}$Pr)].

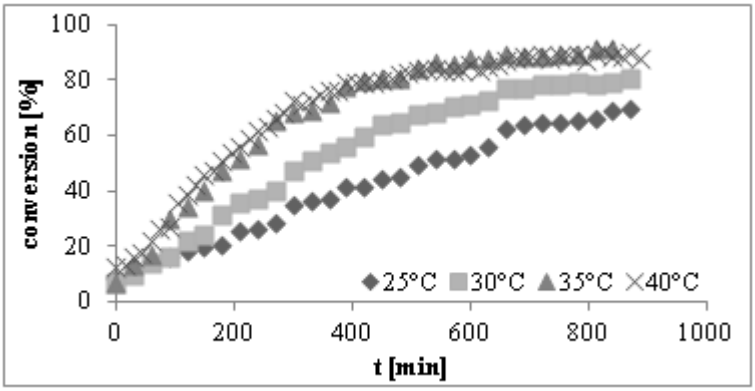


**Figure 5.9.** Time/conversion plots for ROP of *rac*-lactide initiated by [In**L**$^{9}$(O$^{i}$Pr)].

Propagation rate constants $k_{obs}$ for ROP of *rac*-lactide collated in table 5.2 were determined by plots of $-\ln([LA]_0/[LA]_t$ against the reaction time, representatively drawn for ROP of *rac*-LA initiated by [In**L**$^{6}$(O$^{i}$Pr)] at 25 °C (Figure 5.10.).

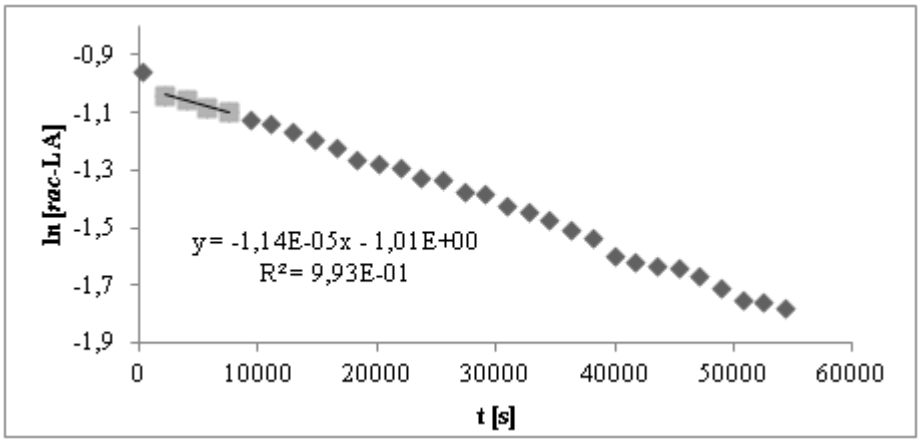


**Figure 5.10.** ln[*rac*-LA]/time plot for ROP of *meso*-lactide initiated by [In**L**$^{6}$(O$^{i}$Pr)] at 25 °C.

ROP of lactide monomers initated by [In**L**$^{6}$(O$^{i}$Pr)] and [In**L**$^{9}$(O$^{i}$Pr)] presumably proceeds via first order kinetic according to

$$-d[LA]/dt = k_{app}[LA] \qquad \textbf{Equation 1}$$

until full conversion is reached. Highest polymerization rate constant for *rac*-lactide was observed for [In**L**$^{9}$(O$^{i}$Pr)] at 313.15 K with $k_{app} = 5.62 \cdot 10^{-5}$ s$^{-1}$. The rate constant at 313.15 K for [In**L**$^{6}$(O$^{i}$Pr)] was found to be as high as for [In**L**$^{9}$(O$^{i}$Pr)] ($k_{app} = 5.33 \cdot 10^{-5}$ s$^{-1}$). Similarity of the rate constants for *rac*-LA polymerization was also apparent at 298.15 K ([In**L**$^{6}$(O$^{i}$Pr)]: $k_{app} = 1.14 \cdot 10^{-5}$ s$^{-1}$; [In**L**$^{9}$(O$^{i}$Pr)]: $k_{app} = 1.22 \cdot 10^{-5}$ s$^{-1}$). However, such similarity was not given at 303.5 and 308.15 K (Table 5.2.).

These values are considerably lower than the rate constants reported for recently reported heteroscorpionate alkylmagnesium complexes ($36.97 \cdot 10^{-3}$ s$^{-1}$).[12] Higher polymerization rate constants were also found for Tolmans catalytic system containing $InCl_3$, BnOH and $NEt_3$ ($k_{app} = 2.7 \cdot 10^{-4}$ s$^{-1}$ at 25 °C).[3]

**Table 5.2.** Rate constants ($k_{app}$) for ROP of rac-lactide initiated by [In**L**$^{6}$($O^{i}$Pr)] and [In**L**$^{9}$($O^{i}$Pr)].

| Entry | T [K] | $k_{app}$ [1/s] for [In**L**$^{6}$($O^{i}$Pr)] | $k_{app}$ [1/s] for [In**L**$^{9}$($O^{i}$Pr)] |
|---|---|---|---|
| 1 | 298.15 | $1.14 \cdot 10^{-5}$ | $1.22 \cdot 10^{-5}$ |
| 2 | 303.15 | $1.44 \cdot 10^{-5}$ | $2.52 \cdot 10^{-5}$ |
| 3 | 308.15 | $2.68 \cdot 10^{-5}$ | $3.76 \cdot 10^{-5}$ |
| 4 | 313.15 | $5.33 \cdot 10^{-5}$ | $5.62 \cdot 10^{-5}$ |

The collected data showed first order dependence on initial initiator concentration. Rate constants for ROP of *rac*-lactide were similar to the rate constants reported for ROP of L-lactide initiated by [In**L**$^{6}$($O^{i}$Pr)] and [In**L**$^{9}$($O^{i}$Pr)].[8,15]

Cumyl substituted initiator [In**L**$^{9}$($O^{i}$Pr)] polymerized lactide monomers faster than *tert*-butyl substituted initiator [In**L**$^{6}$($O^{i}$Pr)]. This trend was reported for bis(phenolate) complexes of aluminum[16] and of group 3 metals.[8,13]

## V.2.4. ROP of *meso*-Lactide

Indium bis(phenolate) isopropoxide complexes [In**L**$^{6}$($O^{i}$Pr)], [In**L**$^{9}$($O^{i}$Pr)] and [In**L**$^{14}$($O^{i}$Pr)] efficiently initiated ROP of *meso*-lactide in toluene. The data are compiled in Table 5.3.

All polymerization experiments were performed until a monomer conversion of ≥ 95% was reached. In all cases, poly(*meso*-lactides) were narrowly distributed with moderate molecular weights. $M_w/M_n$ does not exceed a value of 1.16 for ([In**L**$^{9}$($O^{i}$Pr)]) suggesting a highly controlled polymerization. $M_w/M_n$ decreased with lower catalyst concentrations (Figures 5.11. and 5.12.).

Again, *tert*-butyl substituted complex [In**L**$^{6}$($O^{i}$Pr)] showed a minimally better control over $M_w/M_n$, which are lower for poly(*meso*-lactide) than for poly(*rac*-lactides) formed by [In**L**$^{6}$($O^{i}$Pr)], [In**L**$^{9}$($O^{i}$Pr)] and [In**L**$^{14}$($O^{i}$Pr)]. For [In**L**$^{6}$($O^{i}$Pr)] a linear dependence of $M_n$ on the initial monomer/initator ratio is apparent. Like $M_n$ of poly(*rac*-lactides) formed by [In**L**$^{9}$($O^{i}$Pr)] in THF, $M_n$ of poly(*meso*-lactides) increased with higher initial monomer/initiator ratios reaching a plateau, indicating slower chain propagation. This results from hindered monomer coordination resulting from attachment of long polymer chains at the metal centers.

**Table 5.3.** ROP of *meso*-lactide initiated by [In**L**$^{6}$(O$^{i}$Pr)], [In**L**$^{9}$(O$^{i}$Pr)] and [In**L**$^{14}$(O$^{i}$Pr)] in toluene.[a]

| Initiator | Entry | $[Ln]_0/[LA]_0$ | $M_n$ (g·mol$^{-1}$) ($\times 10^{-4}$)[b] | $M_w/M_n$[b] | $P_s$[c] |
|---|---|---|---|---|---|
| [In**L**$^{6}$(O$^{i}$Pr)]] | 1[d] | 25 | 0.34 | 1.11 | 0.82 |
| | 2[e] | 50 | 0.62 | 1.07 | 0.82 |
| | 3[f] | 100 | 1.11 | 1.04 | 0.87 |
| | 4[g] | 150 | 1.44 | 1.03 | 0.88 |
| | 5[h] | 250 | 1.89 | 1.03 | 0.85 |
| | 6[i] | 500 | 3.07 | 1.02 | 0.89 |
| [In**L**$^{9}$(O$^{i}$Pr)] | 7[d] | 50 | 1.37 | 1.16 | 0.84 |
| | 8[e] | 100 | 1.80 | 1.08 | 0.85 |
| | 9[f] | 200 | 2.32 | 1.07 | 0.90 |
| | 10[g] | 300 | 2.50 | 1.06 | 0.93 |
| | 11[h] | 500 | 2.62 | 1.04 | 0.93 |
| [In**L**$^{14}$(O$^{i}$Pr)] | 12[i,j] | 100 | 1.14 | 1.07 | 0.88 |
| | 13[e] | 100 | 1.86 | 1.08 | 0.89 |

[a] T = 25 °C, $[LA]_0$ = 0.30 M, conversion: > 95%, [b]From GPC analyses; corrected using Mark Houwink parameter 0.58;[11] [c] $P_s$ is the probability of forming syndiotactic tetrads, determined by homonuclear decoupled $^{1}$H NMR; [d] V(toluene) = 0.5 mL, $[Ln]_0 = 6.06 \cdot 10^{-3}$ M; [e] V(Solvent) = 1 mL, $[Ln]_0 = 3.03 \cdot 10^{-3}$ M; [f] V(Solvent) = 2.0 mL, $[Ln]_0 = 1.50 \cdot 10^{-3}$ M; [g] V(Solvent) = 3.0 mL, $[Ln]_0 = 1.01 \cdot 10^{-3}$ M; [i] V(Solvent) = 5.0 mL, $[Ln]_0 = 6.06 \cdot 10^{-4}$ M. [j] conversion 55%.

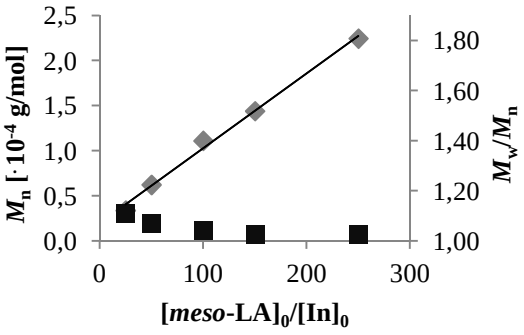


**Figure 5.11.** Dependence of $M_{n,exp}$ (♦) and $M_w/M_n$ (■) on initial monomer/initiator ratio $[rac\text{-LA}]_0/[In]_0$ for ROP of *meso*-lactide in toluene using [In**L**$^{6}$(O$^{i}$Pr)] as initiator.

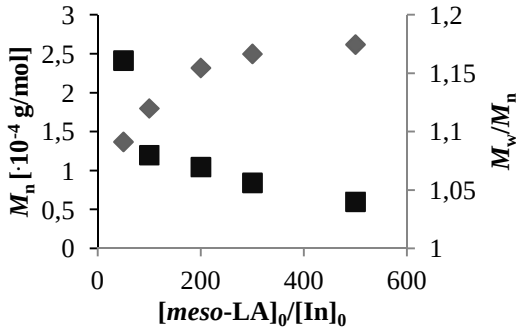


**Figure 5.12.** Dependence of $M_{n,exp}$ (♦) and $M_w/M_n$ (■) on initial monomer/initiator ratio $[rac\text{-LA}]_0/[In]_0$ for ROP of *meso*-lactide in toluene using [In**L**$^{9}$(O$^{i}$Pr)] as initiator.

The produced poly(*meso*-lactides) were highly syndiotactic. [In**L**$^{9}$(O$^{i}$Pr)] with bulky cumyl substitutents ($P_s$ = 0.93) showed a slightly higher syndioselectivity than [In**L**$^{6}$(O$^{i}$Pr)] ($P_s$ = 0.89) and [In**L**$^{14}$(O$^{i}$Pr)] ($P_s$ = 0.89). [In**L**$^{6}$(O$^{i}$Pr)] and [In**L**$^{9}$(O$^{i}$Pr)] showed the trend to polymerize *meso*-lactide slightly more syndioselective at higher initial monomer/initiator ratios. Similar results were achieved by Tolman and his group for heterotactic PLAs ($P_r$ =

0.97) with zwitterionic initiator [{$InCl_3$(deapH)($H_2O$)}$_2$].[3] Rare earth metal bis(phenolate) silylamide complexes generated poly(*meso*-lactides) of comparably high syndiotacticity but with broader polydispersities.[9,13] Bis(phenolate) alkoxide complexes of titanium and zirconium generated poly(*meso*-lactides) with slightly smaller syndiotacticity and higher polydispersities.[17-18]

Narrow $M_w/M_n$ values indicate absence of backbiting reactions, chain termination or transesterification.

Time/conversion plots for ROP of *meso*-lactide in toluene-$d_8$ at specified temperatures initiated by complexes [In**L**$^6$($O^i$Pr)] and [In**L**$^9$($O^i$Pr)] are shown in Figures 5.13. - 5.14.

Rate constants $k_{obs}$ for ROP of *rac*- and *meso*-lactide collated in Table 5.4. were determined by plots of $-\ln([LA]_0/[LA]_t$ against the reaction time, representatively drawn for ROP of *meso*-LA initiated by [In**L**$^6$($O^i$Pr)] at 40 °C (Figure 5.15.).

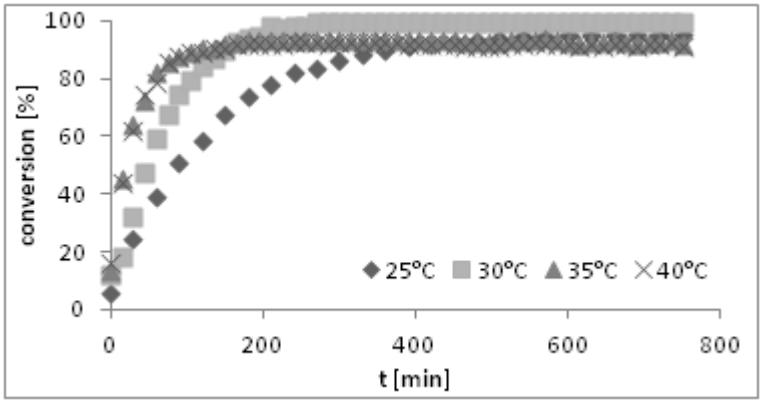


**Figure 5.13.** Time/conversion plots for ROP of *meso*-lactide initiated by [In**L**$^6$($O^i$Pr)].

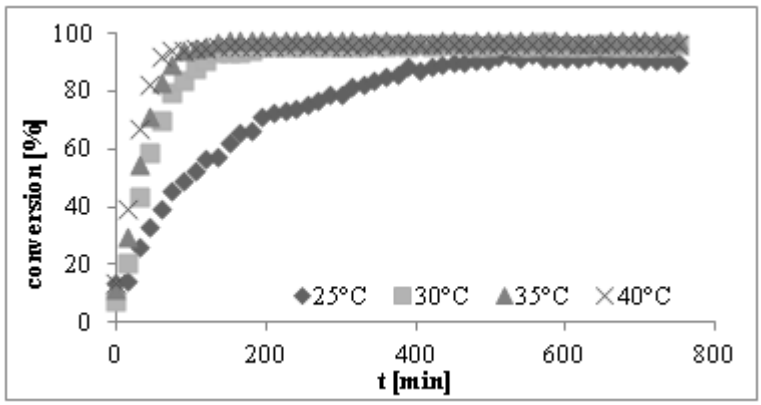


**Figure 5.14.** Time/conversion plots for ROP of *meso*-lactide initiated by [In**L**$^9$($O^i$Pr)].

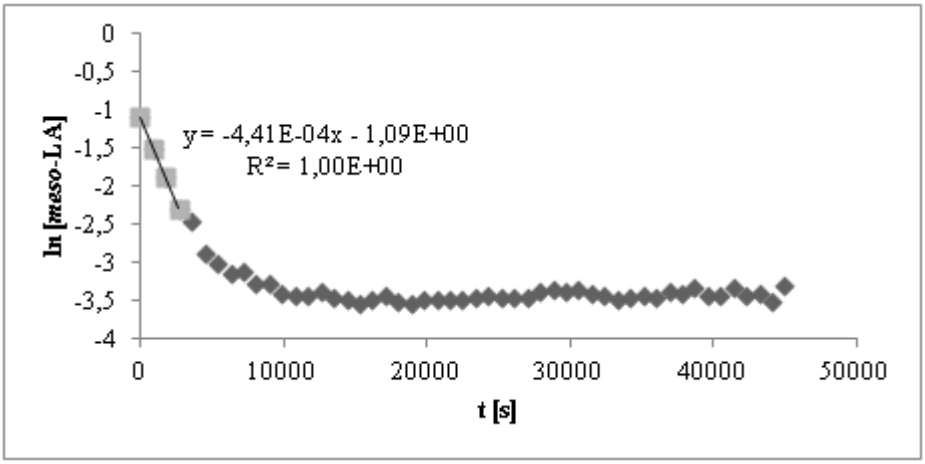


**Figure 5.15.** ln[*meso*-LA]/time plot for ROP of *meso*-lactide initiated by [In**L**$^{6}$(O$^{i}$Pr)] at 40 °C.

**Table 5.4.** Rate constants ($k_{app}$) for ROP of *meso*-lactide initiated by [In**L**$^{6}$(O$^{i}$Pr)] and [In**L**$^{9}$(O$^{i}$Pr)].

| Entry | T [K] | $k_{app}$ [1/s] for [In**L**$^{6}$(O$^{i}$Pr)] | $k_{app}$ [1/s] for [In**L**$^{9}$(O$^{i}$Pr)] |
|---|---|---|---|
| 1 | 298.15 | $1.21 \cdot 10^{-4}$ | $1.26 \cdot 10^{-4}$ |
| 2 | 303.15 | $1.93 \cdot 10^{-4}$ | $3.60 \cdot 10^{-4}$ |
| 3 | 308.15 | $4.32 \cdot 10^{-4}$ | $5.22 \cdot 10^{-4}$ |
| 4 | 313.15 | $4.41 \cdot 10^{-4}$ | $7.68 \cdot 10^{-4}$ |

Because polymerization of *meso*-lactide occurred generally very fast, only the first data points measured were used for the regression fit as side reactions only occur slightly at this early reaction times.

Highest rate constants for ROP of *meso*-lactide was found for [In**L**$^{9}$(O$^{i}$Pr)] at 313.15 K ($7.68 \cdot 10^{-4}$ $s^{-1}$). Under identical conditions, complex [In**L**$^{6}$(O$^{i}$Pr)] was slower ($4.41 \cdot 10^{-4}$ $s^{-1}$). Differenting from ROP of *rac*-lactide, similar rate constants $k_{app}$ for [In**L**$^{6}$(O$^{i}$Pr)] and [In**L**$^{9}$(O$^{i}$Pr)] were only found at 298.15 K ([In**L**$^{6}$(O$^{i}$Pr)]: $1.21 \cdot 10^{-4}$; [In**L**$^{9}$(O$^{i}$Pr)]: $1.26 \cdot 10^{-4}$). Compared to related bis(phenolate) complexes of titanium ([Ti**L**$^{16}$(O$^{i}$Pr)$_2$], $k_{app} = 1.36 \cdot 10^{-5}$ $s^{-1}$ in toluene at 100 °C)[15] or zirconium ([Zr**L**$^{16}$(O$^{t}$Bu)$_2$], $1.49 \cdot 10^{-4}$ $s^{-1}$ in toluene at 100 °C),[14] indium complexes polymerized *meso*-lactide faster with better stereocontrol.

## V.2.5. Determination of the Activation Parameters for the ROP of *rac*- and *meso*-Lactide Initiated by [InL$^6$(O$^i$Pr)] and [InL$^9$(O$^i$Pr)]

Comparison of the Eyring plots for ROP of *rac*-, *meso*- and L-lactide initiated by [In**L**$^6$(O$^i$Pr)], and [In**L**$^9$(O$^i$Pr)] (Figures 5.16. and 5.17.) shows polymerization of *meso*-lactide proceeding faster than of *rac*-lactide. This might be due to higher ring-strain of *meso*-lactide compared to that of D and L-lactide resulting in easier acyl-bond cleavage during the ring-opening.[20] Again, this behavior agrees with observations made for related bis(phenolate) initiators of trivalent metals.

Activation parameters were obtained from resulting Eyring plots where the regression follows Equation 2.[21]

$$\ln\frac{k_{app}}{T} = -\frac{\Delta H^{\#}}{R}\cdot\frac{1}{T} + \ln\frac{k_B}{h} + \frac{\Delta S^{\#}}{R} \qquad \textbf{Equation 2}$$

As expected, rate constants $k_{app}$ increase at elevated temperatures. Activation parameters were determined from the Eyring plots (Figures 5.16. and 5.17.) and are given for 25 °C in Table 5.5.

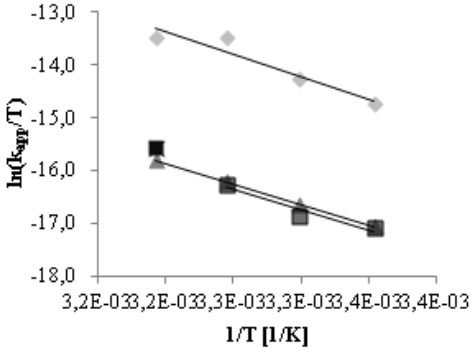


**Figure 5.16.** Dependence of ln($k_{app}$) on 1/T (Eyring Plot) for ROP of *rac*- (■), *meso*- (♦) and L-lactide (▲)[8,18] initiated by [In**L**$^6$(O$^i$Pr)].

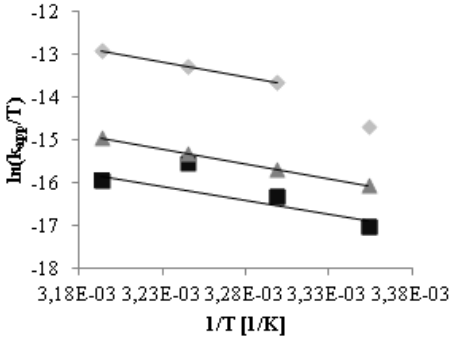


**Figure 5.17.** Dependence of ln($k_{app}$) on 1/T (Eyring Plot) for ROP of *rac*- (■), *meso*- (♦) and L-lactide (▲)[8,18] initiated by [In**L**$^{9}$($O^{i}$Pr)].

**Table 5.5.** Activation parameters for ROP of *rac*-, *meso*- and L-lactide initiated by indium bis(phenolate) isopropoxide complexes [In**L**$^{6}$($O^{i}$Pr)] and [In**L**$^{9}$($O^{i}$Pr)].

| Initiator | Monomer | $\Delta H^{\ddagger}$ [kJ/mol] | $\Delta S^{\ddagger}$ [J/(K · mol)] | $\Delta G^{\ddagger}$ [kJ/mol] |
|---|---|---|---|---|
| **1** | *meso*-LA | 70.4(2) | -83.6(3) | 95.4(0) |
| | *rac*-LA | 62.6(0) | -130.1(0) | 101.4(0) |
| | L-LA | 64.9(3) | -121.6(2) | 101.1(9) |
| **2** | *meso*-LA | 57.2(0) | -122.2(0) | 93.6(4) |
| | *rac*-LA | 52.1(9) | -162.7(3) | 100.7(0) |
| | L-LA | 56.8(4) | -140.8(0) | 98.8(9) |

The $\Delta S^{\ddagger}$ values indicate an ordered transition state in all cases. Data for ROP of *meso*-lactide indicate that less activation energy is needed for initiation of ROP of *meso*-lactide compared to ROP of L- and *rac*-lactide. Fulfilling the expectations, activation parameters for ROP of L- and *rac*-lactide are nearly the same.

## V.2.6. Mechanism of the ROP

In agreement with the generally accepted mechanism for ROP of cyclic esters initiated by metal alkoxides[26], the mechanism of the ROP of lactide monomers initiated by indium bis(phenolate) isopropoxide compounds is suggested to run as shown in Scheme 5.5. The lactide monomer coordinates to the Lewis acidic metal center with the carbonyl oxygen (1).

This is followed by a nucleophilic attack of the isopropoxide on the carbonyl carbon, resulting in insertion of the monomer into the metal isopropoxide bond (2). Ring-opening of the monomer takes place by acyl-bond cleavage (3) and chain propagation proceeds by repeated insertion of lactide monomers (4). Finally, polymerization is terminated by water, forming an OH-end group on the polymer chain.

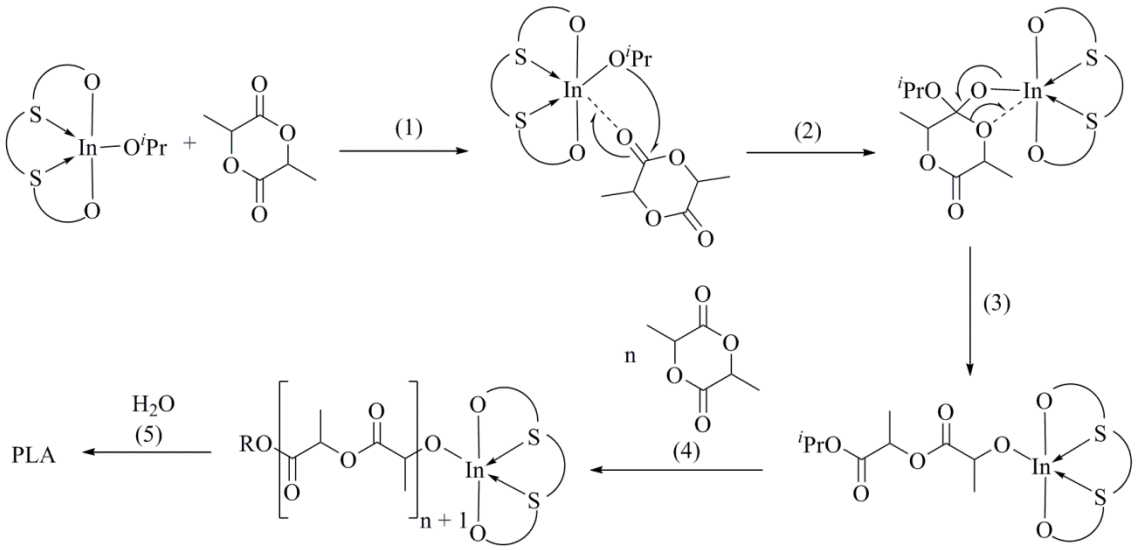


**Scheme 5.5.** Proposed mechanism for ROP of lactide monomers initiated by indium bis(phenolate) isopropoxide complexes [In**L**$^{6}$(O$^{i}$Pr)] and [In**L**$^{9}$(O$^{i}$Pr)].

## V.3. Summary.

Stereoselective ROP of *rac*- and *meso*-lactide initiated by indium bis(phenolate) isopropoxide complexes [In**L**$^{6}$(O$^{i}$Pr)], [In**L**$^{9}$(O$^{i}$Pr)] and [In**L**$^{14}$(O$^{i}$Pr)] was studied. All three complexes initiated the ROP of lactide monomers with a coordination insertion mechanism. Dimeric complex [In**L**$^{6}$(O$^{i}$Pr)] splits into two mononuclear units as a result of lactide coordination to the metal center. All complexes polymerize *meso*-lactide faster than *rac*-lactide. For [In**L**$^{6}$(O$^{i}$Pr)] and [In**L**$^{9}$(O$^{i}$Pr)] polymerization activity for ROP of *rac*- and L-lactide is nearly the same.

Complex [In**L**$^{14}$(O$^{i}$Pr)] produced highly syndiotactic poly(*meso*-lactides) and heterotactic poly(*rac*-lactides). [In**L**$^{6}$(O$^{i}$Pr)] and [In**L**$^{9}$(O$^{i}$Pr)] produced syndiotactic poly(*meso*-lactides), while *rac*-lactide is polymerized to give poly(*rac*-lactides) either isotactically or heterotactically enriched polymers depending on the solvent.

# V.4 Experimental Section

**$In_5(\mu_5\text{-}O)(\mu_3\text{-}O^iPr)_4(\mu_2\text{-}O^iPr)_4(O^iPr)_5$, "$In(O^iPr)_3$"[22] (21)** 1358.223 g/mol

1.0 g of Na (43.5 mmol, 3 equiv.) were reacted in a mixture of 25 mL toluene and 35 mL isopropanol at 80 °C. A suspension of 3.2 g of $InCl_3$ (12.7 mmol, 1 equiv.) in a mixture of 25 mL toluene and 25 mL isopropanol was added slowly. The solution was stirred at 80 °C for 3 h, centrifugated and filtered. After evaporation of the solvent and recrystallization from *n*-pentane, **21** was isolated as a colorless powder in 80% yield (2.78 g, 2.0 mmol). **$^1$H NMR** (THF-$d_8$, 25 °C, 400 MHz), δ (ppm): 1.23 (d, 9 H, $^3J_{HH}$ = 5.9 Hz, OCH(C$H_3$)$_2$), 1.51 (d, 9 H, $^3J_{HH}$ = 5.9 Hz, OCH(C$H_3$)$_2$), 4.43 (sept, $^3J_{HH}$ = 5.9 Hz, OC$H$(CH$_3$)$_2$). **$^{13}$C{$^1$H} NMR** (THF-$d_8$, 25 °C, 100.1 MHz), δ (ppm): 27.8 (OCH(*C*H$_3$)$_2$), 29.2 (OCH(*C*H$_3$)$_2$), 69.4 (O*C*H(CH$_3$)$_2$). **Elemental analysis**, calculated for $C_{39}H_{91}In_5O_{14}$ (1358,22 g/mol): C 34.49, H 6.75; Found: C 30.45, H 7.07.

---

**[In$\mathbf{L}^6$($O^i$Pr)]**[8]

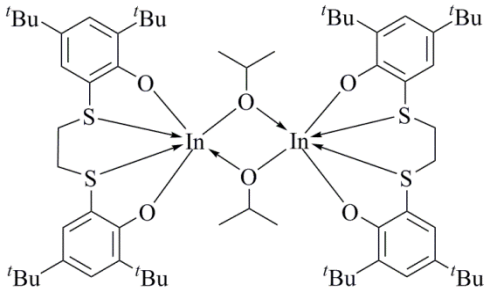


[In$\mathbf{L}^6$($O^i$Pr)]
$C_{70}H_{114}In_2O_6S_4$
1409,55

A solution of 279 mg **21** (0.21 mmol, 1 equiv.) in 3 mL toluene was added dropwise to a suspension of bis(phenol) $H_2\mathbf{L}^6$ (517 mg, 1.03 mmol, 5 equiv.) in 15 mL of toluene at -78 °C and the reaction mixture was stirred for 1.5 h at 60 °C. After removal of the volatiles the yellow residue was dissolved in *n*-pentane and dried under reduced pressure to give [In$\mathbf{L}^6$($O^i$Pr)] as a colorless powder in a yield of 77% (532 mg, 0.39 mmol). **$^1$H NMR** (THF-$d_8$, 25 °C, 400 MHz), δ (ppm): 1.07 (d, $^3J_{HH}$ = 6.1 Hz, 6 H, CH(C$H_3$)$_2$), 1.19 (s, 6 H, C(C$H_3$)$_3$), 1.22 (s, 6 H, C(C$H_3$)$_3$), 1.24 (s, 6 H, C(C$H_3$)$_3$), 1.25 (s, 6 H, C(C$H_3$)$_3$), 1.26 (s, 6 H, C(C$H_3$)$_3$), 1.39 (d, $^3J_{HH}$ = 6.0 Hz, 6 H, In-OCHC$H_3$), 2.13 (d, $^2J_{HH}$ = 11.4 Hz, 2 H, SC$H_2$), 2.21 (d, $^2J_{HH}$ = 11.1 Hz, 2 H, SC$H_2$), 2.95 (d, $^2J_{HH}$ = 11.4 Hz, 2 H, SC$H_2$), 3.11 (d, $^2J_{HH}$ = 11 Hz, 2 H, SC$H_2$), 4.59 (sept, $^3J_{HH}$ = 6.1 Hz, 1 H, In-OC$H$), 4.77 (sept, $^3J_{HH}$ = 6.5 Hz, 1 H, In-OC$H$), 7.05-7.11 (m, 2 H, Ph$H$-5), 7.23 (d, $^4J_{HH}$ 2.6 Hz, 2 H, Ph$H$-5‘), 7.36 (d, $^4J_{HH}$ = 2.7 Hz, 4 H,

Ph*H*-3). **$^{13}$C{$^{1}$H} NMR** (THF-$d_8$, 25 °C, 100.1 MHz), δ (ppm): 28.0 (CH(*C*H$_3$)$_2$), 28.3 (CH(*C*H$_3$)$_2$), 28.9 (C(*C*H$_3$)$_3$), 29.9 (C(*C*H$_3$)$_3$), 30.6 (C(*C*H$_3$)$_3$), 30.8 (C(*C*H$_3$)$_3$), 32.1 (*C*(CH$_3$)$_3$), 32.3 (*C*(CH$_3$)$_3$), 34.9 (S*C*H$_2$), 34,9 (S*C*H$_2$), 36.3 (S*C*H$_2$), 36.7 (S*C*H$_2$), 68.5 (O*C*H), 68.8 (O*C*H), 127.6 (Ph-*C*3), 127.8 (Ph-*C*3‘), 128.2 (Ph-*C*5), 128.3 (Ph-*C*5‘), 128.7 (Ph-*C*2), 129.1 (Ph-*C*2‘), 138.3 (Ph-*C*4), 139.0 (Ph-*C*4‘), 139.6 (Ph-*C*6), 140.3 (Ph-*C*6‘), 162.9 (Ph-*C*1), 163.2 (Ph-*C*1‘). **Elemental analysis**, calculated for $C_{66}H_{102}In_2O_6S_4$ (1351.19 g/mol): C 58.74, H 7.62; Found: C 58.69, H 7.76.

---

**[InL$^{9}$(O$^{i}$Pr)]$^{8}$**

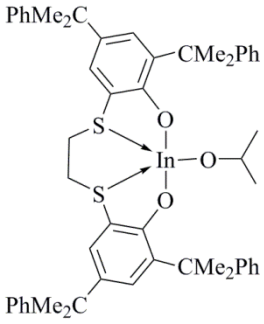


**[InL$^{9}$(O$^{i}$Pr)]**
$C_{53}H_{59}InO_3S_{22}$
923.00

A solution of 300 mg **21** (0.22 mmol, 1 equiv.) in 3 mL of toluene was added dropwise to a suspension of proligand $H_2$**L$^{9}$** (711 mg, 1.03 mmol, 5 equiv.) in 15 mL of toluene at -78 °C and the reaction mixture was stirred for 2.5 h at 60 °C. After removal of the volatiles, the yellow residue was dissolved in *n*-pentane and dried under reduced pressure to give [In**L$^{9}$**(O$^{i}$Pr)] as a colorless powder in a yield of 77% (532 mg, 0.39 mmol). **$^{1}$H NMR** ($C_6D_6$, 25 °C, 400 MHz), δ (ppm): 1.02 (d, $^{3}J_{HH}$ = 5.9 Hz, 3 H, OCH(C*H**3**)$_2$), 1.16 (d, $^{3}J_{HH}$ = 5.9 Hz, 3 H, OCH(C*H**3**)$_2$), 1.49 (s, 6 H, Ph6-C(CH$_3$)$_3$), 1.58 (d, $^{4}J_{HH}$ = 2.1 Hz, 12 H, Ph4-C(C*H*$_3$)$_3$), 1.75 (s, 6 H, Ph6-C(C*H*$_3$)$_3$), 1.78 (d, $^{2}J_{HH}$ = 11.1 Hz, 2 H SC*H*$_2$), 2.23 (d, $^{2}J_{HH}$ = 11.2 Hz, 2 H, SC*H*$_2$‘), 3.55 (sept, $^{3}J_{HH}$ = 5.7 Hz, 1 H, OC*H*(CH$_3$)$_2$), 6.95 - 7.14 (m, 11 H, Ph-*H*), 7.21 - 7.39 (m, 13 H, Ph-*H*). **$^{13}$C{$^{1}$H} NMR** ($C_6D_6$, 25 °C, 100.1 MHz), δ (ppm): 28.1 (C(*C*H$_3$)$_2$Ph), 29.3 (OCH(*C*H$_3$)$_2$), 31.5 (O*C*H(CH$_3$)$_2$), 33.5 (C(*C*H$_3$)$_2$Ph), 36.2 (C(*C*H$_3$)$_2$Ph), 43.2 (C(*C*H$_3$)$_2$Ph), 43.8 (S*C*H$_2$), 125.4 (Ph-*C*2), 126.0 (Ph-*C*), 126.2 (Ph-*C*), 126.7 (Ph-*C*), 127.6 (Ph-*C*), 128.2 (Ph-*C*), 128.5 (Ph-*C*5), 129.0 (Ph-*C*), 129.6 (Ph-*C*), 130.2 (Ph-*C*), 131.1 (Ph-*C*), 137.0 (Ph-*C*5‘), 137.3 (Ph-*C*3), 138.1 (Ph-*C*4), 139.7 (Ph-*C*6), 152.3 (Ph-*C*), 152.5 (Ph-*C*), 162.7 (Ph-*C*1). **Elemental analysis**, calculated for $C_{53}H_{59}InO_3S_2$ (922.00 g/mol): C 68.97, H 6.44; Found: C 68.24, H 6.33.

**[InL$^{14}$(O$^{i}$Pr)]**

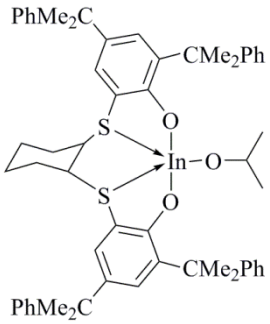


**[InL$^{14}$(O$^{i}$Pr)]**
$C_{57}H_{65}InO_3S_2$
977.07

To a solution of 140 mg **21** (0.10 mmol, 1 equiv.) in 5 mL of toluene a solution of 415 mg $H_2$**L$^{14}$** (0.52 mmol, 5 equiv.) in 3 mL toluene was added dropwise and the solution stirred for 6 h at 70 °C. After removal of the solvent under vacuum at 50 °C and recrystallization from a saturated *n*-pentane/THF mixture, [In**L$^{14}$**(O$^{i}$Pr)] was isolated as light yellow crystals in a yield of 57% (289 mg, 0.30 mmol). **$^{1}$H NMR** (THF-$d_8$, 25 °C, 400 MHz), δ (ppm): 0.84 (dd, $^{3}J_{HH}$ = 6.0 Hz, 6 H, OCH(C*H*$_3$)$_2$), 1.21 (s, 2 H, Cy-*H*), 1.26 (s, 3 H, C(C*H*$_3$)$_2$), 1.30 (s, 2 H, Cy-*H*), 1.31 (s, 3 H, C(C*H*$_3$)$_2$Ph), 1.47 (br, 2 H, Cy-*H*), 1.52 (s, 3 H, C(C*H*$_3$)$_2$Ph), 1.62 (s, 3 H, C(C*H*$_3$)$_2$Ph), 1.63 (s, 3 H, C(C*H*$_3$)$_2$Ph), 1.64 (s, 3 H, C(C*H*$_3$)$_2$Ph), 1.65 (s, 3 H, C(C*H*$_3$)$_2$Ph), 1.68 (br, 2 H, Cy-*H*), 1.75 - 1.90 (s, 2 H, SC*H*), 3.43 (sept, $^{3}J_{HH}$ = 6.0 Hz, 1 H, OC*H*(CH$_3$)$_2$), 6.57 (d, $^{3}J_{HH}$ = 7.3 Hz, 1 H, CMe$_2$Ph-*H*), 6.87 (d, $^{4}J_{HH}$ = 2.5 Hz, 1 H, CMe$_2$Ph-*H*), 6.97 (m, 1 H, CMe$_2$Ph-*H*), 6.98 (s, 1 H, CMe$_2$Ph-*H*), 7.01 (d, $^{4}J_{HH}$ = 2.1 Hz, 1 H, Ph-*H*5‘), 7.01 - 7.03 (m, 1 H, CMe$_2$Ph-*H*), 7.04 (d, $^{4}J_{HH}$ = 2.2 Hz, 1 H, Ph-*H*3), 7.06 (d, $^{4}J_{HH}$ = 2.5 Hz, 1 H, Ph-*H*5), 7.09 (m, 1 H, CMe$_2$Ph-*H*), 7.10-7.12 (br, 2 H, CMe$_2$Ph-*H*), 7.13 (s, 1 H, CMe$_2$Ph-*H*), 7.17 (d, $^{4}J_{HH}$ = 2.1 Hz, 1 H, CMe$_2$Ph-*H*), 7.21 (t, $^{4}J_{HH}$ = 3.4 Hz, 2 H, CMe$_2$Ph-*H*), 7.23 (m, 2 H, CMe$_2$Ph-*H*), 7.25 (m, 2 H, CMe$_2$Ph-*H*), 7.27 (t, $^{4}J_{HH}$ = 1.8 Hz, 1 H, CMe$_2$Ph-*H*), 7.31 (d, $^{4}J_{HH}$ = 2.6 Hz, 1 H, CMe$_2$Ph-*H*), 7.38 (d, $^{4}J_{HH}$ = 2.4 Hz, 1 H, CMe$_2$Ph-*H*). **$^{13}$C{$^{1}$H} NMR** (THF-$d_8$, 25 °C, 100.1 MHz), δ (ppm): 25.8 (Cy-*C*), 26.0 (Cy-*C*), 26.9 (OCH(*C*H$_3$)$_2$), 27.0 (Cy-*C*), 28.1 (O*C*H(CH$_3$)$_2$), 29.3 (Cy-*C*), 30.8 (C(*C*H$_3$)$_2$Ph), 31.2 (C(*C*H$_3$)$_2$Ph), 31.5 (C(*C*H$_3$)$_2$Ph), 32.0 (C(*C*H$_3$)$_2$Ph), 33.1 (C(*C*H$_3$)$_2$Ph), 33.3 (C(*C*H$_3$)$_2$Ph), 33.3 (C(*C*H$_3$)$_2$Ph), 33.9 (C(*C*H$_3$)$_2$Ph), 43.1 (*C*(CH$_3$)$_2$Ph), 43.3 (*C*(CH$_3$)$_2$Ph), 43.4 (*C*(CH$_3$)$_2$Ph), 43.8 (*C*(CH$_3$)$_2$Ph), 51.6 (S*C*H), 51.9 (S*C*H), 68.1 (O*C*H), 125.5 (CMe$_2$Ph-*C*), 125.6 (CMe$_2$Ph-*C*), 126.2 (CMe$_2$Ph-*C*), 126.2 (CMe$_2$Ph-*C*), 126.8 (CMe$_2$Ph-*C*), 127.7 (Ph-*C*3‘),127.8 (Ph-*C*3), 128.1 (CMe$_2$Ph-*C*), 128.4 (CMe$_2$Ph-*C*), 128.7 (Ph-*C*5), 128.7 (Ph-*C*5‘), 130.0 (CMe$_2$Ph-*C*), 133.8 (Ph-*C*6), 133.9 (Ph-*C*6‘), 135.6 (Ph-*C*2), 135.9 (Ph-*C*2‘), 138.2 (Ph-*C*4), 139.7 (Ph-*C*4‘), 152.8 (CMe$_2$Ph-*C*), 152.8 (CMe$_2$Ph-*C*), 153.7 (CMe$_2$Ph-*C*), 162.6 (Ph-*C*1), 163.0 (Ph-

*C*1‘). **Elemental analysis**, calculated for $C_{57}H_{59}InO_3S_2$ (977.07 g/mol): C 70.07, H 6.71; Found: C 69.12, H 6.53.

**General Procedures for Kinetic Measurements.** In a typical experiment, 0.3 mL of a $4 \cdot 10^{-4}$ M (calculated per metal center) initiator stock solution in the specified solvent was injected into a screw cap J. Young Teflon valved NMR-tube in a glove box. After addition of 0.3 mL of a 0.08 M stock solution of the lactide monomer, the NMR tube was placed in the pretempered NMR-spectrometer. After specified time intervals $^1$H NMR spectrum were recorded. After 16 h, the samples were quenched with moist *n*-hexane and filtered. After drying under vacuum the polymers were analyzed in $CDCl_3$ by NMR measurements. GPC analyses were performed in THF.

**Typical Polymerization Procedures.** In the glove box, initiator stock solution in the specified solvent was injected individually into a series of 6 mL vials loaded with a solution of *rac*- or *meso*-lactide in the specified solvents. After specified time intervals, each vial was taken out of the glove box and the reaction quenched with moist *n*-hexane. The polymer was filtered over a funnel, washed with diethyl ether, and dried under vacuum. $^1$H-, $^1$H-{$^1$H}- and $^{13}$C{$^1$H} NMR spectroscopic analysis of the polymers were performed in $CDCl_3$ at 25 °C. GPC analytics were performed in THF.

Kinetic studies were carried out at 298.15, 303.15, 308.15 and 313.15 K for complexes [In**L**$^{6}$($O^i$Pr)] and [In**L**$^{9}$($O^i$Pr)] with an initial monomer/initiator concentration of $[LA]_0/[In]_0$ = 100 and $[LA]_0$ = 0.8 M.

# V.5. References


1 I.-P. Hsieh, C.-H. Huang, H. M. Lee, P.-C. Kuo, J.-H. Huang, H.-I. Lee, J.-T. Cheng, G.-H. Lee, *Inorg. Chim. Acta* **2006**, *359*, 497-504.

2 a) A. F. Douglas, B. O. Patrick, P. Merkhodavandi, *Angew. Chem. Int. Ed.* **2008**, *47*, 2290-2293; b) A. Acosta-Ramírez, A. F. Douglas, I. Yu, B. O. Patrick, P. L. Diaconescu, P. Mehrkhodavandi, *Inorg. Chem.* **2010**. *49*, 5444-5452; c) D. C. Aluthge, B. O. Patrick, P. Mehrkhodavandi *Chem Commun*. **2012**, *48*, 6806-6808; d) I. Yu, A. Acosta-Ramirez, P. Mehrkhodavandi, *J. Am, Chem. Soc*. **2012**, *134* (30), 12758-12773.

[3] a) A. Pietrangelo, M. A. Hillmyer, W. B. Tolman, *Chem. Commun.* **2009**, 2736-2737; b) A. Pietrangelo, S. C. Knight, A. K. Gupta, L. Y. Yao, M. A. Hillmyer, W. B. Tolman, *J. Am. Chem. Soc.* **2010**, *132*, 11649-11657.

[4] M. Hu, M. Wang, P. Zhang, L. Wang, F. Zhu, L. Sun, *Inorg. Chem. Commun.* **2010**, *13*, 968-971.

[5] J.-C. Buffet, J. Okuda, P. Arnold, *Inorg. Chem.* **2010**, *49*, 419-426.

[6] M. P. Blake, A. D. Schwarz, P. Mountford, *Organometallics* **2011**, *30*, 1202-1214.

[7] M. Normand, E. Kirillov, T. Roisnel, J.-F. Carpentier, *Organometallics* **2012**, *31*, 1448-1457.

[8] I. Peckermann, A. Kapelski, T. P. Spaniol, J. Okuda, J. *Inorg. Chem.* **2009**, *48*, 5526-5534,

[9] J.-C. Buffet, A. Kapelski, J. Okuda, *Macromolecules* **2010**, *43*, 10201-10203.

[10] H. Ma, J. Okuda, *Macromolecules* **2005**, *38*, 2665-2673.

[11] a) W. M. Stevels, M. J. K. Ankoné, P. J. Dijkstra, J. Feijen, *Macromolecules* **1996**, *29*, 6132-6138; b) M. Save, M. Schappacher, A. Soum, *Macromol. Chem. Phys.* **2002**, *203*, 889-899.

[12] L. F. Sánchez-Barba, A. Garcés, J. Fernández-Baeza, A. Otero, C. Alonso-Moreno, A. Lara-Sánchez, A. M. Rodríguez, *Organometallics* **2011**, *30*, 2775-2789.

[13] A.Kapelski, J.-C. Buffet, T. P. Spaniol, J. Okuda, *Chem. Asian. J.* **2012**, *6*, 1320-1330.

[14] Eyring equation: $\ln(k_{obs})/T) = (-\Delta H^{\ddagger}/RT) + \ln(k_b/h) + (\Delta S^{\ddagger}/R)$ where r = unviversal gas constant, $k_b$ = Boltzmann's constant, h = Planck's constant.

[15] [In**L**$^{6}$($O^{i}$Pr)] at 25 °C: $k_{obs} = 1.11 \times 10^{-5}$ [1/s]; [In**L**$^{6}$($O^{i}$Pr)] at 40 °C: $k_{obs} = 4.26 \times 10^{-5}$ [1/s]; [In**L**$^{9}$($O^{i}$Pr)] at 25 °C: $k_{obs} = 2.85 \times 10^{-5}$ [1/s]; [In**L**$^{9}$($O^{i}$Pr)] at 40 °C: $k_{obs} = 1.15 \times 10^{-4}$ [1/s].

[16] H. Ma, G. Melillo, L. Oliva, T. P. Spaniol, U. Englert, J. Okuda, *Dalton Trans.* **2005**, 721–727.

[17] J.-C. Buffet, A. Martin, M. Kol, J. Okuda, *Polym. Chem.* **2011**, *2*, 2378-2384.

[18] J.-C. Buffet, J. Okuda, *Chem. Comm.* **2011**, *47*, 4796-4798.

[19] a) T. Ouhadi, C. Stevens, P. Teyssié, *Makromol. Chem. Suppl.* **1975**, *1*, 191-201; b) W. M. Stevels, M. J. K. Ankoné, P. J. Dijkstra, J. Feijen, *Macromolecules* **1996**, *29*, 6132-6138.

[20] M. H. Chisholm, N. W. Eilerts, J. C. Huffman, S. S. Iyer, M. Pacold, K. Phomphrai, *J. Am. Chem. Soc.* **2000**, *122*, 11845-11854.

[21] Eyring equation: $\ln(k_{obs})/T) = (-\Delta H^{\ddagger}/RT) + \ln(k_b/h) + (\Delta S^{\ddagger}/R)$; r = gas constant, $k_b$ = Boltzmann's constant, h = Planck's constant.

[22] a) A. Mehrotra, R. C. Mehrotra, *Inorg. Chem.* **1972**, *11*, 2170-2174; (b) S. Chatterjee, S. T. Bindal, R. C. Mehrotra, *J. Indian. Chem. Soc.* **1976**, 867-869.

# Chapter VI

# Discrete Neutral and Cationic Alkali and Alkaline Earth Metal Complexes – Syntheses, Characterization and ROP of Lactide Monomers

# VI. Discrete Neutral and Cationic Alkali and Alkaline Earth Metal Complexes – Syntheses, Characterization and ROP of Lactide Monomers

## VI.1. Introduction

Application of alkaline earth metal complexes in catalysis gathered increased attention during the last years as they are non-toxic, readily available and inexpensive. Although catalytic applications of alkaline earth metal complexes are relatively rare compared to complexes of ruthenium, rhodium or nickel,[1] they are already applied in hydroamination,[2] polymerization of olefins,[3] alkyne coupling,[4] hydrogenation,[5] pyridine activation[6] and ROP of cyclic esters.[7-41]

Selective ROP of *rac*-lactide by Trispirazolyl-hydroborate complexes of calcium were reported by Chisholm *et al. rac*-Lactide is polymerized rapidly to give heterotactic PLAs ($P_r$ = 0.90) (Scheme 6.1.). [10]

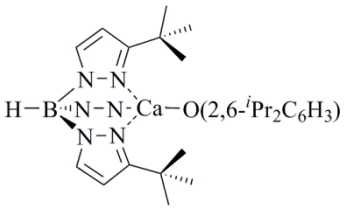


**X**

**Scheme 6.1.** Calcium tris(pyrazolyl)-hydroborate initiator **X** by Chisholm *et al.*[10]

Okuda *et al.* reported alkaline earth metal complexes of the cyclen-derived (NNNN)-type macrocycle 1,4,7-Trimethyl-1,4,7,10-tetraazacyclododecane ($Me_3$TACD)H (**22**), that polymerized *meso*-lactide to give syndiotactically enriched poly(*meso*-lactides) (Scheme 6.2.). Magnesium and calcium complexes **XXIV** and **XXV** are fast initiators reaching full conversion with an initial monomer/initiator ratio of 100 in less than 0.5 h.

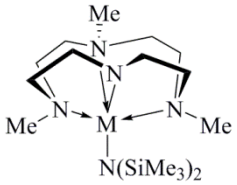


M = Mg (**XXIV**), Ca (**XXV**)

**Scheme 6.2.** Alkaline earth metal complexes **XXIV** and **XXV** bearing one $Me_3$TACD-ligand.[27]

Recently, alkaline earth metal complexes of a chiral polyether have been prepared and used in ROP of lactide monomers (Scheme 6.3., **XXVI**).[41] Syndioselective ROP of *meso*-lactide ($P_s$ = 0.73) and formation of atactic poly(*rac*-lactides) was observed for this class of complexes.

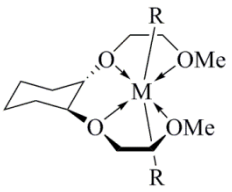


M = Mg, Ca, Sr
R = $N(SiMe_3)_2$, $CH_2SiMe_3$, $\eta^3$-$C_3H_5$

**XXVI**

**Scheme 6.3.** Alkaline earth metal complexes **XXVI** bearing a chiral polyether.[27,41]

Befor recent reports by Carpentier *et al.*, no family of discrete well-defined alkaline earth metal cations supported by alkoxide ligands was known,[14,31] although in 2001 Itoh and Kitagawa published structures of cations of Mg, Ca, and Sr stabilized by (aza-crown-ether)-aryloxide ligands and external Lewis bases.[42] Carpentier *et al.* studied these complexes in the ROP of lactide finding narrowly distributed molecular weights not exceeding $M_w/M_n$ = 1.42 (Scheme 6.4.). Additionally, a variety of different macrocycle containing phenoxy-type proligands was used. The structure of alkaline earth metal complexes of these ligand types is strongly dependant on the cationic radius. While for small $Mg^{2+}$ cations, monomeric complexes were formed, dimeric structures were identified for complexes of $Ca^{2+}$.[14]

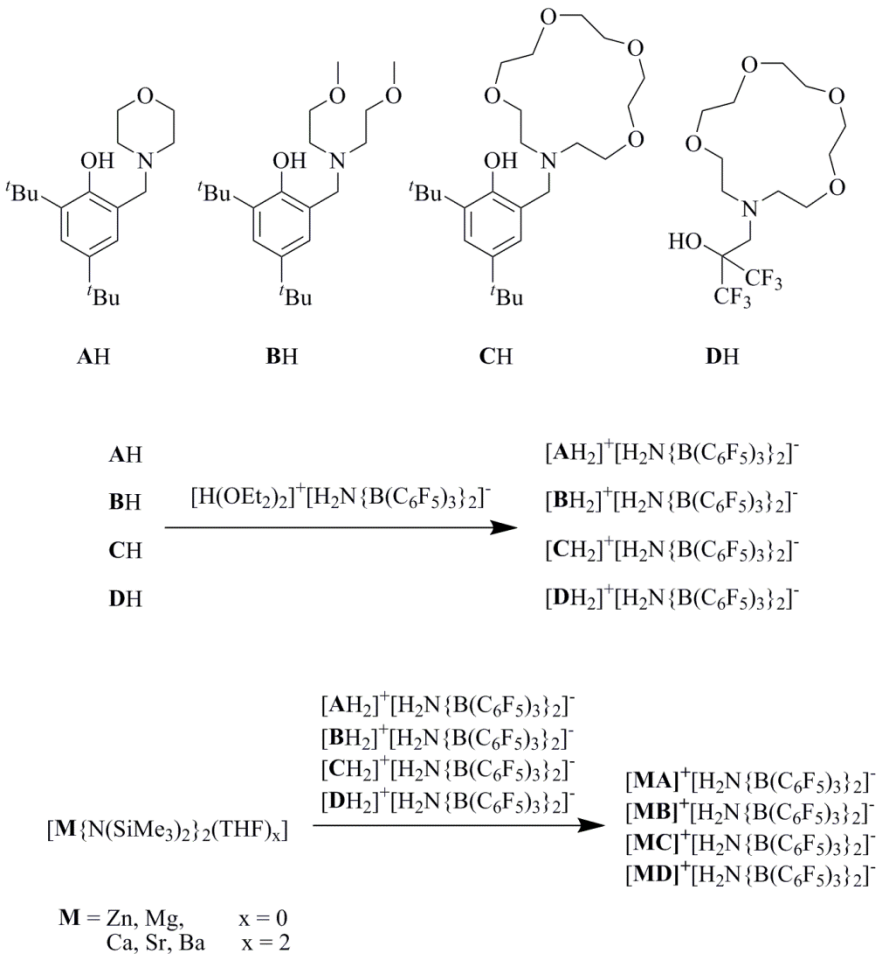


**Scheme 6.4.** Cationic alkaline earth metal complexes bearing a chiral polyether reported by Carpentier *et al.*[14,31]

As early as 1997, Wieghardt *et al.* described azacycloalkane containing phenoxy-type proligands using a simple halide elimination reaction starting from 2-(bromomethyl)-4,6-di-*tert*-butylphenol and 1,3,5-triazacyclononane as well as 1,4-Dimethyl-1,3,5-triazacyclonone (Scheme 6.5).[42]

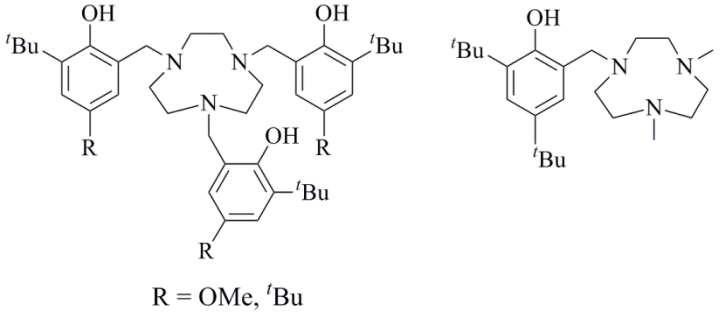


**Scheme 6.5.** Macrocycle containing phenolate ligands by Wieghardt *et al.*[42]

# VI.2. Results and Discussion

This chapter deals with the syntheses of neutral and cationic alkaline earth metal complexes. A new (aza-crown-ether)-phenoxide proligand and its transformation into a cationic intermediate is presented. Subsequent treatment with alkali and alkaline earth metal precursors gives neutral and cationic complexes. Application of these complexes in ROP of lactide monomers will be studied.

## VI.2.1. Syntheses of Neutral and Cationic (Aza-Crown-Ether)-Phenoxide Proligands.

Okuda *et al.* recently published an efficient synthesis of aza-crown-ether proligand ($Me_3$TACD)H **22** in good yields. Reaction of cyclen with three equivalents chloral hydrate gave 1,4,7-triformylcyclen.[43] Reduction with $BH_3 \cdot THF$[44] and subsequent treatment with HCl afforded **22** in 71% yield (Scheme 6.6.).[45]

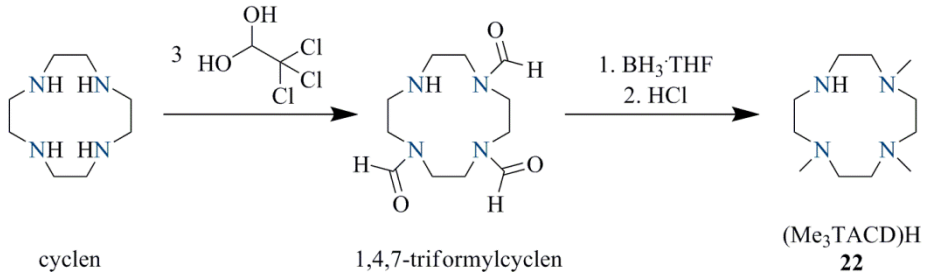


**Scheme 6.6.** Synthesis of ($Me_3$TACD)H **22**.[45]

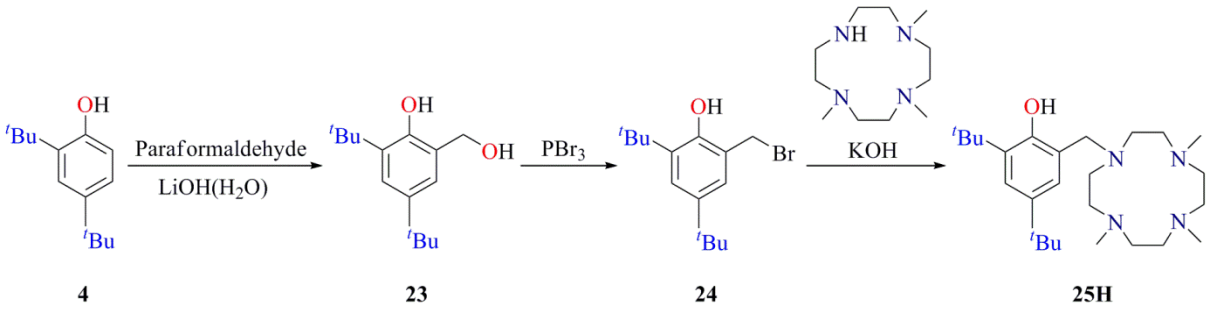


**Scheme 6.7.** Synthesis of **25H**.

To synthesize the new proligand, the literature procedure reported for Itohs proligand 2-{(1,4,7,10-tetraoxa-13-azacyclopentadecan-13-yl)methyl}-4,6-di-*tert*-butylphenol[46] was adapted. **4** was treated with LiOH($H_2O$) and paraformaldehyde to give 2,4-di-*tert*-butyl-6-(hydroxymethyl)phenol[47] (**23**) in a yield of 58%. In the second step, successive addition of $PBr_3$ to a solution of **23** in $CH_3Cl$ afforderd 2-(bromomethyl)-4,6-di-*tert*-butylphenol (**24**) in a yield of 89%.[47] Finally, **24** and **22** were reacted in presence of KOH to give new pentadentate proligand 2,4-di-*tert*-butyl-6-((4,7,10-trimethyl-1,4,7,10-tetraazacyclododecan-1-yl)methyl)phenol **25H** in a yield of 32% (Scheme 6.7.) as a slightly yellow crystalline compound that is easily soluble in toluene, pentane, THF, chloroform, DCM, diethylether, benzene, ethanol and methanol.

NMR as well as the elemental analysis are consistent with the structure consisting of one macrocycle attached to the disubstituted phenol.

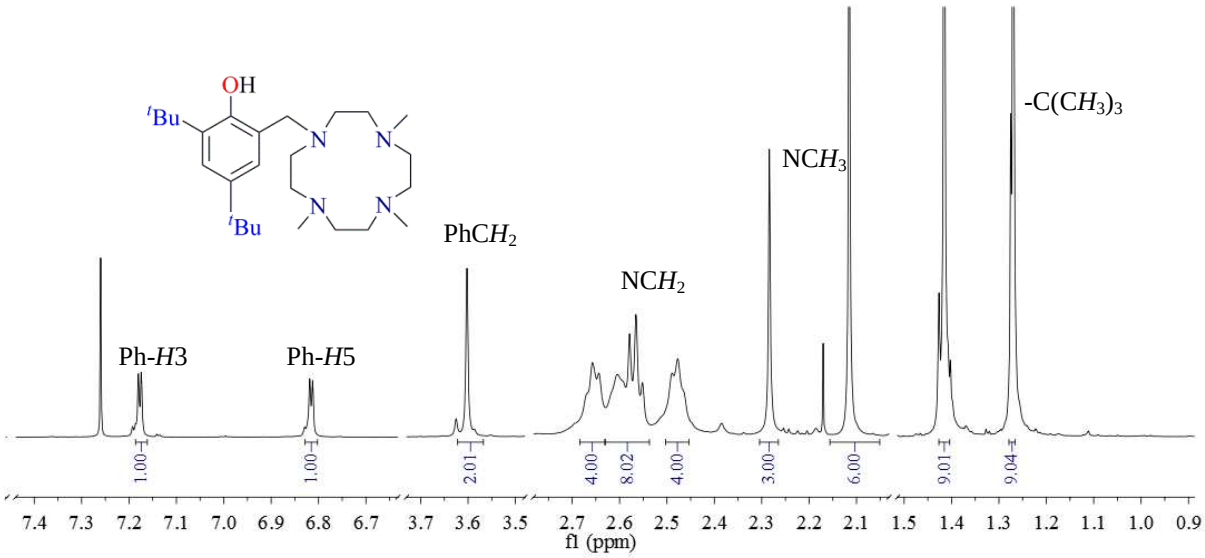


**Figure 6.1.** $^1$H NMR spectrum of **25H** in $CDCl_3$ at 25 °C.

In the $^1$H NMR spectrum of **25H** shown in Figure 6.1., two signals at 2.12 and 2.28 ppm arise for the NC$H_3$ groups at the $Me_3$TACD fragment, while the NC$H_2$C$H_2$N moieties form three broad signals between 2.42-2.53, 2.55-2.62 and between 2.63-2.70 ppm. The PhC$H_2$ protons are identified as a signal at 3.60 ppm while the $^t$Bu groups give two singulets at 1.27 and 1.42 ppm. Aromatic protons Ph-*H*5 and Ph-*H*3 arise as two doublet signals at 6.82 and 7.18 ppm.

Treatment of **25H** with Brønsted acids **$[H(OEt_2)_2]^+[B\{3,5\text{-}C_6H_3Cl_2\}_4]^-$** [48] and **$[H(OEt_2)_2]^+[3,5\text{-}B(C_6H_3(CF_3)_2\}_4]^-$** [48] selectively protonates the proligand resulting in formation of **$[25H_2]^+[B\{3,5\text{-}C_6H_3Cl_2\}_4]^-$** and **$[25H_2]^+[3,5\text{-}B(C_6H_3(CF_3)_2\}_4]^-$** (Scheme VI.6.8.).

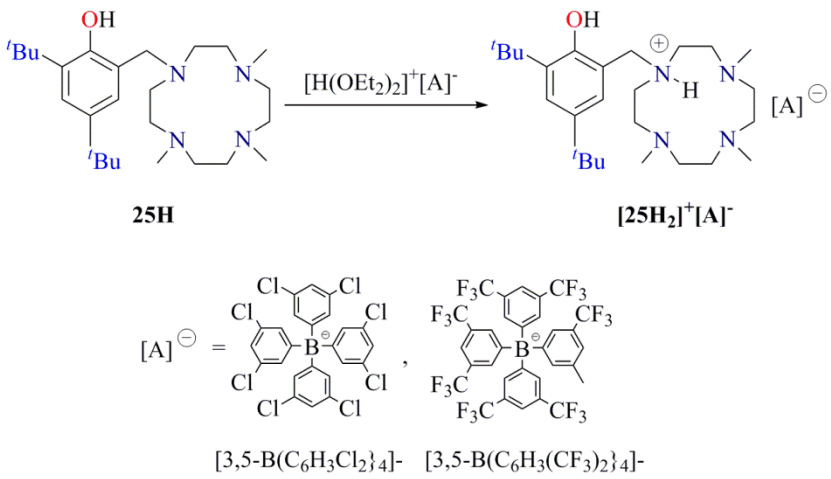


**Scheme 6.8.** Syntheses of **$[25H_2]^+[B\{3,5\text{-}C_6H_3Cl_2\}_4]^-$** and **$[25H_2]^+[3,5\text{-}B(C_6H_3(CF_3)_2\}_4]^-$**.

Successful transformation was confirmed by NMR spectroscopy as well as by elemental analysis. Figure 6.2. shows the $^1$H NMR spectrum of **$[25H_2]^+[B\{3,5\text{-}C_6H_3Cl_2\}_4]^-$**

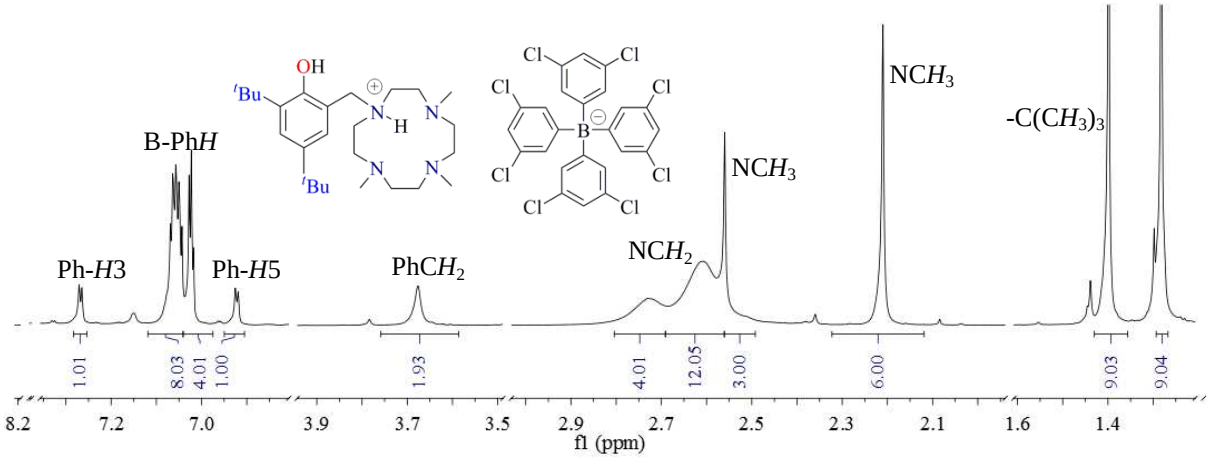


**Figure 6.2.** $^1$H NMR spectrum of **$[25H_2]^+[B\{3,5\text{-}C_6H_3Cl_2\}_4]^-$** in $CD_2Cl_2$ at 25 °C.

For $[\mathbf{25H_2}]^+$, two signals at 1.28 and 1.40 ppm represent the $^t$Bu groups while the NC$H_3$ groups form two singulets at 2.21 and 2.56. For the TACD-ring, two broad signals between 2.57-2.68 and 2.69-2.83 arise. The methylene protons connecting the phenol with the heterocycle in $[\mathbf{25H_2}]^+$ give a singulet at 3.68 ppm, while resonances for the aromatic protons arise at 6.92 and 7.26 ppm. Two multiplet signals at 7.02 and between 7.04-7.09 ppm represent the aromatic protons of $\mathbf{[B\{3,5\text{-}C_6H_3Cl_2\}_4]^-}$. Obviously, $^1$H NMR spectrum of $[\mathbf{25H_2}]^+\mathbf{[3,5\text{-}B(C_6H_3(CF_3)_2\}_4]^-}$ looks quite similar. Clearly, the resonances of the aromatic protons arise at different chemical shifts of 7.58 and 7.74 ppm as broad signals due to neighboured $CF_3$-groups effecting a downfield shift of the resonances.

## VI.2.3. Syntheses of Neutral and Cationic Alkali and Alkaline Earth Metal Complexes Bearing an (Aza-Crown-Ether)-Phenolate Ligand.

**25H** was lithiated by treating a cooled solution of **25H** in *n*-pentane with one equivalent of *n*-BuLi. Within a few seconds, after addition of *n*-BuLi a white precipitate is formed that was identified as **Li25** by NMR-spectroscopic methods and elemental analysis. Synthesis of **K25** was accomplished by reaction of **25H** and K{N(SiMe$_3$)$_2$} in *n*-pentane (Scheme 6.9.).

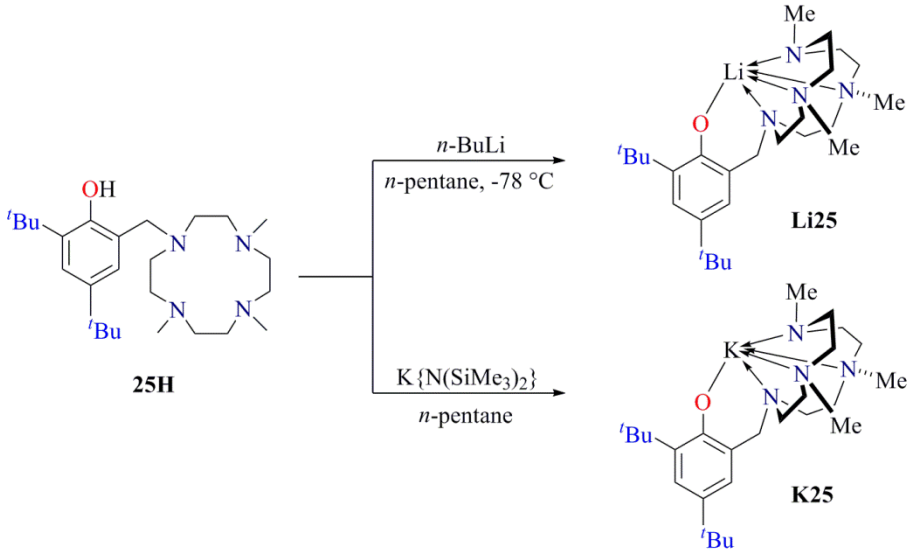


**Scheme 6.9.** Syntheses of **Li25** and **K25**.

The metal centers are coordinated by the phenoxy-oxygen and four amide donors of the $Me_3$TACD fragment. The $^1$H NMR spectrum of **Li25** shown in Figure 6.3. shows splitting of the NC$H_2$ signal into several signals between 2.10 and 2.60 ppm. This signal split is typical for successful complexation of a metal with a $Me_3$TACD ligand showing a rigid geometry. Similar signals have recently been reported for dimeric $[Li_2(Me_3TACD)_2]$[49] or rare earth metal allyl complexes bearing a $Me_3$TACD ligand.[45]

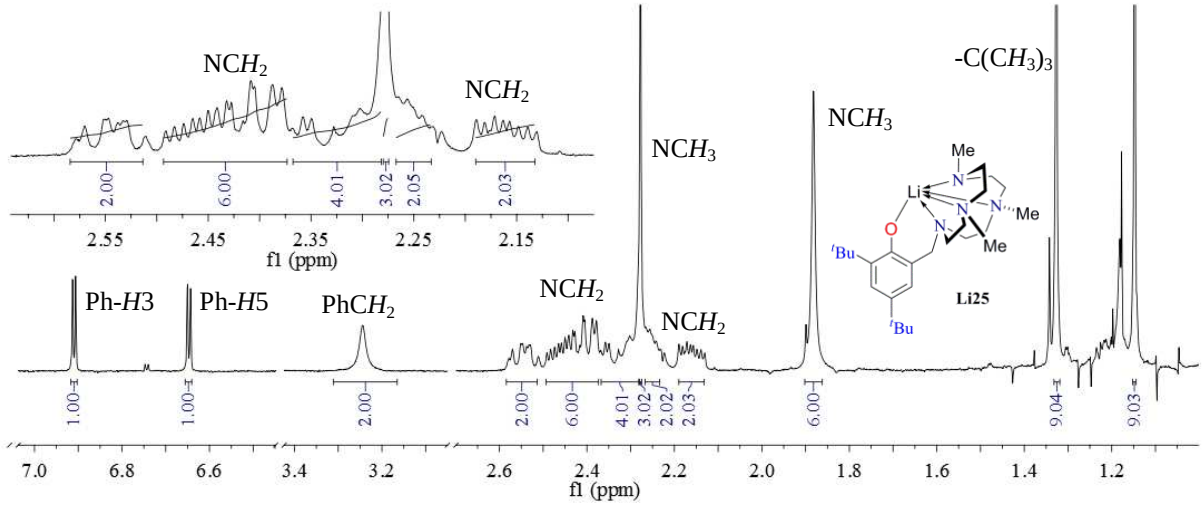


**Figure 6.3.** $^1$H NMR spectrum of **Li25** in $CD_2Cl_2$ at 25 °C.

The $^t$Bu groups form two signals at 1.14 and 1.33 ppm while two signals at 1.88 and 2.28 ppm represent the NC$H_3$ protons. The PhC$H_2$ methylene protons arise as a broad resonance at 3.25 ppm. Compared to the signal of the PhC$H_2$ protons in **H25**, the signal is shifted for **Li25**, resulting from metalation. For Ph*H*3 and Ph*H*5 two doublets at 6.65 and 6.91 ppm were identified. Similar to bis(phenolate) complexes, the signal of the phenolate *ipso* carbon in the $^{13}$C{$^1$H} NMR spectrum of **Li25** at 167.2 ppm (signal of the *ipso* carbon in **25H**: 155.0 ppm) is another characteristic. For **K25**, similar signals than that for **Li25** arise. It is worth to mention, that signals for **K25** are typically broader than for **Li25** due to the larger metal center giving a less rigid compound.

Similar to preparation of **K25**, amine elimination reaction at alkaline earth metal silylamide precursors $[Ca\{N(SiMe_3)_2\}_2(THF)_2]$ as well as $[Mg\{N(SiMe_3)_2\}_2]$ by proligand **25H** led to formation of alkaline earth metal silylamide complexes of the type **[M25{N(SiMe$_3$)$_2$}]** (M = Ca, Mg, Scheme 6.10.).

NMR spectrum and elemental analysis are consistent with the structure of **[Ca25{N(SiMe$_3$)$_2$}]** and **[Mg25{N(SiMe$_3$)$_2$}]** consisting of one ligand **25** and one silylamide group attached to the six-coordinated metal center. Compared to the spectra of **K25** and **Li25**, spectra of **[Ca25{N(SiMe$_3$)$_2$}]** and **[Mg25{N(SiMe$_3$)$_2$}]** differed only slightly. Figure 6.4. shows the $^1$H NMR spectrum of **[Ca25{N(SiMe$_3$)$_2$}]**.

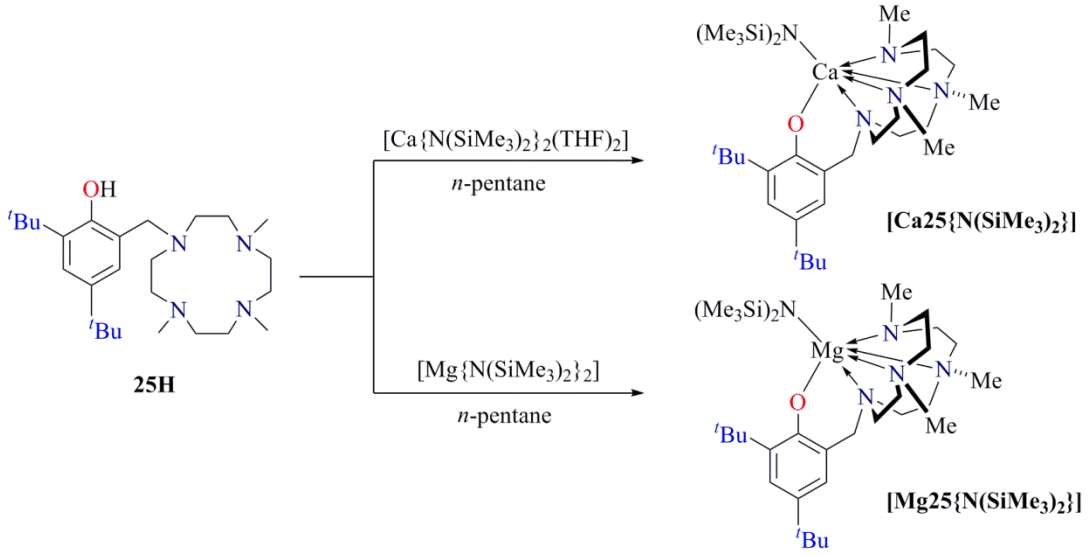


**Scheme 6.10.** Syntheses of alkaline earth metal complexes **[Ca25{N(SiMe$_3$)$_2$}]** and **[Mg25{N(SiMe$_3$)$_2$}]**.

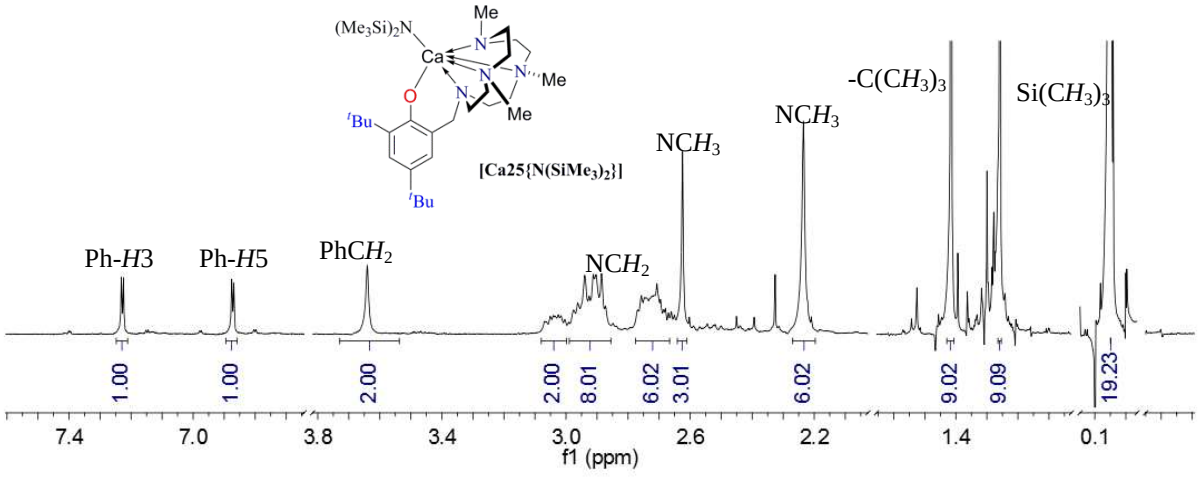


**Figure 6.4.** $^1$H NMR spectrum of **[Ca25{N(SiMe$_3$)$_2$}]** in $C_6D_6$ at 25 °C.

One broad resonance represents the silylamide group at 0.05 ppm. The $^{t}$Bu-groups form two signals at 1.26 and 1.41 ppm while at 2.24 and 2.63 ppm resonances for the NC$H_3$ groups arise. Three resonances between 2.65 and 3.10 ppm represent the ethylene units of the heterocycle while the methylene protons of the pendant arm form a relatively sharp signal at 3.64 ppm. Two doublet signals at 6.87 and 7.23 ppm arise for the aromatic protons of the phenoxy group. In the $^{13}C\{^{1}H\}$ NMR spectrum, the signal for the *ipso* carbon at 164.8 ppm is characteristic for successful metalation. The NMR spectra of [**Mg25{N(SiMe$_3$)$_2$}**] look comparable.

In order to generate cationic fragments of the type **[M25]$^+$** (M = Ca, Mg), alkaline earth metal precursors [Ca{N(SiMe$_3$)$_2$}$_2$(THF)$_2$] and [Mg{N(SiMe$_3$)$_2$}$_2$] were treated with proligand [**25H$_2$**]$^+$**[B{3,5-C$_6$H$_3$Cl$_2$}$_4$]**$^-$ to give **[Ca25]$^+$[B{3,5-C$_6$H$_3$Cl$_2$}$_4$]**$^-$ and **[Mg25]$^+$[B{3,5-C$_6$H$_3$Cl$_2$}$_4$]**$^-$ (Scheme 6.11.).

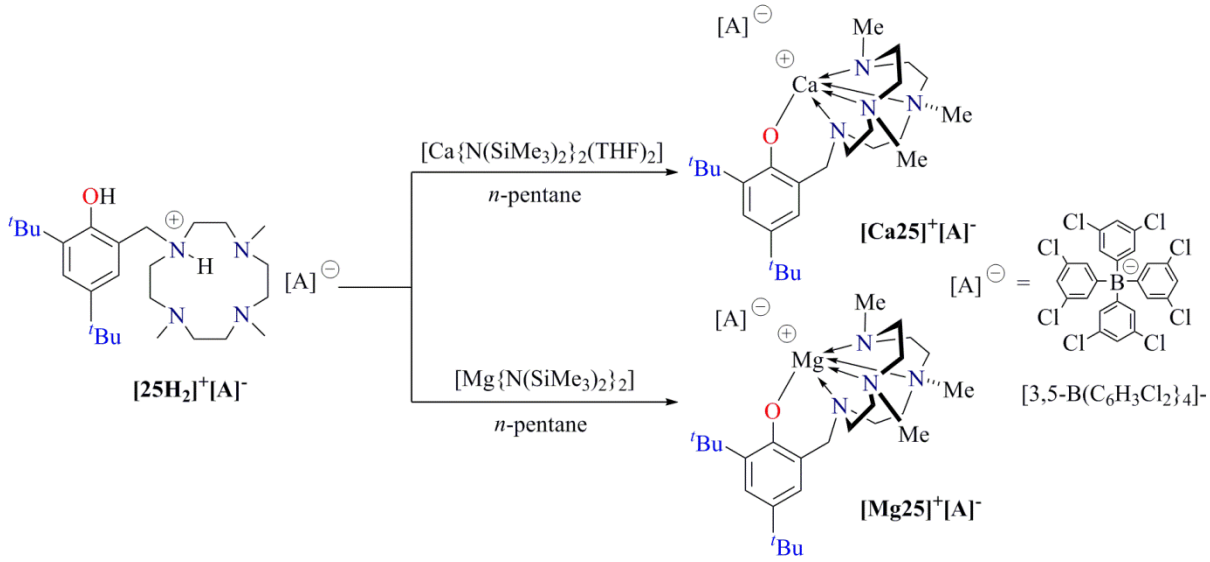


**Scheme 6.11.** Syntheses of cationic alkaline earth metal complexes **[Ca25]$^+$[B{3,5-C$_6$H$_3$Cl$_2$}$_4$]**$^-$ and **[Mg25]$^+$[B{3,5-C$_6$H$_3$Cl$_2$}$_4$]**$^-$.

Both compounds were analyzed by NMR spectroscopy and elemental analysis. Figure VI.5. shows the $^{1}$H NMR spectrum of **[Mg25]$^+$[B{3,5-C$_6$H$_3$Cl$_2$}$_4$]**$^-$. The signals of ligand **25** and of the borate anion appear at nearly the same chemical shifts for [**Mg25]$^+$[B{3,5-C$_6$H$_3$Cl$_2$}$_4$]**$^-$ as for **25** in the spectrum of complex [**Mg25{N(SiMe$_3$)$_2$}**] or for the borate in proligand [**25H$_2$**]$^+$**[B{3,5-C$_6$H$_3$Cl$_2$}$_4$]**$^-$, respectively. Again, a slight difference is observed for the

resonances of the ethylene bridges in the heterocycle for the calcium and the magnesium complex.

While the protons for the magnesium complexes form broad signals with clearly identifiable sharp signals indicating multiple coupling between the protons, in the spectrum of **[Ca25]$^+$[B{3,5-C$_6$H$_3$Cl$_2$}$_4$]$^-$** the resonances for the ethylene units of the heterocycle are very broad indicating fluxional behaviour of the ligand in solution. The ligand can effectively shield the small magnesium center giving a rigid geometry while larger calcium gives a flexible geometry of the complex.

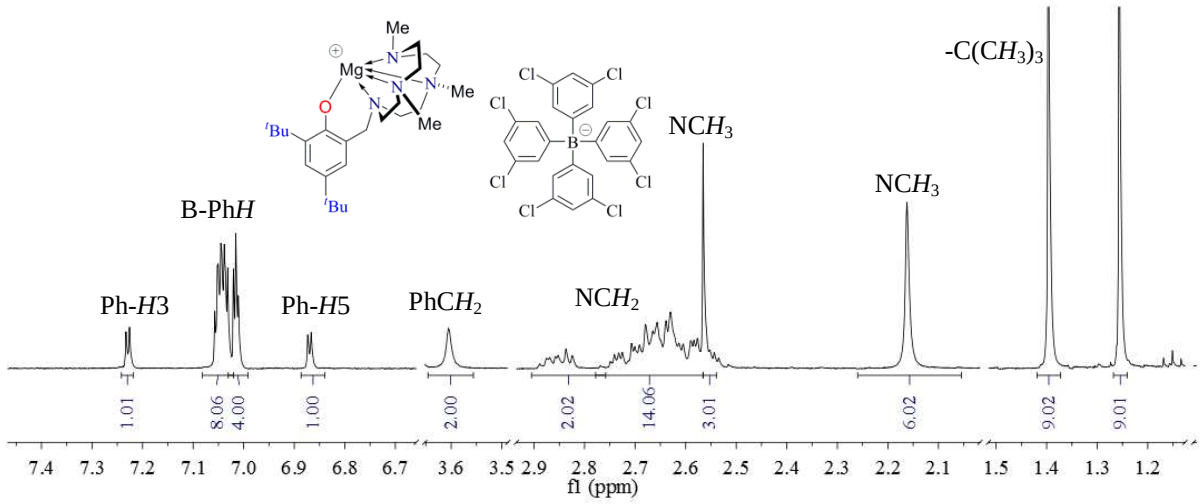


**Figure 6.5.** $^1$H NMR spectrum of **[Mg25]$^+$ [B{3,5-C$_6$H$_3$Cl$_2$}$_4$]$^-$** in $CD_2Cl_2$ at 25 °C.

Single crystals of **[Mg25]$^+$[B{3,5-C$_6$H$_3$Cl$_2$}$_4$]$^-$** suitable for x-ray diffraction analysis were grown from a cooled and saturated solution of the complex in a 1:1 mixture of THF, *n*-pentane and a few drops of 1,2-dichlorobenzene (Table A1, Appendix). Figure 6.6. shows the solid state structure of **[Mg25]$^+$**. The magnesium center in **[Mg25]$^+$** is five-coordinated by the phenoxy group and by the Me$_3$TACD cycle. The nitrogen atoms of the heterocycle and the magnesium center forms a pyramidal substructure as indicated by narrow angles of the amine donors and the magnesium center N1-Mg-N2 81.21(17)°, N2-Mg-N3 81.79(17)°, N3-Mg-N4 81.51(16)° and N1-Mg-N4 81.68(16)°. The bond lengths between magnesium and the nitrogen donors vary between 2.14 Å and 2.21 Å, which is in the typical range of structurally related complexes introduced by Carpentier *et al.* (2.109(2) -2.222(2) Å).[14] Compared to recently reported magnesium complex [Mg(Me$_3$TACD)(N(SiMe$_3$)$_2$)],[41] the bond lengths are

also relatively similar. The bond length between Mg and the amide in [Mg($Me_3$TACD)(N($SiMe_3$)$_2$)] (Mg-N1 1.9828(15) Å) is shorter than the Mg-amine lengths present in [**Mg25**]$^+$ while the bonds from Mg to the amine nitrogens are 2.27 and 2.32 Å. The bond length between Mg and the phenoxy oxygen in **[Mg25]**$^+$ (Mg-O 1.880(4) Å) is shorter than the bond length between Mg and the silylamide group in [Mg($Me_3$TACD)(N($SiMe_3$)$_2$)] (Mg-N 2.0462(14) Å) and very close to the Mg-O bond in Carpentiers mixed phenoxy-macrocycle complex (Mg-O 1.900(2) Å).[14]

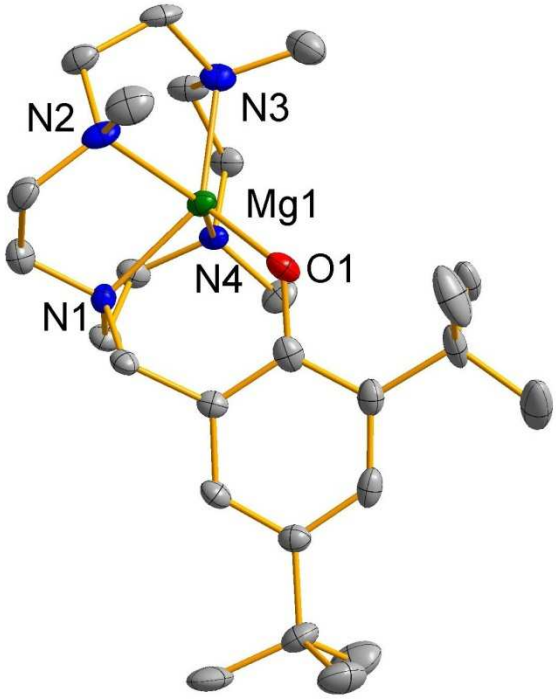


**Figure 6.6.** Molecular structure of [**Mg25**]$^+$. Hydrogen atoms are omitted for clarity. Selected bond lengths (Å) and angles (°): Mg-O1 1.880(4), Mg-N1 2.140(6), Mg-N2 2.207(4), Mg-N3 2.181(5), Mg-N4 2.203(4); N1-Mg-N2 81.21(17), N2-Mg-N3 81.79(17), N3-Mg-N4 81.51(16), N1-Mg-N4 81.68(16), N1-Mg-O1 97.85(16), N1-Mg-N2 78.40(6), N2-Mg-N3 78.56(5), N3-Mg-N4 80.38(5), N1-Mg-N4 77.42(6), N1-Mg-N5 131.51(6).

## VI.2.2. ROP of Lactide Monomers

The new alkali and alkaline earth metal complexes introduced have been used in ROP of lactide monomers. The results are collated in Table 6.1.

**Table 6.1** ROP of lactide monomers initiated by alkali and alkaline earth metal initiators [a]

| Entry | Catalyst | LA | *t* (h) | Conv. (%)[b] | $M_c$ (g·mol$^{-1}$) (×10$^{-4}$)[c] | $M_n$ (g·mol$^{-1}$) (×10$^{-4}$)[d] | $M_w/M_n$[d] | $P_r$[e] | $P_s$[e] |
|---|---|---|---|---|---|---|---|---|---|
| 1 | **Li25** | *rac* | 16 | 98 | 1.42 | 0.05 | 12.1 | - | - |
| 2 | | *meso* | 2 | 96 | 1.38 | 0.66 | 4.45 | - | 0.72 |
| 3 | **K25** | *rac* | 16 | 94 | 1.35 | 0.06 | 17.8 | - | - |
| 4 | | *meso* | 2 | > 99 | 1.44 | 0.99 | 4.50 | - | 0.74 |
| 5 | **[Ca25{N(SiMe$_3$)$_2$}]** | *rac* | 3 | 98 | 1.42 | 0.29 | 4.81 | - | - |
| 6 | | *meso* | 0.5 | > 99 | 1.44 | 0.10 | 4.72 | - | 0.70 |
| 7 | **[Mg25{N(SiMe$_3$)$_2$}]** | *rac* | 3 | 50 | 0.72 | 1.44 | 1.17 | 0.54 | - |
| 8 | | *meso* | 0.5 | > 99 | 1.44 | 0.52 | 3.10 | - | 0.77 |
| 9[f] | **[Ca25]$^+$[A]$^-$** | *rac* | 24 | 50 | 0.77 | 0.25 | 1.16 | - | - |
| 10[f] | | *meso* | 24 | 86 | 1.24 | 0.12 | 1.62 | - | - |
| 11[f] | **[Mg25]$^+$[A]$^-$** | *rac* | 24 | 12 | 0.27 | 0.16 | 1.06 | - | - |
| 12[f] | | *meso* | 24 | 76 | 1.10 | 0.27. | 1.26 | - | 0.68 |

[a] $[In]_0$ = 2.9 mmol·L$^{-1}$, $[LA]_0/[In]_0$ = 100, THF (3 mL) for ROP of *rac*-lactide, Toluene (3 mL for ROP of *meso*-lactide), 25 °C; $[A]^-$ = $[B\{3,5\text{-}C_6H_3Cl_2\}_4]^-$ [b] monomer conversion determined by $^1$H NMR spectroscopy; [c] $M_c$ = ([LA]/[Ln] × conv.% × 144.13); [d] determined by GPC and corrected using Mark-Houwink parameters; [e] $P_r$ is the probability of forming a new *r*-dyad, $P_s$ is the probability of forming a new *s*-dyad; determined by homonuclear decoupled $^1$H NMR spectroscopy; [f] reaction were performed in a mixture of 2.5 mL toluene and 0.5 mL isopropanol.

Resulting from the larger cation radius, **K25** polymerizes lactide monomers only minimally faster than **Li25**. Conversions of more than 94% were achieved for ROP of *rac*-lactide within 16 h while only 2 h are needed to convert more than 98% of the initial *meso*-monomer. In ROP experiments of *rac*-lactide stopped after 2 hours, the formed precipitate gave no useful data in NMR analytics and GPC. Atactic poly(*rac*-lactides) and syndiotactically enriched poly(*meso*-lactides) were produced (Entries 1-4) ($P_s$ = 0.72 with **Li25** and $P_s$ = 0.74 with **K25**). $M_n$ of the polymers are low and the molecular weight distribution is broad (PDI > 4.50, entry 4) indicating only little control.

Not surprisingly, the trend that the initiation rate depends on the size of the metal cation was also observed for alkaline earth metal complexes **[M25{N(SiMe$_3$)$_2$}]** and **[M25]$^+$[B{3,5-C$_6$H$_3$Cl$_2$}$_4$]$^-$** (M = Ca, Mg). **[Ca25]$^+$[B{3,5-C$_6$H$_3$Cl$_2$}$_4$]$^-$** polymerized lactide monomers faster than analogous **[Mg25]$^+$[B{3,5-C$_6$H$_3$Cl$_2$}$_4$]$^-$**. *meso*-Lactide was polymerized faster than *rac*-

lactide by both type of complexes resulting in slightly syndiotactic poly(*meso*-lactides) not exceeding a value of $P_s$ = 0.77. Cationic intermediates **[M25]**$^+$ and isopropanol as co-activator polymerize lactide monomers more controlled than silylamide initiators **[M25{N(SiMe$_3$)$_2$}]** (M = Mg,Ca), as shown by narrow PDI values for **[M25]**.$^+$ While **[M25{N(SiMe$_3$)$_2$}]** is supposed to polymerize via a coordination-insertion mechanism, **[M25]**$^+$ is supposed to polymerize lactide monomers following the cationic pathway.

However, molecular weights measured were low indicating a relatively unefficient catalysis. Compared to results for similar complexes reported by Carpentier, the complexes introduced in this thesis are less efficient. Two effects seem to be the reason for this. Firstly, the size of the macrocycle: As the macrocycle is relatively small, the metal centers are not effectively coordinated, leaving a large coordination sphere for incoming monomers, which costs selectivity.

Secondly the type of the donor atoms seem to have a large effect. While in this thesis, amine donors of the TACD-ring coordinate to the metal center, ether donors are present in the complexes reported by Carpentier *et al.*, as the metal-donor interaction is different. Because Carpentiers studies only focus on L-lactide polymerization, one can not directly compare the results with each other but as *rac*-lactide contains 50% L-lactide a comparison might be valid.[14]

## VI.3. Summary

In this chapter, the new proligand **H25** consisting of one phenoxy unit and a Me$_3$TACD heterocycle connected with each other by a methylene linker was introduced. Protonation of this proligand by a Brønsted acid into a cationic proligand was demonstrated as well as complexation of $Li^+$, $K^+$, $Ca^{2+}$ and $Mg^{2+}$ by treatment of the proligand with precursors of the forementioned metal cations. Characterization by NMR spectroscopy, elemental analysis and by X-ray diffraction analysis of [**Mg25]**$^+$**[B{3,5-C$_6$H$_3$Cl$_2$}$_4$]**$^-$ prove the proligand to coordinate to the metal centers by the phenoxy oxygen and the four amine donors.

The complexes were tested in the ROP of lactide monomers. Alkaline metal complexes showed no useful performance in the ROP experiments while the cationic intermediates of the

alkaline earth metal cations **[M25]**$^{+}$ with M = Ca and Mg generate narrowly distributed polymers. However, no stereoselectivity in the ROP is given by these type of complexes.

## VI.4. Experimental Section

1,4,7-trimethyl-1,4,7,10-tetraazacyclododecane, ($Me_3$TACD)H **(22)**[45]

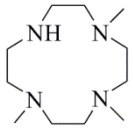


**22**
$C_{11}H_{26}N_4$
214,35

To a stirred solution of 6.00 g Cyclen (34.8 mmol, 1 equiv.) in 40 mL of EtOH, a solution of 17.65 g chloralhydrate (106.7 mmol, 3.07 equiv.) in 40 mL of EtOH was added by dropping funnel over a period of 1.5 h at 25 °C. The resulting solution was stirred at 60 °C for 16 h. After evaporation of the solvent, the resulting colorless oil was purified by flash chromatography using a mixture of DCM/MeOH/$NH_{3(aq.)}$ (25%) 9:1:0.1 to give 1,4-7-Triformylcyclen as a colorless oil in a yield of 70% (6.12 g, 24.3 mmol).

To a stirred solution of 6.12 g 1,4,7-Triformylcyclen in 30 mL of dry THF, 145 mL of a 1M solution of $BH_3$·THF were added and the mixture refluxed for 16 h. After addition of 3 mL MeOH, the solvents were evaporated under vacuum. The resulting colorless precipitate was suspended in a mixture of 50 mL EtOH and 5 mL conc. $H_2SO_4$ and heated to reflux for 2 h. After cooling to 25 °C, 150 mL of an 0.1 mol/L NaOH solution was added and the mixture was extracted three times with DCM. After removing the solvent under vacuum at 30 °C the resulting light red oil was purified by distillation under vacuum at 60 °C to give (**22**) as a colorless oil in a yield of 74% (3.836 g, 17.9 mmol). **$^{1}$H NMR** ($CDCl_3$, 25 °C, 400 MHz), δ (ppm): 2.14 (s, 3 H, NC$H_3$), 2.16 (s, 6 H, NC$H_3$), 2.27 (m, 8 H, NC$H_2$), 2.30 – 2.37 (m, 4 H, NC$H_2$), 2.48 – 2.57 (m, 4 H, NC$H_2$). **$^{13}$C{$^{1}$H} NMR** ($CDCl_3$, 25 °C, 100.1 MHz), δ (ppm): 43.5 (N$CH_3$), 44.5 (N$CH_3$), 45.6 (N$CH_2$), 53.5 (N$CH_2$), 55.0 (N$CH_2$), 55.1 (N$CH_3$). **Elemental analysis**, calculated for $C_{11}H_{26}N_4$ (214.35 g/mol) (%): C 61.64, H 12.23, N 26.14; Found: C 61.16, H 12.56, N 25.97.

2,4-di-*tert*-butyl-6-(hydroxymethyl)phenol[47] (**23**)

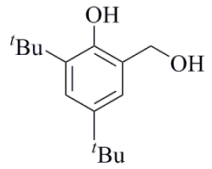


**23**
$C_{15}H_{24}O_2$
236,35

To a stirred solution of 30 g **4** (0.145 mol, 1 equiv.) in 40 mL of MeOH a suspension of paraformaldehyde (4.5 g, 0.15 mol) and LiOH($H_2O$) (0.5 g, 0.012 mol) in 40 mL of MeOH was added dropwise. After refluxing the solution for 12 h, the solvent was removed by rotary evaporation. The orange-brown viscous residue was dissolved in 60 mL *n*-hexane. After filtration and storage of the solution at 0 °C for 16 h a colorless precipitate of **23** in a yield of 58% was formed (20.2 g, 85 mmol). **$^1$H NMR** ($CDCl_3$, 25 °C, 400 MHz), δ (ppm): 1.30 (s, 9 H, C(C*H*$_3$)$_3$), 1.44 (s, 9 H, C(C*H*$_3$)$_3$), 2.10 (tr, 1 H, $^3J_{HH}$ = 5.9 Hz, CH$_2$O*H*), 4.85 (d, 2 H, $^3J_{HH}$ = 5.9 Hz, C*H*$_2$OH), 6.91 (d, 1 H, $^4J_{HH}$ = 2.4 Hz, Ph-*H*6) 7.30 (d, 1 H, $^4J_{HH}$ = 2.4 Hz, Ph-*H*4), 7.55 (s, 1 H, Ph-O*H*). **$^{13}$C{$^1$H} NMR** ($CDCl_3$, 25 °C, 100.1 MHz), δ (ppm): 29.8 (C(*C*H$_3$)$_3$), 31.8 (C(*C*H$_3$)$_3$), 34.4 (*C*(CH$_3$)$_3$), 35.1 (*C*(CH$_3$)$_3$), 66.0 (Ph*C*H$_2$OH), 122.8 (Ph-*C*5), 124.1 (Ph-*C*3), 124.2 (Ph-*C*6), 136.7 (Ph-*C*2), 141.8 (Ph-*C*4), 153.2 (Ph-*C*1). **Elemental analysis**, calculated for $C_{15}H_{24}O_2$ (236.35 g/mol) (%): C 76.23, H 10.24; Found: C 75.04, H 10.24.

---

2-(bromomethyl)-4,6-di-*tert*-butylphenol[47] (**24**)

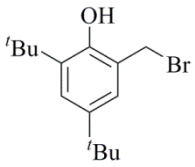


**24**
$C_{15}H_{23}BrO$
299,25

To a stirred solution of 17.5 g **23** (74 mmol, 1 equiv.) in 60 mL of $CHCl_3$, a solution of $PBr_3$ (8.1 g, 2.8 mL, 30 mmol, 0.4 equiv.) in 40 mL $CHCl_3$ was added dropwise. After stirring the solution for 1 h at 25 °C, 100 mL water were added. The organic phase was washed three times with water and dried over $MgSO_4$. The solvent was removed by rotary evaporation. The resulting orange viscous oil was further dried under vacuum to give 19.8 g of **24** (66 mmol, 89%). **$^1$H NMR** ($CDCl_3$, 25 °C, 400 MHz), δ (ppm): 1.30 (s, 9 H, C(C*H*$_3$)$_3$), 1.44 (s, 9 H, C(C*H*$_3$)$_3$), 4.59 (s, 2 H, PhC*H*$_2$Br), 7.11 (d, 1 H, $^4J_{HH}$ = 2.5 Hz, Ph-*H*3), 7.34 (d, 1 H, $^4J_{HH}$ =

2.5 Hz, Ph-*H*5). **$^{13}$C{$^{1}$H} NMR** ($CDCl_3$, 25 °C, 100.1 MHz), δ (ppm): 30.0 (C($CH_3$)$_3$), 31.7 (C($CH_3$)$_3$), 32.8 (Ph$CH_2$Br), 34.5 ($C$($CH_3$)$_3$), 35.1 ($C$($CH_3$)$_3$), 123.4 (Ph-*C*3), 124.9 (Ph-*C*5), 125.8 (Ph-*C*2), 137.3 (Ph-*C*6), 143.1 (Ph-*C*5), 151.8 (Ph-*C*1).

---

**25H**

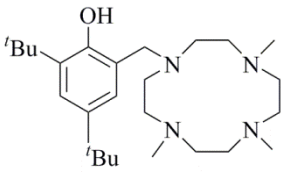


**25H**
$C_{26}H_{48}N_4O$
432,69

To a stirred solution of 3.0 g **22** (14.0 mmol, 1 equiv.) in 40 mL of dry toluene, 1.26 g of KOH (10 mmol, 2.1 equiv.) were added. After stirring for 16 h, a solution of **24** (4.2 g, 14.0 mmol) in 20 mL of toluene was added dropwise. After refluxing the solution for 6 h the solution was cooled to 25 °C, filtered and the solvent removed by rotary evaporation. A yellow brown viscious oil was obtained that was dissolved in a mixture of acetone and acetonitrile to give light yellow crystals of the desired proligand **25H** in a yield of 32% (1.9 g, 4.46 mmol). **$^{1}$H NMR** ($CDCl_3$, 25 °C, 400 MHz), δ (ppm): 1.27 (s, 9 H, C($CH_3$)$_3$), 1.42 (s, 9 H, C($CH_3$)$_3$), 2.12 (s, 6 H, N$CH_3$), 2.28 (s, 3 H, N$CH_3$), 2.42 – 2.53 (br, 4 H, N$CH_2$), 2.55 – 2.62 (br. 8 H, N$CH_2$), 2.63 – 2.70 (br., 4 H, N$CH_2$), 3.60 (s, 2 H, Ph$CH_2$), 6.82 (d, 1 H, $^{4}J_{HH}$ = 2.4 Hz, Ph-*H*5), 7.18 (d, 1 H, $^{4}J_{HH}$ = 2.4 Hz, Ph-*H*3). **$^{13}$C{$^{1}$H} NMR** ($CDCl_3$, 25 °C, 100.1 MHz), δ (ppm): 29.8 (C($CH_3$)$_3$), 31.9 (C($CH_3$)$_3$), 34.2 ($C$($CH_3$)$_3$), 35.1 ($C$($CH_3$)$_3$), 43.3 (N$CH_3$), 45.0 (N$CH_3$), 51.7 (N$CH_2$), 55.6 (N$CH_2$), 55.7 (N$CH_2$), 55.8 (N$CH_2$), 59.5 (Ph$CH_2$), 122.7 (Ph-*C*6), 122.8 (Ph-*C*3), 124.0 (Ph-*C*5), 135.8 (Ph-*C*2), 140.0 (Ph-*C*4), 154.5 (Ph-*C*1). **$^{1}$H NMR** ($C_6D_6$, 25 °C, 400 MHz), δ (ppm): 1.39 (s, 9 H, C($CH_3$)$_3$, 1.73 (s, 9 H, C($CH_3$)$_3$, 2.02 (s, 6 H, N$CH_3$), 2.15 (s, 3 H, N$CH_3$), 2.31 (br, 4 H, N$CH_2$), 2.41 (s, 8 H, N$CH_2$), 2.43 – 2.60 (br., 4 H, N$CH_2$), 3.42 (s, 2 H, Ph$CH_2$), 6.99 (d, 1 H, $^{4}J_{HH}$ = 2.4 Hz, Ph-*H*3), 7.18 (d, 1 H, $^{4}J_{HH}$ = 2.4 Hz, Ph-*H*5), 10.80 (s, 1 H, PhO*H*). **$^{13}$C{$^{1}$H} NMR** ($C_6D_6$, 25 °C, 100.1 MHz), δ (ppm): 30.2 (C($CH_3$)$_3$), 32.1 (C($CH_3$)$_3$), 34.3 ($C$($CH_3$)$_3$), 35.5 ($C$($CH_3$)$_3$), 43.3 (N$CH_3$), 44.7 (N$CH_3$), 52.1 (N$CH_2$), 55.8 (N$CH_2$), 56.4 (N$CH_2$), 56.6 (N$CH_2$), 59.6 (Ph$CH_2$), 122.8 (Ph-*C*6), 123.8 (Ph-*C*3), 124.2 (Ph-*C*5), 136.2 (Ph-*C*2), 140.1 (Ph-*C*4), 155.3 (Ph-*C*1). **$^{1}$H NMR** ($CD_2Cl_2$, 25 °C, 400 MHz), δ (ppm): 1.27 (s, 9 H, C($CH_3$)$_3$), 1.40 (s, 9 H, C($CH_3$)$_3$), 2.09 (s, 6 H, N$CH_3$), 2.25 (s, 3 H, N$CH_3$), 2.42 – 2.49 (br, 4 H, N$CH_2$), 2.50 – 2.65 (br, 12 H, N$CH_2$),

3.60 (s, 2 H, PhC$H_2$), 6.84 (d, 1 H, $^4J_{HH}$ = 2.4 Hz, Ph-*H*3), 7.16 (d, 1 H, $^4J_{HH}$ = 2.4 Hz, Ph-*H*5). **$^{13}$C{$^1$H} NMR** ($CD_2Cl_2$, 25 °C, 100.1 MHz), δ (ppm): 30.0 (C(*C*$H_3$)$_3$), 32.0 (C(*C*$H_3$)$_3$), 34.5 (*C*(CH$_3$)$_3$), 35.3 [*C*(CH$_3$)$_3$], 42.6 (N*C*H$_3$), 43.6 (N*C*H$_3$), 44.9 (N*C*H$_3$), 52.2 (N*C*H$_2$), 55.9 (N*C*H$_2$), 56.2 (N*C*H$_2$), 56.3 (N*C*H$_2$), 59.8 (Ph*C*H$_2$), 123.0 (Ph-*C*6), 123.6 (Ph-*C*3), 124.5 (Ph-*C*5), 136.0 (Ph-*C*2), 140.5 (Ph-*C*4), 155.0 (Ph-*C*1). **$^1$H NMR** (THF-$d_8$, 25 °C, 400 MHz), δ (ppm): 1.26 (s, 9 H, C(C*H*$_3$)$_3$), 1.40 (s, 9 H, C(C*H*$_3$)$_3$), 2.05 (s, 6 H, NC*H*$_3$), 2.21 (s, 3 H, NC*H*$_3$), 2.36 – 2.45 (br, 4 H, NC*H*$_2$), 2.55 – 2.63 (br, 12 H, NC*H*$_2$), 3.60 (s, 2 H, PhC*H*$_2$), 6.84 (d, 1 H, $^4J_{HH}$ = 2.5 Hz, Ph-*H*3), 7.15 (d, 1 H, $^4J_{HH}$ = 2.4 Hz, Ph-*H*5). **$^{13}$C{$^1$H} NMR** (THF-$d_8$, 25 °C, 100.1 MHz), δ (ppm): 30.1 (C(*C*H$_3$)$_3$), 32.3 (C(*C*H$_3$)$_3$), 34.8 (*C*(CH$_3$)$_3$), 35.8 (*C*(CH$_3$)$_3$), 43.6 (N*C*H$_3$), 45.1 (N*C*H$_3$), 52.8 (N*C*H$_2$), 57.2 (N*C*H$_2$), 57.4 (N*C*H$_2$), 58.6 (N*C*H$_2$), 60.0 (Ph*C*H$_2$), 123.1 (Ph-*C*6), 124.5 (Ph-*C*3), 124.8 (Ph-*C*5), 136.4 (Ph-*C*2), 140.4 (Ph-*C*4), 156.7 (Ph-*C*1). **Elemental analysis**, calculated for $C_{26}H_{48}ON_4$ (432.69 g/mol) (%): C 72.17, H 11.18, N 12.95; Found: C 71.64, H 11.19, N 12.27.

---

**[25H$_2$]$^+$[B{3,5-C$_6$H$_3$Cl$_2$}$_4$]$^-$**

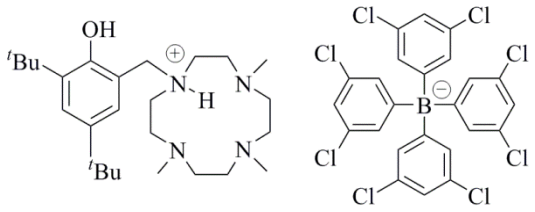

**[25H$_2$]$^+$[B{3,5-C$_6$H$_3$Cl$_2$}$_4$]$^-$**
$C_{50}H_{61}BCl_8N_4O$
1028.48

To a stirred solution of 0.300 g of **25H** (0.69 mmol, 1 equiv.) in 10 mL of dry $Et_2O$, a solution of 0.516 g [H(OEt$_2$)$_2$]$^+$[B{3,5-C$_6$H$_3$Cl$_2$}$_4$]$^-$ (0.69 mmol, 1 equiv.) in 10 mL of dry $Et_2O$ was added at 25 °C. A colorless precipitate was formed within a few seconds. The solution was filtrated and the collected colorless powder dried under vacuum to give **[25H$_2$]$^+$[B{3,5-C$_6$H$_3$Cl$_2$}$_4$]$^-$** in a yield of 68% (0.47 mmol, 0.49 g). **$^1$H NMR** ($CD_2Cl_2$, 25 °C, 400 MHz), δ (ppm): 1.28 (s, 9 H, C(C*H*$_3$)$_3$), 1.40 (s, 9 H, C(C*H*$_3$)$_3$), 2.21 (s, 6 H, NC*H*$_3$), 2.56 (s, 3 H, NC*H*$_3$), 2.57 – 2.68 (br, 12 H, NC*H*$_2$), 2.69 – 2.83 (br, 4 H, NC*H*$_2$), 3.68 (br, 2 H, PhC*H*$_2$), 6.92 (d, 1 H, $^4J_{HH}$ = 2.4 Hz, Ph-*H*3), 7.02 (m, 4 H, BPh-*H*(para), 7.04 – 7.09 (m, 8 H, BPh-*H*(ortho)), 7.26 (d, 1 H, $^4J_{HH}$ = 2.4 Hz, Ph-*H*5). **$^{13}$C{$^1$H} NMR** (THF-$d_8$, 25 °C, 100.1 MHz), δ (ppm): 30.1 (C(*C*H$_3$)$_3$), 31.0 (C(*C*H$_3$)$_3$), 34.6 (*C*(CH$_3$)$_3$), 35.4 (*C*(CH$_3$)$_3$), 42.8 (N*C*H$_3$), 43.7 (N*C*H$_3$), 50.6 (N*C*H$_2$), 50.7 (N*C*H$_2$), 50.8 (N*C*H$_2$), 50.9 (N*C*H$_2$), 54.9 (PhC*H*$_2$), 121.7 (Ph-

*C*6), 123.7 (Ph-*C*5), 124.6 (Ph-*C*3), 125.3 (Ph-*C*2), 131.3 (BPh-*C*2), 133.4/133.5/133.6 (BPh-*C*Cl), 136.2 (Ph-*C*2), 142.4 (Ph-*C*4), 153.7 (Ph-*C*1), 163,5/165.0/165.5/166.0 (BPh-*C*1, $J_{BC}$= 49.5 Hz). **Elemental analysis**, calculated for $C_{50}H_{61}BCl_8N_4O$ (1028.48 g/mol) (%): C 58.39, H 5.98, N 5.45; Found: C 58.59, H 5.88, N 5.37.

---

**$[25H_2]^+[B\{3,5\text{-}C_6H_3(CF_3)_2\}_4]^-$**

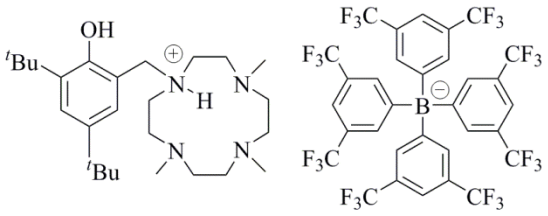

**$[25H_2]^+[B\{3,5\text{-}C_6H_3(CF_3)_2\}_4]^-$**
$C_{58}H_{61}BF_{24}N_4O$
1296.90

To a stirred solution of 0.214 g of **25H** (0.49 mmol, 1 equiv.) in 10 mL dry $Et_2O$ was added a solution of 0.500 g $[H(OEt_2)_2]^+[B\{3,5\text{-}C_6H_3(CF_3)_2\}_4]^-$ (0.49 mmol, 1 equiv.) in 10 mL dry $Et_2O$ at 25 °C. A colorless precipitate was formed after a few seconds. After stirring for 2 h, the solution was filtrated and the solvent evaporated to give **$[25H_2]^+[B\{3,5\text{-}C_6H_3(CF_3)_2\}_4]^-$** in a yield of 68% (0.47 mmol, 0.417 g). **$^1$H NMR** ($CD_2Cl_2$, 25 °C, 400 MHz), δ (ppm): 1.28 (s, 9 H, C(C*H*$_3$)$_3$), 1.41 (s, 9 H, C(C*H*$_3$)$_3$), 2.29 (s, 6 H, NC*H*$_3$), 2.64 (s, 3 H, NC*H*$_3$), 2.65 – 2.83 (br, 12 H, NC*H*$_2$), 2.83 – 2.95 (br, 4 H, NC*H*$_2$), 3.73 (br, 2 H, PhC*H*$_2$), 6.93 (d, 1 H, $^4J_{HH}$ = 2.4 Hz, Ph-*H*3), 7.29 (d, 1 H, $^4J_{HH}$ = 2.4 Hz, Ph-*H*5), 7.58 (br, 4 H, BPh-*H*(*para*)), 7.74 (m, 4 H, BPh-*H*(*ortho*)). **$^{13}$C{$^1$H} NMR** ($CD_2Cl_2$, 25 °C, 100.1 MHz), δ (ppm): 30.0 (C(*C*H$_3$)$_3$), 30.3 (C(*C*H$_3$)$_3$), 34.7 (*C*(CH$_3$)$_3$), 35.4 (*C*(CH$_3$)$_3$), 43.0 (N*C*H$_3$), 44.0 (N*C*H$_3$), 50.8 (N*C*H$_2$), 53.6 (N*C*H$_2$), 53.9 (N*C*H$_2$), 54.2 (N*C*H$_2$), 54.5 (PhC*H*$_2$), 118.1 (dt, $^3J_{CF}$ = 3.7 Hz, BPh-C4), 121.1 (Ph-*C*6), 123.8 (Ph-*C*5), 124.7 (Ph-*C*3), 125.3 (Ph-*C*2), 126.6 (BPh-*C*2), 129.5 (qq, $^2J_{CF}$ = 274.1 Hz), 135.4 (BPh-*C*2), 136.3 (Ph-*C*2), 142.7 (Ph-*C*4), 153.9 (Ph-*C*1), 162.3 (q, $^1J_{BC}$= 49.7 Hz, BPh-*C*1).

**Li25**

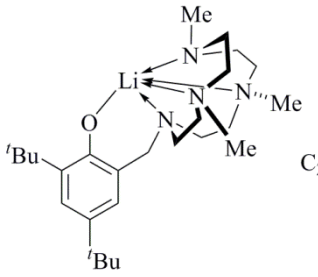


**Li25**
$C_{26}H_{47}LiN_4O$
438,62

To a stirred solution of 0.1 g **25H** (0.23 mmol, 1 equiv.) in 5 mL dry *n*-pentane, 0.09 mL of a 2.5 M solution *n*-BuLi were added at -78 °C. A colorless precipitate was formed within a few seconds. After stirring for 2 h at -78 °C, the solution was allowed to warm up slowly. After evaporation of the solvent, the powder was dissolved in 1 mL THF. After addition of 2 drops of *n*-pentane and storage of the solution for 5 d at -30 °C, colorless microcrystals of **Li25** in a yield of 87% (86 mg, 0.20 mmol) were obtained. **$^1$H NMR** ($CD_2Cl_2$, 25 °C, 400 MHz), δ (ppm): 1.14 (s, 9 H, C(C$H_3$)$_3$), 1.33 (s, 9 H, C(C$H_3$)$_3$), 1.88 (s, 6 H, NC$H_3$), 2.12 – 2.19 (br, 2 H, NC$H_2$), 2.22 – 2.26 (br, 2 H, NC$H_2$), 2.28 (s, 3 H, NC$H_3$), 2.30 – 2.34 (br, 4 H, NC$H_2$), 2.36 – 2.49 (br, 6 H, NC$H_2$), 2.52 – 2.58 (br, 2 H, NC$H_2$), 3.25 (s, 2 H, PhC$H_2$), 6.64 (d, 1 H, $^4J_{HH}$ = 2.4 Hz, Ph-*H*5), 6.90 (d, 1 H, $^4J_{HH}$ = 2.4 Hz, Ph-*H*3). **$^{13}$C{$^1$H} NMR** ($CD_2Cl_2$, 25 °C, 100.1 MHz), δ (ppm): 30.1 (C(*C*H$_3$)$_3$), 32.4 (C(*C*H$_3$)$_3$), 35.7 (*C*(CH$_3$)$_3$), 43.2 (N*C*H$_3$), 44.1 (N*C*H$_3$), 50.8 (N*C*H$_2$), 54.5 (N*C*H$_2$), 54.7 (N*C*H$_2$), 57.7 (N*C*H$_2$), 59.9 (Ph*C*H$_2$), 122.8 (Ph-*C*6), 126.9 (Ph-*C*3), 129.2 (Ph-*C*5), 134.9 (Ph-*C*2), 140.8 (Ph-*C*4), 167.2 (Ph-*C*1). **$^1$H NMR** ($CDCl_3$, 25 °C, 400 MHz), δ (ppm): 1.27 (s, 9 H, C(C$H_3$)$_3$), 1.42 (s, 9 H, C(C$H_3$)$_3$), 2.12 (s, 6 H, NC$H_3$), 2.28 (s, 3 H, NC$H_3$), 2.42 – 2.53 (br, 4 H, NC$H_2$), 2.55 – 2.62 (br, 8 H, NC$H_2$), 2.63 – 2.70 (br, 4 H, NC$H_2$), 3.60 (s, 2 H, PhC$H_2$), 6.82 (d, 1 H, $^4J_{HH}$ = 2.4 Hz, Ph-*H*5), 7.18 (d, 1 H, $^4J_{HH}$ = 2.4 Hz, Ph-*H*3). **$^{13}$C{$^1$H} NMR** ($CDCl_3$, 25 °C, 100.1 MHz), δ (ppm): 29.8 (C(*C*H$_3$)$_3$), 31.9 (C(*C*H$_3$)$_3$), 34.2 (*C*(CH$_3$)$_3$), 35.1 (*C*(CH$_3$)$_3$), 43.3 (N*C*H$_3$), 45.0 (N*C*H$_3$), 51.7 (N*C*H$_2$), 55.6 (N*C*H$_2$), 55.7 (N*C*H$_2$), 55.8 (N*C*H$_2$), 59.5 (Ph*C*H$_2$), 122.7 (Ph-*C*6), 122.8 (Ph-*C*3), 124.0 (Ph-*C*5), 135.8 (Ph-*C*2), 140.0 (Ph-*C*4), 154.5 (Ph-*C*1). **$^1$H NMR** ($C_6D_6$, 25 °C, 400 MHz), δ (ppm): 1.39 (s, 9 H, C(C$H_3$)$_3$), 1.73 (s, 9 H, C(C$H_3$)$_3$), 2.02 (s, 6 H, NC$H_3$), 2.15 (s, 3 H, NC$H_3$), 2.31 (br, 4 H, NC$H_2$), 2.41 (s, 8 H, NC$H_2$), 2.43 – 2.60 (br, 4 H, NC$H_2$), 3.42 (s, 2 H, PhC$H_2$), 6.99 (d, 1 H, $^4J_{HH}$ = 2.4 Hz, Ph-*H*3), 7.18 (d, 1 H, $^4J_{HH}$ = 2.4 Hz, Ph-*H*5). 10.80 (s, 1 H, PhO*H*). **$^{13}$C{$^1$H} NMR** ($C_6D_6$, 25 °C, 100.1 MHz), δ (ppm): 30.2 (C(*C*H$_3$)$_3$), 32.1 (C(*C*H$_3$)$_3$), 34.3 (*C*(CH$_3$)$_3$), 35.5 (*C*(CH$_3$)$_3$), 43.3 (N*C*H$_3$), 44.7 (N*C*H$_3$), 52.1 (N*C*H$_2$), 55.8 (N*C*H$_2$), 56.4 (N*C*H$_2$), 56.6 (N*C*H$_2$), 59.6 (Ph*C*H$_2$), 122.8 (Ph-*C*6), 123.8 (Ph-*C*3), 124.2

(Ph-*C*5), 136.2 (Ph-*C*2), 140.1 (Ph-*C*4), 155.3 (Ph-*C*1). **Elemental analysis**, calculated for $C_{26}H_{47}LiON_4$ (438.62 g/mol) (%): C 71.20, H 10.80, N 12.77; Found: C 69.42, H 10.78, N 12.08.

---

**K25**

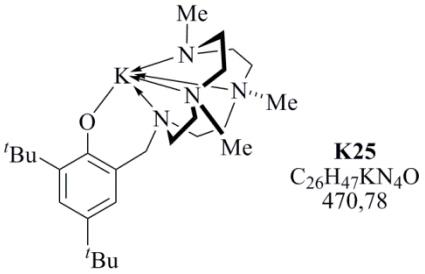


**K25**
$C_{26}H_{47}KN_4O$
470,78

To a stirred solution of 0.143 g **25H** (0.33 mmol, 1 equiv.) in 5 mL of dry *n*-pentane, 0.066 g of $K\{N(SiMe_3)_2\}$ were added at 25 °C. A colorless precipitate was formed within a few seconds. After stirring for 16 h at, the solution was filtrated and the collected colorless powder dried under vacuum to give 141 mg of **K25** (0.30 mmol, 89%). Colorless crystals were obtained from a saturated THF/n-pentane mixture over one week. **$^1$H NMR** ($C_6D_6$, 25 °C, 400 MHz), δ (ppm): 1.35 (s, 3 H, NC$H_3$), 1.40 (br, 2 H, NC$H_2$), 1.56 (s, 9 H, C(C$H_3$)$_3$, 1.65 (br, 6 H, NC$H_3$), 1.83 (s, 9 H, C(C$H_3$)$_3$, 1.85 – 2.0 (br, 6 H, NC$H_2$), 2.0 – 2.21 (br, 8 H, NC$H_2$), 2.40 – 2.62 (br, 2 H, PhC$H_2$), 7.20 (d, 1 H, $^4J_{HH}$ = 2.4 Hz, Ph-*H*5), 7.56 (d, 1 H, $^4J_{HH}$ = 2.4 Hz, Ph-*H*3). **$^{13}$C{$^1$H} NMR** ($C_6D_6$, 25 °C, 100.1 MHz), δ (ppm): 31.1 (C(*C*$H_3$)$_3$), 32.8 (C(*C*$H_3$)$_3$), 34.0 (*C*(CH$_3$)$_3$), 35.8 (*C*(CH$_3$)$_3$), 44.0 (N*C*H$_3$), 41.1 (N*C*H$_3$), 41.3 (N*C*H$_3$), 53.7 (N*C*H$_2$), 53.8 (N*C*H$_2$), 53.9 (N*C*H$_2$), 54.0 (N*C*H$_2$), 59.8 (Ph*C*H$_2$), 123.2 (Ph-*C*6), 127.6 (Ph-*C*3), 128.0 (Ph-*C*5), 128.2 (Ph-*C*2), 135.6 (Ph-*C*4), 168.4 (Ph-*C*1). **Elemental analysis**, calculated for $C_{26}H_{47}KON_4$ (470.78 g/mol) (%): C 66.33, H 10.06, N 11.90; Found: C 65.63, H 10.64, N 10.18.

**[Ca25{N(SiMe$_3$)$_2$}]**

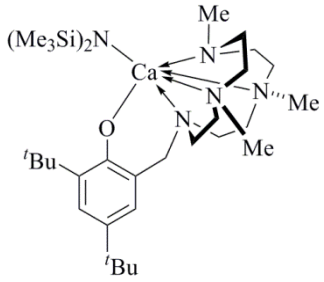


**[Ca25{N(SiMe$_3$)$_2$}]**
$C_{32}H_{65}CaN_5OSi_2$
632,14

To a stirred suspension of 0.200 g of [Ca{N(SiMe$_3$)$_2$}$_2$(THF)$_2$] (0.40 mmol, 1 equiv.) in 5 mL dry *n*-pentane, a solution of 0.171 g **25H** (0.40 mmol, 1 equiv.) in 5 mL dry *n*-pentane was added at 25 °C. A colorless precipitate was formed within a few seconds. After stirring for 16 h at, the solution was filtrated and the collected colorless powder dried under vacuum to give 181 mg of **[Ca25{N(SiMe$_3$)$_2$}]** (0.29 mmol, 72%). **$^1$H NMR** ($C_6D_6$, 25 °C, 400 MHz), δ (ppm): 0.35 (s, 18 H, SiC$H_3$), 1.22 – 1.38 (br, 4 H, NC$H_2$), 1.44 (s, 9 H, C(C$H_3$)$_3$), 1.55 – 1.65 (br, 4 H, NC$H_2$), 1.64 – 1.82 (br, 4 H, NC$H_2$), 1.83 (s, 9 H, C(C$H_3$)$_3$), 1.85 (br, 2 H, NC$H_2$), 1.87 – 1.91 (br, 2 H, NC$H_2$), 1.92 (s, 3 H, NC$H_3$), 2.08 (s, 6 H, NC$H_3$), 2.18 – 2.40 (br, 2 H, PhC$H_2$), 6.98 (d, 1 H, $^4J_{HH}$ = 2.4 Hz, Ph-*H*5), 7.55 (d, 1 H, $^4J_{HH}$ = 2.4 Hz, Ph-*H*3). **$^{13}$C{$^1$H} NMR** ($C_6D_6$, 25 °C, 100.1 MHz), δ (ppm): 7.6 (Si*C*H$_3$), 31.0 (C(*C*H$_3$)$_3$), 32.6 (C(*C*H$_3$)$_3$), 34.2 (*C*(CH$_3$)$_3$), 36.0 (*C*(CH$_3$)$_3$), 47.7 (N*C*H$_3$), 51.7 (N*C*H$_3$), 41.3 (N*C*H$_3$), 51.7 (N*C*H$_2$), 53.0 (N*C*H$_2$), 54.7 (N*C*H$_2$), 55.6 (N*C*H$_2$), 64.6 (Ph*C*H$_2$), 122.3 (Ph-*C*6), 124.1 (Ph-*C*3), 125.4 (Ph-*C*5), 131.8 (Ph-*C*2), 136.8 (Ph-*C*4), 164.8 (Ph-*C*1). **Elemental analysis**, calculated for $C_{32}H_{65}CaN_5OSi_2$ (632.14 g/mol) (%): C 60.80, H 10.36, N 11.08; Found: C 56.45, H 9.61, N 8.87.

---

**[Mg25{N(SiMe$_3$)$_2$}]**

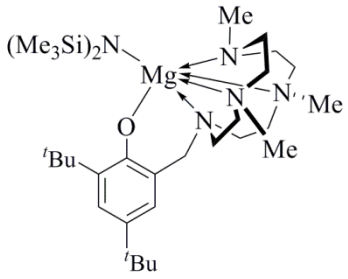


**[Mg25{N(SiMe$_3$)$_2$}]**
$C_{32}H_{65}MgN_5OSi_2$
616,37

To a stirred suspension of 0.160 g of [Mg{N(SiMe$_3$)$_2$] (0.46 mmol, 1 equiv.) in 5 mL dry *n*-pentane, a solution of 0.200 g **25H** (0.46 mmol, 1 equiv.) in 5 mL dry *n*-pentane was added at

25 °C. A colorless precipitate was formed within a few seconds. After stirring for 2 h at, the solution was filtrated and the collected colorless powder dried under vacuum to give **[Mg25{N(SiMe$_3$)$_2$}]** in a yield of 69% (0.32 mmol, 0.196 g). **$^1$H NMR** ($CD_2Cl_2$, 25 °C, 400 MHz), δ (ppm): 0.05 (s, 18 H, SiC$H_3$), 1.26 (s, 9 H, C(C$H_3$)$_3$), 1.42 (s, 9 H, C(C$H_3$)$_3$), 2.23 (s, 6 H, NC$H_3$), 2.62 (s, 3 H, NC$H_3$), 2.67 – 2.77 (br, 6 H, NC$H_2$), 2.85 – 2.99 (br, 8 H, NC$H_2$), 3.00 – 3.07 (br, 2 H, NC$H_2$), 3.64 (br, 2 H, PhC$H_2$), 6.87 (d, 1 H, $^4J_{HH}$ = 2.6 Hz, Ph-*H*5), 7.23 (d, 1 H, $^4J_{HH}$ = 2.4 Hz, Ph-*H*3). **$^{13}$C{$^1$H} NMR** ($CD_2Cl_2$, 25 °C, 100.1 MHz), δ (ppm): 6.7 (Si*C*H$_3$), 29.9 (C(*C*H$_3$)$_3$), 32.1 (C(*C*H$_3$)$_3$), 34.3 (*C*(CH$_3$)$_3$), 35.8 (*C*(CH$_3$)$_3$), 43.8 (N*C*H$_3$), 44.1 (N*C*H$_3$), 50.0 (N*C*H$_2$), 53.6 (N*C*H$_2$), 54.3 (N*C*H$_2$), 57.7 (N*C*H$_2$), 121.4 (Ph-*C*6), 125.3 (Ph-*C*3), 127.1 (Ph-*C*5), 136.9 (Ph-*C*2), 138.2 (Ph-*C*4), 163.4 (Ph-*C*1). **Elemental analysis**, calculated for $C_{32}H_{65}MgN_5OSi_2$ (616.37 g/mol) (%): C 62.36, H 10.63, N 11.36; Found: C 59.87, H 11.07, N 10.26.

---

**[Ca25]$^+$[B{3,5-C$_6$H$_3$Cl$_2$}$_4$]$^-$**

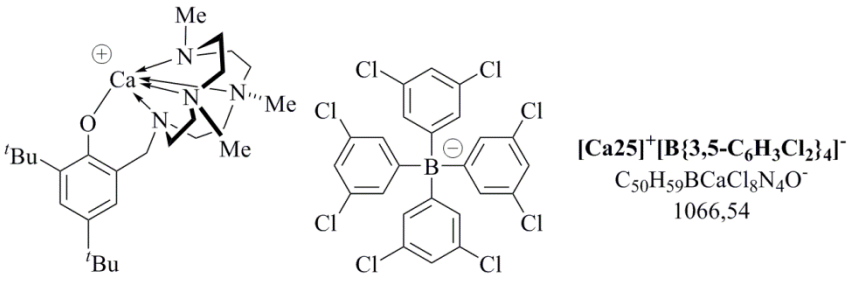


To a stirred solution of 100 mg **[Ca(N(SiMe$_3$)$_2$(THF)$_2$]** (0.2 mmol, 1 equiv.) in 10 mL $Et_2O$, a solution of 204 mg **[25H$_2$]$^+$[B{3,5-C$_6$H$_3$Cl$_2$}$_4$]$^-$** in 10 mL $Et_2O$ was added. The mixture was stirred for 3 h at 25 °C. After removal of the solvent under vacuum, the resulting white powder was recrystallized from $CH_2Cl_2$ to afford 204 mg (0.19 mmol, 95%) of the desired product. **$^1$H NMR** ($CD_2Cl_2$, 25 °C, 400 MHz), δ (ppm): 1.25 (s, 9 H, C(C$H_3$)$_3$), 1.38 (s, 9 H, C(C$H_3$)$_3$), 2.04 (m, 4 H, *β*-THF), 2.28 (s, 6 H, NC$H_3$), 2.36 (s, 3 H, NC$H_3$), 2.37 – 2.49 (br, 4 H, NC$H_2$), 2.51 – 2.79 (br, 12 H, NC$H_2$), 3.50 – 3.80 (br, 2 H, PhC$H_2$), 4.03 (m, 4 H, *α*-THF), 6.86 (d, 1 H, $^4J_{HH}$ = 2.5 Hz, Ph-*H*3), 7.01 (tr, 4 H, BPh-*H*(para)), 7.04 (m, 8 H, BPh-*H*(ortho)), 7.19 (d, 1 H, $^4J_{HH}$ = 2.4 Hz, Ph-*H*5). **$^{13}$C{$^1$H} NMR** ($CD_2Cl_2$, 25 °C, 100.1 MHz), δ (ppm): 24.7 (*β*-THF), 28.7 (C(*C*H$_3$)), 28.8 (C(*C*H$_3$)), 28.9 (C(*C*H$_3$)), 30.6 (C(*C*H$_3$)), 30.8 (C(*C*H$_3$)), 32.9(C(*C*H$_3$)), 34.2 (*C*(CH$_3$)), 43.4 (N*C*H$_3$), 44.0 (N*C*H$_3$), 48.9 (N*C*H$_2$), 49.1

(N*C*H$_2$), 49.3 (N*C*H$_2$), 49.4 (N*C*H$_2$), 64.9 (PhC*H*$_2$), 68.3 (*α*-THF), 121.1 (Ph-*C*6), 122.3 (BPh-C(meta)), 123.5 (Ph-*C*5), 125.9 (Ph-*C*3), 132.1/132.2/132.2/132.3 (BPh-*C*Cl), 132.4 (Ph-*C*2), 134.7 (Ph-*C*4), 163,2/163.7/164.2/164.6 (BPh-*C*1, $J_{BC}$= 49.4 Hz), 163.7 (Ph-*C*1). **Elemental analysis**, calculated for $C_{50}H_{59}BCaCl_8N_4O$ (1066.54 g/mol) (%): C 56.96, H 5.93, N 4.92; Found: C 54.57, H 5.58, N 4.73.

---

**[Mg25]$^+$[B{3,5-C$_6$H$_3$Cl$_2$}$_4$]$^-$**

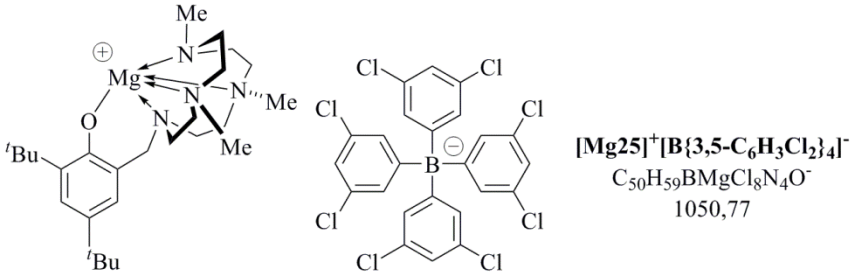


To a stirred solution of 67 mg **[Mg(N(SiMe$_3$)$_2$]** (0.2 mmol, 1 equiv.) in 10 mL Et$_2$O, a solution of 200 mg **[25H$_2$]$^+$[B{3,5-C$_6$H$_3$Cl$_2$}$_4$]$^-$** (0.2 mmol, 1 equiv.) in 10 mL Et$_2$O and 5 mL THF was added. The mixture was stirred for 3 h at room 25 °C. After removal of the solvent under vacuum, the resulting colorless powder was recrystallized from $CH_2Cl_2$ to afford 166 mg (0.158 mmol, 79%) of the desired product. **$^1$H NMR** ($CD_2Cl_2$, 25 °C, 400 MHz), δ (ppm): 1.26 (s, 9 H, C(C*H*$_3$)$_3$), 1.40 (s, 9 H, C(C*H*$_3$)$_3$), 1.82 (m, 4 H, *β*-THF), 2.16 (s, 6 H, NC*H*$_3$), 2.57 (s, 3 H, NC*H*$_3$), 2.58 – 2.74 (br, 14 H, NC*H*$_2$), 2.82 – 2.89 (br, 2 H, NC*H*$_2$), 3.61 (s, 2 H, PhC*H*$_2$), 3.69 (s, 4 H, *α*-THF), 6.87 (d, 1 H, $^4J_{HH}$ = 2.7 Hz, Ph-*H*3), 7.00 – 7.02 (tr, 4 H, BPh-*H*(para)), 7.03 – 7.06 (m, 8 H, BPh-*H*(ortho)), 7.23 (d, 1 H, $^4J_{HH}$ = 2.7 Hz, Ph-*H*5). **$^{13}$C{$^1$H} NMR** ($CD_2Cl_2$, 25 °C, 100.1 MHz), δ (ppm): 26.2 (*β*-THF), 29.9 (C(*C*H$_3$)), 35.8 (C(*C*H$_3$)), 43.3 (*C*(CH$_3$)), 43.8 (*C*(CH$_3$)), 49.4 (N*C*H$_3$), 53.7 (N*C*H$_3$), 53.9 (N*C*H$_2$), 57.3 (N*C*H$_2$), 64.6 (PhC*H*$_2$), 68.3 (*α*-THF), 121.2 (Ph-*C*2), 123.7 (BPh-C(meta)), 125.5 (Ph-*C*5), 127.3 (Ph-*C*3), 133.4/133.5/134.6/133.7 (BPh-*C*Cl), 133.7 (BPh-C(ortho)), 137.3 (Ph-*C*6), 138.4 (Ph-*C*4), 164.5/165.0/165.5/166.0 (BPh-*C*1, $J_{BC}$= 49.5 Hz), 166.0 (Ph-*C*1). **Elemental analysis**, calculated for $C_{50}H_{59}BMgCl_8N_4O$ (1122.87 g/mol) (%):C 57.15, H 5.66, N 5.33; Found: C 57.05, H 5.91, N 4.95.

**Typical polymerization procedure.** In the glove box, stock solution of the initiator in the specified solvent was injected individually to a series of 6 mL vials loaded with a solution of *rac*- or *meso*-lactide in the specified solvents. After specified time intervals, each vial was taken out of the glove box and the solution quenched with moist *n*-hexane. After filtration and drying under vacuum, the polymers were analyzed in $CDCl_3$ by NMR measurements. GPC analyses were performed in THF.

**Polymerization procedure in presence of isopropanol.** To a solution of the lactide monomer in the specified solvent and one equivalent of isopropanol, initiator stock solution was injected. After specified time intervals, each vial was taken out of the glove box and the solution was quenched with moist *n*-hexane. After filtration and drying under vacuum, the polymers were analyzed in $CDCl_3$ by NMR measurements. GPC analyses were performed in THF.

## VI.5. References


1 a) S. Harder, *Chem. Rev.* **2010**, *110*, 3852-3876; b) A. G. M. Barett, M. R. Crimmin, M. S. Hill, P. A. Procopiou, *Proc. R. Soc. A* **2010**, *466*, 927-963, c) C. A. Wheaton, P. G. Hayes, B. J. Ireland, *Dalton Trans.* **2009**, 4832-4846.

2 a) J. Jenter, R. Koeppe, P. W. Roesky, *Organometallics* **2011**, *30*, 1404-1413, b) A. G. M. Barrett, I. J. Casely, M. R. Crimmin, M. S. Hill, J. R. Lachs, M. F. Mahon, P. A. Procopiou, *Inorg. Chem.* **2009**, *48*, 4445-4453.

3 a.) S. Harder, F. Feil, K. Knoll, *Angew. Chem. Int. Ed.* **2001**, *40*, 4261-4264, b) S. Harder, F. Feil, *Organometallics* **2002**, *21*, 2268-2274, c) P. Jochmann, T. S. Dols, T. P. Spaniol, L. Perrin, L. Maron, J. Okuda, *Angew. Chem. Int. Ed.* **2009**, *48*, 5715-5719.

4 A. G. M. Barrett, M. R. Crimmin, M. S. Hill, P. B. Hitchcock, S. L. Lomas, P. A. Procopiou, K. Suntharalingam, *Chem. Commun*. **2009**, 2299-2301.

5 J. Spielmann, F. Buch, S. Harder, *Angew. Chem. Int. Ed.* **2008**, *47*, 9434-9438.

6 P. Jochmann, T. S. Dols, T. P. Spaniol, L. Perrin, L. Maron, J. Okuda, *Angew. Chem. Int. Ed.* **2010**, *49*, 7795-7798.

7 M. Westerhausen, S. Schneiderbauer, A. N. Kneifel, Y. Söltl, P. Mayer, H. Nöth, Z. Zhong, P. J. Dijkstra, J. Feijen, *Eur. J. Inorg. Chem.* **2003**, *18*, 3432-3439.

8 M. S. Hill, P. B. Hitchcock, *Chem. Commun.* **2003**, 1758-1759.

9 M. H. Chisholm, J. Gallucci, K. Phomphrai, *Chem. Commun.* **2003**, 48-49.

10 M. H. Chisholm, J. Gallucci, K. Phomphrai, *Inorg.Chem.* **2004**, *43*, 6717-6725.

11 D. J. Darensbourg, W. Choi, C. P. Richers, *Macromolecules* **2007**, *40*, 3521-3523.

12 D. J. Darensbourg, W. Choi, O. Karroonnirun, N. Bhuvanesh, *Macromolecules* **2008**, *41*, 3493-3502.

13 V. Poirier, J.-F. Carpentier, Y. Sarazin, *Dalton Trans* **2009**, 9820-9827.

[14] Y. Sarazin, V. Poirier, T. Roisnel, J.-F. Carpentier, *Eur. J. Inorg. Chem.* **2010**, *22*, 3423-3428.

[15] Z. Zhong, P. J. Dijkstra, C. Birg, M. Westerhausen, J. Feijen, *Macromolecules* **2001**, *34*, 3863-3868.

[16] D. J. Darensbourg, W. Choi, P. Ganguly, C. P. Richers, *Macromolecules* **2006**, *39*, 4374-4379.

[17] Y. Sarazin, R. H. Howard, D. L. Hughes, S. M. Humphrey, M. Bochmann, *Dalton Trans.* **2006**, 340-350.

[18] M. G. Davidson, C. T. O'Hara, M. D. Jones, C. G. Keir, M. F. Mahon, G. Kociok-Köhn, *Inorg. Chem.* **2007**, *46*, 7686-7688.

[19] B. M. Chamberlain, M. Cheng, D. R. Moore, T. M. Ovitt, E. B. Lobkovsky, G. W. Coates, *J. Am. Chem. Soc.* **2001**, *123*, 3229-3238.

[20] M. H. Chisholm, N. W. Eilerts, J. C. Huffman, S. S. Iyer, M. Pacold, K. Phomphrai, *J. Am. Chem. Soc.* **2000**, *122*, 11845-11854.

[21] M. H. Chisholm, J. Gallucci, K. Phomphrai, *Inorg. Chem.* **2002**, *41*, 2785-2794.

[22] M. H. Chisholm, J. C. Gallucci, K. Phomphrai, *Inorg. Chem.* **2005**, *44*, 8004-8010.

[23] B. Lian, C. M. Thomas, O. L. Casagrande, Jr., T. Roisnel, J.-F. Carpentier, *Polyhedron* **2007**, *26*, 3817-3824.

[24] J. Ejfler, M. Kobylka, L. B. Jerzykiewicz, P. Sobota, *Dalton Trans.* **2005**, 2047-2050.

[25] M. H. Chisholm, J. C. Huffman, K. Phomphrai, *J. Chem. Soc., Dalton Trans.* **2001**, 222-224.

[26] I. L. Fedushkin, A. G. Morozov, V. A. Chudakova, G. K. Fukin, V. K. Cherkasov, *Eur. J. Inorg. Chem.* **2009**, *33*, 4995-5003.

[27] J.-C. Buffet, J. P. Davin, T. P. Spaniol, J. Okuda, *New. J. Chem.* **2011**, *35* (**10**), 2253-2257.

[28] L. F. Sanchez-Barba, A. Garces, J. Fernandez-Baeza, A. Otero, C. Alonso-Moreno, A. Lara-Sánchez, A. M. Rodríguez, *Organometallics*, **2011**, *30*, 2775-2789.

[29] L. Wang, H. Ma, *Macromolecules* **2010**, *43*, 6535-6537.

[30] J. Ejfler, K. Krauzy-Dziedzic, S. Szafert, L. B. Jerzykiewicz, P. Sobota, Eur. *J. Inorg. Chem.* **2010**, *23*, 3602-3609.

[31] Y. Sarazin, B. Liu, T. Roisnel, L. Maron, J.-F. Carpentier, *J. Am. Chem. Soc.* **2011**, *133*, 9069-9087.

[32] Y. Wang, W. Zhao, D. Liu, S. Li, D. Cui, X. Chen, *Organometallics*, **2012**, *31*, 4182-4190.

[33] C.-Y. Sung, C.-Y. Li, J.-K. Su, T.-Y. Chen, C.-H. Lin, B.-T. Ko, *Dalton Trans*, **2012**, *41*, 953-961.

[34] H.-J. Chuang, S.-F. Weng, C.-C. Chang, C.-C. Lin, H.-Y. Chen, *Dalton Trans.* **2011**, *40*, 9601-9607.

[35] V. Poirier, T. Roisnel, J.-F. Carpentier, Y. Sarazin, *Dalton Trans.* **2011**, *40*, 523-534.

[36] A. Garcés, L. F. Sánchez-Barba, C. Alonso-Moreno, M. Fajardo, J. Fernández-Baeza, A. Otero, A. Lara-Sánchez, I. López-Solera, A. María Rodríguez, *Inorg. Chem.* **2010**, *49*, 2859-2871.

[37] P. L. Arnold, I. J. Casely, Z. R. Turner, R. Bellabarba, R. B. Tooze, *Dalton Trans.* **2009**, 7236-7247.

[38] Z. Zheng, G. Zhao, R. Fablet, M. Bouyahi, C. M. Thomas, T. Roisnel, O. Casagrande Jr, J.-F. Carpentier, *New. J. Chem.* **2008**, *32*, 2279-2291.

[39] A. P. Dove, V. C. Gibson, E. L. Marshall, A. J. P. White, D. J. Williams, *Dalton Trans.* **2004**, 570-578.

[40] B. Liu, V. Dorcet, L. Maron, J.-F. Carpentier, Y. Sarazin, *Chem. Eur. J.* **2012**, *18*, 3023-3031.

[41] J. P. Davin, J.-C. Buffet, T. P. Spaniol, J. Okuda, Dalton Trans. **2012**, *41*, 12612-12618.

[42] S. Itoh, H. Kumei, S. Nagatomo, T. Kitagawa, S. Fukuzumi, *J. Am. Chem. Soc.* **2001**, *123*, 2165–2175.

[43] V. Boldrini, G. B. Giovenzana, R. Pagliarin, G. Palmisano, M. Sisti, *Tetrahedron Lett.* **2000**, *41*, 6527-6530.

[44] A. J. Blake, J. P. Danks, W.-S. Li, V. Lippolis, M. Schröder, *J. Chem. Soc., Dalton Trans* **2000**, 3034-3040.

[45] E. Abinet, D. Martin, S. Standfuss, H. Kulinna, T. P. Spaniol, J. Okuda, *Chem. Eur. J.* **2011**, *17*, 15014-15026.

[46] S. Itoh, H. Kumei, S. Nagatomo, T. Kitagawa, S. Fukuzumi, *J. Am. Chem. Soc.* **2001**, *123*, 2165–2175.

[47] A. Sokolowski, J. Müller, T. Weyhermüller, R. Schnepf, P. Hildebrandt, K. Hildenbrand, E. Bothe, K. Wieghardt, *J. Am. Chem. Soc.* **1997**, *119*, 8889-8900.

[48] M. Brookhart, B. Grant, A. F. Volpe Jr., *Organometallics*, **1992**, *11*, 3920-3922.

[49] S. Standfuss, T. P. Spaniol, J. Okuda, *Eur. J. Inorg. Chem.***2010**, 2987-2991.

# Summary

The main objective of the present work is the investigation of the ring-opening polymerization (ROP) of lactide monomers initiated by complexes based on lewis acidic metal centers.

In **Chapter II**, synthesis of new OSSO-type bis(phenols) $H_2\mathbf{L}^{x}$ (x = 24-27) from salt metathesis reactions of 2,4-disubstituted phenols with dibromoalkanes are described (Scheme S1.). The first two bis(phenols) of the OSSO-type bearing a 1-methylcyclohexyl group are presented. $H_2\mathbf{L}^{x}$ (x = 28,29) are generated by reaction of disulfide precursors with cycloalkenes, catalyzed by $BF_3{*}OEt_2$. These proligands expand the number of chiral OSSO-type proligands. The compounds are fully characterized by NMR and elemental analysis.

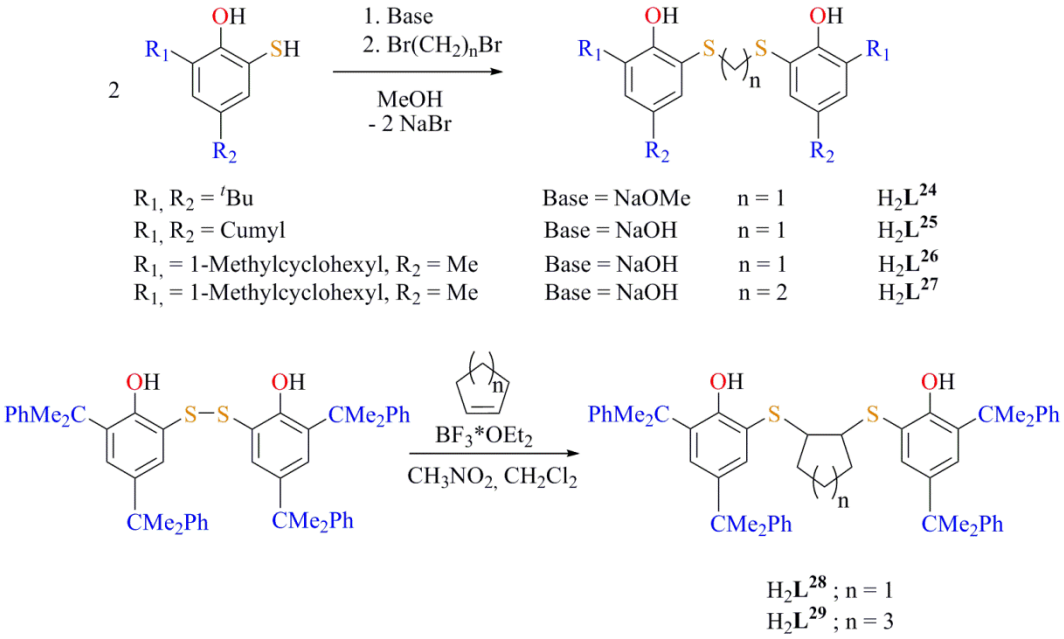


**Scheme S1.** Preparation of OSSO-Type Bis(phenols).

**Chapter III** describes the preparation of scandium and yttrium silylamide bis(phenolate) complexes by reaction of tetradentate bis(phenol) $H_2\mathbf{L}^{14}$ as well as bis(phenols) drawn in Scheme S1 with one equivalent of scandium or yttrium silylamide complexes. The complexes $[Ln\mathbf{L}^{x}\{N(SiMe_2H)_2\}THF]$ (Ln = Sc,Y; x = 14, 24-29) are isolated as colorless or light yellow powders that are highly sensitive towards air and moisture. NMR-spectroscopic analysis and elemental analysis of the complexes as well as X-ray diffraction analysis of complex $[Y\mathbf{L}^{14}\{N(SiMe_2H)_2\}THF]$ proof the prepared compounds to appear monomeric in solution

and in the solid state whe the metal centers adopt a six-coordinated geometry. One bis(phenolate) ligand, one silylamide group and one THF molecule coordinate to the metal center. (Scheme S2.)

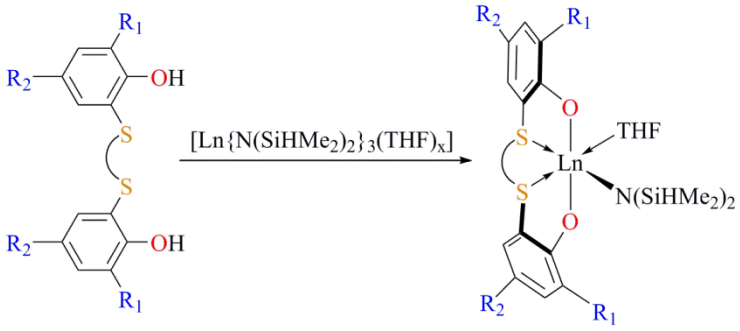


**Scheme S2.** Preparation of rare earth metal silylamide bis(phenolate) complexes.

In **Chapter IV** the application of these complexes in the ring-opening polymerization (ROP) of *rac*- and *meso*-lactide to biodegradable poly(lactide) (PLA) is discussed (Scheme S3.).

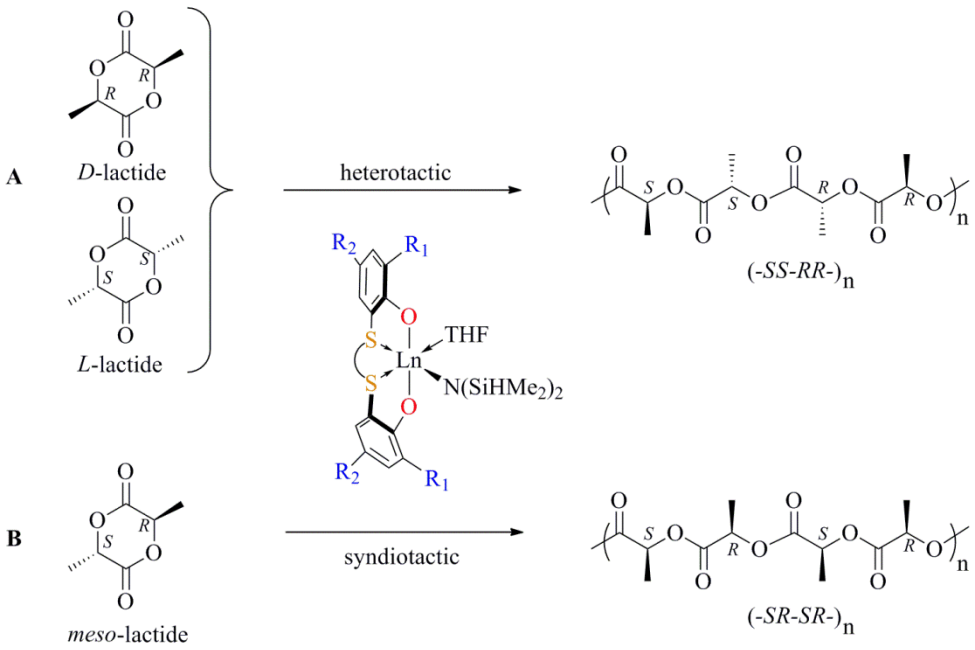


**Scheme S3.** Preparation of heterotactic poly(*rac*-lactides) and syndiotactic poly(*meso*-lactides) by ROP of *rac*- and *meso* lactide initiated by rare earth metal bis(phenolate) silylamide complexes.

The complexes are very active and selective initiators for the ROP of lactide. *rac*-Lactide is polymerized heteroselectively while *meso*-lactide is polymerized syndioselectively. Complexes that polymerize *rac*-lactide highly heteroselective do also show the highest syndioselectivity. Analyses of the microstructure of poly(*meso*-lactides) shows the rare earth

metal bis(phenolate) silylamide complexes to possibly epimerize *meso*-lactide into *rac*-lactide which results in enchainments of *rac*-monomers into the poly(*meso*-lactide) chains, potentially preventing the formation of PLA with syndiotacticity values exceeding $P_s$ = 0.92. Nevertheless, rare earth metal bis(phenolate) solylamide complexes showed fast consumption of lactide monomers

**Chapter V** describes the application of indium bis(phenolate) isopropoxide complexes [In**L**$^{6}$(O$^{i}$Pr)], [In**L**$^{9}$(O$^{i}$Pr)] and [In**L**$^{14}$(O$^{i}$Pr)] in the ROP of *rac*- and *meso*-lactide (Scheme S4). ROP of *rac*-lactide forms atactic PLA while meso-lactide is polymerized predominantly syndioselectively. Mechanistic studies demonstrate a coordination-insertion mechanism occuring. Determination of the activation parameters of the ROP proof the ROP of *rac*- and *l*-lactide being less favored than the ROP of *meso*-lactide.

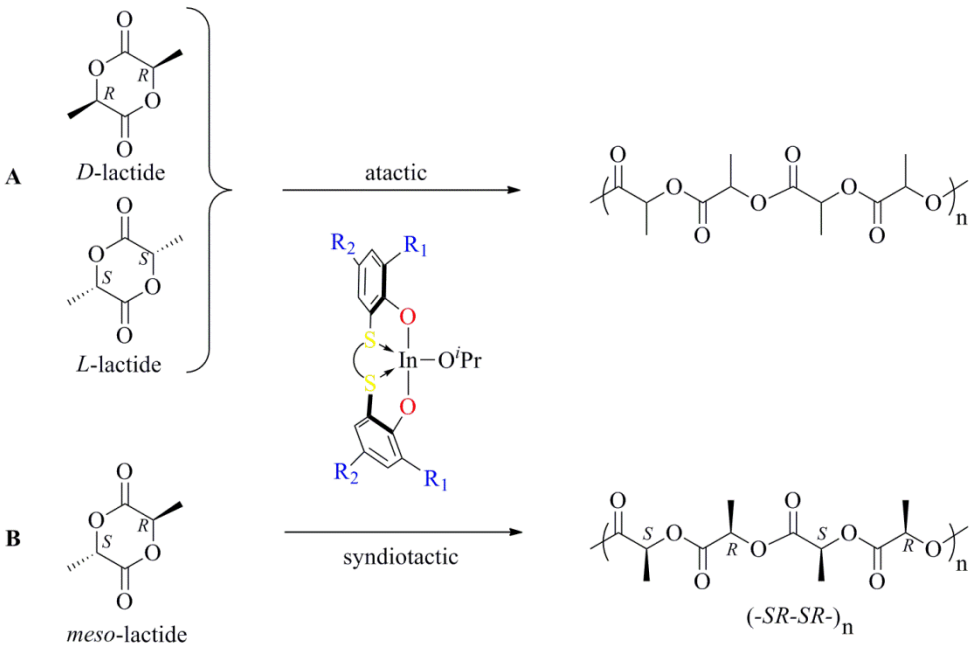


**Scheme S4.** ROP of lactide monomers initiated by indium bis(phenolate) isopropoxide complexes.

**Chapter VI** describes the reactions of alkali metal- and alkaline earth metal precursors with neutral and cationic heterocycle-containing phenol based proligands (Scheme S5). Proligand **25H** is prepared by halide elimination reaction of $Me_3$TACD **(22)** and 2,4-disubstituted-bromomethylphenol. Treatment with silylamides of potassium, calcium and magnesium as well as *n*-BuLi gives the corresponding metal complexes. By treatment of **25H** with Brønsted acids the proligand is transformed into **[25H$_2$]$^+$[A]$^-$**.

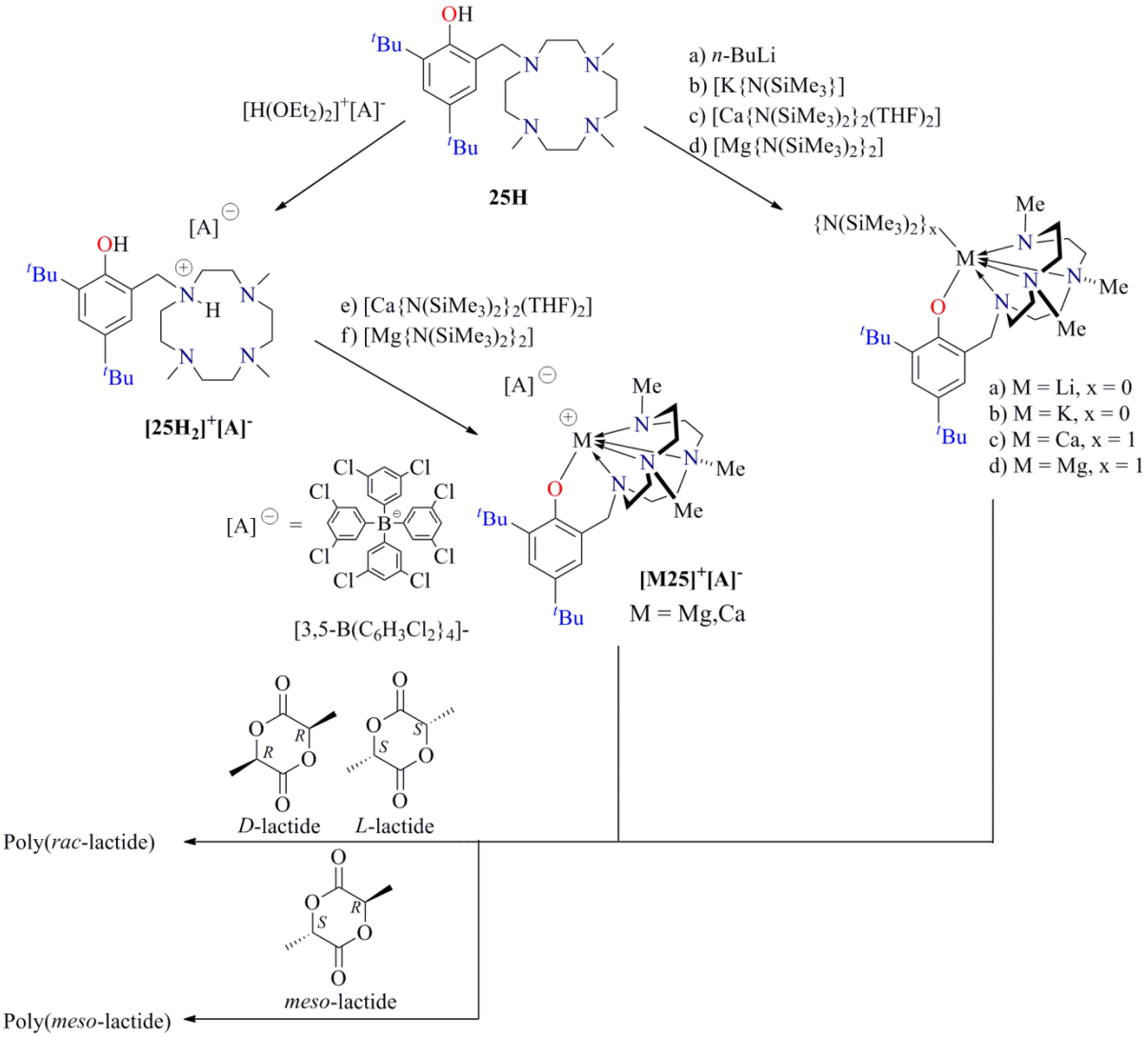


**Scheme S5.** Syntheses of neutral and cationic alkali and alkaline earth metal complexes bearing a phenolate type proligand containing a macrocycle and their application in the ROP of lactide monomers.

Further treatment of **[25H$_2$]$^+$[A]$^-$** with calcium and magnesium silylamide precursors affords the formation of cationic complexes. The complexes are applied in the ROP of *rac*- and *meso*-lactide and produce predominatly atactic polylactides.

## Index of Compounds

**1** 2,4-di(2-phenylpropan-2-yl)phenol, $C_{24}H_{26}O$

**2** 6,6'-disulfanediylbis(2,4-bis{2-phenylpropan-2-yl}phenol), $C_{48}H_{50}O_2S_2$

**3** 2-(bromomethyl)-4,6-di-*tert*-butylphenol, $C_{15}H_{23}BrO$

**4** 2,4-di(*tert*-butyl)phenol, $C_{14}H_{22}OH$

**5** 6,6'-disulfanediylbis(2,4-di-tert-butylphenol), $C_{28}H_{42}O_2S_2$

**6** 2,4-di-*tert*-butyl-6-mercaptophenol, $C_{14}H_{22}OS$

**7** 2-mercapto-4,6-bis(2-phenylpropan-2-yl)phenol, $C_{24}H_{26}OS$

**8** 4-methyl-2-(1-methylcyclohexyl)phenol, $C_{14}H_{20}O$

**9** 6,6'-disulfanediylbis(4-methyl-2-{1-methylcyclohexyl}phenol), $C_{28}H_{38}O_2S_2$

**10** 2-mercapto-4-methyl-6-(1-methylcyclohexyl)phenol, $C_{14}H_{20}OS$

**11** 4-methyl-2-(2-phenylpropan-2-yl)phenol, $C_{16}H_{18}O$

**12** 6,6'-disulfanediylbis(4-methyl-2-{2-phenylpropan-2-yl}phenol),

**13** 2-bromo-4-methylphenol, $C_7H_7BrO$

**14** 1-(benzyloxy)-2-bromo-4-methylbenzene, $C_{14}H_{13}BrO$

**15** 2-(benzyloxy)-5-methylbiphenyl, $C_{20}H_{18}O$

**16** 5-methyl-(1,1'-biphenyl)-2-ol**,** $C_{13}H_{12}O$

**17** 3-(2-bromo-4-methylphenoxy)tetrahydro-2H-pyran, $C_{12}H_{15}BrO_2$

**18** $[Li\{N(SiMe_2H)_2\}]$

**19** $[Sc\{N(SiMe_2H)_2\}_3THF]$

**20** $[Y\{N(SiMe_2H)_2\}_3THF_2]$

**21** "$In(O^iPr)_3$", $In_5(\mu_5\text{-}O)(\mu_3\text{-}O^iPr)_4(\mu_2\text{-}O^iPr)_4(O^iPr)_5$,

**22** 1,4,7-trimethyl-1,4,7,10-tetraazacyclododecane, $(Me_3TACD)H$

**23** 2,4-di-*tert*-butyl-6-(hydroxymethyl)phenol, $C_{15}H_{24}O_2$

**24** 2-(bromomethyl)-4,6-di-*tert*-butylphenol, $C_{15}H_{23}BrOH$

**25 H** 2,4-di-*tert*-butyl-6-((4,7,10-trimethyl-1,4,7,10-tetraazacyclododecan-1-yl)methyl) phenol

# Appendix

All operations unless otherwise noted were performed under an inert atmosphere of argon by using standard schlenk-line or glovebox techniques.

**Solvents and Reagents.** Toluene, *n*-pentane, $CH_2Cl_2$, THF and diethyl ether were purified using *MB SPS-800*. Benzene, MeOH, EtOH and isopropanol were distilled under argon from sodium/benzophenone ketyl prior to use. Deuterated solvents excepting $CD_2Cl_2$ and $CDCl_3$ were distilled under argon from sodium/benzophenone ketyl prior to use. $CD_2Cl_2$ and $CDCl_3$ were distilled under argon from $CaH_2$. *Meso*-Lactide (Uhde Inventa-Fisher) and *rac*-lactide were recrystallized from isopropanol and toluene at – 30 °C, washed with diethyl ether, dried under vacuum and sublimed twice. All other chemicals were commercially available and used after appropriate purification.

**NMR.** NMR spectrum were recorded on a *Bruker Avance II 400 MHz* spectrometer ($^1$H, 400.1 MHz, $^{13}$C-{$^1$H}, 100.6 MHz) or on a *Varian Mercury 200 MHz* at ambient temperature unless otherwise stated. Chemical shifts for $^1$H an $^{13}$C-{$^1$H} NMR spectrum were referenced internally using the residuel solvent resonances and reported relative to tetramethylsilane.

**Metal Titration.** General method for metal titration: 10-30 mg of the compound were dissolved in 1-2 mL of THF and hydrolized by slow addition of a few drops of distilled water. After addition of 1-2 mL aqueous ammonia solution (25%) the total volume was increased to 20-30 mL by addition of distilled water. An indicator tablet was dissolved and titrated with a 0.01 m solution of EDTA disodium salt until the transition point was observed.

**X-Ray diffraction analysis**. Crystallographic data were collected by the group of Prof. Ulli Englert at the institute of inorganic chemistry at RWTH Aachen University on a *Bruker* AXS diffractometer equipped with an *Incoatec* microsource and an APEX area detector using Mo-Kα radiation (graphite monochromator, λ = 0.71073 Å) using ω-scans. The SMART program package was used for data collection and unit cell determination; processing of the raw frame data was performed using SAINT and SADABS; absorption correction was applied with Mulabs as implemented in the program PLATON. Structures were solved by direct methods and refined against $F^2$ using all reflections with SHELXL-97 software as implemented in the program system WinGX. All crystal structures were refined by Dr. Thomas P. Spaniol.

**GPC.** Molecular weight and polydispersity determinations were performed in THF at 25 °C at a flow rate of 1 mL $min^{-1}$ utilizing an *Agilent 110 Series* equipped with a G1310A isocratic pump, an *Agilent 1100 Series* refractive index detector and 8 * 600 mm, 8 * 300 mm, 8 * 50 mm PSS SDV linear M columns. Calibration standrads were commercially available narrowly distributed linear polystyrene samples that cover a broad range of molar masses ($10^3 < M_n < 2 * 10^6$ g/mol).

**GC/MS.** GC/MS analysis was performed on a *Shimadzu GCMS – QP 2010 plus*.

**DSC.** DSC measurements were performed on a *Netzsch 204 Phoenix*.

**Table A1.** Crystallographic Data for [Y**L**$^{14}${N(SiMe$_2$H)$_2$}(THF)] and [M25]$^+$.

| **Compound** | **[YL$^{14}${N(SiMe$_2$H)$_2$}(THF)]** | **[Mg25]$^+$[B{3,5-C$_6$H$_3$Cl$_2$}$_4$]$^-$** |
|---|---|---|
| Empirical Formula | $C_{62}H_{80}NO_3S_2YSi_2$ | $C_{56}H_{63}BCl_8F_2MgN_4O$ |
| Formula weight [g · mol$^{-1}$] | 1096.42 | 1164.82 |
| Crystal size [mm$^3$] | 0.40 x 0.15 x 0.05 | 0.12 x 0.06 x 0.03 |
| Crystal color and habit | Colorless block | Colorless Needle |
| Crystal system | Monoclinic | Triclinic |
| Space group | *P* 2$_1$/*n* | *P*-1 |
| *a* [Å] | 14.9108(11) | 11.612(4) |
| *b* [Å] | 20.1511(16) | 16.237(5) |
| *c* [Å] | 20.9690(16) | 16.460(6) |
| $\alpha$ [°] | 90° | 102.856(9) |
| $\beta$ [°] | 98.940(2)° | 106.909(9) |
| $\gamma$ [°] | 90° | 94.452(9) |
| *V* [Å$^3$] | 6224.0(8) | 2814.5(16) |
| *Z* | 2 | 2 |
| $D_{calc}$ [g · cm$^{-3}$] | 1.209 | 1.374 |
| *T* [K] | 100(2) | 100(2) |
| $\mu$(Mo K$_\alpha$) [mm$^{-1}$] | 1.086 | 0.461 |
| *F*(000) | 2412 | 1212 |
| $\theta$ range [°] | 1.71 - 26.44 | 1.32 – 26.47 |
| hkl indices | -18 18, -25 25, -26 26 | -14 14, -20 20, -20 20 |
| Reflections collected | 73781 | 33103 |
| Independent reflections | 12766 [R(int) = 0.1163] | 11371 [R(int) = 0.1439] |
| Data / restraints / parameters | 12766 / 0 / 688 | 11371 / 0 / 667 |
| $R_1$, $wR_2$ ($I > 2\,\sigma(I)$) | 0.0521, 0.0977 | 0.0753, 0.1430 |
| $R_1$, $wR_2$ (all data) | 0.0981, 0.1125 | 0.1535 |
| Goodness-of-fit on $F^2$ | 1.005 | 0.995 |
| Largest diff. in peak and hole [e· Å$^{-3}$] | 0.578, -0.300 | 0.653, -0.393 |

# Curriculum Vitae

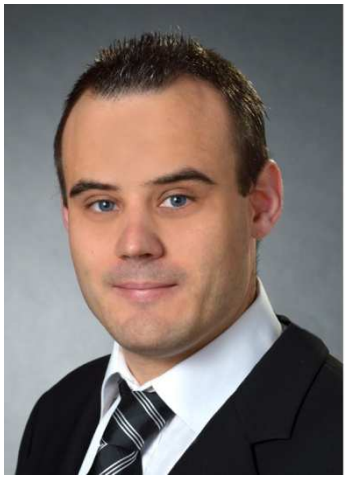

**Personal Data**


| | |
|---|---|
| Name | Andreas Kapelski |
| Date and place of birth | 20/01/1984, D-47495 Rheinberg |
| Address | Junkerstraße 60, D-52064 Aachen |
| Email | andreaskapelski@aol.com |


**Education**

Postgraduate Studies

| | |
|---|---|
| 10/2009-02/2013 | Doctoral Studies at RWTH Aachen University; DE, under supervison of Prof. Dr. Jun Okuda: „Stereocontrolled Ring-Opening Polymerization of Lactide Monomers by Lewis-Acidic Metal Complexes” |

Undergraduate Studies

| | |
|---|---|
| 09/2009 | Graduation (Diplom) |
| 03/2009-09/2009 | Diploma thesis at RWTH Aachen University, DE, under supervision of Prof. Dr. Jun Okuda „Bis(phenolato)-Komplexe des Bismuts“ |
| 10/2004 | Begin of chemistry studies, RWTH Aachen University, DE |

Secondary Education

| | |
|---|---|
| 08/1994-06/2003 | Amplonius-Gymnasium Rheinberg, DE. General qualification for university entrance (Abitur) |
| 08/1990-06/1994 | Gemeinschaftsgrundschule Alpen; DE |

**Practical Intership**

| | |
|---|---|
| 05/2004-06/2004 | Laboratorium für Umweltanalytik und Qualitätskontrolle, Solvay Chemicals & Co.KG, Rheinberg, DE. |

**Language Skills** English (excellent), French (fundamental)

**List of publications**

1) I. Peckermann, A. Kapelski, T. P. Spaniol, J. Okuda „Indium Complexes Supported by 1,4-Dithiaalkanediyl-Bridged Bis(phenolato) Ligands: Synthesis, Structure, and Controlled Ring-Opening Polymerization of L-Lactide", *Inorganic Chemistry* **2009**, *48* (12), 5526.

2) J.-C. Buffet, A. Kapelski, J. Okuda "Stereoselective Polymerization of *meso*-Lactide: Syndiotactic Polylactide by Heteroselective Initiators Based on Trivalent Metals", *Macromolecules* **2010**, *43*, 10201-10203.

3) A. Kapelski, J.-C. Buffet, T. P.Spaniol, J. Okuda "Group 3 Metal Initiators with an OSSO-Type Bis(phenolate) Ligand for the Stereoselective Polymerization of Lactide Monomers, *Chem. Asian. J.* **2012**, *7*, 1320-2330.

**Conference Contributions**

- Poster Presentation: „Sc and Y Bis(phenolato) Complexes for the Ring-Opening Polymerization of Lactides" 15. Vortragstagung der Wöhler Vereinigung für Anorganische Chemie, Freiburg im Breisgau, DE (09/2010)
- Poster Presentation: "Stereocontrolled Ring-Opening Polymerization of Lactide Monomers by Bis(phenolato) Rare-Earth Metal Initiators", 6. Heidelberg Forum of Molecular Catalysis, Heidelberg, DE (07/2011)

- Poster Presentation: „Sc and Y Bis(phenolato) Complexes for the Ring-Opening Polymerization of Lactides" Fourth Annual New Year's Symposium, RWTH Aachen University, DE, (01/2012)
- Poster Presentation: "Stereocontrolled Ring-Opening Polymerization of Lactide Monomers by Bis(phenolato) Rare-Earth Metal Initiators" 5th CaRLa Winterschool, Heidelberg, DE, (03/2012)
- Oral Presentation: "Stereocontrolled Ring-Opening Polymerization of Lactide Monomers by Bis(phenolato) Rare Earth Metal Initiators" 5th CaRLa Winterschool, Heidelberg, DE, (03/2012)

## Acknowledgment

First of all I want to to express my gratitude and respect to my supervisor

**Prof. Dr. Jun Okuda**

for providing me with this interesting and challenging topic, for his sustained support, for his encouragement and for his scientific and personal guidance during my work.

I want to thank **Dr. Thomas P. Spaniol** for his support and encouragement in the group.

Very important to the success of this thesis were the careful homonuclear decoupled $^{1}$H-NMR measurements of the polymer samples and in general the NMR spectra of the synthesized compounds. These measurements were performed by **Toni Gossen** and his team. **Toni**, you are definitely one of the rare examples of a real striking head in the IAC. Keep it that way. I will miss the numerous emotional discussions we had, not only about small signals and the question, which signal to irradiate.

Keeping care about the GPC and DSC is only one of the excellent qualities, I will keep **Dr. Klaus Beckerle** ever in mind for. **Klaus**: Thanks a lot for the numerous discussions about science, society, soccer and students. Força, Wormatia.

**Monika Paul** also did numerous GPC measurement and cared about the chemical ordering. Thank you!

For X-ray data collection, structure solution / refinement and help concerning all crystallographic issues I want to thank **Dr. Thomas P. Spaniol**, **Prof. Ulli Englert** and all the members of his group. And of course **Heiko**, for his ideas concerning the choice of different solvents.

Two students worked on their Bachelor Thesis under my occupation. Their results form an important contribution to this thesis. I am very grateful to **Catherine Hermans** and **David Fabry** for their hard work, patience and passion. It was a pleasure to me, instructing you during your work and beyond. I wish both of you all the best in the future. **David**: Good Luck! **Catherine**: Imagine the moment we first met. And now imagine someone walking up

to us, telling how our friendship will develop. It was a great time, which is hopefully not at its end.

The comfortable feeling I had during the last years is inseparably connected to the people working with me in the group over the last years. Thank you all for making these years so exciting and worth remembering. First of all, I want to thank **Sabine Sandfuss** and **Britta Meier**. **Sabine**: Thank you for everything. As an office neighbor, as a colleague and as a friend. I will miss your presence. **Britta**: Zack….Bumm….Auf Wiedersehen!

Thanks also to **Heiko Kulinna** and **Waldemar Fegler**, whose presences I will also definitely miss in the future. **Heiko**: Mr. Cardigan! We started together our studies in 2004 and we finished our Ph.D. (more or less) together. Thanks for keeping up with me and being patient with me, even in my darkest moments. **Waldemar**: The "Lit"-Master. Your Literature-Alert-System was better than any RSS-Feed. Unfortunately, you look terrible with a mustache.

I also want to thank **Dr.** …. sorry, now he is **Prof. Dr. Ajay Venugopal**. A very intelligant, hard-working and nice post-doc from india working 1.5 years in Aachen. **Ajay**: I am still waiting for your SeleCa-Presentation as a Full Professor! And I will miss these interestingly tasting indian sweets.

**Dr. Jean-Charles Buffet** joined the Okuda group in October 2009 and became my "subgroup leader" for 1.5 years. He instructed and guided me through the work. Consequently his ideas and suggestions were very helpful. **JC**: Je suis trés reconnaissant pour votre soutien et des conseils. Tu m'avez aidé de me familiariser avec le thème dans les premiers mois. Merci bien.

I want to thank **Steve Gotzen** for the numerous discussions about soccer, although he was never interested in joining actively our soccer match. As a trained lab assistant he is additionally a very good chemist! **Steve**: There's just one true Borussia!

**Simone Becher** organized the "paper stuff" for the whole group. In addition, she has always an ear for everybody who needs help. **Simone**: Thank you for caring about so many organisational things, we normally don't recognize in the labs. You do a great job and I will miss our talks in your office and on the terrace. Stay true to you.

**Elise**: "Did you measure a VT?" Bonne chance, Madame Abinet!

**Freddi**: Finally a (unshaved) Post-Doc!

**Phillip**: Thanks for caring about the gloveboxes and the NMR solvents. Enjoy Canada!

**Crispin**: Was there any week without kinetics, crazy working hero?

**Andreas S.**: Burning down the house.

Thanks also to **Dr. Schnupsi**, **Steffi**, **Marie**, **Laura**, **FrauChen**, **Dr. Michael Tauchert**, **Dr. Holger Helten**, **Julien**, **Julian**, **Daniel, Claudio, Thomas D.**, **Ashley**, **Peng**, **Dr. Jung** and **Valeri** for keeping up with me during the last years.

I want to thank my colleagues from the other groups of the IAC, especially **Carina** (Herne West), **Asli**, **Maria**, **Peter**, **Christian** and **Gillo** for their cooperative contributions to make the last years such an enjoybale time.

Representative for all the people working in the institute I want to thank **Peter Rong** (mechanical workshop), **Gertrud Lennertz** (students office), **Jupp Offermanns** (AC-F and AC-A practical courses) and **Dr. Udo Flesch** (administration).

Thanks also to my **parents**, to my sister **Stephanie** and to my **grandparents** for their support and patience.

PS: I will never forget that rainy day when Thomas Spaniol stood at the Mensa entrance, distributing pocket bibles….even in nature science there is space for something spiritual!